19E Deterministic Evaluations

19E.1 Introduction

This appendix documents evaluations which are deterministic in nature. These evaluations were conducted to provide an insight into performance within the plant boundaries and outside the plant boundaries.

Subsection 19E.2 focuses on the containment performance for several specific accident challenges and develops input for the offsite consequence analysis.

Subsection 19E.3 focuses on offsite consequence analysis with the CRAC code to allow a measurement against consequence related goals. Primary inputs come from the MAAP-ABWR analysis of Subsection 19E.2 and the containment event trees in Subsection 19D.5.

19E.2 Deterministic Analysis of Plant Performance

19E.2.1 Methods and Assumptions

This subsection summarizes the methods and assumptions that were used in evaluating the Reactor Pressure Vessel (RPV) and containment responses and determining the resulting source term. The Modular Accident Analysis Program (MAAP) (Reference 19E.2-1) was the primary tool used to determine the fission product source terms. Included in this subsection is a brief description of the code, the basic assumptions about the ABWR configuration, a discussion of those phenomena not explicitly modeled in the MAAP analysis, and the definition of the base case.

19E.2.1.1 Code Description

MAAP was used to determine the vessel and containment responses and the source terms for the ABWR under severe accident conditions. MAAP3.0B was modified to model the configuration of the ABWR. An overview of MAAP3.0B is provided below, followed by a discussion of the changes made in the code to model the ABWR. This new version of the code will be referred to as MAAP-ABWR.

19E.2.1.1.1 MAAP3.0B

MAAP is a computer code developed as a part of the Industry Degraded Core Rulemaking (IDCOR) program to investigate the physical phenomena that might occur in the event of a severe light water reactor accident leading to core damage, possible reactor pressure vessel (RPV) failure, and possible failure of containment integrity and release of fission products to the environment. MAAP development was sponsored by the Atomic Industrial Forum. MAAP includes models for the important phenomena that might occur in a severe light water reactor accident.

MAAP is an integrated code which tracks the progression of hypothetical accident sequences from a set of initiating events to either a safe, stable and coolable state or containment structural failure and fission product release to the environment. MAAP models a wide spectrum of phenomena including steam flashing, water inventory loss, core heatup, cladding oxidation and hydrogen evolution, fission product release from the degraded fuel rods and their transport to the containment and beyond, molten core slump into the lower plenum of the RPV, vessel failure, corium-concrete interactions and further release and transport of fission products. MAAP models all of the engineered safety systems such as emergency core cooling, automatic depressurization, safety relief valves, and decay heat removal. MAAP also allows the user to model operator behavior and deviations in system operation.

MAAP has a modular structure in which separate subroutines are dedicated to modeling specific regions and physical phenomena. The main program directs the program execution through several high level subroutines. The program calls a sequence of system and region subroutines at each time step. These subroutines, in turn, call phenomenology subroutines as

required. The simulation of an entire accident sequence does not require any user intervention during the running of the program. A set of built-in property-library subroutines provide physical properties.

(1) High Level Subroutines

The high level subroutines include the main program, the input and output subroutines, the data storage and retrieval subroutines, and the numerical integration subroutines. Also included in the high level subroutines is a controlling routine, BWROP, which allows user interventions that describe the actions occurring during an accident sequence. The high level subroutines pass global variables by common blocks (not argument lists) and do not contain physical models for the reactor plant. The time integration subroutines, INTGRT and DIFFUN control the time steps and call system and region subroutines at each time step during an accident transient.

(2) System and Region Subroutines

The system and region subroutines include the EVENTS subroutine which sets the event flags (Boolean variables) giving the status of the system and the status of operator interventions. The event flags control code execution. Region subroutines, one for each physical region of the reactor system, define the differential equations for the conservation of internal energy and mass. Other systems subroutines examine the inter-region gas flow rates and calculate the core temperatures and fuel-cladding-coolant interactions. The systems and region subroutines pass global variables by common blocks and operate on them by calling the phenomenology subroutines.

(3) Phenomenology Subroutines

The phenomenology subroutines describe the rates of the physical processes occurring in each region of the reactor plant model. The phenomenology subroutines pass variables by argument lists, and generally do not use or alter global variables. The phenomenology subroutines are generic in nature and can be called by any of the region subroutines or by other phenomenology subroutines.

(4) Property-Library Subroutines

The property-library subroutines give the physical properties (e.g., specific heat and saturation pressure) of the important materials. These subroutines use argument lists to pass variables and do not have side effects on global variables. Property subroutines are called by the phenomenology subroutines.

19E.2.1.1.2 ABWR Modifications

Several modifications to the MAAP3.0B code were required to adequately model the ABWR. The starting point for the modifications was the MAAP3.0B Mark II models. The modified

version of the code is referred to below as MAAP- ABWR. Specific ABWR features which required code changes are listed below.

(1) Containment Configuration

The ABWR configuration is different than previous BWR configurations. MAAP-ABWR models the flow paths between the containment compartments correctly. The high level subroutine DIFFP was modified. The affected regions are:

(a) Suppression Pool Configuration

The ABWR suppression pool configuration required changes in the models to accurately reflect the relationship between water level and volume. The ABWR suppression pool is modeled by applying the Mark III pool model. The affected subroutines are system routine INITAL and phenomenological routine M3POOL.

(b) Lower Drywell

Several alterations were required in order to model the ABWR lower drywell. Flow paths were added to model the vacuum breakers from the wetwell, the vents to the suppression pool and overflow from the suppression pool through the wetwell drywell connecting vents. Core concrete attack in the lower drywell region can result in penetration of the pedestal to the wetwell/drywell connecting vents. When penetration occurs, flow between the lower drywell region and the suppression pool will occur. Models for this flow were incorporated which employ a user supplied concrete penetration limit. The PEDSTL region subroutine was affected, as was the PDFP region fission product subroutine.

(c) Upper Drywell

This region required the removal of the flow path which represented the vacuum breaker in the Mark II model, and the addition of steam and gas venting to the suppression pool via the lower drywell. Affected subroutines are the DRYWEL region and DWFP fission product region subroutines.

(d) Wetwell

The wetwell fission product transport subroutine WWFP was modified to correctly model the ABWR.

(e) Horizontal Vents

The M3VENTA phenomenological subroutine model for the horizontal vents in a Mark III were applied to model the horizontal vents connecting the wetwell/drywell vents and the wetwell in the ABWR.

(2) RHR Heat Exchangers

ABWR has a heat exchanger in each of the three RHR loops. Previously, heat exchangers were modeled in only two loops of the RHR system. Addition of the third heat exchanger required a change in the ECCS system subroutine.

(3) LOCA Location

MAAP-ABWR directs the flow from all LOCA breaks into the upper drywell. However, since there is a small possibility of LOCAs which blowdown into the lower drywell, MAAP-ABWR allows the user to input the RPV Failure Event Code to simulate this event. This change was accomplished by modifying the high level subroutine BWROP and the region subroutine EVENTS.

(4) Recirculation Pump Trip

In the ABWR, four of the Recirculation Pumps (RIPs) trip on either High Vessel Pressure or on Level 3, with the remaining six RIPs tripping on Level 2. MAAP-ABWR allows the user to input these different setpoints. Region subroutine BWRVSL was modified to allow this capability.

(5) Evaporation from a Pool Surface

The evaporation model in MAAP3.0B was found to be non-conservative for the ABWR. The problem arises when the firewater system is used or the passive flooder operates and water from the wetwell floods the lower drywell. The vapor pressure in the lower drywell is much below the saturation point since there was no water in this region prior to water addition. Therefore, steam will begin to evaporate off the surface of the pool in the lower drywell.

In MAAP3.0B, the water in the suppression pool had to heat to the boiling point before evaporation was permitted off the surface of the pool. In MAAP-ABWR, the vapor pressure is conservatively assumed to rise to saturation in two time steps. This model was applied to the wetwell, upper and lower drywells. The PEDSTL, DRYWEL and BWM2WW region subroutines were affected.

19E.2.1.2 ABWR Configuration Basis

19E.2.1.2.1 ABWR Configuration Assumptions

This subsection provides a description of the assumptions which were made about the configuration and systems of the ABWR. These assumptions were made where the design detail was not yet available or was outside the scope of this submittal: for example, the type of concrete to be used in the plant is not specified in the certified design.

(1) Condensate Storage Tank. The configuration for the condensate storage tank is assumed to be consistent with the description in Subsection 19.9.9. This is sufficient

to satisfy the station blackout performance requirements discussed in Subsection 19E.2.1.2.2.

(2) Not Used

(3) Type of Concrete Used for Containment. Limestone Sand concrete was assumed to be used for all portions of the containment building except the lower drywell floor. This assumption will affect the conduction of heat into the containment walls. However, since concrete has very low thermal diffusivity there will be no negative impact on containment performance. Limestone Sand concrete is representative of the concrete which might be used in much of the United States. Basaltic concrete, with a calcium carbonate content of approximately 4 weight percent was assumed for the lower drywell floor.

(4) Not Used

(5) Battery loading profiles will be developed to define appropriate load shedding during Station Blackout (Subsection 19E.2.1.2.2.2(3)). This item has been identified as COL license information in Subsection 19.9.9.

(6) RCIC room temperature will not exceed equipment design temperature without room cooling for at least 8 hours (Subsection 19E.2.1.2.2.2(5)). This item has been identified as COL license information in Subsection 19.9.9.

(7) Control room temperature will not exceed equipment design temperature for at least 8 hours without room cooling (Subsection 19E.2.1.2.2.2(6)). This item has been identified as COL license information in Subsection 19.9.9.

(8) Operator action during station blackout is consistent with the EPGs as specified in Subsection 19E.2.1.2.2.4.

19E.2.1.2.2 Performance During Station Blackout With Failure of the Combustion Turbine Generator

19E.2.1.2.2.1 Summary

A station blackout is defined as the loss of offsite electrical power and the unavailability of onsite AC electrical power (i.e., failure of diesel generators, in most cases). During this period the important plant performance characteristics to be considered are maintenance of core cooling and containment integrity.

The primary means by which the ABWR copes with a station blackout is use of the combustion turbine generator (CTG). The analyses summarized in this subsection show that the ABWR can withstand a station blackout with failure of the CTG without core damage or loss of containment integrity for a period of approximately 8 hours. If AC power is still unavailable beyond this period, core cooling by the RCIC system is assumed to be lost. However, the ACIWA system may be able to prevent core damage. This accident sequence is discussed in Subsection 19E.2.2.3.

The key requirements of core cooling and primary containment vessel (PCV) integrity are treated separately below.

19E.2.1.2.2.2 Core Cooling

The reactor core isolation cooling (RCIC) system provides water to the reactor vessel during a station blackout with failure of the CTG. The following areas are considered to assure RCIC functionality during this event:

(1) Reactor monitoring function

(2) Steam supply to the RCIC turbine

(3) DC battery capacity

(4) Water source inventory (condensate storage tank or suppression pool)

(5) RCIC room temperature

(6) Control room(s) temperature

Each of these functions is addressed below.

(1) Reactor Monitoring Function.

The reactor monitoring of vessel water level and pressure is performed using local detectors with control room indication. Instrument power supply is from the station batteries as either DC or constant voltage constant frequency (CVCF) sources.

(2) Steam Supply to the RCIC Turbine.

The reactor vessel is the source of energy for the RCIC turbine which operates the RCIC pump, maintaining vessel water level. The RCIC turbine will isolate (i.e., trip) at low pressure 0.446 MPa. However, since the operator will be maintaining vessel pressure near 6.619 MPa in accordance with the emergency procedure guidelines (EPGs), there will be more than adequate RCIC turbine pressure for operation. The RPV pressure will be controlled manually at this level (by opening 1 or more SRVs) below the first SRV setpoint to avoid SRV cycling. SRV operability during station blackout is dependent on a DC supply source and a nitrogen supply and these are evaluated in the following discussions. It should be noted that the SRVs will cycle on the spring setpoint if the operator fails to manually control pressure.

(a) Availability of DC Power for SRV Solenoids.

Based on the following evaluation, it is concluded that there is ample DC power for operating SRV solenoids.

The control power for six of the 18 SRVs is taken from the Division I battery. The valves have been considered as part of the load on the Division I battery

for purposes of calculating the time the RCIC would be operable during station blackout. This evaluation leads to the conclusion that the 4000 ampere hour capacity of the Division I battery is sufficient for approximately 8 hours of coping during station blackout with failure of the combustion turbine generator.

Of the remaining 12 SRVs, 6 have their control power supply on the Division II battery and 6 are on the Division III battery. Each of these batteries have a capacity of 3000 ampere hours. Since Divisions II and III would normally be shut down during a station blackout situation with failure of the CTG, these batteries and their associated power distribution equipment would be available to supply power to the SRVs if necessary.

The ambient temperature for Divisions II and III batteries should remain acceptable as there would be very little load on these batteries during station blackout. For this reason, ambient temperature rise due to the lack of HVAC should not be a problem for the batteries and their associated equipment.

Based on the above, Divisions II and III DC supplies should be available on an intermittent basis for use in operating SRVs, as desired. The 6000 ampere hour total capacity of the two batteries would be adequate for many days of operation beyond the approximately 8 hour capability of Division I.

Further, eight of the 18 SRVs are used for the ADS function and thus have alternate power sources. Five of the eight can be supplied by either of two divisions (Divisions I or II). The other three can be supplied by any of three divisions. Control power for each of the ten SRVs which are not used for the ADS function is supplied by one division (four from Division I, three from Division II, and three from Division III). Thus the ability to control reactor pressure is very reliable.

(b) SRV Operability and High Pressure Containment Conditions.

The SRV actuators can open the SRVs without assistance from internal steam pressure when the makeup pneumatic supply is available to maintain the minimum required differential pressure. The SRV accumulators used for the ADS function (Figure 19E.2-1) shall have sufficient pressure and capacity to fully open the SRVs at 0.860 MPaA pressure in the containment, and additional gas is available from outside the containment to ensure the pressure control and depressurization function. The 0.86 MPaA containment pressure is based on the Containment Overpressure Protection System setpoint of 0.72 MPaA $\pm$ 5% (per section 6.2.5.2.6) plus a maximum pressure difference of 0.1 MPa between the wetwell and drywell.

The normal supply of N_2 gas to the SRVs from the atmospheric control system outside the containment may shut off due to low pressure caused by loss of AC power to the heaters or heating boiler which is used to gasify the liquid N_2 supply. However, there is a backup supply of N_2 gas from stored bottles at 14.8 to 5.96 MPa (maximum to minimum) pressure which can be used to open the SRVs in the ADS system.

Use of the stored nitrogen bottles requires operator action to manually open a closed supply valve at the valve location. Gas is then fed to the SRV actuators through the DC powered ADS solenoid valves inside the containment automatically. The ADS supply lines from the N_2 bottles should also be isolated from the normal N_2 supply to other systems by local manual closure of the motor operated crosstie valves which are otherwise inoperable on AC power loss.

The high pressure gas from the N_2 bottles is automatically reduced to the normal required pressure by a self-actuated pressure regulating valve. If the SRVs do not open with the pressure supplied by the self-actuated pressure regulating valve [for example, if containment pressure was equal to 0.860 MPa or if somewhat less than the normal required pressure were supplied], the operator could adjust the setpoint of the pressure regulating valve above the normal required pressure at the local station.

The capacity of a group of ten 45 liter high pressure N_2 gas bottles at 5.96 MPa minimum pressure is about 16 times that needed to open the 8 ADS SRVs, each of which has an actuator piston volume of 16.4 liters (1000 cubic in). Additionally, there are 10 other N_2 bottles that can be valved into service by local manual operation. After the 8 ADS valves are opened there is sufficient N_2 gas to account for at least 7 days leakage from the valve actuators, after which the N_2 bottles must be replaced to hold the ADS valve open. Based on the foregoing, it is concluded that the ADS valves can be operated to depressurize the reactor on loss of normal AC power supplies with the containment at 0.86 MPa. The operator has to manually close and open valves at the valve locations to supply nitrogen from outside the containment to open the 8 SRVs used for the ADS function and to hold them open when the pressure in the RPV drops to near containment pressure.

(3) DC Battery Capacity.

The Division I DC battery will be sized to be capable of operating the RCIC system for approximately 8 hours assuming the expected loading profiles for station blackout with failure of the CTG. These loading profiles will assume acceptable battery area environmental conditions and load shedding, when necessary, and will be defined in detail as the ABWR design progresses.

(4) Water Source Inventory.

The primary water source for the RCIC System is the condensate storage tank (CST) which has been sized to provide sufficient inventory for a minimum of 8 hours in combination with the suppression pool. In the event the CST became depleted, the backup source is the suppression pool. The suction source switches to the suppression pool automatically on high suppression pool level. The RCIC system must be manually overridden to assure that the suction revert to the condensate storage tank to limit heating of the containment.

(5) RCIC Room Temperature.

Failure of the AC power to the room cooling will allow the RCIC room temperature to rise. The ABWR plant will be designed to prevent the room temperature from reaching the equipment design temperature of 340 K (151°F), starting at the normal room temperature of 313 K (104°F), for at least 8 hours.

(6) Control Room Temperatures.

The safety-related equipment required to function during station blackout with failure of the CTG and located in the main, lower and computer control rooms will be designed for a maximum operating temperature of 331 K (136°F). The ABWR plant will be designed to prevent the control room temperature from reaching this equipment design temperature for at least 8 hours, starting at the normal room temperature of 299 K (79°F).

19E.2.1.2.2.3 Primary Containment Vessel (PCV) Integrity

Containment pressure and temperature analyses were performed to determine the containment atmospheric conditions after 8 hours of station blackout conditions with failure of the CTG assuming event initiation at 100% thermal power. An analysis was performed which assumed the RCIC suction was taken from the condensate storage tank for the duration of the event. The drywell and wetwell pressure and temperature were calculated to be less than their design basis of 0.411 MPa and 444 K (340°F) (drywell)/377 K (219°F) (wetwell) after 8 hours. Therefore, PCV integrity is maintained.

19E.2.1.2.2.4 Operator Actions

The loss of normal AC power will lead to indirect turbine trip and reactor scram due to high condenser pressure on loss of circulating water. The subsequent loss of feedwater will cause the RPV to isolate on low water level. Failure of the emergency diesel generators to initiate and failure of the combustion gas turbine will leave the RCIC system as the only source of makeup water to the core. The RCIC system will automatically restore the RPV water level. Operator actions are specified in the EPGs to control the RCIC system and maintain the RPV level between Level 3 and Level 8.

In addition, the operator will be instructed to maintain RPV pressure below the high pressure scram setpoint to avoid SRV cycling by controlling 1 or more SRVs manually. The PCV pressure and temperature will not approach design values for at least 8 hours. Failure of the RCIC (core uncovery) will require the operator to blowdown through the SRVs when the heat capacity temperature limit is exceeded or the water level falls below the top of the active fuel and thereby avoid a high pressure as the core melts.

19E.2.1.2.2.5 Recovery Following Restoration of AC Power

All equipment necessary for restoration of power is located external to the primary and secondary containments in the reactor building. With the exception of the control building, all heat generating sources external to secondary containment are shutdown during station blackout so that the rooms should be at temperatures which allow restart of the support systems under their automatic or manual modes following restoration of AC power. Temperatures in the control building should be such that restart can be accomplished by the operators from the control room. Also, restart could be initiated from the remote shutdown panel or even by local control at the motor control centers and switchgear. Following restoration of power and initiation of the reactor cooling water system, the ECCS areas of secondary containment will be cooled by their safety grade room coolers so normal operation of the safe shutdown systems could be restored. The turbine building electrical systems and the non-safety-related secondary cooling system provide a backup means of restoring cooling to the ECCS equipment areas within secondary containment.

19E.2.1.2.2.6 Conclusions

The ABWR plant is being designed to be capable of maintaining core cooling and containment integrity for at least 8 hours following the loss of offsite and onsite AC electrical power including the combustion turbine generator. This capability assessment follows the general criteria of:

(1) Assuming no additional single failures

(2) Realistic analytical methods and procedures

A summary of the key plant parameters, design basis values and capability assessment is shown in Table 19E.2-2. Note that the response of the ABWR containment to this event would be successful even if the design basis values were exceeded, as long as the ultimate capability were not exceeded.

19E.2.1.2.3 Equipment Survivability

The requirements for equipment survivability are derived from two sources. 10CFR50.34(f) specifies the conditions required for an analysis in which the 100% of the active fuel cladding is oxidized. Additional requirements for demonstrating the survivability of equipment needed to mitigate a severe accident are specified in SECY-90-016. In order to meet these requirements, three categories of events were considered. The first category consists of one

event which responds to the requirements of 10CFR50.34(f) paragraphs (2)(ix)(C) and (3)(v). A non-mechanistic scenario is modelled which results in the requisite oxidation but which follows the rules of design basis analysis. The other two categories respond to the requirements of SECY-90-016. The second category consists of events representing the frequency dominant events ending in in-vessel recovery. Similarly, category three is made up of events representing the frequency dominant events ending in ex-vessel recovery. Together the events in categories two and three represent the vast majority of the core damage frequency.

The list of required instrumentation and equipment was derived from reviews of the safe shutdown equipment list, the EPGs, the PRA, and the severe accident analysis. The list of required equipment varies for the three categories of events described above. The capability of each piece of identified equipment was then compared to the environmental conditions for the appropriate category of events. In reviewing the equipment capability, the environmental qualification standards for assessing compliance to 50.49 were not used as a strict measure. Rather, they were used to provide a measure of confidence that the equipment would survive the expected conditions.

19E.2.1.2.3.1 Definition of Survivability Profiles

For each of the three categories of events, a set of curves representing the bounding environmental conditions for that category were developed for use in evaluating the equipment and instrumentation survivability. These conditions were then compared to the equipment capabilities to provide a measure of confidence that the necessary equipment would survive the expected conditions. It is important to note that the ABWR containment is inerted for all of the events described below. Therefore, there is no containment challenge due to hydrogen burning or detonation.

The basis for each category of events is provided below along with a brief summary of the event progression.

19E.2.1.2.3.1.1 10CFR50.34(f) Category

This category corresponds to an event which could result in the conditions of 10CFR50.34(f)(2)(ix), which specifies that core cooling is degraded sufficiently to result in the generation of 100% oxidation of the active cladding. Core cooling is then recovered before the vessel fails. The PRA has confirmed the results of previous studies which show that the core damage frequency is dominated by accidents initiated from transients. Table 19.3-5 indicates that a very small percentage of all core damage events are initiated by LOCA. Therefore, a transient initiated event is specified for this evaluation.

Best estimate analyses do not result in oxidation of 100% of the active cladding. In order to simulate the hypothetical event, MAAP-ABWR was run using a multiplier to non-mechanistically generate oxidation of the active cladding. Additionally, ECCS was cycled on and off to produce the requisite amount of hydrogen for 100% metal-water reaction. The event progresses as follows:

- An isolation event occurs.
- All core injection is assumed to fail.
- Drywell and wetwell sprays are initiated 30 minutes after the initiation of the accident, water flow is directed through the RHR heat exchanger.
- The core begins to heat up and zirconium begins to oxidize.
- ECCS is recovered.
- Additional hydrogen is generated as the core is quenched.
- Vessel water level is recovered, terminating the event.

Curves representing the environmental conditions during this event are shown in Figures 19E.2-26a through 19E.2-26e. The vessel pressure remains within the range of normal operating pressures for the duration of the accident. Therefore, a curve of the vessel pressure is not included here.

19E.2.1.2.3.1.2 Severe Accidents Recovered In-Vessel

This category is designed to represent the dominant in-vessel recovery sequences. There are four credible sequences of this type. The events are LCHP-IV-N-N, LCLP-IV-N-N, LCLP-IV-R-N, and SBRC-IV-N-N.

In the SBRC-IV-N-N sequence, the RCIC operates for several hours before it fails, due to the loss of sufficient battery power for RCIC controls. As discussed in Subsection 19E.2.2.3(1), the firewater system can be used to prevent core damage in this instance. The probability associated with the successful use of the firewater addition system in the development of the containment event trees is consistent with prevention of core damage. However, this possibility was not modeled in the core damage event trees. Therefore, for consistency, no credit was taken for the prevention of core damage. Nonetheless, the sequence evaluated for SBRC-IV-N-N would not be expected to have core damage. Thus, it is excluded from further consideration for the purpose of assessing equipment survivability.

All of the remaining events in this category are initiated by transients with a presumed loss of core cooling at initiation. The core gradually uncovers and heats up. Some core damage occurs, but core cooling is recovered and the vessel does not fail. In two of the sequences (those in which the seventh character is N), containment cooling is recovered before the rupture disk opens, while in one (with the seventh character R) the rupture disk opens to prevent containment failure. The curves shown in Figures 19E.2-27a through 19E.2-27f represent the bounding environmental conditions for this category of events.

19E.2.1.2.3.1.3 Severe Accidents which Progress Ex-Vessel

This category is designed to represent the dominant ex-vessel sequences. There are six credible sequences of this type. The events are LCHP-FS-N-N, LCHP-FS-R-N, LCLP-FS-N-N, LCLP-FS-R-N, LCLP-PF-N-N, and LCLP-PF-R-N. For the high pressure melt sequences (LCHP), it is known that the drywell spray system is available since the sequence does not result in a penetration overtemperature failure (i.e., the seventh character in the sequence is not P). For the low pressure scenarios, the use of the firewater addition system cannot be distinguished from sequences with the passive flooder. Therefore, both methods of mitigation are considered.

The details of the core melt progression are discussed in Subsections 19E.2.2.1 and 19E.2.2.2. In general the accident progression is as follows:

- A transient results in scram and containment isolation.
- All core cooling is lost and the vessel water level fails, resulting in core uncovery.
- The core melts and vessel breach occurs.
- For the high pressure scenario, debris may be entrained from the lower drywell, so drywell sprays are used to cool the containment and quench the core debris.
- For the low pressure scenario, either the firewater addition system or the passive flooder may be used to cool the molten core debris.

This category is characterized by core melt and vessel failure. As the fuel melts, the gas in the vessel heats up. The containment response is characterized by pressurization due to steam and non-condensible gas generation. When the vessel fails, high temperatures are generated in the drywell for a short period of time due to the introduction of core debris in the lower drywell. High pressure events have significantly different characteristics than low pressure events. Therefore, the resulting environmental conditions are broken down into two sets of bounding profiles. The curves shown in Figures 19E.2-28a through 19E.2-28f represent the bounding environmental conditions for the high pressure category of events. The curves in Figures 19E.2-29a through 19E.2-29f represent the bounding environmental conditions for the low pressure category of events.

19E.2.1.2.3.2 Identification of Required Equipment and Instrumentation

Three primary sources were used to identify the equipment and instrumentation required for the mitigation of either the 10CFR50.34(f) event or a severe accident. 10CFR50.34(f) requires that the equipment required for safe shutdown and containment isolation be considered, while the equipment and instrumentation required to survive severe accident conditions may be extracted from the discussion of the accident sequences in Subsection 19E.2.2. Additionally, all instrumentation which monitor plant variables required for operator actions were reviewed.

19E.2.1.2.3.2.1 Requirements for 10CFR50.34(f)

Safe shutdown is defined in 10CFR50.2 for non-DBA events as hot shutdown. In addition, 10CFR50.34(f) requires that containment integrity be demonstrated. Thus, the critical functions of reactivity control, vessel inventory control, containment isolation and containment integrity were considered.

The functions of reactivity control and containment isolation are required in the very early stages of an accident, during which all parameters are well within their design basis values. Therefore, since the survival of equipment to support these functions is assured, this equipment is not considered here, although the continued maintenance of containment integrity is considered.

The 10CFR50.34(f) event does not impact the secondary containment in excess of the impact of design basis events. Therefore, equipment located in the secondary containment is not considered in this review.

The core cooling function can be performed by the HPCF, the RCIC, or, following depressurization of the vessel, the LPFL mode of RHR or the firewater addition system (ACIWA). The operability of both LPFL and ACIWA will be demonstrated to satisfy equipment survivability for severe accident. Therefore, the survivability of HPCF and RCIC will not be considered.

Maintenance of containment integrity requires that isolation valves remain closed, and that excessive leakage does not occur through the containment penetrations. For the 10CFR50.34(f) event, the RHR system is used to prevent containment overpressurization.

The required instrumentation was developed from Table 7.5-8 which contains a list of all variables required for manual actions. These are obtained from a review of the events included in Chapter 15 as well as the EPGs, as discussed in Subsection 7.5.2.1. In one case, the action which would be specified by the variable is also required if the operator cannot determine the status of the variable. The neutron flux measurement indicates if the reactor is critical. If that the reactor has not been scrammed during an accident, the operator is required to scram the reactor. This same action is specified if the operator cannot determine the neutron flux. Thus, the instrumentation to determine neutron flux is not included as required for survivability.

The exhaust fan radiation monitor is used during normal operation. Upon sensing high radiation levels, the normal exhaust path is isolated and flow is directed through the Standby Gas Treatment System. Isolation also occurs if the monitor fails. For the classes of accidents considered here, the containment will be isolated. Therefore, this instrument will not be affected by the event. Further, the monitor is not a post accident monitoring device, so its survivability is not an issue.

Based on the above discussion, the equipment and instrumentation list contained in Table 19E.2-29 will be used in assessing the survivability for the 10CFR50.34(f) event.

19E.2.1.2.3.2.2 Requirements for Severe Accidents

As discussed above a review of the PRA and severe accident analysis was done to determine the set of equipment required for accident mitigation. Both in-vessel and ex-vessel scenarios were considered. The survivability of all equipment which is used in the development of the containment event trees or in the severe accident analysis is addressed. It is noted for clarification that, although the RCIC system is discussed in the development of the severe accident analysis, it is only used before core damage occurs. This ensures the proper initial conditions for the accident. Therefore, the survivability of RCIC is not addressed.

In-vessel recovery sequences occur when ECCS fails initially and a source of vessel injection is subsequently recovered or activated prior to vessel failure. Since the mean time to recovery for ECCS is approximately 19 hours and core cooling must be recovered within approximately 1 hour of the initiation of the accident, the in-vessel recovery sequences are dominated by cases in which the reactor is blown down and the firewater addition system is used to provide core cooling. In the long term, the RHR system must also be recovered to provide containment heat removal. Therefore, only these systems are considered for equipment survivability.

The instrumentation considered for equipment survivability for severe accidents was derived from the 10CFR50.34(f) instrumentation list developed in Subsection 19E.2.1.2.3.2.1. This ensures that all instrumentation considered in the severe accident analysis is accounted for, since all operator actions for severe accidents have been included in the Emergency Procedure Guidelines. The list contains more instruments than are actually considered in the severe accident analysis. For example, no actions in the PRA or severe accident analysis are based on the wetwell pressure. As in the case of 10CFR50.34(f) instrumentation, the neutron monitoring function is not required to survive the event for either in-vessel or ex-vessel accidents.

For ex-vessel accidents, it is not necessary for the SRVs or the in-vessel instrumentation to survive past the time of vessel failure. Thus, although very high temperatures persist in the vessel for the duration of an ex-vessel accident, the depressurization function, RPV water level instrumentation and RPV pressure instrumentation must only survive approximately one hour after core uncovery.

19E.2.1.2.3.3 Equipment Required For Accident Mitigation

For each required system identified in Table 19E.2-29, the components of the system which are located inside the containment are identified in the discussion which follows. Components which are located outside of containment and are not exposed to containment process fluid, are excluded from the discussion since neither the 10CFR 50.34(f) event nor a severe accident will cause significant changes outside of the containment itself. The basis for equipment survivability is also provided for each piece of critical equipment.

Stainless steel components such as piping, spargers and quenchers will not be threatened by the conditions in the containment. Therefore no further consideration of those components will be given in this discussion.

The valve actuation cabling within the primary containment is composed of concentric-lay coated copper. All of the cabling inside containment is housed in insulation which is a flame retardant cross-linked polyethylene. Additionally, the insulated cable is housed within a thermoplastic chlorinated polyethylene (Hypalon) jacket which provides protection from severe radiation environments. Analysis performed by ORNL (Reference 19E.2-33) shows that the insulation and jacket begins to lose its chemical composition at 673 K (752°F). Finally, eighty percent of the actuation cabling located inside containment is enclosed within metal conduit which further shields the cabling from severe environments. Therefore survival of the cabling for the environments considered is not a concern.

(1) Depressurization System

During a core damage event, the SRVs must be able to remain open during the in-vessel phase of the accident to ensure that any potential vessel failure occurs at low pressure. After vessel failure, SRV operability is not required.

Inside of the primary containment the depressurization system consists of the following equipment and instrumentation:

(a) Nitrogen supply

(b) Nitrogen supply line

(c) Valve actuation cabling

(d) Piping and quenchers

(e) Safety relief valves

(f) SRV solenoid

(g) Temperature and position monitoring instrumentation

For the 10CFR50.34(f) and core melt scenarios with in-vessel recovery, the safety relief valves must survive or fail in the open position for the duration of the event. For the ex-vessel cases, the safety-relief valves must survive only until the vessel fails. Vessel temperature, pressure, and radiation profiles for the ex-vessel cases fall below those for the in-vessel cases. Hence, the in-vessel cases provide an upper bound for this analysis.

The SRVs are held open with a nitrogen actuator. The nitrogen supply is located outside of containment. As discussed in Subsection 19E.2.1.2.2, the nitrogen supply will be adequate to assure SRV operability over a full range of hypothetical accidents.

The nitrogen supply line consists of piping, valves, and condensation tanks, none of which will be threatened by the containment environment. The survivability of the piping and condensation tanks is discussed above. The valves are rated to a pressure

and temperature of 1.8 MPa and 444 K, respectively. The 10CFR50.34(f) and in-vessel scenarios drywell thermodynamic loads do not exceed these conditions. The ex-vessel scenario drywell loads do not exceed these conditions prior to vessel failure, after which equipment required for vessel depressurization is no longer needed. Additionally, the integrity of the valve actuation cabling, system piping, and quenchers within the containment will not be adversely affected during the accident as discussed above.

The vessel pressure does not pose a problem because it remains within design limits. Comparison to radiation qualification limits are based on two day integrated dose rates. The equipment integrated radiation doses are below the equipment qualification integrated dose rates of 2.0E+8 R and 2.0E+9 R for gamma and beta radiation, respectively, as set forth in Table 3I-16.

During the early part of the event, the temperature of the process gas exceeds the SRV design limit. This will not pose a problem for several reasons. First, organic material is only located in the solenoids, which are far enough removed from the process fluid that overheating from that source should not occur. The remainder of the valve is steel. Any deformation that might occur tends to stretch the valves outward due to internal pressure. This deformation does not restrict the valve from relieving pressure. Valve closure is not required. Therefore, valve failure in the open position is acceptable. Finally, the SRV pressure relief capacity is substantially oversized for this event. Thus, vessel depressurization requires the opening of only one valve. Deformation of all 18 SRVs in a manner which would prevent vessel depressurization is not credible.

For the 10CFR50.34(f) and in-vessel scenarios, the drywell temperature and pressure never exceed the SRV design limits. For the ex-vessel scenario, the drywell temperature and pressure remain below the design limits until the vessel depressurizes. These conditions do not pose a problem for SRV survivability.

SRV temperature and position monitoring instrumentation used during depressurization are not needed for accident mitigation. Therefore, their survival is not discussed here.

(2) Residual Heat Removal System (RHR)

In modelling the 100% metal-water reaction scenario (10CFR50.34(f)), the RHR removes heat from containment through drywell and wetwell sprays. This decreases the wetwell airspace pressure enough to avoid COPS activation, eliminating the potential for containment breach. Inside of the primary containment the RHR system consists of piping, spargers, motor-operated valves (MOVs), and check valves. The integrity of the system piping and valve actuation cabling within the containment will not be adversely affected during the accident as discussed above. The valves are rated

for 8.6 MPa and 575 K. Drywell loads do not exceed these conditions for any of the event categories analyzed here. Additionally, heat transfer in the long pipe runs allows the process fluid to remain within survivability limits.

Table 6.3-9 contains pressure and temperature design parameters for the RHR system components.

For the in-vessel core melt scenarios, the LPFL mode of the RHR system may provide low pressure in-vessel core injection which eventually quenches the molten core. Core injection in the core flooder mode utilizes piping from the suppression pool, an RHR heat exchanger, and an injection valve. None of these components are located inside the vessel. The heat exchanger is located outside of primary containment. The injection valve sees maximum ambient drywell conditions of 400 K and 0.7 MPa. This maximum drywell temperature is below the thermal qualification limit of 455 K. Furthermore, the maximum drywell pressure exceeds neither the pump suction piping design pressure of 2.8 MPa, nor the pump discharge piping design pressure of 3.4 MPa.

The RHR system is needed to remove decay heat from the containment during an ex-vessel transient to avoid COPS activation, as is the case in three of the six ex-vessel events identified. As with the 10CFR50.34(f) scenario, the RHR functions in the containment cooling mode which may involve drywell sprays. The drywell spray mode consists of piping, spargers, valves and valve actuation cabling. As above, only the sparger and piping are located inside of the containment, therefore survivability is not threatened. The pressure in the suppression pool exceeds the system qualification pressure of 0.31 MPa. However, the piping is nominally capable of withstanding pressures approximately 2.5 times that based on an implied safety factor (Appendix 3M). The suppression pool temperature slightly exceeds the system qualification temperature of 377 K but this is not a concern because the RHR system component discussed here do not contain organic material.

The process fluids that are used in the RHR system come from either the suppression pool or the RPV. The suppression pool is limited to a maximum pressure of 0.72 MPa by the COPS system. Furthermore, the suppression pool temperature never rises above 430 K, a temperature reached during some ex-vessel accident scenarios. The RHR suction and discharge piping used for suppression pool cooling are rated to a pressure of 0.31 MPa and a temperature of 377 K. As discussed above, however, the piping is nominally capable of withstanding pressures up to 2.5 times the rated pressure. The high suppression pool water temperature does not pose a problem for RHR system components because they contain no organic material. In the shutdown cooling mode, the RHR loop isolates from the RPV at 0.9 MPa. In the low pressure core injection mode, the RHR loop isolates from the RPV at 3.0 MPa. In-board of the isolation valves all components are rated to a pressure of 8.6MPa and a temperature

of 575 K. Because of these ratings, severe vessel conditions do not threaten RHR survivability. Since the reactor pressure will not increase after RHR activation, overpressurization will not occur.

(3) Firewater System

The firewater system may be called upon to inject water into the vessel for a severe accident with in-vessel recovery or for the 10CFR50.34(f) event or through the drywell sprays during a severe accident which progresses ex-vessel. The system is manually initiated. All flow in the system is from outside the containment. Thus, accumulation of radioactive material in the firewater pumping system will not occur. All components of the firewater system are outside of the containment and will not be significantly affected during a severe accident. Inside the containment, the firewater system utilizes RHR valves, piping and spray headers which were discussed in (2).

(4) Passive Flooder

The passive flooder may be needed to provide a water flow path from the suppression pool to the lower drywell after vessel failure. The flow path is opened as a direct result of high temperatures in the lower drywell which occur after debris relocation from the vessel. This system does not contain any active systems, instrumentation or controls. Additionally, the system components are not hindered from performing their functions due to high radiation levels which might exist in the lower drywell after debris relocation from the vessel. Therefore, the system is expected to operate under the required conditions.

(5) Containment Overpressure Protection System (COPS)

The COPS may be needed during a severe accident to relieve high containment pressure. No credit is taken for the COPS system for the 100% metal-water reactor event. The system contains piping, a rupture disk and two valves which are normally open and fail open. To relieve containment pressure, the rupture disk must burst. Activation will not be adversely affected by the radiation in the wetwell airspace during a severe accident. The sensitivity of rupture disk activation to wetwell temperature is discussed in Subsection 19E.2.8.1.2.

(6) Vacuum Breakers

The vacuum breakers may need to open during an accident to relieve high differential pressures between the wetwell and drywell. Vacuum breakers are passive in nature and have no instrumentation or control other than position indication, which is not essential for operations. The vacuum breakers are located on stub tubes high in the wetwell, a location which subjects them to the temperature loads in the wetwell airspace. During the three scenarios considered here, the differential pressures between the wetwell and the drywell do not exceed the design basis. The gas

temperature in the wetwell exceeds the equipment qualification limit of 377 K by approximately 60 K. The valves are composed of steel and organic seals. There is no concern that the temperature in this area will degrade the capabilities of the steel. Tests at Sandia (Reference 19E.2-32) have shown that organic materials are capable of withstanding temperatures exceeding 600 K. The seats for these valves will be selected to survive the temperatures of the accident environment. Per Subsection 6.2.1.1.4.1, the COL applicant will be responsible for ensuring that the vacuum breakers are shielded from pool swell loads. Finally, there is no direct means for debris to reach the vacuum breakers. Therefore, they are not expected to be adversely affected during any of the accidents considered.

(7) RIP Vertical Restraints

The vertical restraints on the RIPs prevent the pumps from being ejected if the RIP attachment welds are destroyed during a core melt event. The restraints are attached to the outer vessel surface and do not experience the severe conditions within the vessel during core melting. Therefore, the integrity of the vertical restraints is not jeopardized during the in-vessel phase of the accident. Since the restraints are metallic the containment conditions will not lead to failure if vessel failure occurs.

(8) Containment Isolation Valves

The containment isolation valves will close very early in the event when all of the parameters are well within the design basis values. The valves will remain closed for the duration of the event. All of the valves attached to the primary system are rated to a pressure of 8.6 MPa. Therefore they will not be threatened by a severe pressure environment during an accident. The remaining containment isolation valves are rated to pressures above the COPS pressure limit of 0.72 MPa. Thus, they will not be threatened by the pressure environment.

The air supply to the air actuated valves automatically closes on a containment isolation signal. Therefore, the valve can not activate and reopen, even if the elastomers in the solenoid fail due to high temperature. Power for motor-operated valves (MOVs) is controlled outside of containment. During a severe accident, the power is shut off, preventing the possibility of MOV self-actuation due to shorting in a high temperature drywell environment. In addition, MOVs are self-locking, indicating they will not relax and allow leakage during the course of the accidents considered here. Since metal seats are specified for the check valves, a severe accident environment will not degrade the valve seats.

(9) Containment Structure

Extensive work has been done to demonstrate containment survivability. The reactor pedestal is considered to have a very high probability of survival as discussed in

Attachment 19EC. All three scenarios considered here have a very high probability of containment integrity as discussed in Appendix 19F.

(10) Containment Penetrations

The containment penetrations consist of mechanical and electrical fixed penetrations as well as operable penetrations. The survivability of these penetrations is discussed in Subsection 19F.3.2.2. The fixed mechanical penetrations are constructed from steel and will not be affected by the conditions in the drywell. The fixed electrical penetrations contain organic seals that can be affected by high temperatures. However, tests at Sandia National Lab (Reference 19E.2-32) have shown that the penetrations maintain their integrity to a temperature of 644 K and 1.025 MPaG. This pressure is beyond the COPS activation pressure and the temperatures in the drywell do not exceed 644 K. Therefore the electrical penetrations will maintain their leak tightness for the bounding severe accident conditions.

The operable penetrations consist of two types, pressure-seating and pressure-unseating. The operable penetration seals may degrade if the drywell temperatures exceed 533 K. However, the pressure-unseating operable penetrations remain in metal to metal contact up to a pressure of 0.46 MPa. Therefore, any leakage will be within design limits for pressures at or below 0.46 MPa, even if the seal temperature limit has been exceeded. Since the remaining operable penetrations are pressure-seating they will have only a fraction of the leakage of the pressure-unseating penetrations as discussed in Subsection 19F.3.2.2. The bounding profiles show that the operable penetration temperature limit of 533 K is only exceeded for high pressure ex-vessel recovery scenarios as shown in Figure 19E.2-28d. For these scenarios the containment pressure does not exceed 0.46 MPa after the temperature limit has been exceeded, as evidenced in 19E.2-28a. Therefore, containment leaktightness will not be degraded.

The radiation loads on the penetrations are below the TID-14844 limits so radiation is not a concern.

(11) Not Used

(12) Pressure and Water Level Instrumentation

The pressure sensors used to measure both water level and pressure in the vessel and in the containment are located outside of containment. The conditions in the vessel and containment are monitored via pressure taps. The pressure sensors will not see the higher vessel or primary containment temperature and radiation doses due to the significant length-to-diameter ratio of the piping used in these sensors. The integrated radiation gamma dose for the pressure sensors is slightly over the equipment qualification limit set forth in Table 3I-16. However, the radiation limits set for

design basis events are extremely conservative. Therefore, there is reasonable assurance that the sensors will survive this condition. Furthermore, the sensors are capable of withstanding very high overpressure events, on the order of 14 MPa, indicating that there is no possibility of damage from high containment pressures.

(13) Temperature Instrumentation

The standard practice is to use thermocouples rated to 575 K and 14 MPa. These ratings are well above the drywell and wetwell thermodynamic loads experienced during a postulated severe accident. Therefore, operation of the thermocouples should not be adversely affected. Comparison to radiation qualification limits are based on two day integrated dose rates. The equipment integrated radiation doses are below the equipment qualification dose rates of 2.0E+8 R and 2.0E+9 R for gamma and beta radiation, respectively, as set forth in Table 3I-16.

(14) Containment Atmospheric Monitoring System (CAMS)

The CAMS monitors hydrogen concentration, oxygen concentration and radiation level in both the drywell and wetwell. The hydrogen and oxygen concentration sensors are located outside of primary containment. The sensors monitor containment gas concentrations via taps located within the containment. Therefore, the condition of the sampled process steam provides the only significant impact on this system. Because long pipe runs connect the primary containment to the sensing devices, heat transfer between the process steam and the pipe walls will prevent degradation of the sensors due to severe thermal conditions. The pressure in the sensed gas will be approximately that of the primary containment. The sensors will be selected to survive these pressures. Finally, the sensors are subjected to a radiation environment provided by the process fluid. However, the integrated dose will be below the design basis values.

The wetwell radiation sensors are not exposed to the temperature and pressure environment of the primary containment. The sensors are located in shafts embedded in the primary containment wall and are isolated from the primary containment environment by a substantial amount of concrete. Both wetwell and drywell radiation sensors are qualified to 595 K and 0.65 MPa. Therefore, there will be no threat to the performance of the wetwell radiation sensor.

The radiation sensors for the drywell are located inside the drywell. Therefore they will be exposed to the drywell environment. The qualification temperature of 595 K is not exceeded in the drywell. The COPS limits the drywell pressure to 0.72 MPa. This is only slightly over the qualification pressure and should not damage the sensors. Therefore the sensors are expected to survive. Also, the wetwell sensors can be used as a backup to the drywell sensors in the unlikely event that the drywell sensors are degraded.

19E.2.1.2.3.4 Summary

Three categories of events — 10CFR50.34(f), in-vessel core melt scenarios, and ex-vessel core melt scenarios — were analyzed to determine equipment and instrumentation required to survive the accident environments resulting from these events. Table 19E.2-29 contains a list of the required equipment and instrumentation for each category. The bounding environments are shown in Figures 19E.2-26a through 19E.2-26e, 19E.2-27a through 19E.2-27f, 19E.2-28a through 19E.2-28f, and 19E.2-29a through 19E.2-29f. The equipment and instrumentation has been shown to survive these environments.

19E.2.1.3 Phenomenological Assumptions

This subsection contains a summary of those phenomena which are not considered in an integral fashion using MAAP. These phenomena fall into two categories: those which are ruled out as being incredible for the ABWR and others which are neglected because they produce an insignificant change to the overall performance of the ABWR under severe accident conditions. A more detailed explanation of some of these phenomena is given in Subsection 19E.2.3.

19E.2.1.3.1 Steam Explosions

Large scale steam explosions are deemed incredible. The geometry of the ABWR will prevent a sufficiently large contiguous mass of corium from falling into water in either the vessel or lower drywell regions. A more detailed description of this phenomenon as well as the justification for its neglect is provided in Subsection 19E.2.3.1. Small steam explosions which do not in themselves threaten the integrity of the vessel or containment are calculated by MAAP. Additionally, a scoping calculation is performed in Subsection 19E.2.6.7 to determine the mass of core material which could participate in a steam explosion without damaging the containment.

19E.2.1.3.2 Degree of Metal-Water Reaction

The metal-water reaction rate used in the integrated analysis is that calculated by the MAAP models. One limit on the generation of hydrogen occurs when all of the zirconium in the cladding is assumed to react with steam to form zirconium oxide and hydrogen gas. The separate effects calculation in Subsection 19E.2.3.2 shows that the containment is capable of withstanding the static pressure that would be generated were this maximum hydrogen production to occur, as required by 10 CFR 50.34(f).

19E.2.1.3.3 Suppression Pool Bypass Due to Additional Failures

This assumption covers one of the potential types of suppression pool bypass. Subsection 19E.2.3.3 shows that the total increased risk due to suppression pool bypass caused by additional failures is within the uncertainty of the PRA ,with the exception of failure of a wetwell/drywell vacuum breaker. Therefore, only the failure of a wetwell/drywell vacuum breaker needs to be considered explicitly. A sensitivity study was performed in Subsection 19E.2.6.11 to examine the impact of vacuum breaker leakage and failure on fission

product release. Subsection 19E.2.7.3 presents an uncertainty analysis which determines the impact of bypass on risk.

19E.2.1.3.4 Effect of RHR Heat Exchanger Failure in a Seismic Event

During a seismic event it is possible for the RHR heat exchangers to fail by shear of their anchor bolts. This could potentially lead to drainage of the suppression pool if the RHR suction lines are not isolated. Calculations were performed which show that the operator has about half an hour to isolate the heat exchanger.

If the heat exchanger is not isolated then the RHR pump rooms will be subjected to additional loading caused by the static head of the water, and potentially by chugging loads as steam discharges from the broken pipe. It is seen that the RHR pump room integrity will not be breached by these loads.

Additional details about the pool drainage and structural loading may be found in Subsection 19E.2.3.4. The impact of suppression pool drainage on fission product release, should this event occur is found in Subsection 19E.2.4.5.

19E.2.1.3.5 Radiative Heating of the Equipment Tunnel

A potential concern for the ABWR during severe accidents is radiative heating of the equipment tunnel. After vessel failure, the corium in the lower drywell could radiate energy directly to the walls of the equipment tunnel. This could potentially reduce the structural material strength, eventually resulting in the tunnel buckling under its own weight.

The adoption of the passive flooder (Subsection 9.5.12) precludes this occurrence since the flooder opens when the temperature of the lower drywell airspace reaches 533 K (500°F). Upon opening, water from the suppression pool would flood the lower drywell, covering the corium. This stops any radiative heat transfer from the corium to the tunnel walls. Therefore, no significant material strength reduction of the equipment tunnel caused by increased temperature is possible.

19E.2.1.3.6 Basemat Penetration

Basemat penetration by the core debris will not lead to containment failure. In each of the sequences considered, the debris will be quenched and cooled before basemat penetration can occur. The passive flooder opens when the lower drywell temperature reaches 533 K (500°F). Even were this to fail, when the sideways penetration of the pedestal walls reach 24 mm (8 inches), water from the suppression pool would flood the lower drywell.

The lower drywell design meets the 0.02 square meters/MWt specification of the EPRI Debris Coolability Requirements for Advanced Light Water Reactors (Reference 19E.2-2). A conservative analysis was performed following the methods of the ARSAP Debris Coolability Requirement (Reference 19E.2-3) and utilizing the concrete ablation rate from CORCON

(Reference 19E.2-4). Assuming a 10-hour delay in adding water to the drywell, this resulted in an ablation depth of 0.9 m (3 ft) before the corium is completely quenched and cooled by the water from the suppression pool.

Additionally, uncertainty analysis was performed in Subsection 19E.2.7.2 to assess the potential for continued core-concrete attack. The study concluded that debris cooling is highly probable for the ABWR design and that there is little impact of contained core-concrete interaction on containment performance.

19E.2.1.3.7 Hydrogen Burning and Explosions

The ABWR containment is inerted. Hydrogen burning and explosions are not possible in an inerted containment. An explicit consideration of the short periods of time when the containment is not inerted is not necessary as discussed in Subsection 19D.5.6.4.

19E.2.1.3.8 Mode of Vessel Failure

In the unlikely event of a core melt sequence with substantial relocation of debris which leads to vessel failure, the vessel failure location is expected to be in the bottom head. A failure of the RIPs has been proposed; however, as discussed below, this is not a credible mechanism for the ABWR. Figure 5.4-2 gives a pictoral description of the location of the RIPs in the RPV. Figure 5.4-1 shows more RIP detail.

Since the core melt progression is expected to contain the corium inside the core shroud, debris would not approach the RIP impellers or RPV RIP nozzles which are located outside the shroud. However, if the shroud is perforated by the corium, the corium might then enter the top of RIP impellers and possibly enter the stretch tube/shaft annulus. This is extremely unlikely since this annulus thickness decreases in the downward direction to 1.5mm (the variance between the 215mm diameter RIP shaft and the 218mm inside diameter of the stationary stretch tube). Any molten material relocating through the RIP would quickly freeze or flow through the pump rather than flowing along the pump shaft.

In the event the corium did flow down the stretch tube/shaft annulus, the motor housing to RPV nozzle weld might fail allowing the RIP/motor to drop. Figure 1.2-3b shows the two RIP vertical restraints which connect the bottom of each RIP motor housing to the RPV bottom head. These restraints prevent the RIP/motor from dropping out of the RPV in case the motor housing weld fails for any reason. Therefore, in the exceedingly unlikely event of RIP failure, the pump will not fall from the vessel, and the penetration through the vessel would be small.

Nevertheless, the corium is expected to freeze and, consequently, not flow down the annulus into the motor housing. Therefore, the RPV RIP nozzle motor housing reactor coolant pressure boundary would not be breached. Failure of the vessel in the lower head region is the expected mechanism for the release of core debris from the vessel.

19E.2.1.3.9 Impact of Suppression Pool Flashing

In the event of Containment Overpressure Protection System (COPS) operation, the wetwell will depressurize fairly quickly. This in turn could cause flashing in the wetwell. The impact of flashing on the pool level was evaluated, and it was determined that the pool would not rise to the elevation of the COPS penetration. The potential for entrainment of contaminated water was also evaluated. It was found that entrainment would not lead to increased offsite risk. The details of this analysis may be found in Subsection 19E.2.3.5.

19E.2.1.4 Definition of Base Case Assumptions

In the context of this study the phrase "base case" is used to describe those studies which determine the nominal response of the ABWR to severe accident conditions using best estimate phenomenological models and no credit for system recovery. Several accident sequences were considered using the base case assumptions. The effects of the base case assumptions on the results of the analysis are determined by means of sensitivity studies and uncertainty analyses as necessary.

19E.2.1.4.1 Core Melt Progression and Hydrogen Generation

Critical to the melt progression of the fuel is the question of blockage in the core. In the base cases it was assumed that blockage occurs as predicted by MAAP-ABWR using the default core melt progression input parameters. This decreases the generation of hydrogen in the core, since there will not be steam flow past the hot zirconium during the later stages of the melt process.

The effect of this assumption on the overall response of the plant is determined by turning off the core blockage model in MAAP. This is done with the sensitivity study in Subsection 19E.2.6.1. For this case steam continues flowing past the fuel rods as they melt. The production of hydrogen continues until there is no more water available for reaction. This leads to a somewhat higher partial pressure of hydrogen, and higher containment pressure.

19E.2.1.4.2 In-Vessel Recovery

For sequences in which there is no core cooling available at the onset of the accident it may be possible to recover core cooling at some later time. It is important to know the time which allows for in-vessel recovery in order to determine the probability of system recovery in the containment event trees, Subsection 19D.5.11.3.3. Recovery is of particular interest for the study of Loss of Offsite Power and Station Blackout sequences.

The base sequences do not model in-vessel recovery. This possibility is considered using a sensitivity study. The MAAP code calculates in-vessel recovery only if a core cooling injection source is recovered before channel blockage occurs. However, the effects of in-vessel recovery can be simulated by the use of a wetwell failure as discussed in Subsection 19E.2.4.2.

19E.2.1.4.3 System Recovery After Vessel Failure and Normal Containment Leakage

All of the base analyses assume that any failed system will remain inoperable throughout the duration of the accident. However, in order to determine the appropriate accident management strategy, it is necessary to understand the behavior of the system if a system were to recover. The recovery of any ECC system would be like the use of the firewater system. Only the recovery of the RHR system will prevent containment overpressurization. If the containment pressure is maintained below the rupture disk setpoint, the only fission product release mechanism is normal containment leakage. This mechanism is discussed in Subsection 19E.2.4.3.

19E.2.1.4.4 Early Drywell Head Failure

One type of loss of containment structural integrity in the containment event trees is early drywell head failure following a high pressure melt sequence. The consequences associated with this event are discussed in Subsection 19E.2.4.4.

19E.2.1.4.5 Consequences of Suppression Pool Drain

In a seismic event, a mode of RHR heat exchanger failure was identified which could potentially result in the draining of the suppression pool into the RHR pump rooms. An analysis was performed to examine the impact of this on pump room integrity (Subsection 19E.2.3.4) which showed that the room would remain intact.

Therefore, the suppression pool may be viewed as having moved into the pump rooms. The pump room will have no ability to withstand the increase in pressure due to decay heat. Rather the room will leak and the pressure will remain near atmospheric pressure. Thus, there will be no holdup of noble gasses. However, since all of the fission products will pass through the pool in the pump room, significant fission product scrubbing of the volatile fission products will occur. Subsection 19E.2.4.5 examines the resulting dose from this type of sequence.

19E.2.1.5 Resolution of Phenomenological Uncertainties

The ABWR is designed to limit the sensitivity to various phenomenological uncertainties. Nevertheless, an uncertainty study was performed. Severe accident phenomenological uncertainties were addressed in an engineering sense. This means that only those parameters that have a major impact on the timing and magnitude of fission product release from the containment were investigated in detail. Each parameter was considered individually, although interactions between some key phenomena were considered.

The uncertainty analysis is a four step process. The first step is a literature survey which identifies all severe accident issues. Second, these issues are screened for their applicability to the ABWR. These two steps are combined in this study. Next sensitivity studies have been performed over a credible range of key parameter values to determine the potential for a significant impact on fission product release and timing. If such impact is demonstrated, then

the issue is carried forward into the final step, a detailed uncertainty analysis. The propagation of uncertainty distributions was not carried out as done in NUREG-1150 (Reference 19E.2-19).

19E.2.1.5.1 Identification and Screening of Phenomenological Issues

The first step in performing an uncertainty analysis is to identify the key phenomena and their associated uncertainties. To do this, the available literature was surveyed as discussed in Subsection 19E.2.5. Some of the severe accident issues were screened out, as they are not applicable to the ABWR design. For example, hydrogen combustion phenomena are not important in the ABWR since the containment is inerted. Issues identified which could have impact on the severe accident performance were included in the sensitivity studies which follow.

19E.2.1.5.2 Sensitivity Studies

Sensitivity studies were performed for the ABWR response to severe accident phenomena in order to determine those issues which may have significant impact on the offsite risk associated with the ABWR design. Given this goal, the ultimate measurement of sensitivity is the offsite dose. At a given site the primary factors which influence the dose are the magnitude and time of release. Therefore, changes in these parameters were used to determine the need for detailed uncertainty analyses.

19E.2.1.5.2.1 Core Melt Progression and Hydrogen Generation

Critical to the melt progression of the fuel is the question of blockage in the core. In the base cases it was assumed that blockage occurs as predicted by MAAP-ABWR using the default core melt progression input parameters. This decreases the generation of hydrogen in the core, since there will not be steam flow past the hot zirconium during the later stages of the melt process.

The effect of this assumption on the overall response of the plant is determined by turning off the core blockage model in MAAP-ABWR. This is done with the sensitivity study in Subsection 19E.2.6.1. For this case steam continues flowing past the fuel rods as they melt. The production of hydrogen continues until there is no more water available for reaction. This leads to a somewhat higher partial pressure of hydrogen, and higher containment pressure. There is virtually no impact on source term, and the time of fission product release is not substantially altered. Therefore, it is judged that the ABWR severe accident performance is not sensitive to in-vessel hydrogen production.

19E.2.1.5.2.2 Fission Product Release from the Core

The base sequences use the Cubicciotti model for fission product release from the fuel. If the release from the fuel occurs at a different rate, any potential release from the containment could be affected through the containment residence time and suppression pool scrubbing. The effect of the release rate on source term is examined in Subsection 19E.2.6.2. The study indicates that there are modest differences in the location of the fission products within the containment. However, because of the depth and subcooling of the suppression pool and the presence of the

COPS, there is no appreciable variation in the release from the containment. Therefore, no further investigation of the impact of fission product release from the fuel is required.

19E.2.1.5.2.3 CsI Revaporization

An important aspect of fission product behavior is the propensity of the aerosols to adhere to the relatively cooler surfaces of the vessel and containment. While the deposition process is fairly well understood, there is considerable uncertainty in the revaporization of the fission products, particularly that of CsI. A sensitivity study was conducted, as reported in Subsection 19E.2.6.3, to examine the impact of delayed revaporization. A variation of fission product behavior inside the containment was observable. However, there is not a substantial difference in the release fraction from the containment. Therefore, no further consideration of CsI revaporization is needed.

19E.2.1.5.2.4 Time of Vessel Failure

The detailed melt progression of a severe accident is subject to considerable uncertainty. The melt progression assumed in MAAP retains the molten core material above the core plate until a local failure of the core plate occurs which results in a large pour of core debris into the lower plenum of the vessel. As a result of this model, the lower head of the vessel fails almost immediately, even though there is water in the lower plenum at the time. In other melt progression models, the molten fuel drips down the fuel rods in a process called candling. Under this assumption, it is possible for molten corium to be relocated in the lower plenum slowly, where it is quenched. This results in a delayed vessel failure after the water in the lower plenum has boiled off.

A sensitivity study was performed in Subsection 19E.2.6.4 to determine the impact of the time and mode of vessel failure on containment performance. It was observed that there is little impact on the base scenarios. However, it was noted that the mode of vessel failure could impact other phenomena such as direct containment heating and core concrete interaction. Discussion of these relationships may be found in Subsections 19E.2.7.1 and 19E.2.7.2, respectively.

19E.2.1.5.2.5 Recriticality During In-Vessel Recovery

A potential challenge to the containment has been identified for accidents in which the core melt is arrested in the vessel. Experiments have indicated the potential for the boron carbide in the control blades to form a eutectic with steel at 1500 K and relocate before the fuel relocates. Thus, if core cooling is recovered after the control material has relocated, there is a potential for the core to return to a critical condition. A sensitivity study was performed in Subsection 19E.2.6.5 to examine the potential for recriticality and the implications of its occurrence for the ABWR design. The study concluded that there was a very short time window during which a return to criticality was possible. Further, even if it should occur, recriticality is not likely to lead to containment failure. Thus, recriticality does not pose a significant threat to the ABWR design and need not be considered in an uncertainty analysis.

19E.2.1.5.2.6 Debris Entrainment and Direct Containment Heating

If a core melt accident occurs in which the reactor pressure vessel is at high pressure at the time of vessel failure, the debris may be entrained out of the lower drywell. If the debris is finely fragmented as it is dispersed, the pressure in the containment can rise rapidly. This process is known as direct containment heating. If the magnitude of the pressure rise is high enough, the containment may be challenged. This would lead to an early failure of the containment structure and large releases of fission products. Therefore, uncertainty analysis was performed. The conclusions of this study are given in Subsection 19E.2.1.5.3.1.

19E.2.1.5.2.7 Fuel Coolant Interactions

Containment challenges from fuel coolant interactions may occur when molten debris reacts rapidly, perhaps explosively, with water. Fuel coolant interactions are most likely to challenge the containment when molten debris falls into water. Examination of the containment event trees indicates that only a very small fraction of all sequences have water in the lower drywell before vessel failure. Despite this low probability, scoping studies were conducted considering both the impulse and static loads. As discussed in Subsection 19E.2.6.7, the shock wave transmitted to the structure provides the limiting loads. Using conservative estimates for the impulse load capability of the pedestal, the structure can withstand the loads associated with a steam explosion involving 9.5% of the core mass. This is three times the mass of a credible fuel coolant interaction in the ABWR. Therefore, the ABWR is very resistant to fuel coolant interactions. This failure mechanism need not be considered further in the containment event trees or the uncertainty analysis.

19E.2.1.5.2.8 Core Concrete Interaction and Debris Coolability

The issue of debris coolability has long been an area of considerable uncertainty in the progression of a core melt accident. If core concrete attack continues, the timing and magnitude of potential fission product release can be affected: the pedestal could be eroded which could threaten containment structure, non-condensable gasses could pressurize the containment leading to early rupture disk opening, and additional fission products could be released from the molten core. The ABWR design has a large drywell floor area and redundant systems which can flood the lower drywell. However, experiments performed to date have been unable to provide conclusive evidence that these features cool the debris sufficiently to prevent core concrete interaction. Therefore, uncertainty analysis was performed as discussed in Subsection 19E.2.1.5.3.2.

19E.2.1.5.2.9 Fission Product Release Location

The adoption of the containment overpressure protection system (COPS) in the ABWR containment design serves to significantly reduce the uncertainties in the timing, location and area of any fission product release. The setpoint of the rupture disk was selected such that there is a small probability of containment failure before the rupture disk opens. The probabilities for containment failure depend on the accident progression. They were calculated as described in

Subsection 19E.2.8.1.1. These values were used, along with the appropriate source terms, in the containment event trees.

19E.2.1.5.2.10 Fission Product Release Flow Area

The presence of the COPS serves to substantially reduce the uncertainties associated with the flow area for the release of fission products from the containment. The limiting flow area was chosen such that any slight variation would not affect the ability of the system to relieve the containment pressure. However, if the drywell head fails before the COPS opens, there is a great deal of uncertainty in the size of the opening. A sensitivity study was performed, as reported in Subsection 19E.2.6.10, which concluded that there is a small impact on the fission product release. In addition, only a small fraction of all releases occur as a results of drywell head failure. Therefore, no further consideration of containment failure area is necessary.

19E.2.1.5.2.11 Suppression Pool Bypass

The suppression pool bypass study of Subsection 19E.2.3.3 was not able to show conclusively that a stuck open vacuum breaker would not lead to an increase in risk. Subsection 19E.2.6.11 considers the potential impact on fission product release of a fully or partially stuck open vacuum breaker. The study concludes that there may be a substantial increase in offsite dose if a vacuum breaker sticks open. Therefore, this issue is examined using a detailed uncertainty analysis. The results of this examination are summarized in Subsection 19E.2.1.5.3.3.

19E.2.1.5.2.12 High Temperature Failure of the Drywell

One of the failure modes identified for the containment was the degradation of the seals for the moveable penetrations in the drywell due to high temperature. In the base analyses discussed in Subsection 19E.2.2, the only sequences which exceeded the threshold temperature of 533 K (500°F) were those in which debris was entrained into the upper drywell and sprays were not available. Sensitivity studies were performed, as reported in Subsection 19E.2.6.12, to determine the potential for other sequences to exceed the threshold temperature which could lead to early fission product release. The largest increase in drywell temperature was only 5 K, which left ample margin to a high temperature failure. Therefore, no further study of this area is necessary.

19E.2.1.5.2.13 Suppression Pool Decontamination Factor

The pressure suppression pool is a very effective means of removing fission products from the gas space in a severe accident. The efficiency of the scrubbing process is typically characterized in terms of a decontamination factor (DF) defined by the mass of debris which enters the pool divided by the mass of debris which leaves the pool. MAAP-ABWR uses correlations based on the SUPRA code to calculate the DF. In order to investigate the sensitivity of the offsite consequences of a severe accident to the suppression pool decontamination factor, a simple sensitivity study was performed as described in Subsection 19E.2.6.13. The MAAP-ABWR code was modified to allow a constant DF of 100, a very conservative value for the ABWR configuration, to be used for all species (except noble gasses, for which the DF is 1.0). This

resulted in an increase in fission product release of about four orders of magnitude. Nonetheless, there was no notable increase in offsite dose above a small conditional probability assuming COPS operation. Thus, there is not a significant impact on dose, even for a DF of 100. Thus, no further consideration of suppression pool decontamination factor is required in an uncertainty analysis.

19E.2.1.5.2.14 Suppression Pool pH

The pH of the suppression pool can affect the chemical form of iodine. This, in turn, has an impact on the release of iodine from the containment. A study was performed, as documented in Subsection 19E.2.6.14, to examine the potential for the suppression pool to become acidic. It was concluded that the pool would remain basic for longer than one day. Therefore, the iodine will remain in the pool and the fission product release will not be affected. Therefore, no further consideration of this phenomenon is required.

19E.2.1.5.3 Uncertainty Analyses

A systematic examination of severe accident challenges was performed as part of the ABWR PRA development. After screening the challenges for their applicability to the ABWR, a sensitivity study was performed to examine their potential impact on the ABWR severe accident performance. As a result of this screening, three issues were identified for more detailed examination as being potentially risk significant. The following provides a discussion of the impact of direct containment heating (DCH), pool bypass, and Core Concrete Interaction (CCI) on containment failure probability and risk profile.

19E.2.1.5.3.1 Direct Containment Heating

A large number of calculations were performed to determine the impact of DCH on the probability of containment failure and offsite risk. The analysis investigated uncertainties in a variety of areas:

- Mode of vessel failure
- Mass of molten core debris at the time of vessel failure
- Potential for high pressure melt ejection
- Fragmentation of debris in the containment

Additional sensitivity studies were performed to examine other phenomena which could affect DCH. The study concluded that a deterministic best estimate for the peak pressure from DCH would not lead to containment failure. Consideration of the uncertainties in the phenomena lead to an estimated CCFP of an extermely small fraction of all core damage events. Since the probability of containment failure due to DCH is very low, there is no measurable impact on offsite dose.

19E.2.1.5.3.2 Core-Concrete Interactions

A large number of calculations were performed as part of the investigation into core-concrete interactions in the ABWR. These calculations addressed uncertainties in the following parameters:

- Amount of core debris
- Debris-to-water heat transfer
- Amount of additional steel in the debris
- Delayed flooding of the lower drywell
- Fire water injection instead of passive flooder operation

The conclusion from all of these uncertainty calculations were:

(1) For the dominant core melt sequences that release core material into the containment, a vast majority result in no significant CCI. An insignificant number of sequences are expected to experience dry CCI.

(2) Even for those low frequency cases with significant CCI, radial erosion remains below the structural limit of the pedestal. After consideration of uncertainties a very small percentage of the sequences with significant CCI will suffer pedestal failure. Combining this conclusion with the first, an even smaller percentage of all core melt sequences with vessel failure will lead to additional drywell failures as a result of CCI.

(3) The time of fission product release is not significantly affected by continued CCI.

(4) The fission product release is dominated by the noble gasses when the containment overpressure protection system operates. This conclusion is unaffected by assumptions on debris coolability. Therefore, the offsite dose for sequences with rupture disk operation is not impacted by core concrete attack.

These conclusions would indicate that the uncertainties associated with CCI have an insignificant influence on the containment failure probability and risk.

19E.2.1.5.3.3 Pool Bypass

Analyses performed in Subsection 19E.2.3.3.3(4) indicate that the only significant mode of suppression pool bypass occurs via the vacuum breakers. Uncertainty analyses and sensitivity studies were performed to assess the effect of pool bypass on risk. Some of the key conclusions of these studies are summarized below:

(1) The probability of a large leakage path between the wetwell and drywell is very small.

(2) There is a small probability that there is a small leakage path between the drywell and wetwell. Based on the Morowitz plugging model, most of these sequences are expected to plug before the rupture disk setpoint is reached. In sequences with plugging, there is no significant increase in the time of fission product release or in offsite dose.

(3) Use of the firewater spray system can prevent early opening of the rupture disk for a bypass path of any size.

The sum of the frequency of pool bypass sequences as a result of vacuum breaker failure with no drywell spray available is an extremely small percentage of all core damage events. Since this value is extremely low there is no impact on offsite dose.

19E.2.2 Accident Sequences

The accident sequences are chosen such that both the core damage accident classes and the containment event tree classes are well represented. Using an early version of the PRA, the more probable classes of accidents were considered in selecting the accident sequences to be studied. Subsequent to the initial review, sequences were added to provide a good estimate of risk.

A complete accident sequence is designated by an eight digit character. The first four characters indicate the general conditions of the accident. The next two digits are used to identify any mitigating systems used. The seventh digit indicates the mode of release, and the eighth character indicates the magnitude of the release. A summary of the accident sequence codes is given in Table 19E.2-3.

The first consideration in selecting accident sequences for analysis was to represent the core damage event trees. To accomplish this each accident class was examined to determine the most severe sequence. The frequency of the event was then considered. If the frequency of the most severe sequence was below the cutoff frequency and if it was significantly smaller than the overall frequency of the class then the next most severe case was examined. Note that all sequences in the final PRA with extremely small probabilities were not completely dismissed. They were retained in the sum of the event class frequencies.

Eight accident sequences were selected for analysis with MAAP. Table 19E.2-4 shows how each accident class relates to the accident sequences analyzed. Each of the eight accident sequences is described below:

- LCLP

  Loss of all core cooling with vessel failure occurring at low pressure represents accident class ID and some IB-1 and IB-3 sequences.

- LCHP

  Loss of all core cooling with vessel failure occurring at high pressure models accident classes IA and IIIA as well as some IB-1 and IB-3 sequences. The results are somewhat non-conservative for some of the Class IIIA sequences because the rate of water loss from the vessel may be somewhat faster for medium break LOCAs. Small break LOCAs will be accurately modeled by this case. Even for the case of the medium break LOCA the results should be reasonably accurate, because the definition of a medium break LOCA is that which does not depressurize the vessel quickly enough to allow the low pressure systems to operate without ADS. Furthermore, the low frequency of Class IIIA events allows their consideration here.

- SBRC

  Station blackout with RCIC operating for 8 hours is class IB-2.

- LHRC

  Loss of heat removal in the containment sequences are characterized by a cooled core but the containment structure fails due to loss of containment heat removal. This sequence embodies class II.

- LBLC

  Large break LOCA with loss of all core cooling represents class IIID.

- NSCL

  Transient with no scram or core cooling; vessel fails at low pressure models class IC.

- NSCH

  Transient with no scram or core cooling; vessel fails at high pressure represents class IE.

- NSRC

  The station blackout with no scram or boron injection sequence assumes that the RCIC system is available for core cooling. The reduced flow to the core reduces the reactor power. Also modeled by this sequence are other loss of offsite power sequences where the operator manually reduces flow to the reactor in order to reduce power. This sequence portrays class IV with successful flow control.

For each accident sequence, there are a variety of mitigating systems which could be used to prevent or reduce the release of fission products to the environment. The fifth and sixth digits of the accident sequence indicator describe the mitigating features which were assumed to operate.

- 00

  This symbol is used when none of the mitigative features are operated, due to failure of the system or the operator, or the absence of the initiating condition for the system.

- IV

  There are several means by which the operator may arrest the core melt in the vessel. If any ECC system is recovered or if the firewater system started before vessel failure occurs, it may be possible to prevent vessel failure, assuring that any fission products generated are scrubbed through the suppression pool via the SRV lines. In-vessel recovery is treated as a sensitivity study in Subsection 19E.2.4.2.

- PF

  The passive flooder system is described in Subsection 9.5.12. This system automatically opens a connection between the suppression pool and the lower drywell region when the temperature of the lower drywell airspace reaches 533 K (500°F). This serves to keep the corium temperature low, preventing core-concrete interaction, and preventing radiative heat transfer from the corium to the containment structures and atmosphere.

  The passive flooder system is designed to cause the lower drywell to be flooded when there is no water overlying core debris in the lower drywell. If there is no overlying water pool the fusible material in the valve will heat up and melt the fusible plug. If there is water overlying the debris pool, the lower drywell will not heat up sufficiently to cause the passive flooder to open. Examination of the Containment Event Trees (Subsection 19D.5.11) shows that the firewater addition system is expected to operate in most of the accident sequences. Therefore, the passive flooder is not needed in the majority of accidents. Rather, the lower drywell flooder is viewed as a passive backup system which floods the lower drywell, in order to keep the temperature in the drywell low, and in order to allow quenching of the core debris.

- FA

  The firewater addition system (also referred to as the AC-independent water addition mode of the RHR System), described in Subsection 5.4.7, allows the operator to manually tie the fire protection system into the residual heat removal (RHR) injection line. If this action is performed within about 15 minutes after the water level reaches Level 1, this will prevent core damage, as described in Subsection 19.3.1.3.1. The firewater system also acts as a mitigating feature after core damage. Under these circumstances, the water from the firewater system pours through the vessel and onto the corium on the floor of the lower drywell. This stops core-concrete attack and radiative heating in the same manner as the passive flooder. In addition, the firewater system adds water to the containment increasing the thermal mass. This reduces the rate of containment pressurization and delays or

prevents significant fission product release. The operator is instructed to turn off the firewater system when the water level in the suppression pool is at the vessel bottom elevation, unless firewater is the only means available for core cooling and the vessel is still intact. Operator actions governing use of the firewater addition system is specified in the emergency procedure guidelines in Appendix 18A.

Information about the hardware connections are supplied in the description of the RHR system in Subsection 5.4.7.1.1.10. In particular, Figure 5.4-10 shows the connections from either the diesel-driven pumps or the fire truck to the RHR system. The connection to the diesel-driven pump are in the RHR valve room. Opening valves F101 and F102 allows water to flow from the fire protection system into the RHR piping. Periodic stroke testing of these valves is required by Table 3.9-8 to ensure valve operability. The fire truck connection is located outside the reactor building at grade level. Both connections to the RHR system are protected by a check valve (F100 and F104, respectively) to insure that RCS pressurization does not result in a breach of the injection path. The nominal flow rate for the firewater addition system is between 0.06 m^3/s with no containment backpressure and 0.04 m^3/s at the COPS setpoint.

- HR

  Containment heat removal is provided by the RHR system. For the base analyses the RHR system is conservatively assumed to be unavailable.

- PS

  Passive flooder and drywell spray both operate. The drywell sprays are one function of the RHR system. During severe accidents, especially those which cause vessel failure to occur at high pressure, the drywell sprays keep the upper drywell cool. This prevents degradation of penetration seals which could result in leakage through the movable penetrations and the release of fission products below the pressure capacity of the containment. The upper drywell drains into the suppression pool. Therefore, the use of the drywell sprays will not prevent the temperature in the lower drywell from increasing. Therefore, the passive flooder will open when the lower drywell becomes sufficiently hot.

- FS

  A firewater addition spray function was added to the firewater system as a backup to the RHR drywell spray. Used in spray mode the firewater system adds external water to the containment increasing the thermal mass of the system. The spray also provides cooling of the upper drywell region. The operator will operate the spray system if the temperature of the drywell rises to a level which could threaten the seals and water level in the vessel cannot be maintained. The firewater spray causes the pressure and the temperature of the upper drywell to decrease rapidly. When the water level in the suppression pool reaches the suppression pool to lower drywell vent the operator is instructed to turn the firewater

system off. If drywell head failure occurs the firewater spray system may be restarted. This causes any fission product aerosols to agglomerate on the spray droplets, reducing the fission product release to the environment. No credit is taken for this action.

There are several mechanisms whereby fission products may be released from the containment to the environment. The mode of release is designated by the seventh character in the accident sequence indicator.

- N

  Normal containment leakage does not allow significant release to the environment as discussed in Subsection 19E.2.4.3.

- P

  Leakage through movable penetrations in the drywell is assumed to occur when the gas temperature exceeds 533 K (500°F) and the pressure exceeds 0.46 MPa. Further discussion of this type of leakage is given in Appendix 19F. If containment heat removal is not recovered drywell head failure or rupture disk opening could follow the onset of leakage.

- R

  An overpressure protection relief rupture disk is described in Subsection 6.2.5.2.6 and in Subsection 19E.2.8.1.

- D

  The drywell head is assumed to fail before the rupture disk opens. The median failure pressure of the drywell head is 1.025 MPa if the temperature in the upper drywell is below 533 K (500°F). However, as discussed in Attachment 19FA, there is a small probability the drywell fails at lower pressure. At higher temperatures, the drywell head is assumed to fail at a lower pressure as described in Appendix 19F.

- E

  Early structural failure of the containment has been proposed for cases which result in the failure of the vessel at high pressure. The effect of an early containment structural failure is examined in Subsection 19E.2.4.4.

- S

  Suppression pool drainage into the RHR pump rooms may be possible following an unisolated RHR suction line break. For these cases the release will be scrubbed but the release of fission products will begin with the onset of fuel damage. These cases are considered in a sensitivity study in Subsection 19E.2.4.5.

The final character in the accident sequence designator is assigned after the sequence has been simulated with MAAP-ABWR. This eighth character indicates the magnitude of the release predicted by MAAP-ABWR. Negligible, low, medium, and high categories were established as follows according to the amount of noble gasses and volatile fission products released:

	Noble Gas	Volatiles
N	<100%	<0.1%
L	<100%	<1%
M	<100%	<10%
H	<100%	>10%

Additionally, the character 0 indicates that no core damage occurred, therefore there is no release of radioactivity.

In the following subsections each of the accident classes is considered in turn. For each general accident condition several possible mitigating actions are considered as suggested by the accident progression.

19E.2.2.1 Loss of All Core Cooling With Vessel Failure at Low Pressure (LCLP)

The initiating event selected for this sequence is a Main Steam Isolation Valve (MSIV) Closure, followed by reactor scram. The feedwater is conservatively assumed to trip, with a coastdown of 5 seconds. Four of the Reactor Internal Pumps (RIPs) trip on high vessel pressure. The SRVs cycle open and closed to relieve the steam pressure. As the water level falls, the remainder of the RIPs trip on low level. The ECC injection systems are assumed to fail.

The sequence of events which includes passive flooder and rupture disk opening for this accident is shown in Table 19E.2-5. Figures 19E.2-2a through 19E.2-2h show the system behavior throughout the accident sequence.

About one half hour after accident initiation, sufficient decay heat has been generated to lower the water level to two thirds core height, and the operator opens one SRV to provide steam cooling. The vessel blows down (Figure 19E.2-2a), while the fuel heats up (Figure 19E.2-2d) and begins to melt. There is little generation of hydrogen gas due to the metal-water reaction during the in-vessel portion of the accident (Figure 19E.2-2f) because the vessel blowdown limits the available steam when the cladding is hot. About two hours after the initiation of the transient, the lower vessel head fails.

The corium falls into the lower drywell along with any remaining water in the lower plenum of the vessel. Rapid corium to water heat transfer quenches the corium (Figure 19E.2-2d) and results in non-equilibrium steam generation causing a pressure increase in the drywell

(Figure 19E.2-2b). Then the pressure decreases slightly as the containment temperature and pressure equilibrate with the pool conditions. Just under one hour is then required to boil away the water in the lower drywell (Figure 19E.2-2e) before the corium begins to heat up (Figure 19E.2-2d). After the water in the lower drywell boils off the drywell pressure decreases because steam is condensed on the containment heat sinks but there is no steam generated.

(1) Passive Flooder Operation (PF)

After the corium in the lower drywell is uncovered, the corium and the gas above it begin to heat up. When the lower drywell atmosphere reaches 533 K (500°F) at about 5 hours (Figure 19E.2-2c), the passive flooder opens. Water then pours from the wetwell into the drywell (Figure 19E.2-2e) to the level of the upper horizontal vent. This covers the corium, quenching it. This generates a small pressure spike (Figure 19E.2-2b). Following this there is again a slight decrease in pressure as the drywell returns to equilibrium with the pool.

Since the peak corium temperature during this process is 1600 K (2400°F) no significant core concrete attack occurs during the heatup of the corium, therefore no additional non-condensable gasses are generated. When the corium is quenched the generation of additional non-condensable gasses is prevented (Figure 19E.2-2f).

After the passive flooder opens the corium is covered by an overlying water pool, causing the temperature of the lower drywell gas to decrease (Figure 19E.2-2c). The small, periodic oscillations seen in the lower drywell water level after the passive flooder opens (Figure 19E.2-2e) are due to a physical instability caused by the small pressure and density differences between the lower drywell and the wetwell.

The oscillations begin when there is a small pressure differential between the wetwell and the lower drywell. The pressure differential causes relatively cool water from the suppression pool to flow into the lower drywell. This reduces the bulk temperature of the lower drywell pool. Since MAAP assumes the pool is well mixed, the surface temperature also decreases, resulting in a decrease in the partial pressure of steam in the lower drywell gas space. This pressure decrease (Figure 19E.2-2b) draws additional water into the lower drywell pool from the suppression pool.

When the elevation of water in the lower drywell is sufficient to eliminate the pressure differential, the flow from the wetwell stops. The cooled water in the lower drywell then begins to heat back up to saturation due to heat loss from the debris bed. Once saturated pool conditions are reached, steaming begins and the lower drywell pressure increases. This could cause reverse flow through the flooder line. The subsequent loss of mass in the lower drywell would cause the region to heat up more quickly, exacerbating the amplitude and period of the oscillations. Therefore, the MAAP-ABWR flooder line model includes a check valve which prevents flow from the lower drywell into the wetwell.

While this instability is based on physical phenomena, MAAP-ABWR overpredicts its severity. MAAP-ABWR models this system as two perfectly mixed pools, with overlying gas spaces at potentially different pressures. In the large scale of the plant, the cool water enters the lower drywell pool underneath the surface boundary layer of the pool. Since the density is slightly higher than that of the bulk pool, it will tend to sink. This will tend to damp the oscillation.

The size of the oscillation is dependent, in part on the time step because the decrease in the bulk pool temperature is a function of the amount of cool water added to the lower drywell. To determine the sensitivity of the containment response to the time step used by MAAP-ABWR, a representative sequence was run using very small time steps. While the results showed a slight decrease in the magnitude and period of the oscillations, no significant effect on the overall transient response was observed.

The upper drywell temperature continues to increase since the remaining fuel in the vessel loses its decay heat energy to the vessel walls and drywell via radiative and convective heat transfer. The pressurization of the containment continues (Figure 19E.2-2b) because the corium is now transferring heat directly to the water which results in steaming.

The containment continues to pressurize until the wetwell pressure reaches 0.72 MPa at 20.2 hours (Figure 19E.2-2b), when the rupture disk opens. No penetration leakage (Appendix 19F) is predicted since the temperature in the upper drywell remains below 533 K (500°F), until well after the rupture disk opens (Figure 19E.2-2c).

Figures 19E.2-2g and 19E.2-2h give the release fractions of the noble gases, cesium iodide, and cesium hydroxide as functions of time. The release of noble gases is nearly complete one hour after the rupture disk opens. The release of the volatile species, CsI and CsOH, occurs over a much longer period of time and is nearly complete at 100 hours. The release fraction of CsI at 72 hours is less than 1E-7.

There is a small probability that the drywell head will fail prior to the rupture disk opening for this case. Assuming the drywell head fails as the wetwell pressure reaches 0.72 MPa at 20.2 hours, drywell head failure will preclude rupture disk opening. Fission product release begins directly from the drywell. Noble gas release is nearly complete at 32 hours, and the volatile fission product release continues until 120 hours. The duration of the release is significantly longer for the drywell head failure sequence since the heat source in the drywell allows only a slow depressurization of the wetwell which contains the noble gases. The CsI release fraction at 72 hours is 7.5E-2, which is much greater than the release for the corresponding rupture disk case.

(2) Firewater Spray (FS)

If the operator fails to initiate the firewater addition system in the first 20 minutes of the accident to prevent core damage, there is still potential for significant benefit from its use after vessel failure is assumed to occur. The results of a sequence using the firewater addition system are given in Table 19E.2-6 and Figures 19E.2-3a through 19E.2-3e.

The firewater system adds water to the containment through the RHR-C injection lines. When trying to prevent vessel failure the operator is instructed to inject water to the vessel via the LPFL line. If very high temperatures are observed in the drywell, the valves are realigned to the drywell spray. The water then pours from the upper drywell into the wetwell via the wetwell/ drywell connecting vents, and eventually overflows into the lower drywell. This cools the corium, preventing core-concrete attack and additional metal-water reaction. Since external water is used, the effective heat capacity of the containment is increased. Furthermore, since the decay heat in the corium is delivered by convection to the water, no significant radiation heat transfer takes place, and the lower and upper drywell atmospheres remain cool. Therefore, no degradation of the movable penetration seals is expected, and no leakage through these penetrations will occur.

In this case it was assumed that the operator starts the firewater system four hours after the initiation of the event. The first four hours of the transient are identical to the LCLP-PF-R-N sequence discussed above. When the firewater system starts a pressure spike (Figure 19E.2-3b) is observed in the drywell which is caused by the evaporation of droplets in a superheated atmosphere. After the containment atmosphere is cooled (Figure 19E.2-3a), the pressure drops fairly rapidly to match the droplet temperature. This causes some water to spill over from the wetwell to the lower drywell (Figure 19E.2-3c).

The firewater addition system continues to add water, first filling the wetwell to the level of the suppression pool return path. At 7 hours, the pressure oscillations in the drywell cause the water level in the wetwell-drywell connecting vents to rise, and overflow into the lower drywell. This causes the drywell pressure to decrease further, in much the same manner as the oscillation discussed in (1) for the passive flooder. After this pressure-induced transient, the water level in the suppression pool continues to rise until, at 16 hours, it overflows. Then water begins to spill into the lower drywell and the mass of water in both the wetwell and the lower drywell increase in proportion to their surface areas (Figure 19E.2-3c). During this time the increase in pressure (Figure 19E.2-3a) is due to the slow compression of the non-condensable gases above the water.

Supplementary calculations have shown that the pressure in the containment is minimized when the water level is near the bottom of the vessel, assuming that the drywell and wetwell are at the same pressure. For this reason, the operator is directed

to turn off the firewater system when the water level in the suppression pool reaches the elevation of the bottom of the vessel, which occurs at 23.6 hours (Figure 19E.2-3c).

After the firewater spray is turned off the pressures in the drywell and wetwell increase (Figure 19E.2-3a) to values consistent with the temperature of the suppression pool and non-condensable gas pressure. The pressure in the drywell regions continues to increase as steam is generated by the corium in the lower drywell. This forces water to be displaced from the lower drywell to the suppression pool via the wetwell/drywell connecting vents. When water can no longer flow directly from the drywell into the wetwell the drywell region begins steaming. This steam flows to the suppression pool where it is quenched. During this period the pressure in the wetwell stays nearly constant while that in the drywell region increases (Figure 19E.2-3a).

At 26 hours the wetwell becomes nearly saturated and the pressure in the wetwell begins to increase along with that in the drywell. At 31.1 hours the pressure in the wetwell has reached 0.72 MPa and the rupture disk opens. After the rupture disk opens the pressure decreases rapidly (Figure 19E.2-3a) and fission product release begins. At about 57 hours the water in the lower drywell boils away leaving the corium uncovered. The gas temperature in the lower drywell increases to 533 K (500°F) (Figure 19E.2-3b) and the passive flooder opens at 61 hours, allowing water to flow from the suppression pool to the drywell (Figure 19E.2-3c). The noble gas release is nearly complete at 35 hours, and the volatile fission product release is nearly complete at 76 hours. The release fraction of CsI at 72 hours is about 1E-7, as shown in Figures 19E.2-3d and 19E.2-3e, respectively.

There is a small probability that the drywell head will fail before the rupture disk opens for this case. Assuming the drywell head fails as the wetwell pressure reaches 0.72 MPa at 31.1 hours, drywell head failure will preclude rupture disk opening. Fission product release begins directly from the drywell. Noble gas release is nearly complete at 69 hours, and the volatile fission product release continues until 90 hours. The CsI release fraction at 72 hours is 5.3E-2, which is much greater than the release fraction for the corresponding rupture disk case.

19E.2.2.2 Loss of All Core Cooling with Vessel Failure at High Pressure (LCHP)

The initiator used for this analysis is a station blackout with loss of all core cooling. For this sequence the operator is assumed to fail to depressurize the vessel. The complete sequence of events for this accident with the passive flooder and drywell spray operating is shown in Table 19E.2-7. Figures 19E.2-4a to 19E.2-4i show the system response to the presumed accident.

The early stages of this transient are identical to those of a LCLP accident. The MSIVs close, the reactor scrams and the feedwater coasts down. The core becomes uncovered at 17 minutes,

and metal-water reaction begins generating hydrogen (Figure 19E.2-4g) as the core heats up. The vessel continues to cycle on the SRV setpoints (Figure 19E.2-4a) as the water in the core boils away, and the core melts. Since the suppression pool temperature is below the suppression pool heat capacity temperature limit at the time of vessel failure, SRV loads are not a concern.

At 2.0 hours the vessel fails. The initial discharge of corium and water from the lower plenum is entrained by the steam from the vessel into the upper drywell and wetwell because the vessel fails at high pressure (Figure 19E.2-4a). As the steam is driven from the lower drywell the corium is carried into the upper drywell and wetwell (Figure 19E.2-4e). That portion of the corium which is blown into the wetwell is immediately quenched. It heats up only very slowly, as the suppression pool heats (Figure 19E.2-4c). The corium which is transferred into the upper drywell is initially cooled (Figure 19E.2-4c) by the atmosphere and by contact with the floor of the upper drywell.

(1) Passive Flooder and Drywell Spray Operation (PS)

The passive flooder opens 30 seconds after the vessel fails as the temperature in the lower drywell reaches 533 K (500°F) (Figure 19E.2-4d). This allows water from the suppression pool to flood the lower drywell, cooling the corium in the lower drywell. This does not, however, ensure that the upper drywell remains cool, since there is corium in this region. In order to prevent leakage through the movable penetrations in the upper drywell, the sprays must be initiated within the first 4 hours of the transient.

When the drywell spray is turned on the temperatures of both the corium and the gas in the upper drywell drop sharply (Figures 19E.2-4c and 19E.2-4d). The containment pressure also drops as steam is condensed by the spray droplets (Figure 19E.2-4b). The rapid depressurization of the lower drywell also causes water to flow from the suppression pool to the lower drywell through the open passive flooder (Figure 19E.2-4f).

After the drywell sprays are turned on, the containment slowly repressurizes (Figure 19E.2-4b). The pressure difference between the wetwell and the drywell is very small because the recirculation of water from the suppression pool to the drywell keeps the steam near the saturation pressure of the suppression pool water. If at any time during this sequence the RHR heat exchangers begin to operate, the containment would depressurize. Containment failure and fission product release would be averted.

If the heat exchangers are not recovered, the rupture disk will open when the wetwell pressure reached 0.72 MPa at 25.0 hours. Upon rupture disk opening, fission products leave the containment. The release of noble gases continues for about 8 hours after the rupture disk opens (Figure 19E.2-4h). The volatile fission product

release continues for about 25 hours. The release fraction of CsI at 72 hours is less than 1E-7 (Figure 19E.2-4i).

There is a small probability that the drywell head will fail prior to rupture disk opening for this case. Assuming the drywell head fails as the wetwell pressure reaches 0.72 MPa at 25.0 hours, drywell head failure will preclude rupture disk opening. Fission product release begins directly from the drywell. Noble gas release is nearly complete at 35 hours, and the volatile fission product release continues beyond 5 days. The CsI release fraction at 72 hours is 2E-4.

(2) Firewater Spray Operation (FS)

It is possible for the operator to delay the time of containment structural failure and reduce the fission product release by adding water to the containment after a loss of core cooling with vessel failure at high pressure. Consider a case which begins identically to LCHP-PS-R-N, a loss of all core cooling occurs and the reactor scrams. The operator is assumed to fail to blowdown the reactor, vessel failure occurs at high pressure and corium is entrained into the upper drywell and wetwell.

It is assumed that the operator turns on the firewater addition spray system 1.9 hours after the start of the accident, just before the passive flooder would operate. The pressure and the upper drywell temperature decrease rapidly. The additional water from the spray is initially directed to the suppression pool. Since the flow from the sprays does not initially enter the lower drywell, the passive flooder opens at 2.0 hours. This begins to flood the lower drywell. The containment then remains in a stable condition for several hours with the containment pressure and suppression pool mass increasing. Water is present in the lower drywell for the remainder of the sequence since the passive flooder is open.

When the suppression pool water level reaches the suppression pool to lower drywell vent, the operator is instructed to turn off the firewater system. The corium in the upper drywell then causes the temperature in the upper drywell to increase.

The continued use of sprays which add water to the containment is prohibited by the EPGs. There is, however, a high probability that the RHR System would have been recovered in this interval. The operator could use this system to maintain low drywell temperatures. To model the potential impact of continued containment pressurization, the heat exchanger is assumed inoperable. The effect of this change in spray water source is an increased rate of suppression pool heating and containment pressurization, leading to an earlier containment failure than would be predicted if the spray continued to be supplied by firewater addition. The wetwell pressure reaches 0.72 MPa at about 50 hours and the rupture disk opens. The volatile fission product release continues for the next 75 hours and the CsI release fraction at 72 hours is less than 1E-7.

There is a small probability that the drywell head will fail before the rupture disk opens for this case. Assuming the drywell head fails as the wetwell pressure reaches 0.72 MPa at 50 hours, drywell head failure will preclude rupture disk opening. Fission product release begins directly from the drywell. The noble gas release is nearly complete at 55 hours and the volatile fission product release continues for more than 5 days. The release fraction of CsI at 72 hours is 1.5E-4.

(3) Passive Flooder Operation

If the operator takes no actions after a high pressure core melt, high temperatures will ensue in the upper drywell and leakage will occur through the large movable penetrations as discussed in Appendix 19F. The sequence of events for this case is summarized in Table 19E.2-8 and is depicted in Figure 19E.2-5a through 19E.2-5e.

The passive flooder opens when the temperature in the lower drywell reaches 533 K (500°F) at 2.0 hours (Figure 19E.2-5b). Water then flows from the wetwell into the lower drywell (Figure 19E.2-5d), quenching the corium in the lower drywell (Figure 19E.2-5c). In contrast, the corium in the upper drywell heats up, after an initial heat loss to the upper drywell atmosphere and structures (Figure 19E.2-5c). This heats the upper drywell atmosphere. The seal degradation temperature of 533 K (500°F) determined in Appendix 19F is reached about in 2.1 hours (Figure 19E.2-5b), but leakage does not start at this time because the pressure is still relatively low (Figure 19E.2-5a).

The containment continues to pressurize, and leakage through the movable penetrations begins at 18.1 hours. This initiates the release of fission products (Figure 19E.2-5e). However, since the leakage is not sufficient to pass all of the decay heat energy, the containment continues to pressurize (Figure 19E.2-5a).

At about 40 hours, the pressure in the drywell dips by about 0.04 MPa. This dip is caused by the flow of water from the suppression pool into the lower drywell which reduces the average temperature of the water in the lower drywell (Figure 19E.2-5d). The temperature decrease results in a decrease in pressure because the drywell is filled with saturated steam. The initial flow of water from the suppression pool causes the pressure of the lower drywell to drop, which in turn causes more water to flow from the suppression pool. The flow stops when enough water has been added to the lower drywell such that the static head above the flooder balances the pressure decrease. While this may be a mathematical artifact of the calculation, it has no serious impact on the analysis.

At about 69 hours into the accident the drywell gas temperature has reached a steady value of 830 K (1035°F) (Figure 19E.2-5b) and the drywell pressure has reached a steady value of 0.66 MPa (Figure 19E.2-5a). The containment does not reach the wetwell rupture disk setpoint pressure of 0.72 MPa, nor does it reach the pressure necessary to fail the drywell head. The drywell head failure pressure at 830 K is

reduced to 0.75 MPa because high temperatures in the drywell weaken the drywell head seal as discussed in Appendix 19F.

The fission product release begins at 18.1 hours (Figure 19E.2-5e). The noble gas release continues well beyond 5 days, while the volatile fission product release is nearly complete at 70 hours. The release fraction of CsI at 72 hours is 8.8E-2.

19E.2.2.3 Station Blackout with RCIC Available (SBRC)

This accident initiator, SBRC, represents a station blackout sequence with failure of the combustion turbine generator (CTG). These are characterized by the unavailability of all AC Power except that obtained from the batteries through inverters. Therefore, the RCIC system and firewater are the only systems available for core cooling. This sequence assumes RCIC operates for approximately 8 hours, providing core cooling (Subsection 19E.2.1.2.2). After the RCIC fails, the operator depressurizes the vessel and begins injection with the firewater addition system which can maintain core cooling indefinitely. However, no containment cooling system is available since all the diesel generators and the CTG were assumed to fail.

Two types of station blackout sequences are considered. In the first, the operator successfully initiates the firewater addition system. This sequence is then similar to class II events. There is no core damage unless the containment structural failure leads to core damage. The sequence of events for the case in which core cooling is maintained is summarized in Table 19E.2-9 and is depicted in Figures 19E.2-6a through 19E.2-6e. The more serious sequence of events is that in which the operator fails to inject with the firewater system. This case is summarized in Table 19E.2-10 and is shown in Figures 19E.2-7a through 19E.2-7f.

A reactor scram occurs immediately upon loss of power. The MSIVs close and the RIPs coast down. Feedwater pumps also coast down and the water level begins to fall. When the water level reaches Level 2, the RCIC system initiates. The steam boiled off in the core is routed to the suppression pool through the SRVs.

Initially, the RCIC suction is taken from the condensate storage tank (CST). After 1.3 hours, the suppression pool level high-high alarm is reached, and RCIC suction switches to the suppression pool. Later, at 4.4 hours, the high suppression pool temperature alarm occurs, and the operator manually switches RCIC suction back to the CST. The reactor is maintained in this quasi-steady condition, with the suppression pool heating up, and the containment pressurizing, for approximately 8 hours. After the RCIC system is presumed to fail, the water in the vessel continues to boil off to the suppression pool. The pool begins to overflow the drywell at about 9 hours.

The data in Figures 19E.2-6a through 19E.2-6e, in which core cooling is maintained by the addition of firewater, begins at 6 hours. The sequence in which core cooling is maintained is identical to the sequence in which it is not until the addition of firewater at about 10 hours.

Thus, Figures 19E.2-7a through 19E.2-7f can be substituted for Figures 19E.2-6a through 19E.2-6e for the first 6 hours.

(1) Firewater Addition Prevents Core Damage

It is possible for the operator to prevent core damage during an SBRC sequence by using the firewater system to inject water into the vessel after the RCIC is assumed to fail. To do this, operator must depressurize the reactor and align the valves to begin injecting with the firewater addition system.

Before RCIC failure, the containment pressure increases slowly while the RCIC operates (Figure 19E.2-7b). After RCIC failure the water level in the vessel drops quickly. At 9.8 hours the water level reaches 2/3 core height and the operator depressurizes the vessel. As the vessel pressure falls, the containment pressure increases quickly. During the blowdown the water level in the suppression pool has become sufficient to cause the water to begin to overflow from the wetwell into the lower drywell region (Figure 19E.2-6e). After the blowdown, when the firewater system is injecting, the pressure rises more slowly since only decay heat is being added to the suppression pool (Figure 19E.2-6a). The decay heat addition causes a slight volumetric expansion of water in the suppression pool. Since the water level in the suppression pool is already at the overflow point, the expansion results in flow to the lower drywell and causes a slight decrease in suppression pool mass.

The depressurization causes the water to flash to steam, lowering the water level in the vessel (Figure 19E.2-6d). MAAP-ABWR predicts that the core heats up to about 1150 K (1610°F) during this time (Figure 19E.2-6c). Therefore, core damage will not occur. When the pressure reaches the shutoff head of the firewater addition system, 1.96 MPa, water injection begins and the core cools rapidly. The water level in the vessel then rises until it reaches level 8 (Figure 19E.2-6d). The operator then maintains water level between level 8 and level 3.

When the wetwell pressure reaches 0.72 MPa after 32.3 hours, the drywell head is presumed to fail. However, because no core damage has occurred there is no release of fission products.

(2) Passive Flooder Operation

If the operator fails to use the firewater addition system after the RCIC fails, then core damage will occur. The sequence of events for this case is shown in Table 19E.2-10. The system response to this accident is shown in Figures 19E.2-7a to 19E.2-7f.

Eight hours after the loss of offsite power, RCIC is assumed to fail. The water level begins to fall, although the rate of the water level decrease is slower than that for the LCLP sequence because the decay heat is lower. The operator depressurizes the vessel when the water level reaches two-thirds core height by opening one SRV (Figure 19E.2-7a) at 9.7 hours (SRV operability is discussed in

Subsection 19E.2.1.2.2). If the operator fails to begin injection using the firewater system then the fuel melts slowly, and the vessel fails at 12.3 hours.

The corium and the lower plenum water then fall to the lower drywell floor. The containment continues to pressurize as this water boils (Figure 19E.2-7b). At 21.1 hours the lower drywell dries out (Figure 19E.2-7e) and the corium begins to heat up (Figure 19E.2-7d). The corium radiates energy to the lower drywell gas (Figure 19E.2-7c). When the gas temperature reaches 533 K (500°F) at 23.5 hours, the passive flooder opens.

When the passive flooder opens water pours from the wetwell into the lower drywell (Figure 19E.2-7e). This quenches the corium and causes the drywell pressure to increase rapidly to the rupture disk rupture pressure, 0.72 MPa in about 4 minutes.

The fission product release for this sequence (Figure 19E.2-7f) begins at 23.5 hours, the time of rupture disk opening. The noble gas release lasts about 3 hours. The volatile fission products are released slowly over the next 75 hours. The CsI release fraction at 72 hours is less than 1E-7.

There is a small probability that the drywell head will fail prior to rupture disk opening for this case. Assuming the drywell head fails as the wetwell pressure reaches 0.72 MPa at 23.5 hours, drywell head failure will preclude rupture disk opening. Fission product release begins directly from the drywell. Noble gas release is nearly complete at 38 hours, and the volatile fission product release continues until 105 hours. The CsI release fraction at 72 hours is 3.4E-1, which is much greater than the release for the corresponding rupture disk case.

19E.2.2.4 Loss of Containment Heat Removal (LHRC)

This case, LHRC, was simulated using an MSIV closure event with loss of the drywell coolers, since this event isolates the reactor immediately, and will therefore direct the most heat to the suppression pool of any Class II event. The sequence of events is shown in Table 19E.2-11. Figures 19E.2-8a through 19E.2-8c show the system response to this sequence.

For most of these sequences ECCS suction is initially drawn from the CST. When the high suppression pool level is reached the suction is switched to the suppression pool. However, for simplicity, no credit was taken for the CST inventory. The effect of this assumption is to underestimate the mass of water in the suppression pool, thus overpredicting the increase in suppression pool temperature and containment pressure. Additionally, in the later stages of this transient the operator could switch the suction for the ECCS back to the condensate storage pool or use the firewater addition system, either of which provides a source of makeup water to the suppression pool.

MSIV closure causes scram and feedwater trip. As the water level falls core cooling (RCIC) initiates. Since the reactor is isolated all of the decay heat is directed to the pool, causing the

pool temperature to increase (Figure 19E.2-8b). When the suppression pool temperature reaches suppression pool temperature limit, the operator blows down the reactor in accordance with the EPGs. As the vessel pressure falls, RCIC trips due to insufficient turbine pressure. The water level falls, and the HPCF system initiates.

The containment pressurizes very slowly. At 21.7 hours, the pressure reaches 0.72 MPa, (Figure 19E.2-8a) and the rupture disk opens. After the rupture disk opens, the suppression pool begins to boil off (Figure 19E.2-8c). The system will remain in this quasi-steady state for a very long time.

If at any time during this transient a source of makeup water to the containment can be used, the reactor can be maintained indefinitely in this state. As mentioned above, either the firewater addition system or the water in the CST could provide a source of makeup water to the containment.

If makeup water is not supplied, the water level in the suppression pool will eventually become so low that the core cooling pumps are unable to draw sufficient suction, and core cooling could be lost. The transient was simulated for 72 hours in this analysis and that condition was not reached. When there is insufficient suppression pool suction the operator could still maintain core cooling by switching the ECCS suction back to the CST. The CST has at least 8-hour capacity for core cooling based on the station blackout performance assessment (Subsection 19E.2.1.2.2).

If core cooling is lost, the water in the vessel will begin to boil off slowly, and eventually, core melt will occur, no earlier than three hours after the loss of core cooling. The analysis of this transient was not carried any further because there is a very long time for the operator to take the necessary action to terminate the event.

19E.2.2.5 Large LOCA with Failure of All Core Cooling (LBLC)

A main steamline break is assumed to represent the LBLC case, since it has the largest flow area and will cause the most rapid loss of coolant from the vessel. The sequence of events for this case is similar to that for LCLP (loss of core cooling with vessel failure at low pressure), however, the core melt will occur earlier for the LBLC case. The sequence of events for the LBLC case with the passive flooder and rupture disk opening is shown in Table 19E.2-12. The system response to this event is given in
Figures 19E.2-9a through 19E.2-9d.

The feedwater system is conservatively assumed to trip at the initiation of the event for this analysis. The reactor scrams on a high drywell pressure signal, and the MSIVs close as the vessel pressure drops. The core uncovers in 2.8 minutes and the fuel begins to heat up. Vessel failure occurs at 1.4 hours.

At the time of vessel failure, the corium and water from the lower plenum fall into the lower drywell. The corium is quenched by this lower drywell water. The water in the lower drywell then begins to boil away (Figure 19E.2-9c), pressurizing the containment (Figure 19E.2-9a).

(1) Passive Flooder Operation

After the water in the lower drywell is boiled away by the decay heat energy in the corium, the corium begins to heat up, raising the lower drywell temperature (Figure 19E.2-9b). When the gas temperature in the lower drywell reaches 533 K (500°F) at 5.7 hours the passive flooder opens automatically. Water flows into the lower drywell (Figure 19E.2-9c) and the temperature drops as steam is generated (Figure 19E.2-9b).

After the passive flooder opens the containment pressurizes slowly (Figure 19E.2-9a) as steam is generated in the lower drywell. The entire containment remains cool (Figure 19E.2-9b) since the corium is covered.

When the wetwell pressure reaches 0.72 MPa, at 19.1 hours (Figure 19E.2-9a), the rupture disk opens. The fission product release occurs over the next 105 hours (Figure 19E.2-9d). The CsI release fraction at 72 hours is less than 1E-7.

There is a small probability that the drywell head will fail prior to rupture disk opening for this case. Assuming the drywell head fails as the wetwell pressure reaches 0.72 MPa at 19.1 hours, drywell head failure will preclude rupture disk opening. Fission product release begins directly from the drywell. Noble gas release is nearly complete at 31 hours, and the volatile fission product release continues until 100 hours. The CsI release fraction at 72 hours is 2.2E-2, which is much greater than the release for the corresponding rupture disk case.

(2) Firewater Spray

If the operator initiates the firewater addition system to add water to the containment through the RHR line then the time to containment structural failure will be delayed. For this analysis it is assumed that the operator begins injection 4 hours after the start of the accident. The sequence of events after vessel failure for this sequence is similar to that for the LCLP-FS-R-N sequence shown in Figures 19E.2-3a to 19E.2-3e.

When the firewater system is initiated there is some splashing of water into the lower drywell. This prevents the code from predicting operation of the passive flooder.

Eventually, at about 11 hours, the suppression pool overflows into the lower drywell. Water is added to the containment via the firewater system until the water level in the suppression pool reaches the level of the vessel bottom. During this time there is no boiling in the lower drywell. The containment pressurizes slowly due to the compression of the non-condensable gasses. At 23.4 hours the firewater system is shut off. As in the LCLP-FS-R-N case [Subsection 19E.2.2.1(2)], the containment

pressure first increases very slowly as the water in the lower drywell heats to saturation. Then after boiling begins, the pressure rises more rapidly.

The wetwell pressure reaches 0.72 MPa at 29.5 hours, the rupture disk opens, and fission product release begins. At about 62 hours the lower drywell has dried out leaving the corium uncovered. This causes the gas temperature in the lower drywell to increase to 533 K (500°F) causing the passive flooder to open. The release of volatile fission products is nearly complete at 67 hours. The release fraction of CsI at 72 hours is less than 1E-7.

There is a small probability that the drywell head will fail before the rupture disk opens for this case. Assuming the drywell head fails as the wetwell pressure reaches 0.72 MPa at 29.5 hours, drywell head failure precludes rupture disk opening. Fission product release begins directly from the drywell. Noble gas release is nearly complete at 60 hours, and the volatile fission product release continues until 95 hours. The CsI release fraction at 72 hours is 2.4E-2, which is much greater than the release fraction for the corresponding rupture disk case.

19E.2.2.6 Concurrent Loss of All Core Cooling and ATWS with Vessel Failure at Low Pressure (NSCL)

The sequence chosen to represent the NSCL case is a station blackout case with failure to scram. This sequence is analogous to the LCLP case, with the additional failure of reactivity control. The sequence of events for this case, if the operator does not initiate the firewater addition system is given in Table 19E.2-13. Some of the important parameters are depicted in Figures 19E.2-10a through 19E.2-10d.

Upon loss of power, the MSIVs close and the feedwater and recirculation pumps trip. All automatic and manual attempts to insert control rods are assumed to fail. The SRVs open to relieve the vessel pressure. Furthermore, all injection pumps, including the RCIC and SLC pumps fail to inject water into the vessel. Because of the increased power level the water level in the vessel falls rapidly and the core is uncovered in 3.7 minutes.

The temperature of the uncovered core now begins to rise (Figure 19E.2-10b), and core damage begins. At 30 minutes the operator is assumed to initiate ADS and the vessel blows down. When the vessel fails at 1.3 hours, the pressure is sufficiently low to prevent entrainment. The corium, together with any water in the lower plenum, falls into the lower drywell (Figure 19E.2-10c).

The corium is quenched in the lower drywell by the water from the lower plenum. The water then boils, causing the drywell pressure to rise (Figure 19E.2-10a). All of the water is boiled off at 1.9 hours (Figure 19E.2-10c).

(1) Passive Flooder

If no actions are taken by the operator to initiate the firewater system, the passive flooder will open when the temperature of the lower drywell reaches 533 K (500°F)

at 4.4 hours. At that time, water from the wetwell will pour into the lower drywell, covering the corium. This prevents core concrete attack and metal-water reaction from occurring because the corium is not sufficiently hot for either reaction to occur (Figure 19E.2-10b).

The containment pressure then begins to rise slowly as steam is generated (Figure 19E.2-10a). The rupture disk opens at 18.7 hours, and the fission products are released (Figure 19E.2-10d). The noble gas release lasts about 2 hours. The volatile fission product release lasts about 85 hours. The CsI release fraction at 72 hours is less than 1E-7.

There is a small probability that the drywell head will fail prior to rupture disk opening for this case. Assuming the drywell head failure will preclude rupture disk opening. Fission product release begins directly from the drywell. Noble gas release in nearly complete at 33 hours, and the volatile fission product release continues until 100 hours. The CsI release fraction at 72 hours is 8.5E-2, which is much greater than the release for the corresponding rupture disk case.

(2) Firewater Spray

If the operator begins injection using the firewater addition system after vessel failure has occurred, then the time of drywell head failure can be delayed. The sequence of events for this case is similar to the LCLP-FS-R-N case shown in Figures 19E.2-3a through 19E.2-3e.

For this sequence, where neither scram or core cooling was successful, the operator is assumed to initiate the firewater system within 4 hours. When the firewater system is initiated, there is some splashing of water into the lower drywell. This prevents the passive flooder from opening. The firewater addition serves to keep the drywell cool, and increases the thermal mass of the suppression pool, slowing the containment pressurization rate. The water level in the suppression pool reaches the spillover height at about 15 hours. When the water level of the suppression pool reaches the bottom of the vessel, at 23.7 hours, the operator is assumed to turn off the system.

The containment pressurization rate then increases, and the rupture disk opens at 30.7 hours. At about 57 hours the water over the corium boils away leaving the corium uncovered. The gas temperature in the lower drywell increases to 533 K (500°F) and the passive flooder opens at 61 hours. The volatile fission product release continues for the next 8 hours. The release fraction of CsI at 72 hours is less than 1E-7.

There is a small probability that the drywell head will fail before the rupture disk opens for this case. Assuming the drywell head fails as the wetwell pressure reaches 0.72 MPa at 30.7 hours, drywell head failure will preclude rupture disk opening. Fission product release begins directly from the drywell. Noble gas release is nearly complete at 62 hours, and the volatile fission product release continues until 85

hours. The CsI release fraction at 72 hours is 6.4E-2, which is much greater than the release fraction for the corresponding rupture disk case.

19E.2.2.7 Concurrent Loss of All Core Cooling and ATWS with Vessel Failure at High Pressure (NSCH)

The NSCH sequence is analogous to the LCHP sequence described in 19E.2.2.2 with the additional failure of reactivity control. The main effect of failure to scram or inject boron is to decrease the time of vessel failure, since the reactor stays at power for the first few minutes of the transient. However, the power level soon drops due to additional voiding in the core. The sequence of events for the NSCH sequence where the passive flooder is the only mitigating system is given in Table 19E.2-14. Figures 19E.2-11a through 19E.2-11d illustrate the key parameters.

Following an isolation event the water in the vessel boils rapidly, and the core becomes uncovered in 3.6 minutes. If the operator fails to blow down to low pressure, a high pressure vessel melt occurs in 1.3 hours. Since the suppression pool temperature is below the suppression pool heat capacity temperature limit at the time of vessel failure, SRV loads are not a concern. As with an LCHP event, corium is entrained into the wetwell and upper drywell (Figure 19E.2-11c).

(1) Passive Flooder (PF)

If the operator does not initiate the firewater system then the passive flooder will open at 1.4 hours when the temperature of the gas in the lower drywell reaches 533 K (500°F) (Figure 19E.2-11b). This immediately cools the corium in the lower drywell and the gas temperature in this region drops to near the saturation temperature.

The only heat sinks available to remove the decay heat generated by the corium in the upper drywell region are the concrete walls and the atmosphere. Since the heat transfer to the concrete is not very effective, the gas temperature in the upper drywell increases steadily. Shortly after the passive flooder opens the temperature in the upper drywell exceeds the penetration leakage temperature threshold (Figure 19E.2-11a). However, since the pressure is only 0.25 MPa, leakage does not occur at this time but is delayed until 17.8 hours when the drywell pressure reaches 0.46 MPa as shown in Figure 19E.2-11a.

At 47.7 hours, the pressure in the drywell dips sharply by about 0.06 MPa. This dip is caused when the pressure difference between the wetwell and lower drywell sides of the passive flooder allows water to flow from the suppression pool into the lower drywell, which is now filled with water. The initial flow of water from the suppression pool causes the temperature of the lower drywell pool to decrease which in turn results in depressurization of the lower drywell. This induces more water to flow from the suppression pool. The flow stops when enough water has been added to the lower drywell so the static head above the flooder balances the pressure

decrease. While this may be only a mathematical artifact of the calculation, it has no serious impact on the analysis.

At about 67 hours into the accident the drywell gas temperature has reached a steady value of 850 K (1070°F). At the same time the drywell pressure has reached a steady value of 0.67 MPa (Figure 19E.2-11a). The containment does not reach the rupture disk setpoint pressure of 0.72 MPa, nor does it reach the pressure necessary to fail the drywell head. The drywell head failure pressure at 850 K is reduced to 0.71 MPa because high temperatures in the drywell weaken the drywell head seal as discussed in Appendix 19F.

Fission product release begins when drywell penetration leakage starts, at 17.8 hours. The initial release rate is very small (Figure 19E.2-11d) because of the small penetration leakage. The noble gas release continues well beyond 5 days, while the volatile fission product release is nearly complete at 65 hours. The release fraction of CsI at 72 hours is 7.3E-2.

(2) Firewater Spray Addition (FS)

The scenario in which the operator begins the firewater spray after vessel failure has occurred is the analog to the LCHP-FS-R-N case considered in Subsection 19E.2.2.2(2). The only major differences after the spray is initiated are the temperature of the pool, and consequently the pressure in the containment.

Comparisons of the LCHP-PF-P-M and NSCH-PF-P-M pressure histories (Figures 19E.2-5a and 19E.2-11a, respectively) shows that the additional power generated in the ATWS sequence causes the pressure for this case to be about 0.02 MPa higher than the non-ATWS sequence. This increase in pressure represents the additional power generated in the first hours of the ATWS transient. After this time the power level will drop to decay heat levels because of a strong negative void coefficient in the core.

Therefore, since the difference in the pressures of the two cases is small, the transient considered here, a simultaneous loss of all core cooling and failure of reactivity control with vessel failure at high pressure, in which the operator start the firewater spray system after vessel failure, will behave like the LCHP-FS-R-N case considered in 19E.2.2.2(2). No further analysis of this sequence was performed.

19E.2.2.8 Concurrent Station Blackout with ATWS (NSRC)

The final sequence considered here, NSRC, is the case where a station blackout occurs with failure of the combustible gas turbine and all reactivity control fails. In this sequence the RCIC is the only system available to provide core cooling. The sequence of events for this case is given in Table 19E.2-15 and some of the key parameters are shown in Figure 19E.2-12a through 19E.2-12f.

Upon the loss of power, the reactor isolates immediately. The vessel pressure increases and SRVs cycle to control pressure (Figure 19E.2-12a). The water level falls rapidly and at 1.1 minutes, the RCIC system begins injecting. The water level continues to fall and at 2.2 minutes the top of the core becomes uncovered.

Although the top few nodes heat up to about 850 K (1070°F), the core does not melt at this time due to steam cooling (Figure 19E.2-12d). The power level during this time is about 4% (Figure 19E.2-12c). This amount is that required to boil the water injected by RCIC. During this time the containment pressurizes fairly rapidly due to the relatively high rate of steam generation (Figure 19E.2-12b).

All of the water added by the RCIC System is converted to steam in the core. The steam flows through the SRVs to the suppression pool where it is quenched, adding to the mass of the pool. At 1.9 hours the suppression pool begins to overflow into the lower drywell.

If the operator is unable to shutdown the reactor by means of either the rods or boron injection then the containment pressure will reach the RCIC turbine exhaust pressure limit in 3.6 hours (Figure 19E.2-12b). This causes the RCIC to trip. As there is no other source of vessel injection available, the water level in the vessel will drop and the core will begin to melt, as seen by the increasing fuel temperature in Figure 19E.2-12d. At the same time the power will drop to the decay heat level because of increasing voids (Figure 19E.2-12c).

(1) Passive Flooder

The operator depressurizes the reactor 10 minutes after the RCIC is tripped. Vessel failure ensues at 5.6 hours. Corium and water fall into the lower drywell (Figure 19E.2-12e). A short time later, at 8.6 hours, the wetwell pressure reaches 0.72 MPa and the rupture disk opens. The containment begins to depressurize (Figure 19E.2-12b) and fission product release begins. The lower drywell dries out at about 30 hours and the passive flooder opens soon after. The noble gas release occurs within the first 5 hours after the rupture disk opens, while the volatile fission product release continues for 100 hours. The release fraction of CsI at 72 hours is less than 1E-7.

There is a small probability that the drywell head will fail prior to rupture disk opening for this case. Assuming the drywell head fails when the wetwell pressure reaches 0.72 MPa at 8.6 hours, drywell head failure will preclude rupture disk opening. Fission product release begins directly from the drywell. Noble gas release is nearly complete at 19 hours, and the volatile fission product release continues until 50 hours. The CsI release fraction is 4.8E-1 at 72 hours, which is much greater than the release for the corresponding rupture disk case.

(2) Firewater Sprays Operated

The operator can delay the release of fission products by initiating the firewater spray before the rupture disk opens. If the firewater spray begins at 6.1 hours, 30 minutes after vessel failure, the fission product release does not begin until 26.4 hours. Upon firewater spray initiation the containment pressure and temperature decrease. At 22 hours the level has reached the bottom of the vessel and the operator is instructed to turn off the spray. The containment begins to pressurize until, at 26.4 hours, the wetwell pressure reaches 0.72 MPa and the rupture disk opens. The containment rapidly depressurizes and fission product release begins. At 49 hours the lower drywell dries out, leaving the corium uncovered and the passive flooder opens at 52 hours. The noble gas release is nearly complete at 33 hours, while the volatile fission product release continues until about 120 hours. The CsI release fraction at 72 hours is 1E-7.

There is a small probability that the drywell head will fail before the rupture disk opens for this case. Assuming the drywell head fails as the wetwell pressure reaches 0.72 MPa at 26.4 hours, drywell head failure will preclude rupture disk opening. Fission product release is nearly complete at 38 hours, and the volatile fission product release continues until 85 hours. The CsI release fraction at 72 hours id 2.0E-1, which is much greater than the release fraction for the corresponding rupture disk case.

19E.2.2.9 Summary

Table 19E.2-16 gives a summary of the critical parameters for the accident sequences discussed above. For each sequence considered in the analysis which results in fission product release, the time of vessel failure, the start of fission product release and the time of rupture disk opening are given. Also shown are the duration of the release and the release fraction for CsI after 72 hours.

19E.2.3 Justification of Phenomenological Assumptions

Several separate effects studies were performed to supplement the MAAP analyses of severe accident sequences. These studies were performed to address the technical issues which could potentially have impact on the ABWR response to postulated severe accidents. They were selected for consideration based on the results of past PRA experience within the industry.

19E.2.3.1 Steam Explosions

A steam explosion is caused by thermal energy release to water, which causes rapid steam formation, expansion, and substantial pressure or impact loads on structures. It is possible that the high thermal energy content of molten core debris can cause a steam explosion if it enters water under conditions favorable to rapid heat transfer.

The potential for an ex-vessel steam explosion for a postulated severe accident in the ABWR plant is evaluated in this subsection, and is found to be extremely low.

19E.2.3.1.1 The Steam Explosion Process

Figure 19E.2-13 helps explain the process of steam explosions. It is postulated that a loss of cooling mechanism causes the reactor core to melt, followed by vessel breach and discharge of molten core debris with high thermal energy into the lower drywell, which is assumed to contain a stagnant pool of water. The energy transfer rate to water depends on the volume of submerged debris and available surface area for heat transfer. If many small particles of molten debris enter or form in the water, heat transfer will be rapid. Larger particles have less surface area per unit volume, and correspondingly slower heat transfer. Moreover, internal heat diffusion in large particles can limit the heat transfer rate to the water.

High velocity discharge of liquid debris into air can form spray-size droplets before they enter a water pool. However, for most cases debris discharge in the ABWR is expected to occur by gravity draining from a depressurized vessel, which could form larger droplets in air, about 24 mm. Smaller droplets would be formed by a stream of molten debris falling through water. An event called triggering can occur if the energy transfer from droplets forms additional droplets from the debris stream and rapidly mixes them with surrounding water. Both external triggering and self-triggering can cause steam explosions. External triggering has been employed in experiments by the use of submerged explosive devices, which include exploding wires, primicord, and blasting caps. The corresponding energy release of external triggers promotes the rapid breakup of molten debris into small particles.

Self-triggering sometimes is caused by debris stream impingement and shattering on submerged structures. If triggering suddenly creates increased surface area for heat transfer, the rapid formation of the steam causes water acceleration, which can create substantial pressure and impact forces.

19E.2.3.1.2 Previous Studies

Analytical and experimental studies of steam explosion phenomena are summarized in a 1983 IDCOR study (References 19E.2-5 and 19E.2-6). Analytical models and experimental studies reported in the literature are discussed from the standpoint of necessary conditions required to produce large scale steam explosions. It was determined that the following specific conditions had to be satisfied for steam explosions to occur:

(1) Many tonnes of molten core debris must enter the water.

(2) The debris must be coarsely fragmented into about one centimeter diameter or smaller particles and thoroughly mixed with water.

(3) A trigger must initiate a localized explosion which subsequently fragments adjacent particles into submillimeter size, and rapidly mixes them with the surrounding water in less than a millisecond, promoting rapid vaporization.

(4) A continuous liquid slug must cover the vaporization zone so that it can be propelled upward like a missile by the explosive interaction.

It was concluded in the IDCOR study that for both in-vessel and ex-vessel steam explosions, the formation of tonnes of coarsely fragmented molten core debris dispersed in water, with the associated large steam generation rates, is fundamentally inconsistent with a continuous overlying liquid slug required for efficient energy transfer. That is, steam explosions do not provide a set of credible physical processes leading to failure of either the primary system or the reactor containment building. The IDCOR conclusion and the conclusion of this analysis differ from the earlier WASH-1400 report (Reference 19E.2-7), in which energetic steam explosions were believed possible, leading to early containment failure.

Molten debris discharge from a reactor vessel at high pressure is more likely to be atomized and enter the pool as small droplets, which can rapidly transfer thermal energy and increase the potential for a steam explosion. However, the major conclusion from data and analytical models discussed in the IDCOR study (Reference 19E.2-5) imply that low vessel pressure and gravity discharge of molten core debris in ABWR has an extremely low potential for generating a steam explosion.

The IDCOR study (Reference 19E.2-5) reports that in various experiments it was possible to cause a steam explosion with an external trigger, which broke the molten metal into small drops and mixed them with surrounding water. Several experiments were reported in which iron thermite was observed to undergo self-triggering prior to a steam explosion. However, the thermite at a temperature of 3000 K apparently remained liquid during the triggering process, offering only surface tension resistance to molten droplet formation. Molten core debris is expected to be discharged at the liquidus temperature of 2600 K. The outer surface of small droplets freezes rapidly after entering water, perhaps even while falling a long distance through air, so that further droplet division requires more energy to fracture the outer crust formed than it does to overcome liquid surface tension. This helps explain why self-triggering can be observed with some highly superheated metals, but is much less likely with molten core debris.

Experimental work reported in the IDCOR study was performed in small scale test facilities, which leads to questions about how accurately the experiments represent full size severe accident steam explosion response. Theofanous (Reference 19E.2-8) addressed the scaling concern by formulating the basic phenomena of steam explosions, and comparing computer solutions for different scales. Calculated pressure and volume fractions of steam, melt, and coolant, were compared on a normalized time scale, and show that for properly scaled molten debris pours, comparable behavior can be expected in scales as low as 1/8 of full size. Most of the experiments discussed in the IDCOR report (Reference 19E.2-5) were at smaller scales, which leaves the scaling question short of full resolution. However, it is expected that the basic theoretical formulations, which are consistent with experimental phenomena at small scales, can be extrapolated to evaluate the potential for steam explosion in full size applications. That is largely the IDCOR approach which leads to the conclusion of low steam explosion potential during a severe accident in a full scale reactor.

19E.2.3.1.3 Theoretical Considerations

The theoretical considerations of this study are based on simplified, bounding analyses which tend to be conservative in the promotion of steam explosions. These considerations are used to evaluate the geometric conditions expected for a molten debris pour into water, the heat transfer and steam formation rates, pressure rise and water hydrodynamic response time. It is concluded from these considerations that the potential of an ex-vessel steam explosion in ABWR is extremely low.

(1) Estimated Debris Droplet Formation Size

Hydrodynamic instability causes droplet formation when two parallel, adjacent liquid streams with different densities travel at different velocities. Figure 19E.2-14a shows the heavier liquid, of density ρ_h, on the bottom, flowing horizontally with velocity v_h, underneath the lighter liquid, of density ρ_L, flowing with velocity v_L. The condition for unstable interface waves can be obtained from Lamb (Reference 19E.2-9) in the form

$$\frac{8\pi^3\sigma}{\lambda^3} + \frac{2\pi g(\rho_h - \rho_L)}{\lambda} - \frac{4\pi^2\rho_h\rho_L(v_h - v_L)^2}{\lambda^2(\rho_h + \rho_L)} < 0 \qquad (19E.2\text{-}1)$$

where σ is the surface tension of the heavier liquid and λ is the wave length. An unstable wave can grow to the amplitude at which it detaches from the heavier liquid and forms a droplet of approximate diameter λ, or radius $r \approx \lambda/2$.

Figure 19E.2-14b shows a corium stream of density ρ falling vertically at velocity V through stationary fluid of density ρ_∞. Here, the gravity term does not play a role in wave growth, and Equation 19E.2-1 gives the approximate minimum stable radius of droplets formed as

$$r_{min} > \frac{\pi\sigma(\rho + \rho_\infty)}{\rho\rho_\infty V^2} \qquad (19E.2\text{-}2)$$

If the debris stream discharge is determined by gravity draining, its downward velocity at distance z from the debris surface in the reactor is $V = \sqrt{(2gz)}$. Droplet sizes formed in air and water would be different because density ρ_∞ plays a strong role in Equation 19E.2-2.

When the debris stream first enters the water pool, it undergoes deceleration, a, due to the drag force. Under these conditions, the forces on the debris stream resemble those of Figure 19E.2-14a, except that the term g in Equation 19E.2-1 must be replaced by –(a + g). Stability of the frontal surface of liquid debris in contact with

water can be evaluated by setting $v_L = v_h = 0$ in Equation 19E.2-1. It follows that the expected stable droplet size formed is

$$r_{min}^2 \approx \frac{\pi^2 \sigma}{(a+g)(\rho - \rho_\infty)} \qquad (19E.2\text{-}3)$$

If a mass of debris M enters the pool at velocity V_0, the drag force causes a deceleration

$$a = \frac{C_d A \rho_\infty V_0^2}{2M} \qquad (19E.2\text{-}4)$$

where

A = the projected area of M, and

C_d = the drag coefficient.

(2) Debris Stream Broadening in Water

Equation 19E.2-4 gives an approximate deceleration of a debris mass entering the pool. If an average debris mass

$$M \approx A_0 L \rho$$

decelerates at

$$a = dV/dt = (dV/dy)(dy/dt) = VdV/dy$$

in the pool, its velocity at depth y below the water surface is obtained by integrating Equation 19E.2-4 with $V_0 = V$, which gives

$$\frac{A}{A_0} = \exp \frac{C_d \rho_\infty y}{\rho L} \qquad (19E.2\text{-}5)$$

The stream area broadens about 11% for an approximate C_d of 1.0. A debris stream which broadens in the pool would re-absorb small interface droplets formed by instability in the water. This action would tend to reduce the formation of many small interface droplets for high heat transfer into the water. It follows that substantial droplet formation in the water pool would have to occur by self-triggering. The dynamics of steam formation and the triggering process are discussed after a consideration of steam formation from a single debris droplet.

(3) Steam Formation, Single Debris Droplet

The amount of steam formed if all debris droplet thermal energy is transferred to an associated water mass M_w at P_∞ is given by

$$M_w = \frac{E'}{h_{fg}(P_\infty)} \tag{19E.2-6}$$

where

E' = the energy remaining for steam formation after heating M_w from a subcooled state to saturation.

That is, if E is the droplet total thermal energy,

$$E' = E - E_{sc} \tag{19E.2-7}$$

where

E_{sc} = the energy required to saturate the water mass,

$$E_{sc} = M_w c_v (T_{sat} - T_{sc}) \tag{19E.2-8}$$

The maximum volume of steam formed at ambient pressure is

$$V_g = \frac{E' v_{fg}(P_\infty)}{h_{fg}(P_\infty)} \tag{19E.2-9}$$

If the steam volume is spherical, its radius is

$$R_\infty^3 = 3V_\infty / 4\pi \tag{19E.2-10}$$

(4) Thermal Response Time of Corium Droplet

An idealized spherical debris droplet of radius r at temperature T undergoes convection cooling to the ambient fluid at a heat transfer rate,

$$q = 4\pi h r^2 (T - T_\infty)$$

Assuming uniform droplet internal temperature, the droplet internal thermal energy relative to its surroundings,

$$E = (4/3)\rho\pi c_v r^3 (T - T_\infty) \tag{19E.2-11}$$

is diminished at a rate q, for which

$$T - T_\infty = (T_i - T_\infty)\exp(-t/\tau_h)$$

where the time constant τ_h gives the convective time response as

$$\tau_h = \rho c_v r/3h \qquad (19E.2\text{-}12)$$

The internal conduction of heat occurs with an approximate time constant (Reference 19E.2-10),

$$\tau_c = 2r^2/\alpha \qquad (19E.2\text{-}13)$$

Either τ_c or τ_h may control the heat transfer rate to surrounding water. Figure 19E.2-14a gives the conduction and convection response times in terms of droplet radius for convection bounds defined by an enhanced film boiling coefficient of 3.0 times the Berenson horizontal flat plate value (Reference 19E.2-11), and with a nucleate boiling coefficient. Debris droplets at the liquidus temperature of 2600 K with surface waviness are expected to undergo enhanced film boiling heat transfer. Enhancement factors between 3.0 and 6.0 have been observed at liquid surfaces disturbed by gas bubbling (Reference 19E.2-12). The convective response time is seen to be proportional to the droplet radius in Figure 19E.2-14a. It is seen that internal conduction could become limiting for droplet sizes above 0.2 mm radius if nucleate boiling occurred, and above 10 mm radius if enhanced film boiling dominated the surface heat transfer.

(5) Hydrodynamic Response Time

A steam bubble formed by a single debris droplet grows to an equilibrium radius R_∞ at ambient pressure. The growth time depends on its rate of expansion, which can be estimated from the Rayleigh equation (Reference 19E.2-9) for a spherical bubble,

$$RR'' + \left(\frac{3}{2}\right)(R')^2 = (P_b - P_\infty)/\rho_l \qquad (19E.2\text{-}14)$$

where primes indicate derivatives with respect to time.

Since the pressure of the gas inside the bubble is not known it is necessary to introduce additional equations for the growth rate of the bubble. The rate at which mass enters the bubble may be approximated by

$$h_{fg}m'_g = hA_b(T_i - T_\infty)\exp(-t/\tau_h) \qquad (19E.2\text{-}15)$$

where τ_h is given by Equation 19E.2-12.

An energy balance for the bubble growth may also be written:

$$P_b V' - h_{fg} m'_g + U' = 0 \qquad (19E.2\text{-}16)$$

Assuming an ideal gas

$$U = P_b V_b / (k - 1) \qquad (19E.2\text{-}17)$$

If the bubble is further assumed to be spherical, one may combine Equations 19E.2-16 and 19E.2-17 to yield

$$12\pi k P_b R^2 R' + 4\pi P'_b R^3 = 3 m'_g h_{fg} (k-1) \qquad (19E.2\text{-}18)$$

Combining this equation with the mass rate Equation 19E.2-15 and the Rayleigh bubble Equation 19E.2-14 forms a system of three differential equations in the two dependent variables P and R. These equations were solved numerically assuming values of the constants which are typical of a corium-steam system. The initial conditions and other assumed parameter values are shown in Table 19E.2-17. A hydrodynamic time constant

$$\tau_L = R / R' \qquad (19E.2\text{-}19)$$

was obtained which is plotted in Figure 19E.2-14a.

Figure 19E.2-14a shows that τ_L is less than the convective heat transfer response times for either nucleate or enhanced film boiling. Therefore, in cases where the heat transfer from the debris droplets is controlled by convection, the surrounding water with a shorter dynamic time response gently expands with the steam bubble without permitting a high pressure difference to form. It follows that steam volume formation for the range of debris droplets shown in Figure 19E.2-14a is primarily determined by the droplet surface heat transfer rate.

(6) Conditions for Self-Triggering

Self-triggering could occur if the mechanical energy ΔW released from a molten debris droplet was sufficient to form additional droplets and mix them with surrounding water. The process of self-triggering is shown in Figure 19E.2-16. A debris droplet of radius r rapidly transfers its thermal energy to an associated water region from which steam is formed. The expanding steam performs a net amount of work on its surroundings. If part of the expansion work is sufficient to form one or more debris droplets and mix them with surrounding water, a propagating event

could occur, creating the potential for a steam explosion. The work required to form a debris droplet of radius r is approximately

$$\Delta W_\sigma = 4\pi\sigma r^2 \quad (19E.2\text{-}20)$$

where

σ = the surface tension of the liquid.

If the work required for mixing a new droplet with surrounding water is conservatively neglected, the condition for triggering is

$$\Delta W = \Delta W_\sigma \quad (19E.2\text{-}21)$$

An estimate of the expansion work done by a steam bubble which expands to volume V_∞ is given by

$$\Delta W = (P - P_\infty)V_\infty \quad (19E.2\text{-}22)$$

where P is an average pressure during expansion. The term $(P - P_\infty)$ can be approximated from the Rayleigh bubble equation, written as

$$P - P_\infty = \rho_L(RR'' + 3(R')^2/2) \quad (19E.2\text{-}23)$$

The bubble wall acceleration, R", is negative during the expansion. This can be shown from a large amplitude solution to the Rayleigh equation for the sudden appearance of a high pressure bubble which expands adiabatically (Reference 19E.2-13). If the term RR" is neglected, Equation 19E.2-23 yields a higher $P - P_\infty$, resulting in a conservatively high estimate of expansion work. The bubble wall velocity is estimated from the maximum size given by Equation 19E.2-10 and the convection response time of Equation 19E.2-12, that is, R_∞/τ_h. It follows that the debris droplet radius which could promote self-triggering can be estimated from

$$r_{\text{self-trig}} > \frac{2\sigma}{9\rho_L h^2}(\rho c_v)^{1/3}\frac{(h_{fg})^{5/3}}{[v_{fg}(T_i - T_\infty)]^{5/3}} \quad (19E.2\text{-}24)$$

(7) Conditions for a Steam Explosion

It is assumed that many droplets of molten debris have formed and are in the process of forming a submerged volume of steam, as shown in Figure 19E.2-17. The steam formation time corresponds to the convection response time τ_h of Equation 19E.2-12, since all droplets transfer heat simultaneously. The total involved water mass M_L

provides an equivalent inertia during steam expansion. The equation of motion for M_L can be written as

$$(P - P_\infty)A_L = M_L y'' \quad (19E.2\text{-}25)$$

where

$M_L = \rho_L A_L L$

The solution for y, based on an average pressure, is

$$y = (P - P_\infty)t^2 / 2\rho_L L$$

for which the approximate hydrodynamic response time for the overlying pool is

$$\tau_p^2 = \left.\frac{2y\rho_L L}{(P - P_\infty)}\right|_{y = L} \quad (19E.2\text{-}26)$$

The average pressure is estimated from

$$P \approx P_\infty(2V_{total} / A_L L) \quad (19E.2\text{-}27)$$

The total steam volume V_{total}, if formed at ambient pressure, can be obtained from Equation 19E.2-9 with E' replaced by

$$E'_{total} = NE' \quad (19E.2\text{-}28)$$

where N is the total number of debris droplets participating in the steam formation process. It is possible for a steam explosion to occur if the condition

$$\tau_p \gg \tau_h \quad (19E.2\text{-}29)$$

is satisfied. That is, if water motion is sluggish relative to the submerged steam formation, then it is possible to accelerate M_L to high velocity, accompanied by high pressure and impact.

19E.2.3.1.4 Application to ABWR

Table 19E.2-17 gives approximate values of the important parameters, partially explained in Figure 19E.2-18, which were used in evaluating the potential for an ex-vessel steam explosion in the ABWR.

First, the expected corium droplet sizes were found. The debris stream velocity and radius entering the water pool were obtained as V = 11 m/s, and R_0 = 3.7 cm. This then allowed the

computation of the stable droplet sizes formed by the debris stream falling through air and water:

r_{air} = 24mm

r_{water} = 0.03mm

However, debris stream broadening in the water will prevent small droplets from forming at the interface. The stream deceleration when entering the water was about 178 m/s^2, based on a cylindrical debris mass of approximately 3.7 cm radius and an equal length. This yielded droplet sizes of

r_{decel} = 2.5 mm

The expected average debris droplet size in the water corresponds to the instability of deceleration. With this information, the important response times for bubble growth were determined:

τ_h = 9.2s convection

τ_c = 1.8s internal conduction

τ_L = 0.006s bubble growth, single droplet

That is, steam bubble growth from debris particle energy is limited by the convective heat transfer rate.

Equation 19E.2-24 shows that self-triggering could occur if a debris droplet radius is greater than 8.3 mm, and therefore is unlikely in the ABWR for the expected droplet size of 2.5 mm.

A conservative, bounding analysis was considered in which it was assumed that a debris mass in the pool was broken up into small droplets of the expected 2.5 mm radius. The resulting heat transfer and hydrodynamic response times were evaluated according to the conditions for a steam explosion given in Equation 19E.2-29.

It was assumed that a debris stream which extended throughout the pool depth was the participating mass, corresponding to

$$M_d = \rho\pi R_0^2 L = 213\text{kg}$$

with a total thermal energy of

$$E = M_d c_v (T_{di} - T_\infty) = 256\text{MJ}$$

The mechanical work of steam expansion is

$$\Delta W = P_{\infty} E \frac{v_{fg}(P_{\infty})}{h_{fg}(P_{\infty})} = 19.3 MJ$$

This indicates that about 7% of the total thermal energy is converted into mechanical energy. This is far higher than the 1% to 3% range reported in experiments (Reference 19E.2-5), and is therefore highly conservative for assessing the potential for a steam explosion.

If the participating liquid mass is equivalent to the total in the lower drywell if the passive flooder were somehow to fail open before vessel failure,

$$M_L = \rho_L A_L L = 485,000 kg$$

Then the corresponding hydrodynamic response time is

$$\tau_{\rho} = 0.38 s$$

The convection heat transfer response time, found previously is

$$\tau_h = 9.2 \text{ s}$$

It follows that the condition for a steam explosion given in Equation 19E.2-29 is not satisfied, even for this bounding case, which employs the highly conservative 7% thermal energy conversion. Therefore, the steam explosion potential in ABWR is extremely low.

19E.2.3.2 100% Metal-Water Reaction

An analysis of the capability of the ABWR to withstand 100% fuel-clad metal-water reaction was performed in accordance with 10 CFR 50.34(f). Since the system is inerted, the containment atmosphere will not support hydrogen combustion. Therefore, it is necessary only to consider static loads on the containment.

A simple analysis was performed to determine the effect of the added hydrogen mass and heat energy associated with 100% fuel-clad metal-water reaction. Since the design basis accident for peak containment pressure is a large break LOCA, this accident was chosen as the basis for the analysis.

In order to simplify the analysis several conservative assumptions were made. Since it is not possible to release the hydrogen before the first pressure peak, only the second peak is considered. The hydrogen is distributed in the same manner as the nitrogen. All of the metal-water reaction heat energy is assumed to be absorbed by the suppression pool water. Finally, no credit was taken for the drywell and wetwell heat sinks.

Consideration of 100% fuel clad metal-water reaction results in a peak pressure of about 0.618 MPa. The governing service level C (for steel portions not backed by concrete)/factored load category (for concrete portions including steel liner) pressure capability of the containment structure is 0.770 MPa which is the internal pressure required to cause the maximum stress intensity in the steel drywell head to reach general membrane yielding according to service level C limits of ASME-III, Division 1, Subarticle NE-3220. Therefore, the ABWR is able to withstand 100% fuel clad metal-water reaction as required by 10 CFR 50.34(f).

19E.2.3.3 Suppression Pool Bypass

19E.2.3.3.1 Introduction

This subsection reviews the potential risk of certain suppression pool bypass paths and demonstrates that, with the exception of the wetwell drywell vacuum breakers, they present no significant risk following severe accidents. Because of this insignificance, only the vacuum breakers require further consideration in the ABWR PRA. The approach used in this evaluation is similar to that submitted to the NRC in support of the GESSAR (Reference 19E.2-14) review.

The result of this evaluation is that the remainder of these potential bypass paths contribute a small percentage of the total plant risk and therefore do not need to be specifically evaluated further in the PRA.

(1) Definition of Suppression Pool Bypass

Suppression Pool Bypass is defined as the transport of fission products through pathways which do not include the suppression pool. In such cases, the scrubbing action for fission product retention is lost and the potential consequences of the release are higher.

The potential for suppression pool bypass has been a subject of analysis since the early days of WASH-1400 (Reference 19E.2-7). The “V” sequence which represented a break of the low pressure line outside of the primary containment was one of the more dominant release sequences in WASH 1400. The IDCOR analysis and BMI-2104 also reviewed sequences in which the suppression pool scrubbing action was not obtained in the release pathway.

In order to review the importance of suppression pool bypass pathways, the potential mechanisms, probabilities and source locations were reviewed to identify where fission products might be released outside of the containment. The analysis has conservatively focused on the station blackout event because it leads to a higher likelihood of suppression pool bypass and because it is considered one of the more probable initiating events for core damage sequences.

The principal conclusion of the review is that, with the exception of certain lines addressed in containment event trees of the PRA, suppression pool bypass pathways do not contribute significantly to risk. Consequently, the probabilistic risk

assessment does not require a separate evaluation of bypass sequences, unless the bypass develops during the course of an event, for example, as a result of low suppression pool water level. Such cases are considered in Subsection 19.5.7.

Nevertheless, certain bypass lines which result from piping failures outside of the primary containment are included in this review in order to assess their significance.

(2) Mechanisms for Suppression Pool Bypass

All lines which originate in the reactor vessel or the primary containment are required by sections of 10 CFR 50 to meet certain requirements for containment isolation. Lines which originate in the reactor vessel or the containment are required by General Design Criteria 55 and 56 to have dual barrier protection which is generally obtained by redundant isolation valves. Lines which are considered non-essential in mitigating an accident are also required to automatically isolate in response to diverse isolation signals. Other lines which may be useful in mitigating an accident are considered exceptions to the General Design Criteria (NUREG 0800, Section 6.2.4) and are permitted to have remote manual isolation valves, provided that a means is available to detect leakage or breaks in these lines outside of the primary containment.

A potential mechanism for suppression pool bypass is the “Ex-containment LOCA” which results from the combined failure of a line outside of the primary containment along with the failure of its redundant isolation valves to close. If this combination of events occurs, the operator is made aware of the situation through leakage detection alarms and is instructed by plant procedures to manually isolate the lines, if possible, when the sump water level in areas outside containment exceeds a predetermined point.

Because of these provisions, the probability of suppression pool bypass occurring from the “Ex-containment LOCA” is extremely small since it requires the simultaneous failures of a piping system, redundant and electrically separate isolation valves and the failure of the operator to take action. Subsection 19E.2.3.3.4 summarizes an evaluation of the core damage frequency from ex-containment LOCAs.

The plant design criteria ensure a highly reliable system for containment isolation. Nevertheless, even though there is diversity in the types of valves, all types have experienced failures at operating nuclear plants and certain events, such as station blackout events, may make the early isolation of some lines impossible. This subsection evaluates the significance of bypass paths in order to justify that no additional treatment in the PRA is necessary.

(3) Methodology for Evaluation of Suppression Pool Bypass

The evaluation of suppression pool bypass pathways is based on a methodology which evaluates the potential relative increase in offsite consequence from bypass events over those events with suppression pool scrubbing. Then, knowing this amount of increase, if it can be shown that the probability of bypass is sufficiently low as to offset the increased consequence, the added risk from these pathways will be insignificant.

The justification for this approach is as follows:

Risk = Total [Event core damage Frequency x Consequence] (19E.2-30)

$$= F_{nbp} \times C_{nbp} + F_{bp} \times C_{bp} \quad (19E.2\text{-}31)$$

Where:

F_{nbp} = The total core damage frequency of non-bypass events

C_{nbp} = The consequence of a non-bypass event

F_{bp} = The total core damage frequency by bypass events which are equivalent to a complete bypass of the suppression pool

C_{bp} = The consequence of a complete bypass event

If the total bypass risk is to be insignificant, the last term in Equation 19E.2-31 must be much less than the first, or:

$$\frac{F_{bp}}{F_{nbp}} \ll \frac{C_{nbp}}{C_{bp}} \quad (19E.2\text{-}32)$$

The total bypass and non-bypass event frequencies (F) noted above are the total core damage frequencies for these events assuming that all events have the same consequence. Since this is seldom the case, the bypass frequency must be defined such that the proper consequence is applied. This is accomplished through evaluation of flow split fractions (f) as discussed below.

The total bypass frequency can be expressed as:

$$F_{bp} = F_{cd} \times \sum_{i} P_{cbpi} \quad (19E.2\text{-}33)$$

where:

F_{cd} = The total core damage frequency,

P_{cbpi} = The total conditional probability of full suppression pool bypass path i, given a core damage event

The conditional probability of full bypass can be further refined by the expression:

$$P_{cbpi} = P_{bpi} \times f_i \quad (19E.2\text{-}34)$$

where:

f_i = The fraction of fission products generated during a core damage event which pass through line i [Subsection 19E.2.3.3.3(1) discusses this term in more detail].

The flow split fraction (f) is defined as the ratio of the flow rate which passes out of the bypass pathway to the total flow rate of aerosols generated during the core melt process. The line flow split reduces the consequence associated with smaller lines due to inherent flow restrictions in those lines as compared with the consequence of larger lines. The flow split fraction accounts for this consequence reduction by reducing the equivalent bypass probability.

P_{bpi} = The conditional probability of bypass in line i [Subsection 19E.2.3.3.3(2) discusses this term in more detail].

The conditional probability of bypass is established through a detailed evaluation of each potential bypass pathway, establishing the failure which must occur for a bypass path to develop and assigning a probability to that failure.

Core damage events result in essentially two types of release: releases which bypass the suppression pool and those that do not. With this simplification, the total non-bypass frequency can also be defined as:

$$F_{nbp} = F_{cd} - F_{bp} \quad (19E.2\text{-}35)$$

Inserting Equations 19E.2-33, 19E.2-34 and 19E.2-35 into Equation 19E.2-32 yields:

$$P_{bpi} \times f_i \ll C_{nbp} / C_{bp} \quad (19E.2\text{-}36)$$

Assuming F_{bp} is much less than F_{cd} which would be consistent with the basis for containment isolation.

If Equation 19E.2-36 is satisfied, then the total bypass risk is insignificant.

(4) Criteria for Exclusion of Bypass Sequences in the PRA

As noted previously, if it can be shown that the probability of bypass is sufficiently low as to offset the increased consequence, the risk resulting from release through bypass pathways will be insignificant.

To establish a threshold for this frequency, the consequence ratio (right side of Equation 19E.2-36) was evaluated using the MAAP-ABWR and CRAC codes to establish the approximate order of magnitude for evaluation purposes.

For non-bypass case, the offsite dose from normal containment leakage following core damage was used as a basis. The "NCL" case of Reference 19E.2-42 is the consequence from normal containment leakage; "Case 7" of Reference 19E.2-42 may be used as an approximation of the full suppression pool bypass consequence. There is no credit for plate-out or holdup in the reactor building. Therefore, phenomena such as hydrogen burning in the reactor building will have no impact on this analysis.

The corresponding ratio is based on values in Reference 19E.2-42 and can be used in the evaluation of pool bypass significance. Further evaluation of "Ex-containment LOCA" suppression pool bypass paths in the PRA is not necessary if it can be shown that the total bypass probability is significantly less than this consequence ratio.

19E.2.3.3.2 Identification and Description of Suppression Pool Bypass Pathways

Identification of the potential suppression pool bypass pathways was based on information in the ABWR Standard Safety Analysis Report and supporting piping and instrument diagrams. The potential pathways are shown in matrix form in Table 19E.2-18.

Table 19E.2-1 summarizes the results of reviewing the ABWR design for lines which are potential pathways. For each line the table provides the line sizes, pathways and type of isolation up to the second isolation valve. The bypass lines identified in Table 19E.2-1 were derived from a systematic review of the ABWR P&IDs and other drawings.

Several lines in Table 19E.2-1 were excluded from further consideration on the basis of a variety of judgements discussed in the table notes. In general, the exclusion was based on deterministic rather than probabilistic arguments. For instance, the CUW return line to feedwater and LPFL Loop A were included in Table 19E.2-1 and excluded from further analysis because the bypass path is protected by the feedwater check valves.

The remaining lines are considered potential sources for significant fission product release following severe accidents. Although the probability that these lines could release a significant

amount of fission products is extremely small, they are reviewed further in Subsection 19E.2.3.3.3 to assess the importance of these releases.

19E.2.3.3.3 Evaluation of Bypass Probability

Equation 19E.2-36 of Subsection 19E.2.3.3.1 establishes the need for evaluation of the flow splits and failure probability for each line not excluded in Table 19E.2-1. This subsection provides the basis for the evaluation of each of these factors.

(1) Evaluation of Bypass Flow Split Fraction (f_i)

To assess the fraction of aerosol release which bypass the suppression pool a flow split fraction is needed, the flow split fraction (f) is defined as the ratio of the flow rate which passes out of a bypass pathway to the total flow rate of aerosols generated during the core melt process. Two generalized bypass paths have been evaluated:

(a) a path from the RPV which passes to the reactor building with the remainder passing to the suppression pool through the SRVs, and

(b) a path from the drywell to the reactor building with the remainder passing to the suppression pool through the drywell vents.

The flow split fraction may be defined as:

$$f = \frac{W_j}{W_j + nW_k} \qquad (19E.2\text{-}37)$$

where

W_j = the flow rate which passes through the bypass pathway

W_k = the vent flow rate in a single line (SRV or drywell vent) which passes to the suppression pool

n = the number of flow paths to the suppression pool

This can be simplified into the form:

$$f = \frac{f'}{1 + f'} \qquad (19E.2\text{-}38)$$

where

f' = W_j/nW_k

From the formula for turbulent compressible fluid flow (Reference 19E.2-15)

$$W = 1891\ Yd^2[(dP)/KV]^{1/2} \qquad (19E.2\text{-}39)$$

where

W = Flow rate(lb/h) (1 lb = 0.454 kg)

Y = Expansion factor

d = Internal diameter (in) (1 in = 25.4 mm)

(dP) = Differential pressure (psid) (1 psid = 6.89×10^3 Pa)

K = Resistance coefficient = f "L/D + K'

f " = Friction factor

L/D = Pipe length to diameter ratio, including corrections for valves, bends

K' = Additional factors for entrance and exit effects

V = Specific volume of fluid (f^3/lb) (1 f^3/lb = 0.0623 m^3/kg)

Solving for f ',

$$f' = \frac{1891 Y_j d_j^2[dP/KV]^{1/2}}{1891 n Y_k d_k^2[dP/KV]^{1/2}} = \frac{Y_j d_j^2[dp/K]^{1/2}}{n Y_k d_k^2[dp/K]^{1/2}} \qquad (19E.2\text{-}40)$$

Equation 19E.2-40 may be rearranged to show:

$$f' = (1/n)[Y_j/Y_k][d_j/d_k]^2[dP_j/dP_k]^{1/2}[K_k/K_j]^{1/2} \qquad (19E.2\text{-}41)$$

The expressions in Equation 19E.2-41 were evaluated numerically for the actual line configurations to arrive at the flow split fractions used. The following assumptions were made in this analysis:

(a) Containment pressure following the core melt is assumed to be at an average of 0.411 MPa during the post core melt period. Although the containment pressure could eventually increase to a higher level, the average is used to assess the total amount of release since a release would be occurring throughout this period. This pressure is typical of those calculated in severe accident analyses (Figures 19E.2-2a through 19E.2-12a).

(b) Prior to RPV melt-through, the reactor pressure vessel (RPV) is maintained at a relatively low pressure [0.790 MPa] by the automatic depressurization system or equivalent manual operator action. Four ten inch safety relief valves (ADS valves) are conservatively assumed to be open to release RPV effluent to the suppression pool. This is consistent with the minimum instructions in the EPGs. Ten 0.7 m horizontal vent paths are assumed to be uncovered consistent with the ABWR design configuration. For conservatism the vents are assumed to be one-quarter uncovered.

(c) The pressure drop in the bypass path between the fission product source and the release point is a function of whether the line produces sonic or sub-sonic velocities. For RPV sources, an average 0.790 MPa internal RPV pressure is assumed during the core melt process. This is based on an average 0.411 MPa drywell pressure and an assumed SRV design which closes the SRV when a differential pressure of about 0.345 MPa exists between the main steamline and the SRV discharge line.

Depressurization of the RPV or containment throughout the bypass path is not considered. The assumption is made that pressure is continuously generated during the severe accident in sufficient quantity to uncover the SRV discharge or drywell vents.

(d) The pressure from the non-bypass path between the fission product source and the suppression pool release point depends on the suppression pool level. The suppression pool level is assumed to be higher than normal because of the depressurization of the RPV to the Suppression pool through the SRVs. For RPV sources, the SRVs experience about a 6.0 m (20 ft) elevation head over the SRVs during the core melt process. For drywell sources a 4.5 m (15 ft) elevation head is experienced over the upper horizontal vent. For the station blackout sequence, the effect of ECCS system operation on suppression pool level has been ignored.

(e) The length of lines discharging to the suppression pool and through the bypass paths affects the resistance coefficient in Equation 19E.2-39. Based on the ABWR arrangement drawings this length is estimated to be approximately 25 m (85 ft.). For the drywell sources, the path to the suppression pool is estimated to be 1.5 m (5 ft.).

Other values used in the calculation are listed below:

Parameter	Assumed Value	Basis
Resistance Coefficient	(K=f'L/D)	
Friction Factor	0.011 to 0.018	Reference 19E.2-15 (pg A-25) (Size dependent)
Line Diameter (D)	Various	Line size (Table 19E.2-1)
Other Resistances (K)		Reference 19E.2-15
Gate valve	13	(pg A-30)
Check valve	135	
Globe valve	340	
Entrance effects	0.5	
Exit effects	1.0	
Expansion Factor (Y)	0.6 to 0.9	Reference 19E.2-15 (pg A-22) (dP, K dep.)

Table 19E.2-19 shows samples results (f ' from Equation 19E.2-41) for a line with two motor-operated valves. In the evaluation of individual bypass lines the actual configuration is used. The evaluation of flow split fractions is considered to be conservative for several reasons:

(i) Bypass release paths would normally be expected to be more restricted than evaluated due to smaller lines, more valves and pipe bends, valves being partially closed or pipe breaks being smaller than the piping diameter.

(ii) No credit is taken for additional retention of fission products in the reactor building, in piping or through radioactive decay.

(iii) For drywell sources, a higher than analyzed differential pressure should exist between the drywell and wetwell. This will lead to lower flows through the bypass path.

(2) Evaluation of Failure Probabilities (P_{bpi})

The failure probabilities used for the detailed calculation of the bypass probabilities are summarized in Table 19E.2-20. The bases for these probabilities are provided below:

(a) Failure to close probability with a common mode failure probability (P_1) is assumed for failure of both valves in a single line to close.

(b) Current operating plants evaluate MSIV leakage against a leakage requirement of 0.33 m^3/h per valve. 50% of valves are assumed to fail this local leak rate test at this level and about 10% are assumed to typically exceed 18 m^3/h level:

		Probability	
Group	**Leakage**	**Per Valve**	**Per Line**
G1	<0.33 m^3/h	0.5	0.5
G2	0.33 m^3/h to 18 m^3/h	0.4	0.2
G3	>18 m^3/h	0.1	0.01

The MSIV leakage probability (P2) is assigned a value to correspond to the total line leakage probability. Flow split fractions were determined and a weighted average flow split fraction (weighted by the line leakage probabilities) was determined for use in the evaluation.

(c) The probability (P3) of flow passing to the main condenser is judged to be governed by the failure of the bypass valve to close. Once flow passes to the main condenser, the condenser is assumed to fail (P4) via the relatively low positive pressure rupture disks.

(d) The main steamline break probability (P5) was line break probability (P15).

(e) Normally open pneumatic (P6) and DC motor operated valves (P7) have failed to close. Causes include improper setting of torque switches leading to valve stem failure, undetected valve operator failures and improper packing materials or lubricants. These failure rates in general are not significantly affected by the valve environments. A common-cause failure among air-operated valves was considered for lines containing redundant series valves.

(f) Normally open AC solenoid and motor-operated valves are subject to a common mode failure (P8) if motive power is unavailable such as during a Station Blackout event. For station blackout events these valves will have a conditional failure probability to close of 1.0.

However, since a loss of power is not expected to result from a break outside containment, an industry failure rate may be used. For those lines with redundant valves, a common cause failure probability was assumed.

(g) Check valves have been observed to fail in such a way as to permit full reverse flow, a condition necessary to permit suppression pool bypass for some lines. Maintenance errors associated with testable check valves have also been observed. The failure rates for check valves allowing complete reverse flow (P9) was based on 7000 hours of operation per operating cycle. A common-cause failure among check valves was considered for lines containing redundant series check valves. Only Feedwater and the SLC paths contain more than one check valve.

(h) When power is available, some normally closed valves open during an event in response to an injection signal, even though the actual injection fails (a requirement for a core damage to occur).

The probability that ECCS valves are not closed by an operator (P10) is considered remote during a severe accident. For station blackout events, since the valves do not open, these lines do not contribute to potential bypass risk.

(i) Some normally closed valves may be open at the beginning of the event. The failure probability (P11) for these valves assumes they are open 4 hours during a 7000-hour operating cycle and that the operator fails to recognize the open path and close the valve.

(j) Some valves may be opened by the operator during the course of the event. Such action may be in compliance with written procedures or it may occur due to confusion in following a procedure. The probability that valves are inadvertently opened (P12) is considered a violation of planned procedures.

(k) Pipe rupture is extremely rare in stainless steel piping. However, carbon steel piping has been observed to fail under certain conditions. Except for the CUW break, four line segments outside of the containment are assumed for each bypass line (CUW system estimated to have 50 segments). The intermediate line size [80A to 150A (3 to 6 inches)] break probability is assumed to be twice that of the large line size [greater than 150A (6 inches)].

For pipe failures in an individual bypass line, it was presumed that an undetected break in an unpressurized line could occur at any time. Therefore, the conditional probability of a bypass path was then taken to be the same as the failure rate during a one-year period (which was estimated to be 7,000 hours). This approach of estimating pipe failure probability is judged to be conservative.

Whether the bypass path is the initiator or occurs simultaneously with the event is inconsequential in the evaluation based on the following discussion. The approach

taken in the bypass study is to consider the presence of a bypass path as an independent event from the events which caused the core damage in a specific sequence. This approach is acceptable because for large breaks the associated systems are not in general relied upon to prevent core damage and no consequence of these failures have been identified which would affect the systems preventing core damage. Therefore whether the break is an initiator or consequential does not affect the final evaluation. Similarly, none of the systems associated with the smaller bypass lines are associated with preventing core damage. Therefore, they too are not associated with the cause of the core melt.

The ACRS has expressed concern regarding the failure of the CUW suction in combination with failure of the isolation valves to close. The concern is that the isolation valves must close under high differential pressure conditions and the entire secondary containment may be subjected to high temperature and humidity conditions that may fail the ECCS systems. In addition, there may be a flooding situation that could have a high consequence if it leads to an eventual loss of suppression pool and CST inventory or flooding of other ECCS rooms. Such an event would not be consistent with this presumed independence of the assumed conditional probabilities.

If a break in the CUW suction line were the postulated LOCA, the containment isolation valves would be expected to close, terminating the event. NRC concerns over Motor Operated Valve (MOV) closure capability are being addressed as an industry activity. In this evaluation it was assumed that the valves fail to close due to a common cause failure. Should the isolation valves fail to close, the operator can close the CUW remote manual shutoff valve. If all three valves should fail to close, the system arrangement assures that the core is not uncovered and EPGs require depressurization and controlling water level below the break elevation which both slows the break flow and terminates any long-term release from the break. Therefore, if the EPG actions are taken, no additional consequence of the event occur.

The system arrangement routes the CUW lines above the core to avoid a potential siphon of the core inventory. In the event of an unisolated CUW line break, lowering the RPV level to below the shutdown cooling suction and depressurizing the RPV would be sufficient to terminate the break flow without causing core damage. These actions are included in Subsection 19D.7.

(3) Evaluation of Bypass Probability

Table 19E.2-21 summarizes the results of these evaluations. For each potential bypass pathway, it shows the flow split fraction based on the line size and valve configuration, the equation to calculate the bypass probability, the results of the probability calculations using the data from Table 19E.2-20 and the bypass fraction for the line. The table also includes reference to the sketch (Figure 19E.2-19a to 19E.2-19k) which illustrates the potential pathways.

(4) Evaluation of Results

Subsection 19E.2.3.3.1(4) provides a conservative justification that certain bypass paths do not substantially increase the offsite risk. The bypass fraction is shown in Table 19E.2-21, for all potential paths not addressed in the containment event trees.

Potential bypass through the Wetwell-Drywell Vacuum Breakers are included in the containment event trees. (Subsection 19D.5).

Based on the above discussion, it can be concluded that suppression pool bypass paths and Ex-Containment LOCAs not addressed by the containment event trees do not contribute a significant offsite risk and do not need further evaluation in the PRA.

19E.2.3.3.4 Evaluation of Ex-Containment LOCA Core Damage Frequency

(1) Introduction

To provide a separate assessment of the importance of bypass paths, a more comprehensive analysis of the frequency of core damage from LOCAs outside containment was conducted using event tree and fault tree techniques.

Conservative and simplified event trees of LOCA outside containment events were developed and included as Figures 19E.2-20a through 19E.2-20c. The end-point for these trees is core damage with or without bypass of the containment.

(2) Assumptions

The following definitions and considerations were applied in development of the trees.

- V_1—Line Break Outside

  The frequency of piping breaks in small, medium or large breaks outside of containment and which communicate directly with the reactor vessel. The lines are grouped by type of isolation. The basis for each event initiation frequency is the line size and the total number of lines considered. The basis for the pipe break frequency is provided in Subsection 19E.2.3.3.3 (2)(k).

- X_1—Line Isolation

  The conditional probability of automatic isolation valves failing to close given the ex-containment LOCA. Values used and the manner in which probabilities were combined are shown on Figures 19E.2-20a through 19E.2-20c.

- P_1—Operator Action

  The conditional probability that operator fails to act to manually isolate the ex-containment LOCA. Such a failure to act could be due to a lack of

instrumentation availability or mechanical failure. For most bypass paths considered, the very conservative assumption was made that no operator action is taken. For ECCS discharge lines and warm-up lines the operator is assumed to act to close an open valve, if needed. The basis for the value chosen [Subsection 19E.2.3.3.3(2)] is based on general operator awareness of the potential for these paths to be unisolated. Although the leak detection system is adequate to alert the operator of a break in the system, instrumentation failure is not considered to provide a strong contribution to the failure probability. For CUW and RCIC line breaks, operator action within one hour was assumed.

- Q_1—Other Divisions not Affected

  For most lines it is conservatively assumed that the LOCA affects the division in which the break occurs. This factor represents the conditional probability that the LOCA also affects the required makeup for core cooling from other electrical divisions. It is assumed that such failure results from environmental effects from flooding or pressurization/steam effects.

  A systematic evaluation of potential cold flooding due to ex-containment breaks was summarized in Appendix 19R, "Probabilistic Flooding Analysis." Flooding in the reactor building is assumed to disable the system affected and potentially flood the Reactor Building corridor, but not disable other makeup equipment due to the water-tight doors contained in the design. The analysis of an unisolated CUW break in Subsection 19R.4.5 shows that no cooling systems will be damaged due to flooding.

  Compartment pressurization and environmental effects of high pressure LOCAs in secondary containment were considered in the development of Figures 19E.2-20a through 19E.2-20c. Equipment in the ABWR design is arranged with consideration of divisional separation. A high energy line break in a division would cause the blowout panels from the division to relieve the initial pressure spike to the steam tunnel. Subsequent pressurization of the room could eventually cause a release of the energy into the adjacent divisions.

  As doors from the corridor and penetrations are forced open, the environment of the adjacent divisions could be affected by the presence of steam. However, the equipment is qualified to 373 K (212°F) and 100% humidity. Where a LOCA could occur in an area adjacent to a separate division, a value was assumed for Q_1, based on engineering judgment, to represent the possibility for failure of these adjacent systems. For the CUW line break outside containment, Q_1, was assumed to be 1.0 because equipment in all three safety divisions will experience a high temperature and steam environment. The impact of this environment is reflected in the coolant makeup unavailability (Q_o).

For line breaks in the turbine building the effect of the break would not impact the divisional power distribution and, for these sequences, the Q_1 value was judged to be negligible.

Although line routing are not specified, the analysis assumes that breaks inside reactor building equipment rooms affect the division in which the breaks occur; LOCAs outside of the secondary containment are not assumed to fail a division of equipment.

- Q_0—Coolant Makeup

  This factor represents the conditional probability of core cooling failure by all sources of cooling with consideration to those affected by the ex-containment LOCA. The values used are derived from an evaluation of the PRA fault trees.

  The conditional probability when one or more electrical divisions are affected were derived by disabling the most limiting division in the LOCA event trees and then calculating the resulting conditional probability. Only the medium LOCA CUW or RCIC line breaks could potentially affect all divisions since larger lines are in containment or the steam tunnel and smaller lines do not contain sufficient energy to affect all divisions.

  For LOCAs which occur in the reactor building, the event is assumed to fail the division in which the break occurs. For other LOCAs, such as LOCAs in the turbine building, no divisional impact is assumed.

  Consideration of inventory depletion due to the LOCA outside containment is addressed by EPGs which specify that coolant makeup sources using inventory sources outside of containment be used as the preferred source. In the ABWR design small breaks can be accommodated by any of the high pressure coolant makeup systems (RCIC, HPCF B and HPCF C) which are in separate divisions and which draw water from the condensate storage tank. Since condensate is effectively an unlimited supply for small breaks and makeup capability exists, no additional concern is necessary for the small break LOCAs outside of containment.

  Medium and large breaks outside of containment can be accommodated by any of the three divisions in the short term following a break without concern for inventory loss in the RPV. All penetrations, except the RPV/CUW bottom head drain (a unique situation addressed separately in Subsection 19.9.1 by an event specific procedure), are above the top of active fuel so that core uncovery due to inventory depletion is not a concern. In the longer term, the break will depressurize the RPV which effectively reduces the loss of inventory from the break to a level well within the makeup capacity of other available systems which

makeup from sources outside of containment, such as condensate. Due to the reduction in loss rate through the break, significant time is available for operators to compensate for the usage of water and flooding in the affected area. Furthermore, operators are assumed to follow plant procedures in isolating the break or controlling RPV level to a level below the affected penetration, if necessary. Adequate instrumentation and long term makeup from condensate sources would normally be available.

(3) Conclusion

For each of the event trees shown in Figures 19E.2-20a through 19E.2-20c the total non-bypass and bypass core damage frequencies were evaluated.

Ex-containment LOCA events without bypass represent a small fraction of the total core damage frequency . Therefore, they are justified as not being further evaluated in the PRA.

Although the consequence from bypass events is greater than for non-bypass events, the total frequency of bypass events concurrent with core damage is extremely small. The core damage frequency of ex-containment LOCAs with bypass are an extremely small percentage of the total evaluated core damage frequency. Large LOCAs can be excluded from further consideration on the basis of low probability. Exclusion of Intermediate and Small bypass sequences is based on the additional consideration of the reductions in consequences of the ex-containment LOCAs due to the flow splits provided by restrictions due to line sizing. This is discussed in Subsection 19E.2.3.3.3.

In addition, since significant margin exists between the current PRA results and the safety goals, it can be concluded that the bypass events do not significantly contribute to the offsite exposure risk.

19E.2.3.3.5 Suppression Pool Bypass Resulting from External Event Analysis

The effect of external events on the Suppression Pool Bypass evaluation is discussed in Appendix 19I to determine if a significant potential for bypassing the suppression pool results from component failures induced by a seismic event. Only seismic events were considered to provide a significant challenge to the creation of bypass paths beyond that already considered in the PRA.

19E.2.3.4 Effect of RHR Heat Exchanger Failure in a Seismic Event

A failure of the RHR heat exchanger mounting can conservatively be postulated to shear the pipe between the RHR pump discharge and the RHR heat exchanger. About 30 minutes is available for the operator to close the RHR suction valve to the suppression pool. If no power is available, or if the operator failed to close the suction valve(s), the suppression pool will drain to the RHR equipment rooms.

This subsection describes the analysis of these sequences which concludes that structural integrity of the RHR equipment room will be maintained and that, in effect, the suppression pool scrubbing is transferred from the wetwell to the RHR equipment rooms.

19E.2.3.4.1 RHR Equipment Room Flooding

The RHR equipment rooms drain to a sump. This sump also receives drains from the HPCF equipment room (in two cases) and from the RCIC room (in one case).

The analysis of the resulting loads in the RHR equipment and the basis for concluding that the room will remain intact is described in the following paragraphs.

19E.2.3.4.2 Dynamic Loads Induced by Chugging

The dynamic loads on the RHR equipment room wall resulting from a postulated break of the RHR pump discharge pipe were estimated using applicable test data. The most limiting wall is assumed to run parallel with the discharge pipe at a distance of approximately 1.22 m (4 ft) from the piping. The length of this wall is 13.1 m (43 ft), the height is 6.1 m (20 ft). The RHR pump discharge piping is assumed to run 0.61 m (2 ft) above the equipment room, with the rupture located exactly opposite to the middle of the wall (worst case).

The dynamic loads result from the discharge of the containment atmosphere through the broken pipe into the water pool in the RHR equipment room. It was conservatively assumed that the entire volume of the equipment room was flooded with the suppression pool water.

The gas discharged from the broken pipe will be initially almost pure nitrogen, later a mixture of nitrogen and steam with decreasing nitrogen content, and finally, after all the nitrogen is purged out of the containment, pure steam. The mean flow rates through the broken pipe will be a function of pressure in the containment, which in turn will initially depend on the accident scenario. In the long term, however, the mass flow rate will be driven by the steam generated from the decay heat. It is assumed that there will be no pressurization of any airspace remaining in the RHR equipment room.

This situation is similar to the discharge of the drywell atmosphere through the drywell vents into the suppression pool during a LOCA. The test results from LOCA tests conducted for a wide range of break sizes demonstrate that the highest wetwell pressure loads due to this discharge are experienced late in the event during the “chugging” regime characterized by low mass fluxes <48.9 kg/s•m^2(<10 lbm/s•ft^2) and high steam/air ratios (<1% air). At higher mass fluxes the “condensation oscillation regime” and higher air contents, the loads were substantially lower.

To estimate the chugging loads on the RHR room wall, the Mark III PSTF test data were used. The Mark III data were chosen because of the horizontal orientation of the vents and because no pressurization of the airspace above suppression pool which approximates the situation in the ABWR RHR room. The highest chugging loads on the wall seen during the Mark III

experiments were 0.790 MPa. These pressures were observed on the drywell wall adjacent to the vent exit into the pool. Because of the close proximity of the pressure sensor to the source of the pressure disturbance (the collapsing steam bubble) this pressure can be considered to be the actual bubble pressure.

The period between the pressure spikes was typically 1 to 5 seconds or more. Following the peak pressure spike, a series of lower amplitude pressure oscillations were observed, with frequencies that were in the range of the natural frequencies of the vents and water pool. The maximum amplitude of these oscillations was typically less than 10% of the maximum pressure spike.

Given the RHR equipment room geometry, and using a conservative pressure attenuation model (supported by the Mark III experimental data), it was calculated that the peak, spatially averaged, dynamic wall pressure will be below 0.028 MPa, if the maximum bubble pressure of 0.790 MPa is assumed. With higher flowrates and higher non-condensable contents in the discharge, the loads are expected to be lower. Therefore, this conclusion should also cover a range of severe accidents during which non-condensable gases (e.g., H_2, CO_2) are generated from metal-water reaction and/or corium-concrete interaction.

19E.2.3.4.3 RHR Equipment Room Structural Integrity

The structural integrity of the RHR equipment room structure was evaluated for the loads resulting from the seismic-induced flood. The RHR room is located at the reactor building basemat level in each of the three divisions. The wall is approximately 13 m (43.64 ft) wide, 6.5 m (21.32 ft) tall, and 0.5 m (1.64 ft) thick.

The compartment walls were examined for their abilities to withstand a 2g earthquake which is the median peak ground acceleration required to fail the heat exchanger mounting causing the postulated room flooding. No structural damage is predicted, although some concrete cracking is inevitable. After the earthquake, the wall would be structurally sound to withstand the loads imposed by flooding as described below.

The seismic-induced flood imposes loadings to the room in the form of hydrostatic and hydrodynamic pressures. It is assumed that no damaging aftershocks would occur during flood. From the above discussion the most significant hydrodynamic load is caused by chugging. The pressure transient on the wall is idealized by a sharp pressure spike with a maximum amplitude of about 0.028 MPa preceded by a half cycle sinusoidal and followed by a decay sinusoidal with much smaller amplitudes.

To find the dynamic effect on the wall response, the pressure transient described above is approximated by an isosceles triangular pulse with a peak value of 0.028 MPa. For this type of loading, the maximum dynamic amplification factor is about 1.5 regardless of structural frequencies. For conservatism, the equivalent static chugging pressure is taken to be 0.143 MPa.

Under the combined hydrostatic pressures of a fully flooded condition and equivalent static chugging pressure uniformly distributed over the entire wall, the stress analysis was performed and the resulting maximum moment is found to be about 44% of the ultimate moment capacity in accordance with the ultimate strength design method for reinforced concrete. The maximum shear stress is within the ACI-349 code allowable. The leaktight RHR room access door was also evaluated and is found to be structurally sound against flood loadings.

In summary, the structural integrity of the RHR room can be maintained for the seismically-induced flood.

19E.2.3.5 Impact of Flashing During Venting

The adoption of the Containment Overpressure Protection System (COPS) in the ABWR design limits the potential release from the containment in the unlikely event that containment failure is immanent. In the absence of significant suppression pool bypass, the fission products will be scrubbed as they pass through the suppression pool. The predominant conditions in the suppression pool yield very high decontamination factors for all fission products except the noble gasses. Given the extremely low releases from the gas space which result from suppression pool scrubbing before the rupture disk opens, the potential release resulting from the rapid depressurization at the time the rupture disk opens must be considered.

It is shown that the initial decompression wave generated by the opening of the COPS rupture disk is not large enough to lower the pool surface to its saturation pressure and therefore no initial swell due to vapor flashing occurs. The suppression pool does not start to flash until the wetwell has depressurized to the pool saturation pressure.

Comparison of the time constant for blowdown with the time constant for the pressure wave propagation around the wetwell demonstrates that the suppression pool acts as a one-dimensional body for the purpose of this analysis. This allows the calculation of the pool swell height. Comparison of this level to the location of the containment penetration indicates that there is no potential for water to enter the COPS piping. This eliminates the need for consideration of both water loads on the COPS piping and of fission product transport with water. It is also necessary to consider the potential for water droplets to be entrained from the pool surface and carried into the COPS piping. Calculation of entrainment at the surface of the suppression pool is considered using the work of Rozen, et. al. (Reference 19E.2-17) and is found to have an insignificant impact on fission product release.

19E.2.3.5.1 Response of Suppression Pool Surface to Decompression Wave

19E.2.3.5.1.1 Summary

Sudden opening of the containment overpressure protection system (COPS) rupture disk causes a gas discharge from the ABWR pool airspace. The associated decompression wave which enters the airspace spreads to the pool surface. It is necessary to determine how the pool surface responds to the arriving decompression. If the decompression wave causes pool pressure to fall

below the saturation pressure, rapid vapor formation would cause the pool to swell as a flashing steam/water mixture. However, if the arriving decompression does not cause the pool pressure to fall below its saturation value, flashing would not occur, and the pool would respond as a compressed liquid.

The theoretical modeling used to determine pool response from operation of the COPS includes prediction of:

- The gas discharge rate
- The velocity and decompression disturbances originating where the COPS enters the airspace
- Expansion of the decompression into the airspace, and its attenuation with distance
- Decompression transmission from the airspace into the pool at the water surface
- The pool water dynamic and thermodynamic response

It was found that the originating decompression wave entering the containment airspace was 38.8 kPa, dropping below the initial 721 kPa air pressure. The decompression wave leaving the COPS pipe of 0.275 m (0.9 ft) radius would reach the pool surface a distance of 4 m (13.12 ft) away, attenuating from 38.8 kPa to 2.67 kPa. Since sound speed and density of water are much higher than corresponding values in air, a decompression wave entering the water is nearly twice that arriving in the air, or about 5.34 kPa. The decompression is not large enough to cause pool pressure to drop below its saturation pressure of 330 kPa at its initial temperature of 410 K, or 137°C (738 R or 278°F). The pool surface would move upward at only 0.0044 m/s (0.014 fps) for the transmitted decompression.

19E.2.3.5.1.2 The Gas Discharge Rate

The COPS pipe has a radius R and area A. The open COPS rupture disk has a flow area a. Since the airspace pressure P_o is 721 kPa and discharge is into the atmosphere at 101 kPa, the initial air flow is expected to be choked in the valve throat at a choked mass flux of (Reference 19E.2-37)

$$G_{gc} = \left(\frac{2}{k+1}\right)^{(k+1)/2(k+1)} \sqrt{k g_0 P_0 \rho_{g0}} \qquad \text{(19E.2-41a)}$$

The quasi-steady mass flow rate through the pipe and valve is expressed as

$$m = G_{gc} a \qquad \text{(19E.2-41b)}$$

Assuming isentropic flow from the airspace to the throat, and expressing the airspace sound speed as:

$$C_{g0} = \sqrt{(kg_0P_0)/\rho_{g0}} \tag{19E.2-41c}$$

the discharging mass flow rate is obtained in the form,

$$\frac{m}{AC_{g0}\rho_{g0}} = \left(\frac{2}{k+1}\right)^{(k+1)/2(k+1)}\frac{a}{A} \tag{19E.2-41d}$$

19E.2.3.5.1.3 Disturbance Entering the Airspace

It is assumed that the COPS valve opens instantly, causing an instantaneous quasi-steady flow in the attachment pipe. This assumption gives the maximum pipe velocity, which corresponds to a maximum initial decompression wave.

Acoustic theory can be applied if pressure disturbances do not create Mach numbers much greater than 0.2. An area ratio of a/A = 0.132 (diameter ratio of d/D = 0.364) with an airspace state described by

P_0 = 721 kPa

T_0 = 410 K (278°F)

g_0 = 6.16 kg/m^3 (0.384 lbm/ft^3)

C_{g0} = 406 m/s (1332 fps)

yields a gas velocity in the pipe of 31 m/s (102 fps). The corresponding mach number is 31/406 = 0.076, which justifies treating the decompression as an acoustic wave.

It is further assumed that the discharge begins suddenly, imposing the pipe flow velocity of 31 m/s at its entrance. In order to employ spherical propagation of the acoustic wave, an imaginary hemisphere of pipe radius R = D/2 = 0.55/2 m = 0.275 m (0.902 ft) has twice the pipe flow area, reducing the entrance velocity on the hemisphere to 31/2 = 15.5 m/s (50.8 fps). The acoustic equation,

$$\delta P_0 = \frac{C_\rho \delta V}{g_0} \tag{19E.2-41e}$$

can be employed to show that the corresponding decompression disturbance is P_0 = 38.8 kPa (5.6 psid).

19E.2.3.5.1.4 Expansion Into Airspace

The acoustic decompression wave propagation is governed by the spherical wave Equation19E.2–41b,

$$\frac{\partial^2 P}{\partial t^2} - \frac{C^2 \partial}{r^2 \partial r}\left(r^2 \frac{\partial P}{\partial r}\right) = 0 \qquad \text{(19E.2-41f)}$$

with the boundary and initial conditions at r = R of

$$P = P_0 - \delta P_0 \qquad \text{(19E.2-41g)}$$

a boundary condition as r approaches infinity of

$$P = P_0 \qquad \text{(19E.2-41h)}$$

and initial conditions at t = 0 of

$$P = P_0 \qquad \text{(19E.2-41i)}$$

$$\frac{\partial P}{\partial r} = 0 \qquad \text{(19E.2-41j)}$$

A solution for the outgoing decompression wave is given by

$$\frac{\delta P}{\delta P_0} = \frac{R}{r} e^{-(Ct/r - r/R + 1)} H_s\left(t - \frac{r - R}{C}\right) \qquad \text{(19E.2-41k)}$$

where H_s is the Heaviside step function, which is zero for negative arguments, and 1.0 for positive arguments. A pressure disturbance in the airspace will travel from r = R to another r at the acoustic speed C, which requires a time (r - R)/C. When it does arrive, H_s is 1.0, and the arriving magnitude is

$$\delta P = \frac{R}{r} \delta P_0$$

It is seen from Equation (19E.2-41k) that even after the decompression arrives at r, its amplitude decays exponentially with time. This feature is excluded from the analysis for conservatism.

If the water surface is a distance r = 4 m away from the COPS pipe, the arriving decompression wave will have an amplitude of only 2.67 kPa.

19E.2.3.5.1.5 Transmission into the Pool

The arriving decompression wave undergoes both simultaneous transmission and reflection at the pool surface interface. Acoustic theory for a plane wave arriving at a flat surface discontinuity of density and sound speed gives the ratio of transmitted to oncoming pressure disturbances as

$$\frac{\delta P_{transmitted}}{\delta P_{oncoming}} = \frac{2}{1 + \rho_1 C_1 / \rho_2 C_2} \qquad (19E.2\text{-}41l)$$

where subscripts 1 and 2 refer to the airspace and water in this case. A water density and sound speed of 1000 kg/m3 and 1220 m/s yields a transmitted/oncoming pressure of

$$\frac{\delta P_{transmitted}}{\delta P_{oncoming}} = 1.99$$

That is, the decompression wave arriving at the pool surface nearly doubles from the oncoming value to 5.34 kPa. The plane wave analysis employed here is based on left and right traveling waves which add to satisfy continuity and energy conservation at the interface (Reference 19E.2-38). A similar analysis for spherical waves is obtained from the method of images to provide a plane surface of symmetry. The local pressure transmission and reflection amplitudes are the same as those obtained from the plane wave analysis (Reference 19E.2-38).

19E.2.3.5.1.6 Water Dynamic and Thermodynamic Response

The 5.34 kPa decompression wave transmitted into the water pool does not lower the initial 721 kPa pressure anywhere near the 330 kPa saturation pressure. Therefore, the arriving decompression cannot cause rapid pool flashing and swelling. Steam formation will occur in the pool later when continued decompression of the airspace lowers the pressure below saturation.

The water is expected to respond acoustically to the arriving decompression, taking on a velocity obtained from Equation 19E.2-46, written for the liquid as

$$\delta V_L = \frac{g_0 \delta P}{\rho_L C_L} \qquad (19E.2\text{-}41m)$$

where subscript L refers to the water, and δP is the transmitted pressure disturbance. The resulting pool velocity is only 0.0044 m/s (0.014 fps).

19E.2.3.5.2 Critical Time Constants for Blowdown Response

The time constant for the depressurization of the wetwell airspace is calculated from critical flow considerations. Comparing this value to the time constant for propagation of a pressure wave around the wetwell annulus allows one to determine if non-uniform effects in the suppression need to be considered in calculating the suppression pool response.

The depressurization time constant for the wetwell airspace is estimated based on the critical flow through the rupture disk opening and the ideal gas law. There are two sources of steam to the wetwell airspace: the blowdown through the vent system of steam and non-condensable gas from the drywell, and the boiling or steaming of the suppression pool which results from the pressure decrease. If both of these sources are neglected, the time constant for the depressurization of the wetwell will conservatively be underestimated. If one further neglects the effects of any temperature change which results from the blowdown (a second order effect), the rate of depressurization is:

$$\frac{dP}{dt} = \frac{0.665 A R T \sqrt{P \rho_g}}{V_w M_{a,W}} \qquad (19E.2\text{-}42)$$

where:

P = pressure

A = rupture disk flow area

R = universal gas constant

ρ_g = density of gas

V_w = volume of wetwell airspace

$M_{a,w}$ = molecular weight of gas species in wetwell.

Conservatively assuming the wetwell vapor space has only steam, for a blowdown from 0.65 MPa to atmospheric conditions, the assumptions above yield a time constant on the order of 9 minutes. A typical time constant for a pressure wave going around the torus which comprises the wetwell is about 0.5 seconds. Comparison of these two numbers indicates clearly that the entire suppression pool will participate in the blowdown. Thus, two dimensional effects may be neglected.

19E.2.3.5.3 Pool Swell

In order to maximize the potential level in the suppression pool, the analysis assumes that the firewater system has added enough water to fill the pool. The level in the suppression pool rises above the bottom of the vessel because water is transferred from the drywell to the suppression pool. Two sources of steam which may lead to level swell are included in this discussion. The

first steam source is the flow from the drywell through the connecting vents into the suppression pool. The second source of steam which could lead to level swell is the flashing of the pool itself as the system depressurizes.

19E.2.3.5.3.1 Pool Swell Due to Suppression Pool Flashing

Pool swell due to the flashing of the suppression pool may be estimated by use of a drift flux model. Vapor flashing during the wetwell depressurization will be slow and vapor formation will not occur explosively. The suppression pool depressurization rate is much slower than LOCA depressurization rates so the effect of bubble acceleration is less severe. The drift flux model is regularly applied in licensing calculations for LOCA depressurizations occurring over approximately 100 seconds. The suppression pool depressurization occurs over approximately 500 seconds, and begins at a much lower pressure than typical LOCA situations. The drift flux model is appropriate for this scenario because the suppression pool depressurization rate is slow.

The drift flux calculation neglects the contribution of the vapor in the wetwell air space to the flow out of the rupture disk. All vapor flowing out of the rupture disk is assumed to flow from the surface of the pool. This assumption is conservative because it maximizes vapor generation in the suppression pool.

A uniform void generation rate is assumed at each point in the liquid. The average void fraction is then given by:

$$\bar{\alpha}_p = \frac{j_g / U_\infty}{2 + C_0 j_g / U_\infty} \qquad (19E.2\text{-}43)$$

(Reference 19E.2-1) where the mass flow rate, W_p, at the top of the pool determines the superficial gas velocity:

$$j_g = W_p / A\rho_g \qquad (19E.2\text{-}44)$$

and the drift velocity, U_∞, is given by:

$$U_\infty = 1.53\left[\sigma g\left(\frac{\rho_1 - \rho_g}{\rho_1^2}\right)\right]^{1/4} \qquad (19E.2\text{-}45)$$

where:

σ = Surface tension of liquid

g = Acceleration due to gravity

ρ_l = Density of liquid

Then, by assuming the mass of the pool is approximately equal to the initial pool mass, the average void fraction is used to calculate the average pool height:

$$h = \frac{h_0 \rho_l}{\bar{\alpha}_p \rho_g + (1 - \bar{\alpha}_p)\rho_l} \quad (19E.2\text{-}46)$$

where:

h_0 = initial pool height.

19E.2.3.5.3.2 Pool Swell Due to Flow From Drywell

A drift flux model is also used to determine the void fraction in the region of the pool above the horizontal vents due to flow from the drywell. The horizontal vents are located at the inner wall of the suppression pool annulus. If quenching of steam in the suppression pool (which is subcooled at the onset of the blowdown) is neglected, the void fraction in the region above the vents is a constant:

$$\alpha = \frac{j_g / U_\infty}{1 + C_0 j_g / U_\infty} \quad (19E.2\text{-}47)$$

(Reference 19E.2-1) where the terms are analogous to those defined for Equations 19E.2-43 through 19E.2-45, but now refer to drywell conditions. Comparison of Equation 19E.2-47 to Equation 19E.2-43 indicates that the pool swell elevation is much more sensitive to through flow from the drywell than it is to flashing of the suppression pool.

After the void fraction has been determined, the pool level can be calculated using the relationship in Equation 19E.2-46. However, the difficulty in applying these equations to the case with flow from the drywell is the determination of the appropriate area which participates in the pool swell. Therefore, in order to determine if pool swell is a concern, the problem is considered in reverse. That is, the increase in pool height needed to raise water to the elevation of the vents is assumed to be present. This allows the calculation of a void fraction and effective area for flow. If one then assumes that there is a semi-circular region of influence around each of the vents, the critical radius may be determined:

$$r = \sqrt{\frac{2A}{10\pi}} \tag{19E.2-48}$$

If this value is less than the distance between the inner and outer walls of the suppression pool, then pool swell is not expected to lead to carryover of water into the COPS.

19E.2.3.5.3.3 Steam Source

The gas flow through the rupture disk comes from three possible sources: the wetwell vapor space, the drywell vapor space and flashing of the suppression pool. In this calculation of pool swell, the wetwell vapor source is neglected. This results in a somewhat conservative estimate of the pool swell. In order to determine the fraction of flow from each of the sources, the response of the suppression pool and the drywell to a change in wetwell pressure is calculated. Comparison of these values allows the ratio of the flow rates from suppression pool flashing and drywell throughflow to be determined.

The pool flashing rate is determined by consideration of the conservation of energy equation in the suppression pool:

$$\frac{d}{dt}(m_p h_f) = W_p h_g \tag{19E.2-49}$$

where:

m_p = mass of water in the suppression pool,

h_f = specific enthalpy of saturated liquid,

h_g = specific enthalpy of saturated vapor.

Taking the derivative on the left hand side of the equation and introducing the derivative of enthalpy along the saturation curve, one concludes that:

$$W_p = \frac{m_p \frac{dh_f}{dP}}{h_{fg}} \dot{P} \tag{19E.2-50}$$

The ideal gas law is used in the drywell to derive the relationship:

$$W_D = \frac{\dot{P} V_D M_{a,D}}{R T_D} \tag{19E.2-51}$$

where all terms were defined previously and the subscript D refers to the conditions in the drywell.

The ratio of the flow rates from the drywell to pool flashing is found by combining Equations 19E.2-50 and 19E.2-51:

$$\frac{W_D}{W_P} = \frac{V_D M_{a,D} h_{fg}}{R T_D m_P \frac{dh_f}{dP}} \qquad (19E.2\text{-}52)$$

Pool swell is of chief concern for cases in which the firewater addition system has been used to add water to the containment. The suppression pool mass for this case is about 7.0E6 kg. An upper bound estimate of the mass flow ratio assumes that the drywell contains nitrogen at relatively low temperature 373 K (100°C) and that the suppression pool is hot 410 K (137°C). Under these conditions the flow rate ratio is 0.043. These conditions will not occur in the ABWR, since the drywell cannot be cool when the containment pressure is high. However, this value is useful to gain an understanding of the range of Equation 19E.2-52. The bounding calculation shows that less than 5% of the flow through the COPS is being drawn through the horizontal connecting vents. Therefore, the primary contributor to pool swell is flashing of the suppression pool.

19E.2.3.5.3.4 Application to ABWR

The scenarios used in the suppression pool level swell calculations are identical to the accident sequences described in Subsection 19E.2.2.1, Loss of All Core Cooling With Vessel Failure at Low Pressure (LCLP), leading to the opening of the Containment Overpressure Protection System Rupture Disk (R). These results are typical of all initiating events leading to the opening of the rupture disk. The passive flooder actuation scenarios will lead to the highest pool water temperature; thus the passive flooder cases are limiting for the onset of flashing. The firewater addition scenarios will lead to a higher water level swell for given thermal hydraulic conditions because the initial water height is higher.

Figures 19E.2-2 a-j show the drywell and wetwell conditions during a passive flooder actuation scenario. This scenario occurs when the passive flooder (PF) opens to cover the corium. This scenario leads to the maximum suppression pool water temperature. Figure 19E.2-2j shows that the maximum suppression pool temperature is 410 K.

Figures 19E.2-3 a-g show the drywell and wetwell conditions during a firewater addition scenario. This scenario occurs when the firewater system (FS) is actuated four hours after the initiation of the event. This scenario leads to the maximum suppression pool water level. Figure 19E.2-3f shows that the maximum suppression pool level is 14.5 m.

Pool swell is maximized at high temperature (410 K, 137 °C) and high water level (14.5 meters, corresponding to an elevation of 1.35 m). The geometry of the containment and the bounding conditions are shown in Figure 19E.2-25. It is presumed that the rupture disk has just opened. Since the pool swell elevation is more sensitive to flow from the drywell, the upper bound value for the mass flow ratio found above is used. For the limiting suppression pool conditions, the

average void fraction due to pool flashing is about 4%. This results in a pool swell of 0.65 meters, corresponding to an elevation of 2.0 meters. Since the bottom of the COPS penetration is at an elevation of 4.25 meters, this mechanism alone will not lead to flooding of the COPS penetration.

If the pool level were to rise an additional 2.25 meters near the outer wall of the suppression pool due to flow from the drywell, the COPS penetration could be flooded. A void fraction of 13% due to through flow from the drywell is required for this additional pool swell. Applying Equations 19E.2-47, 19E.2-48 and the upper bound value from Equation 19E.2-52, one arrives at an radius of 0.84 meters for the region affected by flow from the drywell. This area would be located near to the horizontal connecting vents at the inner wall of the suppression pool. Since the distance between the inner and outer walls of the suppression pool is 7.5 meters, one may safely conclude that pool swell will not threaten the COPS under these conditions.

TRAC calculations have been performed regarding suppression pool swelling during depressurization. TRAC uses two-fluid modeling instead of the drift flux model.

The TRAC level swell model has been qualified against test data. The PSTF experimental blowdown facility was used to provide information on liquid flashing due to a depressurization, and the subsequent swell of the liquid level. When compared with the TRAC model of the PSTF test, it was found that “the two-phase level comparisons show close agreement (± 10%)” (Reference 19E.2-39) The TRAC PSTF qualification validates the TRAC suppression pool swelling results.

A TRAC study of a typical Mark II containment (Reference 19E.2-36) showed a maximum pool level swell height of 0.79 m above the initial pool level. When the Mark II suppression pool level swell is calculated with the drift flux model used for the ABWR calculations, a maximum pool level swell of 2.33 m is obtained. This is almost three times as high as the TRAC two-fluid modeling results. This result demonstrates that the ABWR pool swell calculation is conservative.

19E.2.3.5.4 Carryover Due to Entrainment

The entrainment of water droplets by the steam flow through the suppression pool is potentially a concern since the water could carry fission products through the COPS to the environment. A very simple estimate analysis based on the work by Kutateladze (Reference 19E.2-18) indicates the potential entrainment for a pool of water sparged from below. The threshold for the entrainment of a droplet is based on the velocity of the steam from the surface of the suppression pool:

$$U_{threshold} = 2.7\left[\sigma g\left(\frac{\rho_l - \rho_g}{\rho_g^2}\right)\right]^{1/4} \qquad (19E.2\text{-}53)$$

Assuming the properties of steam at the rupture disk setpoint, the threshold velocity is about 6 m/s. The superficial velocity from the surface of the suppression pool is 0.02 m/s, assuming all of the flow through the COPS was passed through the suppression pool. Thus, there is more than two orders of magnitude between the superficial velocity which would be observed under the conditions of interest and the threshold for entrainment. This indicates there will be no significant entrainment from the surface of the pool.

A more sophisticated analysis is possible using the work of Rozen, et. al. (Reference 19E.2-17) to estimate even very low amounts of entrainment. This method uses the superficial velocity of steam rising from the pool and the pressure of the system to determine the typical droplet size and the ratio of liquid mass to vapor mass which is entrained from the surface of the pool.

For cases in which the firewater system has been used to add water to the suppression pool, the distance between the bottom of the COPS penetration (elevation 4.25 meters) and the pool surface (elevation 1.35 meters) is 2.9 meters. Assuming the maximum pool swell of 0.65 meters, discussed above, the height between the COPS and the pool surface is 2.25 meters. The correlation selected to calculate carryover is conservative for cases in which the water pool is at least two meters below the COPS penetration.

Using this correlation, the ratio of liquid mass to vapor mass is about 4E-6. If one considers an energy balance on the suppression pool before and after the rupture disk opens, it can be determined that just over one tenth of the suppression pool flashes to steam during the blowdown. Thus, the fraction of suppression pool liquid which might be transported from the suppression pool as a liquid is 4E-7.

The fission products in the suppression pool will exist as a dissolved salt and as sediment on the bottom of the pool. Therefore, the fraction of the fission products which can be carried out the COPS by entrainment will be some fraction less than the ratio of the liquid entrained from the pool surface. However, a release fraction of 4E-7 will not lead to significant offsite dose.

19E.2.3.6 Behavior of Access Tunnels

If core debris is entrained out of the lower drywell and into the access tunnels, it is possible that the integrity of the tunnels could be compromised. This depends on several key factors, such as the amount of debris entrained into the tunnels, whether the debris remains in the tunnels, the heat transfer characteristics between the debris and the tunnel walls, and the strength and loading of the tunnel material.

19E.2.3.6.1 Potential for Debris to Enter Tunnel

Based on the configuration of the lower drywell and the equipment contained therein, it is highly unlikely that debris will be carried into the tunnels unless there is significant debris entrainment. Based on work at INEL, (Reference 19E.2-35) local failure of the lower head is expected. In fact, the drain plug located at center of the bottom head appears to be the dominant

failure location. A localized failure should result in a concentrated discharge from the center of the lower head. Immediately below the reactor vessel are the CRD mechanisms. Splashing off of the CRDs is not judged to result in a significant amount of debris transport to the tunnels. Since the debris is likely to be discharged from the center of the CRD array, radial movement through a forest of vertical structures is not expected and transport of the debris outside of the CRD array is not judged to be likely. In fact, the CRDs will tend to columnate the flow, since they are long, vertically oriented and have little change in cross section along their length.

Approximately 6 meters below the bottom of the vessel is the equipment platform constructed from thin steel grating material. This grating is located at about the elevation of the tunnel bottom. No other structures exist at or above this elevation to divert the discharging debris into the tunnel. The grating surface area is small compared to the overall cross sectional area of the lower drywell and the thermal properties of the debris would result in immediate melting of the grate. Further, the center of the equipment platform, where the debris is likely to flow, does not have any grating to allow movement of the CRDs during refueling. Thus, the presence of the equipment platform is not expected to result in significant splashing of the debris into the tunnels.

Using Ishii's methodology, debris entrainment thresholds were only reached for high pressure melt ejection events with very large vessel failure areas (Subsection 19EA.3.6.2). Based on work done at INEL and contained in the expert elicitations in NUREG 1150, and consistent with the DCH analysis in Attachment 19EA, a very small probability is assigned to a large (> 2 m^2) vessel failure area. Combining this with the probability of a high pressure core melt with melt ejection, this scenario constitutes only a small percentage of all core damage events. Thus, the potential for debris entrainment and the transport of debris to the access tunnels is judged to be quite low for the ABWR.

19E.2.3.6.2 Bounding Calculation Assuming Debris Enters Tunnel

Bounding calculations are performed to address those very low probability scenarios in which debris is transported into the tunnels.

Each access tunnel is a circular steel tube, approximately 11 meters long and 4.6 meters in diameter. The thickness of the steel is 2 cm. The bottom of the tunnel is located 7.4 meters below the bottom of the RPV. Since the low water level in the suppression pool is 6.2 meters below the RPV, the portion of the tunnel that will be in contact with core debris will be submerged. The opening from the tunnel to the lower drywell is a rectangle centered on the tunnel axis. The height of the personnel access is 3.55 meters and the height of the equipment access is 3.8 meters; both are 2.2 meters wide. Due to the reduction in area at the lower drywell wall intersection (i.e. the curb that is formed at the entrance to the tunnel), it will be assumed that any debris transported into the tunnel will remain there. The material properties used in this analysis are provided in Table 19E.2-30.

19E.2.3.6.2.1 Amount of Debris Entrained into Access Tunnels

As noted above, debris can only be entrained during a high pressure core melt scenario. NUREG-1150 indicates an upper bound of 40% for the core debris that exits the vessel at the time of vessel failure, albeit at a low probability . It is judged more likely that only 10% will exit during the initial blowdown. Therefore, 10% debris mass is used for this analysis. From previous estimates of debris entrainment discussed above and the fact that the access tunnels are dead end volumes, it is likely that the debris will not be entrained into the tunnels. However, it is assumed that all of the debris exiting the vessel will be entrained along the lower drywell walls, and since each tunnel occupies 6.5% of the perimeter of the lower drywell, 0.65% of the core debris, 1675 kg, will enter each access tunnel during the blowdown. This debris is assumed to be instantaneously carried into the tunnel and will quickly spread to a depth of 3.5 cm. In addition, it is assumed to be molten with little superheat. This is consistent with the direct containment heating analysis contained in Attachment 19EA.

19E.2.3.6.2.2 Heat Transfer to the Tunnel Wall

As soon as the debris comes into contact with the tunnel shell, the interface will immediately assume a temperature that is between the steel and debris temperatures. This initial contact temperature can be calculated by assuming that both the steel and debris are semi-infinite slabs and equating the heat flux at the interface.

$$q''_i = \frac{k_C(T_{C,0} - T_i)}{\sqrt{\pi\alpha_C t}} = \frac{k_{St}(T_i - T_{St,0})}{\sqrt{\pi\alpha_{St} t}} \qquad (19E.2\text{-}54)$$

For $T_{C,0}$ = 2500 K, and $T_{St,0}$ = 373 K, the initial contact temperature is 1087 K. The interface will remain at this temperature until the thermal boundary reaches the outside of the shell; it will then increase (as will be discussed below) because the heat transfer to the water can not keep up with the heat supplied by the debris. The thickness of the thermal boundary can be expressed as

$$\delta_{thermal} \cong \sqrt{\pi\alpha t} \qquad (19E.2\text{-}55)$$

It takes approximately 19 seconds for the thermal boundary to reach the water side of the tunnel shell. The thermal boundary in the debris, on the other hand, takes more than 200 seconds to reach the upper surface of the debris.

In order for the steel shell to achieve steady state, the water on the outside of the steel shell must be able to remove heat as fast as it is supplied by the debris. Steady state conduction through steel 2 cm thick with surface temperatures of 373 K and 1087 K is 1.07×10^6 W/m^2. The critical heat flux for a downward oriented horizontal plate at one atmosphere is only 4.5×10^5 W/m^2 (Reference 19E.2-34). Although the critical heat flux increases with pressure, steady state can not be achieved in this situation.

19E.2.3.6.2.3 Tunnel Wall Integrity

In order to simplify the effect of transient behavior, bounding calculations are performed to estimate the times associated with the transient. As the thermal boundary layers penetrate the materials, the magnitude of the heat flux at the interface is falling. Assuming that the debris behaves as a semi-infinate slab, the time at which the debris begins to supply less than CHF to the interface can be calculated by

$$q''_{CHF} = \frac{k_C \Delta T_C}{\sqrt{\pi \alpha_C t}} \qquad (19E.2\text{-}56)$$

Approximating the effect of the heat of fusion by assuming the bulk corium temperature to be 3000 K and assuming the interface temperature remains 1087 K, approximately 194 seconds are required for the heat flux at the interface to drop to CHF. If the steel shell can maintain its integrity for longer than this time, the tunnel could remain intact.

The time for the entire thickness of steel to heat to 1200 K (the temperature at which the steel is assumed to lose all strength) can be compared to the time to supply less than CHF. If it is long compared to 194 seconds, the tunnel may remain intact. This time is computed by equating the total heat supplied by the debris to the heat transferred to the steel while the thermal boundary layer is growing plus the heat necessary to raise the steel from its steady state temperature profile to a uniform 1200 K. (Note that the heat transferred during the boundary layer growth takes into account, in a crude way, the heat that is given up to the water prior to dryout. It is assumed that after 19 seconds, critical heat flux has been reached, and there is essentially no heat transfer to the water.)

$$\int_0^t q''_{C,0}\,dt = \int_0^{19} q''_{St,0}\,dt + \rho_{St} C_{P,St} \int_0^{\delta_{St}} (1200 - T_{St}(x))\,dx \qquad (19E.2\text{-}57)$$

The debris is assumed to be infinite during this time, and the steel is assumed to behave as an infinite slab during the first 19 seconds. It is also assumed that the contact temperature is constant, at 1087 K, during the entire time. Solution of this indicates that the tunnel shell will reach 1200 K at approximately 46 seconds. Thus, this rather crude analysis indicates that the tunnel may fail in the unlikely event that debris is entrained.

19E.2.3.6.3 Impact of Tunnel Failure

Failure of the tunnel wall would occur at the lowest point. This would result in a flow path from the lower drywell vapor space into the suppression pool. As indicated earlier, there will initially be at least 1 meter of water above the bottom of the tunnel. Thus, no fission product bypass of the pool would occur. Since the event being considered is a high pressure melt scenario with entrainment of debris, the operator must initiate the firewater addition system in drywell spray mode to prevent high temperature failure of the drywell. This action will indirectly result in

additional water being added to the suppression pool as it spills from the upper drywell, through the connecting vent system to the wetwell. Thus, several meters of water would be present above the tunnel failure elevation to provide scrubbing of fission products.

19E.2.3.6.4 Conclusion

It is unlikely for core debris to be entrained or splashed into the access tunnels. A small percentage of all core damage sequences could lead to debris entering the tunnels.

However, in the event that it does, the tunnel steel will reach temperatures that may compromise its integrity. The heat transfer through the thin steel wall is so high that the water on the outside of the tunnel quickly goes into dryout, and the heat can no longer be removed at a rate sufficient to maintain the tunnel integrity.

Failure of the tunnel wall would occur at the lowest point and would result in a fission product release path into the suppression pool. However, since several meters of water will be present above the tunnel failure site, fission products would be scrubbed and no containment bypass would result.

19E.2.4 Supplemental Accident Sequences

In order to quantify the PRA, sequences were analyzed using MAAP-ABWR to assess the effects of recovery. Additionally, some sequences with unusual characteristics, such as those having early containment structural failure, are considered in this subsection.

19E.2.4.1 Time of Firewater System Initiation

The firewater spray initiation times used in the base analyses are simply assumptions used for the purpose of the study. This subsection examines the possible variation in accident progression which would result if the time of spray initiation is varied from that assumed in the base studies.

For example, in some cases the firewater system is not initiated for four hours. As a consequence of the accident progression, as modeled in the CETs, it is known that the operator failed to initiate the firewater injection system. Thus, it is logical to assume that the operator does not initiate the system immediately after vessel failure. If the system were operated immediately, the containment water level would reach the level of the bottom of the vessel somewhat sooner (a maximum of four hours earlier in this example). At this time the operator would be directed to terminate injection. As seen in Figure 19E.2-3a, the containment pressure rises at this time eventually leading to opening of the rupture disk. The change in time of rupture disk opening in this case would be about four hours earlier than that in the base analysis.

On the other hand, if the operator did not initiate the firewater addition system in the assumed four hour period, more of the water initially in the lower drywell would boil off. Eventually, the debris in the lower drywell will begin to heat up. This would lead to actuation of the passive

flooder in the lower drywell. This would quench the debris and keep the drywell cool. If at some later time the firewater system is initiated, the thermal mass of the suppression pool would be increased as in other sequences with firewater addition. Since the containment water level would reach the bottom of the vessel later than in the nominal case, the firewater injection would be terminated later, leading to later opening of the rupture disk. The effect on the magnitude of fission product release would be negligible. Although the later time of release might argue for delaying the initiation of the firewater system, the effect on risk is judged to be outweighed by the simplicity of telling the operator to initiate the firewater system as soon as possible in all circumstances.

The operator is instructed to initiate the firewater addition system as soon as it is determined that the water level in the vessel cannot be maintained using other systems. However, if the firewater system is not initialized quickly, the passive flooder will open allowing the lower drywell to be flooded from the suppression pool. Thus, the assumed time for initiation of the firewater addition system does not have a significant impact on the accident progression or on any eventual fission product release.

19E.2.4.2 In-Vessel Recovery

This subsection examines the in-vessel recovery sequence to determine how fission product scrubbing should be modeled for these sequences.

The potential for recovery of vessel injection systems before vessel failure occurs is believed to be an important feature in the mitigation of severe accidents. The sequences with fifth and sixth characters IV in the accident sequence designator in the containment event trees have core melt arrest in the vessel. For the ABWR any of the ECC Systems or the firewater addition system is capable of adding sufficient water to the vessel to prevent core damage, and in theory, to halt the core melt progression once it has begun. It is expected that the ECC Systems can prevent core damage if injection is delayed for as much as half an hour after accident initiation. The firewater system prevents core damage if injection is begun within 20 minutes after the loss of injection.

In MAAP, it is not possible to halt core damage once the first channel region has blocked. It is expected the in-vessel recovery would be possible for at least one hour from the initial loss of injection. Since this occurs very shortly after the onset of core damage, it is very difficult to determine the effects of in-vessel recovery on fission product release directly.

However, the salient feature of core melt arrest in the vessel is suppression pool scrubbing. If the core melt is arrested in the vessel then all of the fission products which leave the vessel must do so via the SRVs. These discharge through quenchers at the bottom of the suppression pool, ensuring fission product scrubbing. Although LOCA events may allow an unscrubbed release into the containment, the probability of a LOCA with failure of the COPS is a very low frequency event and may be neglected.

Fission product scrubbing is also provided if the release is from the wetwell airspace, as would occur for cases with COPS operation. The release fractions associated with this type of release are examined in the base analyses of Subsection 19E.2.2. The results of that study are applied to in-vessel recovery in the effects analysis of Subsection 19E.3.

19E.2.4.3 System Recovery After Vessel Failure and Normal Containment Leakage

This subsection describes the determination of containment leakage when pressures are below the ultimate pressure capability of the containment.

The majority of accidents for the ABWR do not lead to COPS operation or containment structural failure. In these accidents the RHR system is recovered to cool the containment following core damage. These sequences are indicated by the characters HR in the fifth and sixth digits of the accident sequence designator in the containment event trees. Although COPS does not open and there is no COPS operation or structural failure of the containment in these cases, there will still be a small release of fission products due to normal containment leakage. These sequences are binned as NCL in the containment event trees.

To estimate the fission product release associated with normal containment leakage following core damage a sensitivity study was performed using MAAP-ABWR. A loss of all core cooling with vessel failure at low pressure case was chosen for the analysis. The transient was run for three days. The RHR System was assumed to be initiated in suppression pool cooling mode just before the wetwell pressure reached the COPS setpoint. The containment leakage area was chosen such that the leak rate was equal to the technical specification limit of 0.5% per day at rated pressure.

Two cases were run for this sensitivity study, one with leakage from the drywell and the other with leakage from the wetwell. In both cases the first appreciable fission product release occurs at about three hours. The noble gas release fraction at 72 hours is 0.052% for the cases with drywell leakage and 4.4% for the case with wetwell leakage. The magnitude of the noble gas release for the wetwell leakage case is larger than that for the drywell leakage case because the noble gases are forced through the SRVs and wetwell/drywell connecting vents and into the wetwell as the steaming rate in the drywell increases. Thus, the amount of noble gases available to escape through the leak is greater in the wetwell than in the drywell. The CsI release fraction at 72 hours is 2.3E-5 for the case with drywell leakage and less than 1E-7 for the case with wetwell leakage. The volatile fission product release is much less for the case with wetwell leakage because of the benefit of fission product scrubbing provided by the suppression pool.

In quantifying the offsite dose associated with containment leakage, a conservative approach has been adopted. The larger release will be used for each species. That is, the noble gas release of 4.4% will be used with the CsI release fraction of 2.3E-5. While this is somewhat conservative there will not be a large impact on risk.

19E.2.4.4 Early Drywell Head Failure

This subsection describes the modeling of fission product release for cases with early drywell head failure resulting from a high pressure core melt.

In Subsection 19D.5 the frequency of the vessel failing at high pressure leading directly to loss of containment integrity was estimated. These sequences are indicated by the character E in the seventh digit of the accident sequence code. This sensitivity study examines the potential fission product release associated with such an event. Only two types of sequences can lead to this occurrence: a loss of all core cooling with vessel failure at high pressure (LCHP), or a concurrent ATWS and loss of all core cooling with vessel failure at high pressure (NSCH). The LCHP event was chosen to represent this case as it has a higher probability of occurrence.

The history of this event is identical to the LCHP events described in Subsection 19E.2.2.2 until the time of vessel failure. It is assumed that the drywell head fails at vessel failure. There is no significant effect of the drywell failure on the entrainment of corium into the upper drywell, or on the opening of the passive flooder.

The pressure in the containment remains low, usually less than 0.2 MPa. Just before the three hour mark MAAP-ABWR predicts that the drywell tear becomes plugged by aerosols using the Morowitz plugging model. The pressure rises to a peak value of 0.3 MPa before the aerosols are blown out and the containment pressure falls to about 0.2 MPa.

The fission product release for this sequence is much higher than that for the base case (LCHP-PF-P-H). Fission product release begins at the time of vessel failure (2.0 hours). The noble gas release is very slow since most of the noble gasses are trapped in the wetwell. After 61 hours the noble gas release is essentially complete. The volatile fission product release is predominantly governed by the revaporization of the fission products from the vessel internals. After 72 hours this revaporization is nearly complete. The CsI and CsOH release fractions are about 24% and 16%, respectively.

Since the fission product release is significantly higher than that for the base case, this information will be included in the consequence analysis of Subsection 19E.3.

19E.2.4.5 Suppression Pool Drain

This subsection describes the modeling of sequences in which the suppression pool water drains to the RHR pump rooms.

The draining of the suppression pool has been proposed as a potential mechanism for the loss of containment integrity following a seismic event. These sequences are designated with the seventh digit S in the accident sequence code. The water from the suppression pool would flood the pump rooms as discussed in Subsection 19E.2.3.4. This analysis indicates that the pump room integrity will not be lost.

However, there is a pipe chase that leads up from the top of the pump room which has no capacity to withstand high pressure. There is no effective fission product holdup if heat exchanger failure and suppression pool drain occur. This sensitivity study evaluates the fission product release associated with this structural failure mode.

Since this failure is caused by a seismic event it is assumed that if one heat exchanger fails, causing the suppression pool to drain into the RHR pump rooms then all three heat exchangers fail. A comparison of the total floor area of the pump rooms to that of the suppression pool shows that the water level in the pump rooms would rise to more than three meters, assuming equal gas space pressures in the wetwell and the pump rooms. As the wetwell pressurizes due to the accident, the water level would increase further. Therefore, the suppression pool may be envisioned as being displaced to the pump rooms rather than being lost. Any release of fission products to the atmosphere must pass through the RHR suction line, into the pump room, and are then scrubbed in the pool now located in the pump room.

The pump rooms will leak to the corridor through a total of six doors at an assumed rate of 1.14 m^3/h (5 gpm) per door. This is less than 5% of the suppression pool volume per day. This will have negligible impact on the water level in the pump rooms.

For simplicity, the fission product release following heat exchanger failure and suppression pool drain was modeled by assuming a large opening in the wetwell above the normal water level. No significant pressure head was allowed to develop in the wetwell. A loss of all core cooling event with vessel failure at low pressure and passive flooder operation was chosen (LCLP-PF) to model the transient. Dryout of the lower drywell, which could occur if no water was added to that region, was not modeled since the suppression pool elevation in this analysis was sufficient to prevent this occurrence.

The fission product release occurs as fission products are released from the fuel. The fission products exit the vessel through the SRVs. Scrubbing occurs as the fission products are blown through the RHR suction line into the pool in the RHR pump rooms. The only delay associated with any release of fission products which are not trapped in the pool is the dilution effect brought about by a large wetwell gas volume. This effect is analogous to that which would occur in the reactor building.

The release of fission products begins as the fuel begins to melt at about 0.5 hours. The noble gas release was essentially complete at 8 hours. The release of volatile fission products was very small due to scrubbing. The final release fraction of CsI after 84 hours was less than 1.E-5.

19E.2.5 Identification and Screening of Phenomenological Issues

The first step in performing an uncertainty analysis is to identify the key phenomena and their associated uncertainties. To do this, various sources have been surveyed (References 19E.2-19 through 19E.2-27).

The following provides a summary of the key literature reviews. Some of the severe accident issues are screened out as not being applicable to the ABWR design. At the end, a list of sensitivity issues will be presented for investigation in the ABWR PRA.

19E.2.5.1 Review of NUREG/CR-4551 Grand Gulf and Peach Bottom Analyses

The ABWR containment shares some similarities in design to the Mark III BWR containment. The NUREG-1150 study of Grand Gulf was used to identify phenomena and issues which may need to be addressed in the ABWR uncertainty analysis. In addition, the Peach Bottom (Mark I) analysis was also reviewed for insights. The results of the NUREG-1150 Grand Gulf and Peach Bottom containment analyses are presented below.

19E.2.5.1.1 Grand Gulf

The Grand Gulf accident progression event tree (APET) consists of 125 event headings. The events treated in the Grand Gulf (GG) APET can be grouped into ten categories based on similar accident progression phenomena or characteristics. This grouping is summarized on Table 19E.2-22 along with the Grand Gulf APET events which fall into each group. A summary of the phenomena and issues addressed by each event group are discussed below:

(1) Damage State Grouping Events

The first fifteen events in the GG APET and Event 20 were sorting type events which summarized the plant damage state for a sequence based on the availability of various core injection and containment systems, the timing of core damage, the availability of AC and DC power and the vessel pressure.

(2) Structural Capacity/Initial Containment Status

Four events (Events 16 - 19) summarized the early status of containment integrity and pool bypass and defined the structural capacities of the containment and drywell to quasi-static and impulse loading.

(3) Systems Behavior/Operator Actions

Twelve events defined operator actions and systems availability during the course of the accident progression including whether hydrogen ignitors were available, the status of containment sprays and whether the containment was vented. These event questions were generally asked prior to core damage, during core damage, at vessel failure and late after vessel failure. Other events considered were reactor vessel pressure during core damage, upper pool dump, SRVs sticking open, and restoration of in-vessel injection during core damage.

(4) AC/DC Power Availability

Six events were related to AC and DC power availability/recovery during core damage, following vessel failure and late in the accident progression.

(5) Criticality

One event assessed whether the debris would be in a critical configuration after core injection recovery.

(6) Hydrogen Related Phenomena/Issues

Forty-eight events in the GG APET were related to assessing the impact of hydrogen production and combustion on containment and drywell integrity. These hydrogen event questions were asked at numerous time periods throughout the accident progression: during core damage, at vessel failure, following vessel failure and late in the accident sequence.

The hydrogen production event questions considered hydrogen production in-vessel during core damage and that released at vessel failure and during core concrete interactions (CCI). Several events were included to assess the transient concentrations of hydrogen, oxygen and steam in the drywell and containment throughout the accident progression and to determine if regions were inert (or non-inert) to deflagrations or detonations during various time periods.

For distinct time periods throughout the accident progression the probability of ignition of hydrogen diffusion flames, uncontrolled deflagrations, and detonations were considered along with the efficiencies of the burns and the peak burn pressures (and detonation impulse loads). Additional events compared these loads with the containment and drywell structural capacities and determined if failure or leakage would result.

(7) Containment/Drywell Pressurization and Failure

Twenty-two events assessed containment and drywell pressure and level of leakage resulting from a combination of loads (gradual overpressurization from steam and non-condensable gases) not directly associated with hydrogen combustion. This set of events also assessed the response of the reactor pedestal and drywell to the pressure loads resulting from energetic events which may occur at vessel failure including steam explosions and rapid steam generation in the reactor cavity, blowdown of the reactor vessel from high pressure and high pressure melt ejection.

(8) Core-Concrete Interactions/Pedestal Failure

Seven events were directed at assessing the behavior of debris in the reactor cavity following vessel failure. These events determined whether there was a water supply to the debris, whether the debris was coolable, (and if not) the nature of the resulting CCI and whether the CCI would result in pedestal failure.

(9) Steam Explosion Related

Five events assessed the likelihood and consequences of steam explosions occurring in-vessel or ex-vessel in the reactor cavity. In-vessel steam explosions which failed the upper reactor vessel head, drywell and containment (alpha mode failure) or which failed the lower head of the vessel were considered. The probability of large ex-vessel steam explosions occurring and failing the pedestal (by impulse loading) were also evaluated.

(10) Core Damage Progression and Vessel Breach

Four events were related to assessing the general in-vessel accident progression and vessel failure characteristics. These events evaluated the amount of core debris in the initial core slump, the amount of debris mobile in the lower head at vessel failure, the mode of vessel failure and whether an HPME occurred.

19E.2.5.1.2 Peach Bottom

The major phenomena considered in the Peach Bottom APET which were not addressed in the GG APET were liner melt-through and over temperature failure of the containment (drywell) penetrations.

19E.2.5.1.3 Application of NUREG/ CR-4551 Results to ABWR

Since the ABWR containment is inerted, the GG APET events associated with details of hydrogen production and combustion are not relevant.

The remaining GG APET areas are generally considered applicable to the ABWR. Insights from the GG APET have been factored into the ABWR containment event tree analysis considering differences between the two designs.

The design of the ABWR lower drywell is very different than the Peach Bottom pedestal cavity. The manway used to gain access to the lower drywell is about 5 meters above the floor. The liner, which represents the containment boundary, in the lower drywell is protected by a layer of sacrificial concrete at least one meter thick. Therefore, the debris will not come in contact with the liner in a manner which could lead to liner melt-through. Therefore, liner melt-through is not addressed in the ABWR analysis.

However, in the unlikely event of vessel breach with the vessel at high pressure, it is considered possible that debris transported into the upper drywell may threaten containment integrity as a result of a general heatup of the upper drywell atmosphere if the drywell sprays are not available. As discussed in Attachment 19EA, the debris will not be transported as a contiguous mass. Therefore, the formation of a debris pool in the upper drywell is not a credible event. However, there may be some debris in the upper drywell which could lead to long-term high temperature failure of the containment. The effects of high upper drywell temperature are considered in the CET in assessing the probability of drywell failure.

19E.2.5.2 Review of NUREG-1335

Table A.5 from NUREG-1335 is included here as Table 19E.2-23. This table includes a list of the parameters identified by the NRC to be addressed in an Individual Plant Examination (IPE). All of these will be addressed in the final list of sensitivity analyses to be carried out for the ABWR except for those discussed below:

(1) Combustion in Containment

As noted above, the ABWR containment is inerted and, therefore, combustion will not result in a challenge to containment.

(2) Induced Failure of the Reactor Coolant System

This is mainly an issue for PWRs. The thin walls of the reactor coolant system outside of the vessel may fail to due extended exposure to elevated temperature and pressure. For typical conditions in a BWR during an accident, induced failures are judged to not occur.

(3) Direct Contact of Debris on Containment

Due to the configuration of the ABWR cavity, under a low pressure vessel failure scenario, core debris will be retained in the cavity and will not come in direct contact with the containment boundary. For a high pressure melt scenario, debris that is entrained into the upper drywell will be dispersed and will not result in the coherent flow of debris to the containment shell needed to cause containment failure.

19E.2.5.3 Review of Recommended Sensitivity Analyses for an Individual Plant Examination Using MAAP 3.0B (EPRI).

This document was reviewed to ensure that there were no new issues that had not previously been identified in the above documents. In this document, the following key issues are highlighted for BWR sensitivity analyses:

(1) Hydrogen Generation In-vessel,

(2) Mass of Molten Core released at vessel failure,

(3) CsI re-vaporization,

(4) Debris Coolability,

(5) Containment Failure Mode,

(6) Chemical form of Iodine.

All of these issues are being addressed in the ABWR sensitivity and uncertainty analysis. Some issues are being considered indirectly in the framework of the phenomenological issues they affect. For example, the mass of molten core released at vessel failure is considered in terms of the impact on high pressure melt ejection, direct containment heating and core debris coolability. The chemical form of Iodine is dominated by the effect of suppression pool pH, and is discussed in that context.

19E.2.5.4 Review of ALWR Requirements Document

The EPRI ALWR Requirements Document includes a top-level section referred to as the Key Assumptions and Guidelines (KAG) which defines the manner in which a probabilistic risk assessment is to be performed for advanced plants. Paragraphs 6.2 and 6.3 address those parameters which could be important for the containment response:

(1) Parameters related to hydrogen burns,

(2) Core Debris Coolability,

(3) Pressure capacity of the containment failure location and failure size,

(4) High Pressure Melt Ejection,

(5) Ex-vessel combustible gas generation,

(6) Operator Actions,

(7) Suppression pool scrubbing,

(8) Iodine composition and revaporization.

As stated previously, hydrogen burning is precluded in the ABWR design by use of an inerted containment. Operator actions are being considered in a separate study. The remainder of these issues are included in the ABWR sensitivity and uncertainty analyses.

19E.2.5.5 Summary and Conclusions

Table 19E.2-24 is the list of issues to be investigated in an ABWR sensitivity analysis and has been derived from the documents described above.

19E.2.6 Sensitivity Analysis and Scoping Studies for Phenomenological Issues

Sensitivity studies were performed for the ABWR response to severe accident phenomena in order to determine those issues which may have significant impact on the offsite risk associated with the ABWR design. Given this goal, the ultimate measurement of sensitivity is the offsite dose. At a given site the primary factors which influence the dose are the magnitude and time of release. Therefore, changes in these parameters were used to determine the need for detailed uncertainty analyses. The issues investigated in the ABWR sensitivity analysis is given in Table 19E.2-24.

19E.2.6.1 Core Melt Progression and Hydrogen Generation

This subsection examines the effect of the MAAP core melt progression modeling on the hydrogen generation due to metal-water reaction.

The progression of a severe accident during the period when the core is melting is important in predicting the amount of hydrogen produced during the core melt. The standard melt progression using MAAP is characterized by molten corium forming blockages in the channels which prevent steam from flowing in the channels. This model has two major effects on the melt progression. First, once a region has been blocked, it is impossible for that region to be cooled since no water can flow into the channel to arrest the core melt. Therefore, a core melt can not be arrested in the vessel after the onset of core damage. Secondly, the blockage of the channel prevents steam from flowing past the hot, uncovered portion of the fuel. This serves to limit the metal-water reaction which can occur in the vessel.

Metal-water reaction in a BWR is dominated by the oxidation of zirconium. This reaction has two important consequences in a severe accident. First, the reaction is exothermic, that is it adds energy to the containment. Second, as oxygen from the steam is consumed in the oxidation reaction, hydrogen gas is generated which adds to the partial pressure of the non-condensable gasses in containment. Both of these effects tend to increase the pressurization rate of the containment and shorten the time to fission product release.

A sensitivity study was performed to determine the effects of the blockage model on hydrogen generation. Four cases were examined, two at low pressure (corresponding to LCLP-FS-R-N and LCLP-PF-R-N) and two at high pressure (LCHP-PF-P-M and LCHP-PS-R-N). These cases were identical to their respective base cases, described in Subsection 19E.2.2, except that the model parameter for blockage and hydrogen generation (FCRBLK, Reference 19E.2-1) was set to prevent blockage and to cause the metal-water reaction to continue past the eutectic temperature of the corium.

For the cases at low pressure, the amount of zirconium oxidation increased from 6.3% of the active clad to 15.8%. The time of vessel breach decreased from 1.8 hours to 1.1 hours. For the dominant case with the firewater system operating, the rupture disk opens at 30.6 hours as compared to 31.1 hours for the base case. The CsI release to the environment increases slightly to about 1.E-6; however, the release is still negligible and will not affect the offsite dose. For the case with passive flooder operation, the time of rupture disk opening decreased from 20.2 hours to 16.7 hours. The change in the magnitude of fission product release was negligible.

The blockage model had a more pronounced effect on the amount of zirconium oxidized for the high pressure cases. The fraction of zirconium oxidized for the no blockage case was 35.9%, increased from 5.1% for the case which included the blockage model. For the LCHP-PS-R-N case, the time to rupture disk opening is decreased from 25.0 to 20.0 hours. The impact on the magnitude of fission product release is negligible.

However, for the LCHP-PF-P-H case the effect of an increase in pressure is more significant because leakage through the movable penetrations is assumed to occur at 0.46 MPa. The time fission product release begins for this case is reduced from 18.1 hours in the base case to 7.1 hours with increased hydrogen production. Additionally, the magnitude of the CsI release fraction at 72 hours is increased from 8.7% to 12.5%.

The difference in the effects of blockage on hydrogen production can be best explained by considering the steam flow past the hot fuel cladding. For cases with vessel failure at low pressure, the reactor is blown down before significant heatup of the cladding has occurred. Although the blockage model does not predict complete blockage until shortly before vessel failure, the loss of water in the core region which occurs during the blowdown effectively terminates the metal-water reaction after only 6.3% of the active cladding has been oxidized. The conditions found in the high-pressure vessel failure cases are more conducive to hydrogen generation for three reasons:

(1) Higher steam temperature in the vessel prior to vessel failure,

(2) A greater mass of water in the core region, and

(3) A longer time before vessel failure.

Despite these conditions, the blockage model causes slightly less of the zirconium to be oxidized by MAAP-ABWR for base cases with vessel failure at high pressure than for cases with vessel failure at low pressure. The blockage model used in the base cases presumes that molten material forms blockages in the core which prevent steam flow past the fuel cladding. This terminates zirconium oxidation and limits hydrogen production. The core is fully blocked in the high-pressure melt sequence at 1.2 hours, while in the low-pressure sequence full blockage is delayed until 1.8 hours.

When the blockage model is disabled, the effect of the blowdown becomes more apparent. The lower water level in the low-pressure core melt sequence results in less steam generation from decay heat and less hydrogen generation. Therefore, much more hydrogen is generated in the high-pressure case which has more steam available for metal-water reaction.

In summary, the blockage and eutectic cutoff models used in MAAP reduce the hydrogen generation by a factor of 2 to 7 compared to the cases where these models are not used. For the more dominant LCLP-FS-R-N, LCLP-PF-R-N and LCHP-PS-R-N sequences there is very little change in release and time to rupture disk operation. The only case which resulted in a significant impact on the timing and magnitude of fission product release is the LCHP-PF-P-H sequence. However, examination of the containment event trees in Subsection 19D.5 indicates the probability of this event is very small. Therefore, it is judged that the ABWR severe accident performance is not sensitive to in-vessel hydrogen production.

19E.2.6.2 Fission Product Release From Core

The base sequences shown in Subsection 19E.2.2 use the Cubicciotti model for fission product release from the fuel. If the release from the fuel occurs later than the time predicted by the MAAP model then there could be more airborne fission products available for release from the containment. Also, as the accident progresses, the decontamination factor associated with the suppression pool will decrease as the pool heats up. Conversely, if the release is more rapid, the fission products will pass through the SRVs or the drywell to the suppression pool earlier. This will result in more efficient scrubbing of the fission products.

The effect of the release rate can be modeled in MAAP-ABWR by use of the variable SCALFP (Reference 19E.2-1) which decreases the release rate. Since early releases will result in lower releases from containment, this possibility will not be examined. In order to investigate the sensitivity of the dose to the release rate from the fuel, the LCLP-PF-R-N sequence was run with SCALFP changed from its nominal value of 1.0 to 10.0. This reduces the rate of release by an order of magnitude.

The behavior of the noble gases is not noticeably altered by the slower release. Some variation of the volatile release is observed. The most risk significant of the volatile fission products, CsI, is used as the measure of the behavior of the fission products. In the nominal case approximately 65% of the fission products are carried into the suppression pool shortly after vessel failure. A small percentage of the CsI is found in the drywell at this time, but the majority of the remaining fission products remain in the vessel where they are slowly revaporized. Finally, after the rupture disk opens, the flow through the vessel is sufficient to cause vaporization of the remaining 25% CsI in the vessel. The final release fraction of CsI through the rupture disk to the environment is less than 1.E-7.

The same basic trends may be observed in the behavior of the sequence with SCALFP equal to 10. However, the amount of material in each location varies substantially during the progression of the accident. At the time of vessel failure only 25% of the CsI has been swept to

the suppression pool. About 20% of the CsI is still present in the corium which relocates to the lower drywell. The remaining 55% of the material remains in the vessel, either in the fuel itself or on the various cool surfaces of the vessel. Slow release of CsI from the vessel then occurs until the time of the rupture disk opening when the fraction of CsI in the vessel and that in the suppression pool are both about 40%. The amount of fission products in the drywell remains relatively unchanged during this period. As in the nominal case, the remaining CsI leaves the vessel soon after the rupture disk opens. The final release fraction of CsI to the environment is also 1.E-7 for this case.

Despite the large variations in the location of the fission products within the containment during the accident, there is no appreciable variation in release from the containment due to the presence of the containment overpressure protection system in the design. Therefore, no further investigation of the impact of fission product release from the fuel is required.

19E.2.6.3 CsI Revaporization

An important aspect of fission product behavior is the propensity of the aerosols to adhere to the relatively cooler surfaces of the vessel and containment. While the deposition process is fairly well understood, there is considerable uncertainty in the revaporization of the fission products. MAAP assumes that the fission products are revaporized such that the local vapor pressure is consistent with the temperature of the surface. However, it has been proposed that chemical reactions may occur on the deposition surfaces which bind the fission products. This could result in delayed revaporization as the heat sink temperature slowly rises due to the decay heat of the fission products.

In the vessel of a BWR, most of the fission product deposition occurs on the steam dryers. After the fission products are deposited, they slowly begin to heat the dryers due to the decay heat they carry. As the temperature of the dryer increases, the fission products are revaporized. Thus, the impact of chemical binding of fission products to the dryers may be simulated by assuming a larger dryer mass. This causes the dryer temperature to rise more slowly, which in turn slows the re-evolution process. For this study, the dryer mass was doubled and the base sequence LCLP-PF-R-N was recalculated.

As in the discussion of fission product release in Subsection 19E.2.6.2, the CsI will be used as the representative fission product compound. There is no real difference in the timing of the key events. However, comparison of the results of this calculation to the base sequence described in Subsection 19E.2.2.1 shows that there is 2% to 5% more CsI in the vessel at any time during the transient. Nonetheless, there is not a substantial difference in the release fraction from the containment. In both cases the release fraction of CsI at 72 hours is about 1.E-7. Based on this small release fraction, no further consideration of CsI revaporization is necessary.

19E.2.6.4 Time of Vessel Failure

The detailed progression of a core melt during a severe accident is subject to considerable uncertainty. The core melt progression assumed in MAAP retains the corium above the core plate until local core plate failure occurs, resulting in a large pour of core debris into the lower plenum of the vessel. Before this time, water in the lower plenum has very little impact on the accident progression because heat transfer to the lower plenum water pool is very small. Consequently, the lower plenum is nearly full of water at the time of core plate failure.

Due to the large amount of core debris poured into the vessel head at the time of core plate failure, local failure of the instrument tubes is predicted very soon after debris enters the lower plenum. Therefore, there is insufficient heat transfer to the corium to quench it in the vessel; and, molten corium and water are relocated to the lower drywell. Figure 19E.2-2e shows that approximately 85,000 kg of water falls into the lower drywell at the time of vessel failure for a low pressure core melt scenario (LCLP).

In other melt progression models the molten fuel drips down the fuel rods in a process called candling. Under this assumption, it is possible for molten corium to be relocated in the lower plenum slowly, where it is quenched. Vessel failure could then be delayed until all water in the lower plenum is boiled off and the corium is reheated. This delay allows more time for operator action which could prevent vessel failure from occurring.

During the time when the water in the lower plenum is boiling, steam would continue to flow past the fuel rods which could result in increased hydrogen production. The impact of hydrogen production on the containment response is discussed in Subsections 19E.2.3.2 and 19E.2.6.1 which conclude that increased metal-water reaction will not have a significant impact on the offsite risk.

More important than the hydrogen generation is the behavior of the fission products assuming this type of core melt progression. As modeled in the MAAP program, a significant fraction of the volatile fission products are not swept into the suppression pool as they are released from the melting fuel. Rather, they are retained on the relatively cool surfaces in the vessel such as the steam dryers. Later, as these structures heat up, the fission products are revaporized. If the vessel is still intact, the fission products will be swept directly into the suppression pool via the safety relief valves where most of the volatile species will be retained.

For typical sequences using MAAP-ABWR, up to 80% of the volatile fission products are deposited on vessel surfaces just prior to vessel failure. These fission products would be released to the drywell atmosphere very slowly and would only be swept into the suppression pool gradually as steam is generated in the drywell and the containment pressurizes. A low pressure core melt sequence (LCLP-PF-R-N) was rerun with a modified version of MAAP-ABWR in which vessel failure was delayed until the water in the lower plenum had been boiled dry. In this sequence, only about 30% of fission products remained in the vessel at the time of vessel failure. This indicates that MAAP-ABWR base analysis may overpredict the airborne

fission products in the drywell. This could result in a significant conservatism for sequences in which the drywell head is presumed to fail. Therefore, the base analysis is conservative as regards the in-vessel effects of debris coolability in the lower head and time of vessel failure.

The assumed core melt progression model will have minor impact on the long-term ex-vessel portion of a severe accident. In the base analyses shown in Subsection 19E.2.2, there is an initial quenching of the corium in the lower plenum followed by a period of time in which the water in the lower drywell boils off. The corium then reheats and the passive flooders open. The influx of water through the flooders quench the corium. If the corium is retained in the vessel until the water from the lower plenum was boiled off, then the initial quenching of debris in the lower drywell will not occur and the passive flooder will open earlier relative to the time of vessel failure. However, this will not have a significant effect on the overall plant response to a severe accident.

The potential for the debris to be cooled in the lower plenum may have an important effect on some of the phenomena which are important immediately after vessel failure. If the debris is not coolable, as was assumed in the base analyses, there may be a large amount of molten debris at the time of vessel failure. If, on the other hand, the debris is cooled in the lower plenum, the penetrations may be expected to fail when only a small fraction of the material is molten. Both of these possibilities are considered in the direct containment heating and debris coolability uncertainty studies contained in Subsection 19E.2.7.

19E.2.6.5 Recriticality During In-Vessel Recovery

A potential challenge to the containment has been identified for accidents in which the core melt is arrested in the vessel. Experiments have indicated the potential for the boron carbide in the control blades to form a eutectic with steel at 1500 K and relocate (Reference 19E.2-28). This is considerably less than the temperature at which the fuel relocates (2500 K). Thus, as the core heats up and begins to melt, there may be regions of the core which are uncontrolled. If the vessel were reflooded after the onset of control blade relocation there is a potential for regions of the core to become critical raising the power level. This could increase the rate of containment pressurization and could potentially lead to operation of the rupture disk or to containment failure.

There are several mechanisms which tend to reduce the potential that the core becomes critical. First, when the cold water is injected into the hot core, it is likely that the any fuel which had been at very high temperature will shatter and form a rubble bed. Analyses performed by PNL (Reference 19E.2-29) indicate that the rubble bed geometry is subcritical since it is undermoderated. Similarly, if there has been substantial relocation of fuel from the upper part of the core, the lower portion of the core will be undermoderated and will probably be subcritical. Finally, if recriticality occurs, boron can be injected via the SLC system to return the core to a subcritical state.

Presuming that the core recriticality occurs as a result of in-vessel recovery, the power level would rise to a level determined largely by the rate of injection. Thus, in effect, a partial ATWS condition develops. As with any ATWS condition, voiding in the core tends to limit the power generation. Thus, the more injection available to the core, the higher the power level. Depending on the precise configuration of the core and control material, it is possible that some of the fuel is damaged locally. However, since coolant is necessary for power generation above the decay heat level, widespread melting of the fuel is inconsistent with the increased power level associated with recriticality.

The steam generated in the core would flow through the SRVs to the suppression pool which would begin to heat up, pressurizing the containment. The emergency operating procedures direct the operator to inject boron via the SLC system and to reduce the water level. Boron injection terminates the recriticality event. Lowering the water level reduces the power generation to a level which can be removed from the containment via the containment heat removal system. If no steps are taken to reduce the power level or to terminate the event, the containment will continue to pressurize leading to opening of the rupture disk and possibly to containment failure. In either case, any fission products released from the fuel in the period in which the core was melting and not retained in the suppression pool could be released from containment.

In order to examine the potential for recriticality to the ABWR containment a low-pressure core melt sequence was examined in detail to estimate the length of time in which recriticality is possible. Qualitative judgements are made about the potential for fuel shattering and the effects of fuel relocation. Additionally, a transient was run using a modified version of MAAP-ABWR to provide a conservative estimate of the minimum time available for the injection of boron should recriticality occur.

19E.2.6.5.1 Potential for Recriticality

In examining the potential for recriticality it is important to recognize that the heating and relocation of the core does not occur uniformly. Variations in the time of uncovery, heat transfer to other structures and the decay power cause the core heatup to progress from the top central portion of the core to the outer and lower regions. In general, once a portion of the core begins to heat up, it heats quickly until it reaches its melt point and begins to relocate.

A MAAP-ABWR calculation of a low-pressure core melt sequence was examined in detail to investigate the heatup and melting behavior of the core. The ABWR core has been modeled using a mesh of ten axial and five radial nodes such that each cell has equal volume. Each node is assumed to have a single temperature. The relocation of the boron carbide is not modeled in MAAP. However, judicious examination of the MAAP analysis can give useful insights.

Before looking at the MAAP-ABWR analysis, consider the possibility for temperature differences between the fuel and the control blades. The source of energy for the heating of the core is the decay heat in the fuel. This leads to the observation that the temperature of the control

blades should be less than that of the bulk of the core. Any temperature difference between the control material and the fuel would tend to decrease the time window for recriticality. In order to estimate the temperature difference, a simple radiation calculation is performed which neglects heat transfer to the steam and assumes that the heat transfer between the fuel and the control blade will cause both to heat up at the same rate. Thus,

$$\frac{\dot{Q}_{blade}}{\dot{Q}_{decay}} = \frac{(mc_p)_{blade}}{(mc_p)_{blade} + (mc_p)_{fuel} + (mc_p)_{can}} \quad (19E.2\text{-}58)$$

where:

$\dot{Q}$ = Rate of heat addition,

mc_p = Thermal mass.

Using approximate values for the thermal masses, only about 10% of the decay energy will go the control blade.

For an indication of the temperature difference between the blade and the fuel when the blade begins to melt, a simplified radiation heat transfer calculation is performed. The channel box walls are neglected and black body radiation is assumed.

$$\dot{Q}_{blade} = (FA)_{blade}\sigma(T^4_{fuel} - T^4_{blade}) \quad (19E.2\text{-}59)$$

where:

FA = Effective area for radiation heat transfer,

σ = Stefan-Boltzman coefficient,

T = Temperature.

The view factor from the control blade to the fuel is taken to be one which neglects the effects near the center of the cross. These assumptions tend to minimize the temperature difference. Assuming a decay heat level of 2% rated power and incipient melting of the control blades, the lower bound on the temperature difference between the fuel and the control blades is about 15 K. Even if different assumptions were made, maximizing the temperature difference, the fuel and control material temperatures would be very close to each other at these high temperatures. Therefore, the use of a single temperature for the fuel and the control blade is a reasonable assumption.

A MAAP-ABWR calculation of a low-pressure core melt sequence was examined to determine the core heatup and relocation characteristics. The core was nodalized using 5 radial rings and 10 axial levels. About 48 minutes after the start of the accident, the temperature in the inner rings of levels 8 and 9 exceeded 1500 K, the temperature at which relocation of the control material might begin. Within a minute levels 6 and 7 also exceed 1500. At 52 minutes, the fuel exceeds the temperature for zirconium melting (2100 K); and, by 55 minutes, there is widespread melting of the core in this region.

After the fuel exceeds the melt point for zirconium, any remaining cladding will be highly oxidic. It is judged to be highly likely that the rapid addition of cold water to the vessel would result in local shattering and relocation of the fuel. Thus, one would not expect a region which has exceeded the zirconium melt point to become recritical.

As time progresses, the region which might be devoid of control material moves downwards. At the same time, fuel from the upper regions of the core also relocates filling these regions with fuel. This reduces the mass ratio of the moderator to the fuel reducing the potential for recriticality. Therefore, it is judged that the critical interval for recriticality is a period of about 7 minutes.

The probability of recovering core cooling in this interval is fairly small. In order for recriticality to occur, there must be a system (or operator) failure that deprives the core of all cooling for about 50 minutes, then injection must be recovered in a time window of about seven minutes. Based on the standard models for recovery of systems and operator error, it is concluded that the probability of this occurrence is small. Therefore, the probability of a recriticality event occurring is small.

19E.2.6.5.2 Implications of Recriticality

Despite the judgement of a low potential for recriticality, an assessment of the effects of a recriticality event are examined. If vessel injection is recovered and some portion of the core becomes critical, the power level would rise above the decay heat level. As long as core injection continues, the fuel would be cooled, thus, no significant fuel damage would occur. However, the additional power generation could increase the rate of containment pressurization. The operator could terminate the recriticality event by initiation of the SLC system or mitigate the event by controlling the vessel injection flow rate.

To bound the impact on the containment, a calculation was performed to determine the earliest time at which the rupture disk could open given a recriticality event. This time indicates the time available to terminate recriticality via the stand-by liquid control system or, as a minimum, to reduce the power level via flow control and slow the rate of pressurization.

MAAP was not designed to analyze recovery scenarios. The model does not contain criticality models, nor can it assess power associated with a degraded core configuration. However, with one minor modification, it is possible to force an ATWS to occur late in an accident which, in

effect, is a recriticality event with the entire core uncontrolled. MAAP-ABWR includes the Chexal-Layman correlation for power during an ATWS. This result will bound the power generation in a recriticality event.

The low-pressure core melt scenario discussed above was used to estimate the time to rupture disk opening during a recriticality event. It was assumed that recovery of injection occurred at approximately 50 minutes. In order to determine the minimum time to rupture disk operation, all of the LPFL and HPCF systems were presumed to be available. A full ATWS condition was forced at the time of injection recovery. Based on the Chexal-Layman correlation, MAAP-ABWR predicts a power level of 15%. The containment pressurizes to the rupture disk setpoint about 55 minutes after recovery of injection. During this time the operator has ample indication that the reactor is critical since the containment pressure is rising very rapidly.

This estimate overpredicts the power level and, thus, underpredicts the time until the rupture disk might open for several reasons:

(1) As discussed above, it is expected that only a small region in the core will become critical. Most of the core will be shut down. Thus, the bulk of the core will generate power at decay heat level. The Chexal-Layman correlation represents the condition where the entire core is uncontrolled. Thus, the power level associated with recriticality will be a fraction of the ATWS power predicted by Chexal-Layman.

(2) The Chexal-Layman correlation is based on conditions at rated reactor pressure. At low pressure, the void fraction will be considerably higher. This causes the power level to be substantially reduced at low pressure. Many of the recovery scenarios will occur with the vessel at low pressure. For these cases, the use of Chexal-Layman is conservative. If the vessel is at high pressure, the LPFL systems will not have sufficient head to inject and the power level will be lower than that calculated here.

(3) It is highly unlikely that the all of the ECC systems will be recovered at the same time. As shown in Subsection 19D.5, the dominant core damage event in the ABWR is initiated by a transient with failure of all core cooling (Classes IA and ID). These sequences represent a majority of all core damage events. The simultaneous recovery of all ECC systems is not credible for these scenarios. At a given pressure the power level is directly proportional to the flow rate. Thus, the power should be about one fifth that given here since it is highly likely that only one ECC system is recovered.

(4) Even if all injection systems were to inject, the operator is instructed to reduce the core flow if the power rises above decay heat level. Studies of ATWS at high pressure have shown that the use of flow control will reduce the power to about 4%. Analyses performed for the success criteria in Subsection 19.3.1.3.1(2) show that the containment can be maintained below Service Level C by use of flow control and the containment heat removal system (Reference 19E.2-30).

Thus, one hour is a very conservative estimate of the time until the opening of the rupture disk. It is expected that the actual time until the containment pressure reached the rupture disk setpoint would be several hours. If the operator initiates SLC injection as directed in the Emergency Procedures, the recriticality event would be terminated. Therefore, the risk associated with a recriticality event is not judged to be significant.

19E.2.6.5.3 Conclusions

The potential for recriticality, as well as the implications of its occurrence, was examined. It was concluded that the time window in which recriticality could occur is very small and that only a small portion of the core could become critical at any time of recovery of injection. A very conservative calculation was performed which assumed that the entire core was uncontrolled and all ECC systems were used. This bounding calculation indicates the containment does not exceed the rupture disk setpoint for at least one hour after recovery. It is expected that the actual time until rupture disk operation would be several hours. This allows ample time for the operator to terminate the event by use of the stand-by liquid control system or to mitigate the event by reducing the rate of injection to the vessel and initiating containment heat removal. Thus, it is concluded that recriticality does not pose a significant threat to the ABWR design.

19E.2.6.6 Debris Entrainment and Direct Containment Heating

If a core melt accident occurs in which the reactor pressure vessel is at high pressure at the time of vessel failure, the debris may be entrained out of the lower drywell. If the debris is finely fragmented as it is dispersed, the pressure in the containment can rise rapidly. This process is called direct containment heating (DCH). The magnitude of the pressure rise is dependent on the amount of debris involved in the event. If a large fraction of debris participates in the DCH event the containment may be challenged. Since this would lead to an early failure of the containment structure in the drywell, the fission product releases from this type of scenario are judged to be high. Therefore, it was decided to bypass the performance of a sensitivity study for this case and perform a detailed uncertainty analysis. The results of this uncertainty analysis can be found in Subsection 19E.2.7.1.

19E.2.6.7 Fuel Coolant Interactions

Challenges of the containment during a severe accident may result from fuel coolant interactions. Fuel coolant interactions are most likely to challenge the containment when molten debris falls into water. Examination of the containment event trees indicates that a very small percentage of all sequences have water in the lower drywell before vessel failure. Both the impulse and static loads are considered. Fuel coolant interactions (FCI) may occur either at the time of vessel failure when corium and water fall from the lower plenum of the vessel, or when the lower drywell flooder opens after vessel failure has occurred.

Fuel coolant interactions were addressed in the early assessment for the ABWR response to a severe accident. Subsection 19E.2.3.1 examined the hydrodynamic limitations for steam explosions and concluded that there was no potential for a large scale steam explosion. The pressurization of the containment from non-explosive steam generation was calculated in the analyses for the accident scenarios. Attachment 19EB examines the available experimental database for its relevance to the ABWR configuration, and provide a simple, scoping calculation to estimate the ability of the ABWR containment to withstand a large, energetic fuel coolant interaction.

Four potential failure modes are considered. The transmission of a shock wave through water to the structure may damage the pedestal. Similarly, a shock wave through the airspace can cause an impulse load. However, since the gas is compressible, the shock wave transmitted through the gas will be much smaller than that which can be transmitted through the water. Therefore this mechanism is not considered here. Third, loading is caused by slugs of water propelled into containment structures as a result of explosive steam generation. Finally, the rapid steam generation may lead to overpressurization of the drywell.

The details of the analysis are presented in Attachment 19EB. The studies show that the limiting loading mechanism is the shock wave transmitted to the structure. Using a conservative bound for the impulse load capability of the pedestal, the structure can withstand the loads associated with a steam explosion involving 9.5% of the core mass. This is three times the mass of a credible fuel coolant interaction in the ABWR. Therefore, the ABWR pedestal is very resistant to fuel coolant interactions. This failure mechanism need not be considered further in the containment event trees or the uncertainty analysis.

19E.2.6.8 Core-Concrete Interaction and Debris Coolability

The issue of debris coolability has long been an area of considerable uncertainty in the progression of a core melt accident. In the ABWR design the lower drywell floor area is large in order to facilitate the spreading of the core debris. The firewater addition system, as well as the passive flooder design, ensure that debris will always be covered by water in the event of a severe accident.

However, experiments performed to date have been unable to provide conclusive evidence that these features cool the debris sufficiently to prevent core concrete interaction from occurring. If core concrete interaction were to continue unabated, there are two possible challenges for the ABWR containment design. First, the generation of non-condensable gas would contribute to the slow pressurization of the containment, even if containment heat removal is available. Second, if the concrete were eroded to a sufficient depth, the pedestal walls could be weakened to the point that the vessel was no longer sufficiently supported. If the vessel then tipped or fell, the piping attached to the vessel could cause the containment penetrations to tear, most likely in the drywell region of the containment.

The time of fission product release from the containment for either of these mechanisms would be fairly late but is dependent on the heat transfer from the corium to the overlying pool of water. Additionally, continued core concrete interaction can lead to an increase in the amount of fission product release. Since core concrete interaction can lead to a mode of drywell failure and because of the high visibility of this issue, it was decided to bypass the sensitivity study and to perform detailed uncertainty analysis for the dual issues of debris coolability and core concrete interaction.

19E.2.6.9 Fission Product Release Location

The adoption of the rupture disk in the ABWR containment design serves to significantly reduce the uncertainties in the timing, location and area of any fission product release. As discussed in Subsection 19E.2.8.1, the Containment Overpressure Protection System (COPS) is highly reliable. The setpoint of the rupture disk, 0.72 MPa, was selected such that there is a very small probability that the containment structure fails. As shown in Subsection 19F.3.1.2, the weakest portion of the ABWR containment is the drywell head. The median failure pressure of the drywell head is estimated to be 1.03 MPa abs. The other portions of the containment have an estimated failure pressure of 1.34 MPa. Thus, it is expected that most fission product releases will be via the rupture disk.

A fragility curve for the drywell head, Figure 19FA-1, shows the uncertainty in the failure pressure for the drywell head. The uncertainty of the rupture pressure for the COPS is very small as discussed in Subsections 19E.2.8.1.1 and 19E.2.8.1.2. Integrating over these two distributions, one can determine the probability that the drywell head fails before the COPS actuates. Because of the pressure difference between the wetwell and the drywell, three cases must be considered. For sequences in which the firewater system is used and water is added to the containment, as described in Subsection 19E.2.2, there is a small chance that the drywell head will fail. For sequences without water addition to the containment, the drywell head failure probability is even smaller. These probabilities are used in the quantification of the containment event trees in Subsection 19D.5. The third case applies to sequences with no pressure difference between wetwell and drywell. In these cases the drywell head failure probability is smaller yet.

19E.2.6.10 Fission Product Release Flow Area

The presence of the COPS serves to substantially reduce the uncertainties associated with the flow area for release of fission products from the containment. In the unlikely event that fission products are released from the containment, the release will almost always be via the COPS. Since this is an engineered feature of the plant, the uncertainties associated with the available flow area are very small. The COPS is designed to allow steam flow equivalent to 2.4% rated power. Since the decay heat level will be less than 1% at the time COPS operation is required, it is judged that the containment response is not sensitive to any small variation in the COPS effective flow area.

However, for the few cases discussed in Subsection 19E.2.6.9, the pressurization of the containment leads to failure of the drywell head. For these cases there is substantial uncertainty in the failure area. Therefore, two sensitivity cases were analyzed. In the first case the nominal failure area of 0.0129 m^2 (20 sq in) was increased by a factor of two. In the second case the failure area was divided by two. This broad range should bound any possible variations in the failure flow area.

The results for the three cases are identical until the time of drywell head failure. After drywell head failure the basic trends of the data are unchanged. The containment pressure is larger for cases with the smaller failure area than for those with larger areas. There is also a small variation in source term for the three cases. In the nominal case the release fraction of CsI is 9.7%. For the larger flow area, the release fraction increases to 12.6%; while, for the smaller flow area, the release drops 4.2%. Considering the upper bound, doubling the flow area increases the release by only 30%. Since a small percentage of all releases are a result of drywell head failure, the change in offsite consequences will be small. Therefore, no further consideration of containment failure area is necessary.

19E.2.6.11 Suppression Pool Bypass

The BWR containment is designed such that all gas generated in the vessel and the drywell passes through the suppression pool. This serves to quench the steam in the gas stream, which substantially decreases the pressurization rate of the containment. In addition, any fission products carried in the gas stream are scrubbed and retained in the suppression pool. Since the ABWR is designed such that any fission product release is from the wetwell airspace, this substantially reduces the risk in the unlikely event of a severe accident.
Subsection 19E.2.3.3.3(4) examined mechanisms which could result in suppression pool bypass, and determined that the only pathway which could significantly increase risk is vacuum breaker failure or leakage. The results of a sensitivity study performed to examine the impact of vacuum breaker performance is summarized in this subsection. Details of the analysis can be found in Subsection 19EE.3.

The dominant severe accident sequence [Loss of all core Cooling with vessel failure occurring at Low Pressure (LCLP)] was chosen to evaluate plant performance. MAAP-ABWR runs were made with effective vacuum breaker area, $A/\sqrt{K}$, varying from 0 to 2030 cm^2 (315 in^2). The upper bound corresponds to one fully open vacuum breaker. Five variations were analyzed. In each case the overpressure relief rupture disk opened when the wetwell pressure reached 0.72 MPa. The five scenarios were:

(1) Bypass leakage begins after passive flooder activation; aerosol plugging is neglected.

(2) Bypass leakage is present from the beginning of the accident; aerosol plugging is neglected.

(3) Bypass leakage begins after passive flooder activation; aerosol plugging of the vacuum breaker opening is considered.

(4) Bypass leakage is present from the beginning of the accident; aerosol plugging of the vacuum breaker opening is considered.

(5) Bypass leakage is present from the beginning of the accident and the operator initiates the firewater spray system.

Suppression pool bypass can lead to a significant increases in fission product release. Releases can be on the order of 10 to 20% for a fully stuck open vacuum breaker. For sequences in which the firewater addition system is used in spray mode, the time to release is not significantly affected. However, for sequences without sprays, the time from the beginning of the accident until the onset of the release can be significantly reduced. The use of the Morowitz blockage model results in a significant improvement in the calculated risk associated with suppression pool bypass. Nonetheless, there is a substantial increase in consequences associated with large bypass areas. Therefore, suppression pool bypass is examined with a detailed uncertainty analysis in Subsection 19E.2.7.3.

19E.2.6.12 High Temperature Failure of Drywell

One of the failure modes identified for the containment was the degradation of the seals for the moveable penetrations in the drywell due to high temperature (Subsection 19F.3.2.2). In the base analyses discussed in Subsection 19E.2.2, the only sequences which exceeded the threshold temperature of 533 K (500°F) were those in which debris was entrained into the upper drywell and sprays were not available. In these cases the debris can radiate directly to the upper drywell structures. For the other sequences, the debris is covered by water so elevated temperature in the upper drywell is dependent on heat transfer from remaining fuel in the vessel to the upper drywell.

To ascertain the sensitivity of the drywell temperature to parameters which could affect it, several sensitivity studies were performed. All of the studies were performed using a low-pressure core melt sequence. The LCLP-PF-R-N sequence, with passive flooder operation, was selected since cases with firewater spray available are not expected to result in high drywell temperatures.

In the first calculation performed, the mass of equipment in the drywell was decreased to reduce the thermal mass in the upper drywell. The mass was arbitrarily decreased to half of the nominal value used in the base analyses. The temperature in the upper drywell at the time the rupture disk opened decreased from its nominal value of 500 K (441°F) to 487 K (418°F). While this result is somewhat counterintuitive, it can be easily explained. In the early stages of the accident, the temperature in the drywell is higher in the sensitivity case. This results in a small increase in the amount of fuel which melts and relocates into the lower drywell. Consequently,

there is less heat generation in the vessel and less radiative heat transfer to the upper drywell. The overall containment performance is not affected by the slight decrease in temperature.

A second analysis was then performed in which the mass of equipment in the upper drywell was increased by a factor of two. In this case the upper drywell temperature at the time of rupture disk opening is virtually unchanged from the nominal case. In the very long term, well after the rupture disk opens, there is a slight increase in temperature compared to the nominal case as one would expect based on the previous result. However, there is no significant impact on containment performance.

The final sensitivity case performed considered the impact of increasing the convective heat losses from the vessel to the drywell 50% above its nominal value. A slight increase in the upper drywell gas temperature was observed in this case. At the time the rupture disk opened, the upper drywell temperature was 505 K (450°F) as compared to 500 K (441°F) in the nominal case. The overall containment performance is not affected by this slight change.

In summary, the three sensitivity studies performed to assess the sensitivity of the drywell temperature to the detailed modeling assumptions indicate that the ABWR is not sensitive to those parameters which affect drywell temperature. Therefore, no further study of this area is necessary.

19E.2.6.13 Suppression Pool Decontamination Factor

From the standpoint of severe accidents, one of the most important features of a pressure suppression containment is the suppression pool. The suppression pool not only quenches any steam which enters it, reducing the rate of containment pressurization, it also traps the fission products carried with the gas flow. This process, known as scrubbing, significantly reduces the amount of fission product aerosols available for release from the containment.

The efficiency of the scrubbing process is typically characterized in terms of a decontamination factor (DF) defined by the mass of debris which enters the pool divided by the mass of debris which leaves the pool. MAAP-ABWR uses correlations based on the SUPRA code to calculate the DF. These correlations typically result in very high retention of fission products in the pool for all species of interest except the noble gasses which have a DF of 1.0.

In order to investigate the sensitivity of the offsite consequences of a severe accident to the suppression pool decontamination factor, a simple sensitivity study was performed. The MAAP-ABWR code was modified to allow a constant DF to be input for all species except the noble gasses. Two calculations were then repeated assuming a conservative DF of 100. None of the other fission product removal mechanisms were affected by the change.

The two cases selected for study were both low-pressure core melt sequences. In the first sequence, LCLP-FS-R-N, the firewater system is assumed to be available, while in the second case, LCLP-PF-R-N, the passive flooder operated to cool the debris. Both cases indicated a

significant increase in the fission product release. For the case with the firewater system available, the fraction of CsI release increased from 1.5E-7 to 1.2E-3. For the case with the passive flooder the results were similar, the CsI release increased from 1.2E-7 to 1.6E-3.

CRAC cases were run in order to determine the effect of these changes on the consequences of release. The probability of the dose is dependent on the weather. There is virtually no impact until a conditional probability of 0.04. Thus, there will not be a significant impact on offsite dose, even for a very conservative DF of 100. Thus, it has been shown that the consequences of a severe accident are not very sensitive to variation in the suppression pool decontamination factor. No further consideration of this phenomena is required in uncertainty analysis.

19E.2.6.14 Suppression Pool pH Control

The chemical form of iodine may be affected by the acidity of the suppression pool. If the pool becomes acidic (pH <7) the formation of volatile and organic forms of iodine may be enhanced. Experiments have indicated the potential for the radiolytic formation of nitric acid (HNO_3) in the suppression pool. This can then lead to the conversion of I^- to I_2 in the pool. The gas species remain in equilibrium with the I_2 in the pool, with the relative amounts governed by a partition fraction between the water- and gas-borne species. Reference 19E.2-31 states, "If the pH is controlled so that it stays above 7, a reasonable value for the I^- converted to I_2 is 3.E-4 ...[Calculation] indicates a small production of volatiles for PWRs but virtually none for BWRs".

Calculations were performed following the methods of Reference 19E.2-31 to determine the potential for the formation of nitric acid to lead to an acidic suppression pool. These sequences differed by consideration of varying initial suppression pool pH, caused by the transport of CsOH to the pool as a result of the accident. In each calculation, the pH of the pool is monitored over time as nitric acid is formed radiolytically. The results of two calculations which bound the expected transfer of CsOH to the pool are given below. In both cases, the transfer of CsI to the pool is assumed to be the same as that for CsOH.

Initial CsOH fraction in pool	**10%**	**80%**
Time (h)	**pH**	**pH**
0	9.65	10.56
1	9.65	10.56
10	9.63	10.53
24	9.59	10.49

The results of these calculations indicate that the pH of the suppression pool will not drop to the acidic range within 24 hours of accident initiation. Therefore, nitric acid formation due to radiolysis will not have a significant impact on the source term. No further consideration of this phenomenon is necessary.

19E.2.7 Detailed Phenomenological Uncertainty Studies

19E.2.7.1 Direct Containment Heating

Direct Containment Heating (DCH) is the sudden heatup and pressurization of the containment resulting from the fragmentation and dispersal of core material in the containment atmosphere. DCH is a concern for sequences in which the vessel fails at high pressure since the steam flow from the vessel provides the motive force for entrainment. In the event of a sufficiently large DCH event, the containment could fail at the time of vessel failure. This would lead to very high releases to the environment. In the past DCH has been addressed for Pressurized Water Reactors. BWRs have very reliable vessel depressurization systems. Thus, the frequency of accidents with the vessel remaining at high pressure is extremely low. However, with the many sources of low-pressure injection available to the ABWR to prevent core damage, the frequency of all core damage sequences is very low. Therefore, high pressure core melts appear as contributors to the total core damage frequency, albeit with a very low probability.

A detailed uncertainty analysis utilizing decomposition event trees (DETs) was performed to assess the peak drywell pressure resulting from a DCH event. This analysis is given in Attachment 19EA. A large number of calculations were performed to determine the impact of DCH on the probability of containment failure and offsite risk. The analysis investigated uncertainties in a variety of phenomena:

(1) Mode of vessel failure,

(2) Mass of molten core debris at the time of vessel failure,

(3) Potential for high pressure melt ejection,

(4) Fragmentation of debris in the containment.

Additional sensitivity studies were performed to examine other phenomena which could affect DCH. The study concluded that a deterministic best estimate for the peak pressure from DCH would not lead to containment failure. Consideration of the uncertainties in the phenomena lead to a very small CCFP for all core damage events. Additional sensitivity analyses were considered which indicate that an upper bound on the impact of DCH is a small percentage. Even in this limiting case, the probability of DCH failing containment is well below the goal of 10%. Furthermore, since the probability of containment failure due to DCH is very low, there is no measurable impact on offsite dose.

19E.2.7.2 Debris Coolability

The issue of debris coolability has long been an area of considerable uncertainty in the progression of a core melt accident. In the ABWR design, the lower drywell floor area is large in order to facilitate the spreading of the core debris. The firewater addition system, as well as the passive flooder design, ensure that debris will always be covered by water in the event of a severe accident.

However, experiments performed to date have been unable to provide conclusive evidence that these features cool the debris sufficiently to prevent core concrete interaction from occurring. If core concrete interaction were to continue unabated, there are two possible challenges for the ABWR containment design. First, the generation of non-condensable gas would contribute to the slow pressurization, even if containment heat removal is available. Second, if the concrete were eroded to a sufficient depth, the pedestal walls could be weakened to the point that the vessel would no longer sufficiently supported. If the vessel then tipped or fell, the piping attached to the vessel could cause the containment penetrations to tear, most likely in the drywell region of the containment. Additionally, continued core concrete interaction can lead to an increase in the amount of fission product release.

A detailed uncertainty analysis utilizing decomposition event trees (DETs) was performed to determine the potential for continued core concrete interaction and its impact on the containment response. This analysis is given in Attachment 19EC. A large number of calculations were performed. These calculations addressed uncertainties in the following parameters:

(1) Amount of core debris,

(2) Debris-to-water heat transfer,

(3) Amount of additional steel in the debris,

(4) Delayed flooding of the lower drywell,

(5) Fire water injection instead of passive flooder operation.

The conclusions from all of these uncertainty calculations were:

(1) For the dominant core melt sequences that release core material into the containment, a large percentage result in no significant CCI. An insignificant number of sequences are expected to experience dry CCI.

(2) Even for those low frequency cases with significant CCI, radial erosion remains below the structural limit of the pedestal. After consideration of uncertainties, only a small percentage of the sequences with significant CCI will suffer pedestal failure.

Combining this conclusion with the first, an extremely small percentage of all core melt sequences with vessel failure will lead to additional drywell failures as a result of CCI.

(3) The time of fission product release is not significantly affected by continued CCI.

(4) The fission product release is dominated by the noble gasses when the containment overpressure protection system operates. This conclusion is unaffected by assumptions on debris coolability. Therefore, the offsite dose for sequences with rupture disk operation is not impacted by core concrete attack.

These conclusions would indicate that the uncertainties associated with CCI have an insignificant influence on the containment failure probability and risk.

19E.2.7.3 Suppression Pool Bypass

Suppression pool bypass (the passage of gas and vapor from the drywell directly into the wetwell airspace) can lead to increased fission product releases. As shown in Subsection 19E.2.3.3.3(4), the only mode of suppression pool bypass that has the possibility of significantly increasing risk is vacuum breaker leakage. Attachment 19EE determined the probabilities and consequences for vacuum breaker leakage areas from zero to that corresponding to one vacuum breaker stuck fully open.

Fission product release fractions were determined with MAAP-ABWR using the dominate accident sequence [Loss of all core Cooling with vessel failure occurring a Low Pressure (LCLP)] modified to include a path between the drywell and the wetwell airspace. Plugging of leakage paths by fission products was considered for small pathways. Leakage probabilities were determined by reviewing recent operating experience of wetwell to drywell vacuum breakers in BWRs with Mark I, II and III containments.

Suppression pool bypass does not significantly add to the risk associated with the ABWR because the bypass areas resulting in increased releases are offset by low probabilities of occurrence. No leakage and, correspondingly, no impact on plant risk is expected to occur for almost all of the accident demands. Small amounts of leakage have a small probability per event, and can result in medium volatile fission product releases (1 to 10% of initial inventory). Volatile fission product releases on the order of 10 to 20% of initial inventory can result when large amounts of suppression pool bypass are present. However, the impact on plant risk is still negligible because the probability of large leakage is very small.

19E.2.8 Severe Accident Design Feature Considerations

Although the frequency of core damage is very low in the ABWR design, features were added to the design to ensure a robust response of the containment to a severe accident. This subsection discusses the important considerations for the severe accident design features.

19E.2.8.1 Containment Overpressure Protection System

ABWR has a very low core damage frequency. Furthermore, in the unlikely event of an accident resulting in core damage, the fission products are typically trapped in the containment and there is no release to the environment. Nonetheless, in order to mitigate the consequences of a severe accident which results in the release of fission products and to limit the effects of uncertainties in severe accident phenomena, ABWR is equipped with a Containment Overpressure Protection System (COPS). This system is intended to provide protection against the rare sequences in which structural integrity of the containment is challenged by overpressurization. It has been determined that these rare sequences comprise a small percentage of the hypothesized severe accident sequences.

The COPS is part of the atmospheric control system and consists of two 200A (8-inch) diameter overpressure relief rupture disks mounted in series on a 250A (10-inch) line which connects the wetwell airspace to the stack. The second rupture disk, located at the inlet to the plant stack, has a very low setpoint, less than 0.03 MPa differential pressure. The setpoint of the inner rupture disk, located near the containment boundary, will be selected such that the COPS opens when the wetwell pressure is 0.72 MPa. The COPS provides a fission product release point at a time prior to containment structural failure. Thus, the containment structure will not fail. By engineering the release point in the wetwell airspace, the escaping fission products are forced through the suppression pool. In a core damage event initiated by a transient in which the vessel does not fail, fission products are directed to the suppression pool via the SRVs, scrubbing any potential release. In a severe accident with core damage and vessel failure or in a LOCA which leads to core damage, the fission products will be directed from the vessel and drywell through the drywell connecting vents and into the suppression pool again ensuring any release is scrubbed. Eventually, if the containment pressure cannot be controlled, the rupture disk opens. Any fission product release to the environment is greatly reduced by the scrubbing provided by the suppression pool.

In the absence of the COPS, unmitigated overpressurization of the containment will result in failure of the drywell head for most severe accident scenarios (Some high-pressure core melt sequences result in fission product leakage through the moveable penetrations in the drywell rather than drywell head failure.). To compare the consequences of severe accidents resulting in fission product releases via drywell head failure to those with releases through the COPS, MAAP-ABWR was used to simulate a series of severe accident sequences for both release mechanisms. These severe accident sequences are described in Subsection 19E.2.2. Failure pressure of the drywell head was assumed to be equal to its median ultimate strength, 1.025 MPaG. The results of these runs show releases of volatile fission products, after 72 hours, for the COPS cases to be several orders of magnitude less than for the corresponding drywell head failure cases. Most accident sequences show this large difference in releases between drywell head failure and COPS cases.

19E.2.8.1.1 Pressure Setpoint Determination

Several factors were considered in determining the optimum pressure setpoint for the rupture disk. The results of the previous analysis show that it is desirable to avoid drywell head failure. This can be assured by providing a rupture disk pressure setpoint below the pressure that would begin to challenge the structural integrity of the containment. However, as the pressure setpoint is reduced, the time to containment failure and fission product release is also reduced. Thus, the setpoint of the rupture disk must optimize these competing factors: minimizing the probability of drywell head failure while maximizing time before fission product release to the environment.

The service level C capability of the containment serves as one indication of a lower bound for the structural integrity of the containment. As shown in Appendix 19F, the service level C for the ABWR is 0.77 MPa, limited by the drywell head. Thus, it is desirable to set the rupture disk setpoint below this value.

The distribution of drywell head failure pressure and the distribution of rupture disk burst pressure were also considered in determining the burst pressure. As stated in Attachment 19FA, the drywell head failure pressure is assumed to have a lognormal distribution with a median failure pressure equal to its ultimate strength of 1.025 MPaG. The variability of rupture disk opening pressures is best modeled with a normal or Gaussian distribution. Typical high quality rupture disks exhibit a tolerance of ±5% of the mean opening pressure. Tests have shown that this ±5% tolerance spans ±2 to ±2.5 standard deviations of the rupture disk population. This analysis of the Containment Overpressure Protection System conservatively assumes that only ±2 standard deviations are included within the ±5% tolerance. Because the setpoint of the outer rupture disk is very low, the variability of the pressure is neglected in comparison to the variability of the inner, high pressure disk.

A critical parameter in determining the risk of drywell head failure before rupture disk opening is the pressure difference between the drywell and wetwell. Late in an accident the drywell is at higher pressure than the wetwell. For a given rupture disk setpoint, the probability of drywell head failure increases as the pressure difference increases. The maximum drywell to wetwell pressure difference is 0.1 MPa. This pressure difference occurs for cases in which firewater spray was activated after vessel failure but terminated before containment failure. Cases without firewater spray have pressure differences of no more than 0.05 MPa.

A COPS setpoint of 0.72 MPa at 366 K (200°F) was chosen. The residual risk of drywell head failure may be calculated by combining the two distributions with an offset corresponding to the pressure difference between the wetwell and the drywell. A 0.72 MPa setpoint results in a small probability of drywell head failure prior to rupture disk opening for a 0.1 MPa drywell to wetwell pressure difference. For a drywell to wetwell pressure difference of 0.05 MPa, the drywell head failure probability prior to rupture disk opening is smaller. This is judged to be an acceptable level of risk.

19E.2.8.1.2 Variability in Rupture Disk Setpoint

Nickel was chosen as the material for the rupture disk for evaluation purposes due to its relative insensitivity to changes in temperature. At temperatures above room temperature the opening pressure of a typical nickel rupture disk will decrease by about 2% for a 56 K (100°F) increase in temperature. Thus, in order to estimate the uncertainty due to variations in the temperature of the ABWR rupture disk, a sensitivity study was performed in which the pressure setpoint of the rupture disk was varied.

The nominal pressure setpoint of the rupture disk is 0.72 MPa at 366 K (200°F). Two cases were examined using MAAP-ABWR in this sensitivity study. For both cases the LCLP-PF-R sequence was used as the base case. First, the rupture disk pressure setpoint was reduced to 0.708 MPa which corresponds to a rupture disk temperature of 422 K (300°F); and, second, the pressure setpoint was increased to 0.735 MPa which corresponds to a temperature of 311 K (100°F). This temperature range, from 311 to 422 K (100 to 300°F), bounds all anticipated rupture disk temperatures.

The elapsed time to rupture disk opening was within 0.8 hours of the base case value of 20.2 hours for both cases tested. Higher rupture disk temperatures (i.e. lower pressure setpoints) reduce the time to rupture disk opening and lower rupture disk temperatures (i.e. higher pressure setpoints) increase the time to rupture disk opening. There were no significant changes in fission product release. For both cases the CsI release fraction at 72 hours remained less than 1E-7.

Another parameter affected by the variation in the rupture disk temperature is the probability of drywell head failure prior to rupture disk opening in a severe accident. Using the rupture disk and drywell head failure distributions, it was determined that the probability of drywell head failure prior to rupture disk opening increased slightly for the case with the rupture disk temperature of 311 K (100°F). With a rupture disk temperature of 422 K (300°F), the probability decreased slightly. The rupture disk temperature variation has a similar effect on the severe accident sequences in which the firewater spray system is activated. The probability of drywell head failure prior to rupture disk opening increases slightly for the case with the rupture disk temperature of 311 K (100°F) and decreases slightly for the case with the rupture disk temperature of 422 K (300°F).

The results of this sensitivity study show that variations in rupture disk temperature, which cause small variations in rupture disk opening pressure, have a minor effect on the performance of the ABWR Containment Overpressure Protection System.

19E.2.8.1.3 Sizing of Rupture Disk

The size of the rupture disk has also been optimized. If the rupture disk is too small, it could be incapable of venting enough steam to prevent further containment pressurization. On the other hand, if the rupture disk is too large, level swell in the suppression pool could introduce water

into the COPS piping. If this were to occur, the piping could be damaged or there could be carryover of waterborne fission products from the containment.

A 200A (8-inch) rupture disk was selected. This is sufficient to allow 35 kg/s of steam flow at the opening pressure of 0.72 MPaA and corresponds to a energy flow of about 2.4% rated power. The minimum acceptable flow rate is 28 kg/s of steam flow at the same pressure. For virtually all severe accident sequences, the rupture disk would not be called upon until about 20 hours after scram. The decay heat level at this time is about 0.5%. Thus, there is ample margin in the sizing of the rupture disk for severe accidents.

An additional accident was considered in the selection of the rupture disk size. In the event of an ATWS with the additional failure of the standby liquid control system, the operator is directed to lower water level to control power. Analysis has shown that the RHR system is capable of removing the energy generated by the ATWS from the containment (Subsection 19.3.1.3.1). If the additional failure of containment heat removal is assumed, a simple calculation indicates that an the rupture disk area is just sufficient to limit the containment pressure below service level C.

Calculations were also performed to investigate the potential effects of pool swell and fission product carryover at the time of COPS operation. These analyses (Subsection 19E.2.3.5) indicate that pool swell does not threaten the integrity of the COPS piping and that no significant entrainment of fission products will occur due to carryover.

19E.2.8.1.4 Not Used

19E.2.8.1.5 Suppression Pool Bypass

A comparison of performance for cases with suppression pool bypass flow through an open vacuum breaker valve was also considered. Cases were run with bypass effective area varying from 5 to 2030 cm^2 (0.0054 to 2.19 ft^2). A fully open vacuum breaker has a flow area of 2030 cm^2. The dominant the Loss of All Core Coolant with Vessel Failure at Low Pressure sequence was considered with Passive Flooder Operation since previous analysis has shown that the firewater system is capable of mitigating bypass.

No credit was taken for aerosol plugging of the bypass leakage in this analysis; and, therefore, the results are conservative. Also, it was assumed that the bypass leakage was present from the beginning of the accident sequence. As the bypass area increases, the fraction of fission product aerosols which pass through the suppression pool decreases. Thus, the benefit of a wetwell release of fission products is significantly reduced as the bypass area increases.

For effective bypass areas less than 50 cm^2 (0.054 ft^2), CsI releases at 72 hours from the COPS cases were smaller than for the corresponding drywell head failure cases. However, the differences in CsI releases at 72 hours were only factors of 2 to 4 rather than several orders of magnitude. The time difference between drywell head failure and rupture disk opening was 4

to 8 hours for these small bypass areas. For bypass effective areas greater than 50 cm^2 (0.054 ft^2), CsI release fractions at 72 hours are on the order of 10% for both the drywell head failure cases and the COPS cases. On the other hand, the time difference between rupture disk opening and drywell head failure is only 2 to 4 hours for these larger bypass areas. These relatively small time differences will not significantly affect the magnitude of the offsite dose. Attachment 19EE has a complete discussion of suppression pool bypass flow through vacuum breaker valves.

19E.2.8.1.6 Potential Impact of Hydrogen Burning and Detonation

Hydrogen burning and detonation are not a concern for the ABWR containment because the containment is inerted with hydrogen. There could be a potential for burning in the COPS system and the stack after the rupture disk opens. However, due to the design and operation of the COPS system, this issue does not have an impact on risk.

Hydrogen burning and detonation will be precluded in the piping associated with the COPS system. The piping will be inerted during operation with rupture disk located at the inlet of the stack. This, combined with initial purging of the piping, will ensure that the inertion of the containment will extend out to the stack, and prevent burning of hydrogen in the portion of the COPS system which is within the reactor building. Therefore, there will be no concern of the leading edge of the containment atmosphere mixing with the gas in the piping and causing a burn. After passing of the leading edge of the gas flow, the mixture in the piping will be identical to that in the containment. The gas flow through the system will prevent the backflow of air into the COPS piping.

Hydrogen burning could occur in the plant stack as the gas flow enters the stack. The stack is a non-seismic structure located on top of the reactor building. Because of this configuration, the reactor building has been designed to withstand the loads associated with the collapse of the plant stack. Furthermore, no credit is taken in the analysis for the plant stack to reduce the offsite dose by providing for an elevated release. All releases were presumed to occur at the elevation of the top of the reactor building. Therefore, hydrogen burning or detonation in the stack will have no impact on the consequences of a severe accident as modeled in this analysis.

No burning will occur within the COPS piping. Furthermore, no credit was taken for the plant stack to reduce the source term to the environment and the reactor building can withstand the collapse of the plant stack. Therefore, hydrogen burn or detonation in the COPS system will have no impact on risk and no further consideration of this phenomenon is required.

19E.2.8.1.7 Summary

A wetwell pressure setpoint of 0.72 MPa for the overpressure relief rupture disk meets the design goal. The probability of containment structural failure is minimized while maximizing the time to fission product release in a severe accident. The small probability of containment structural failure if the pressure reaches the rupture disk setpoint in a severe accident, combined

with the already low core damage frequency and reliable containment heat removal, produces an extremely low probability of significant fission product release. In addition, the elapsed time to rupture disk opening is greater than 24 hours for most severe accident sequences.

19E.2.8.2 Lower Drywell Flooder

19E.2.8.2.1 Introduction

This subsection provides the bases for sizing the lower drywell flooder system. The system is described in detail in Subsection 9.5.12.

The lower drywell flooder provides an alternate source of water to the lower drywell once it contains core debris. The primary water source is the firewater addition system. Water present in the lower drywell cools the core debris and establishes a water pool above the debris. Water absorbs heat by first heating up to saturation conditions and then boiling away. Debris cooling requires that the water absorb the heat generated in the debris bed and the latent and sensible heat released by the debris as its temperature decreases. Quenching prevents or mitigates core concrete interaction (CCI). An overlying water pool also scrubs fission products which may be released from the debris bed.

The flooder system is comprised of ten piping lines. Each line originates in one of the ten vertical pipes which are part of the drywell to wetwell connecting vent system. The vents are arranged symmetrically around the perimeter of the lower drywell. The flow through each flooder line will be initiated by melting a temperature-sensitive fusible plug (or fusible link) that in turn triggers the fusible plug valve to fully open and remain open.

The minimum acceptable flow rate for the flooder system corresponds to the flow rate which can just absorb the heat generated in the debris bed. Minimum acceptable flow is calculated in Subsection 19E.2.8.2.2. The expected flow rate in the flooder system can be obtained by applying Bernoulli's equation to the flooder geometry. This calculation is presented in Subsection 19E.2.8.2.3.

19E.2.8.2.2 Minimum Acceptable Flow Rate

Heat is generated in the debris bed by fission product decay and zirconium oxidation. Any flooder flow in excess of the amount required to remove generated heat will participate in quenching the debris and establishing a water pool above the debris bed. As shown in Attachment 19EC, the time required to quench the debris is not a critical parameter in determining containment performance. Therefore, the minimum acceptable flow rate for the lower drywell flooder system is the rate which will completely absorb all the heat generated in the debris bed.

The decay heat generation rate at the time when debris is expected to first enter the lower drywell during credible accident scenarios is approximately 1% of rated power (39 MW). Thirty-nine megawatts can be used as a first approximation of the decay heat generation rate of

the debris bed in the lower drywell. This assumption is highly conservative because the entire core mass will never completely relocate into the lower drywell. Furthermore, noble gasses and volatiles will escape from the molten debris, carrying away the decay heat associated with these two constituents (approximately 20% of the total).

Heat can also be generated in the bed by exothermic reactions of the debris constituents. The most energetic reactions involve oxidation of zirconium by water vapor and carbon-dioxide. The only source of significant amounts of oxidizing agents is the concrete beneath the debris bed. The water above the bed will not contribute significantly to oxidation because the surface of the bed will form a crust which will quickly be depleted of zirconium. NUREG-5565 indicates that a typical ablation rate for concrete is 5.08 cm (2 inches) per hour. The generation rate, assuming that the H_2O and CO_2 released during ablation completely react with zirconium, is 3.6 MW. Combining these two sources of heat yields a debris bed heat generation rate of 43 MW.

The heat absorption capability of the suppression pool water is 2,350 MJ/m^3. Therefore, the minimum acceptable flow rate for the lower drywell flooder system is 0.018 m^3/s (18 liters/s). Assuming a four-inch throat, as discussed in Subsection 19E.2.8.2.3, this flow can be provided by two lines of the lower drywell flooding system. Alternatively, if nine flooder lines are active, this system flow corresponds to a minimum individual line flow of 2 liters/s.

19E.2.8.2.3 Expected Flooder Flow Rate

The flow rate through the flooder system will be governed by the flow area, the hydrostatic driving head and head losses in the lines.

The flow area depends on the diameter of the flooder lines and the number of lines that are participating. Assuming that one flooder fails to operate, the flow area is

$$A_f = \frac{\pi}{4} d_f^2 n_f = 0.073 m^2 \quad \text{(19E.2-60)}$$

where:

d_f = diameter of lines (0.1016 m, 4 in), and

n_f = number of lines (9, assuming one fails).

The elevation of the flooder line exit below the water level in the drywell-to-wetwell connecting vents determines the hydrostatic head, Figure 19E.2-23. Due to steaming in the drywell, the drywell pressure is greater than the wetwell pressure and the water level in the drywell-to-wetwell connecting vents is assumed to be depressed to the bottom of the first row of horizontal vents. This leaves a hydrostatic head, Δz, of 0.375 meters to the inlet of the flooder lines.

Form and frictional head losses decrease the flow through the flooder lines. Form losses are due to entrance and exit effects as well as the 90° elbow and valve. A loss coefficient, k, of 3 conservatively accounts for all the head losses in the flooder system.

Applying Bernoulli's equation to steady, irrotational flow and assuming that the level of the suppression pool does not change (since the surface area of suppression pool is much greater than the flooder flow area) yields a flooder flow rate of

$$\dot{v}_{fl} = A_f\sqrt{\frac{2g\Delta z}{1+k}} = 0.099 m^3/s \quad (19E.2\text{-}61)$$

where:

$\dot{v}_{fl}$ = the total volumetric flow rate through nine lines, and

g = the acceleration of gravity.

For a liquid density of 980 kg/m^3, this corresponds to a system flow rate of 97 kg/s and an individual line flow rate of 10.8 kg/s. This is the expected flow rate through the flooder system assuming complete expulsion of the fusible plug and minimum hydrostatic driving head.

19E.2.8.2.4 Time to Fill Lower Drywell

Water that enters the lower drywell provides cooling to the debris bed. It also establishes an overlying liquid layer. Neglecting the subcooling of the flooder water, heat transfer from the debris bed to the water will result in vaporization. The amount of flooder flow which is vaporized is

$$\dot{V}_{vap} = \frac{\dot{Q}}{h_{fg}\rho_{liq}} \quad (19E.2\text{-}62)$$

where:

$\dot{V}_{vap}$ = volume rate at which flooder water is vaporized,

$\dot{Q}$ = heat transfer from the debris bed to the flooder water,

h_{fg} = latent heat of vaporization of water,

ρ_{liq} = density of water.

The amount of flooder flow which can contribute to filling the lower drywell is

$$\dot{v}_{fill} = \dot{v}_{fl} - \dot{v}_{vap} \quad (19E.2\text{-}63)$$

The time to fill the lower drywell to the exit of the flooder is

$$t_{fill} = \frac{V_{fill}}{\dot{v}_{fill}} \quad (19E.2\text{-}64)$$

where

V_{fill} = the volume of the lower drywell below the flooder exit.

The flooder exit will be 1.15 meters above the lower drywell floor. The surface area of the lower drywell floor is 88.25 m^2. Thus,

$$V_{fill} = 101.5 m^3$$

Flooder actuation is expected to occur approximately five hours after reactor scram during most severe accident scenarios. The decay heat level at this time is approximately 1% of the rated power. Assuming the entire core relocates to the lower drywell, the debris bed will have a decay heat generation rate, Q_d, of 39 MW. If all of this heat is transferred to the flooder water, the rate and time to fill the lower drywell are

$$\dot{v}_{fill,\,d} = 0.080 m^3/s$$

$$t_{fill,\,d} = 21 \text{minutes}$$

The maximum heat flux from the surface of a debris bed that has been experimentally observed (Subsection 19EB.2.2) is 2 MW/m^2. The lower drywell has a surface area of 88.25 m^2. Thus, the maximum cooling rate of the debris bed, Q_{max}, is 177 MW. For this heat transfer rate, the rate and time to fill the lower drywell are

$$\dot{v}_{fill,\,max} = 0.016 m^3/s$$

$$t_{fill,\,max} = 1.8 \text{hours}$$

In practice, this high heat flux is not expected to be maintained as the debris is quenched. Nonetheless, the time to fill the lower drywell to the elevation of the flooder exit will be bounded by these two values, 21 minutes and 1.8 hours. This difference in timing will not have

a significant impact on the fission product release from the containment since the steam produced during debris quenching will carry any fission products released during this time into the suppression pool.

19E.2.8.2.5 Consequences of One Flooder Line Opening First

Core debris that enters the lower drywell will be distributed fairly uniformly. The lower drywell floor was designed so that debris spreading would not be hindered. The temperature of the lower drywell air space and structures should be even more uniform because of convective and radiative heat transfer from debris material. Cooler regions will tend to absorb more heat than warmer ones resulting in temperature equalization.

However, if highly non-uniform debris dispersal occurs, it has been postulated that one flooder line could open and its operation could delay or even prevent the other lines from activating. In the worst physical case, the initiation of one flooder line causes crust formation without completely quenching the debris. The crust limits heat transfer from the surface of the debris bed. Core-concrete interaction (CCI) will occur if surface heat transfer is reduced enough.

CCI results in large quantities of gases being formed under the surface of the crust. The gases will increase in pressure due to continued generation until the crust ruptures or they escape from the edges of the bed. In either case, the gases will pass from the debris bed into the lower drywell airspace. The passage either will be unobstructed with gasses exiting the debris above the water elevation or through an overlying layer of water. Since only one flooder line is presumed active, the water layer, if it exists, will be thin and no significant amount of heat will be transferred from the gas to the liquid.

Concrete has an ablation temperature of approximately 1500 K. The released gases from core concrete interaction will be at least at this temperature. Higher temperatures may be reached by the gases as they interact with debris material in their exit. Thus, gases enter the lower drywell air space at very high temperature. The CCI gases will increase the temperature of the lower drywell air space. More flooder lines will become active as the lower drywell temperature increases. For this reason, the activation of a single flooder line is transient condition at worst and is not expected to adversely affect the operation of the other lines.

19E.2.8.2.6 Valve Opening Time

The fusible plug valve is designed to open when the lower drywell temperature reaches 533 K. The fusible material is made up of an alloy mixture of two or more of the following metals: tin, silver, bismuth, antimony, tellurium, zinc and copper. Alloy contents are chosen so that the plug melts when its temperature reaches 533 K.

The melting points of the individual metals are as follows:

Metal	Melting Point (K)
Antimony (Sb)	903
Bismuth (Bi)	544
Copper (Cu)	1356
Silver (Ag)	1233
Tellurium (Te)	722
Tin (Sn)	505
Zinc (Zn)	692

To estimate the opening time, a calculation has been made for a pure bismuth plug. Bismuth was used because it has the closest melting point to 533 K.

Heat transfer from the surrounding stainless steel pipe to the plug is by conduction. Heat transfer from steam in the lower drywell to the stainless steel pipe is by convection. The pipe also receives radiative heat from the debris on the lower drywell floor. Heat transfer to the bottom of the valve was neglected. The debris bed surface temperature and lower drywell gas temperature were estimated using a representative MAAP-ABWR sequence. Using these assumptions, the valve opening time was calculated to be less than approximately 10 minutes depending on the steam absorbtivity. This is a representative time from when the lower drywell gas space reaches 533 K until the flooder line becomes active.

19E.2.8.2.7 Estimation of Net Risk

In order to assess the net risk of the passive flooder system, a sensitivity study was performed using three failure probabilities for the passive flooder node, P, in the containment event trees. In these cases, the failure probability of the passive flooder was incrementally increased from its base case value.

The overall results are not sensitive to this parameter. Failure of the passive flooder leads to an increase in the probability of Dry CCI. Thus, the probability of Dry CCI increases by the same increments for the three sensitivity cases. However, the base case results for Dry CCI are so small that a very large magnitude increase does not impact other results significantly.

The principal conclusions of the sensitivity studies are:

(1) Pedestal failure does not increase since it is dominated by the Wet CCI sequences.

(2) The only probabilistic output which shows any significant variation is drywell head seal overtemperature leakage (Pen OT) which exhibits an increase of magnitude with an increase in the passive flooder failure probability. The change in seal leakage is much less than the change in passive flooder failure probability since high RPV pressure sequences with entrainment of debris to the upper drywell and failure of the upper drywell sprays dominate the seal leakage sequences in the base analysis.

(3) Even for the case where the passive flooder is assumed to be unavailable, the frequency associated with the Dry CCI is extremely small. Since only the Dry CCI cases have failure of the passive flooder, this frequency represents an upper bound for the impact of passive flooder failure on offsite dose.

Thus, it is seen that the lower drywell flooder has negligible impact on net risk. Therefore, no chart of the impact on risk was created. The value of the lower drywell flooder system is not measured as a direct impact on risk. Rather, it should be viewed as a passive system which serves to limit the impact of uncertainty in operator actions and allows the ABWR design to mitigate a severe accident in a purely passive manner.

19E.2.8.2.8 Summary

The passive flooder meets its design goal of preventing or, at least, mitigating core concrete interaction in the lower drywell. The flow rate required to remove the heat generated in the debris bed is 0.018 m^3/s which can be provided by two of the ten flooder lines. The expected flow rate is 0.099 m^3/s (nine of the ten lines active). If the expected flow rate is achieved, a one-meter layer of water will be established above the bed in a time between 21 minutes and 1.8 hours after flow initiation. One flooder line opening first is not expected to prevent the other lines from opening during a severe accident in which significant amounts of core debris is present in the drywell. The flooder lines will become active within ten minutes of the lower drywell gas space reaching 533 K. The passive flooder has negligible impact on the net risk of the plant since it provides a redundant function to the firewater addition system.

19E.2.8.3 Corium Shield

During a hypothetical severe accident in the ABWR, molten core debris may be present on the lower drywell floor. The EPRI ALWR Requirements Document specifies a floor area of at least 0.02 m^2/MWt to promote debris coolability. This has been interpreted in the ABWR design as a requirement for an unrestricted lower drywell floor area of 79 m^2.

The ABWR has two drain sumps in the periphery of the lower drywell floor which could collect core debris during a severe accident if ingression is not prevented. If ingression occurs, a debris bed will form in the sump which has the potential to be deeper than the bed on the lower drywell floor. Debris coolability becomes more uncertain as the depth of a debris bed increases. Therefore, debris should be kept out of the sumps.

The two drain sumps have different design objectives. One, the floor drain (HCW) sump, collects water which falls on the lower drywell floor. The other, the equipment drain (LCW) sump, collects water leaking from valves and piping. Both sumps have pumps and instrumentation which allow the plant operators to determine water leakage rates from various sources. Plant shutdown is required when leakage rate limits are exceeded for a certain amount of time. A more complete discussion on the water collection system can be found in Subsection 5.2.5.

Debris will be prevented from entering into the lower drywell sumps by shield walls (corium shields) built around their periphery. The shields will be constructed from material which will prevent or minimize interactions with the core debris. The shield for the floor drain sump will have channels at floor level that allow nearly unrestricted water flow at rates on the order of and somewhat greater than the leakage limits. The channels will be sized so that they plug with core debris during a severe accident; thus preventing debris ingression into the sump. The equipment drain sump will be solid. A complete description of corium shields can be found in Attachment 19ED.

19E.2.9 References

19E.2-1 "MAAP-3.0B Computer Code Manual", EPRI NP-7071-CCML, November 1990.

19E.2-2 "Advanced Light Water Reactor Utility Requirements Document", Volume II; EPRI Report NP-6780-L.

19E.2-3 Advanced Reactor Severe Accident Program, "Technical Support for the EPRI Debris Coolability Requirement for Advanced Light Water Reactors, Task 8.3.5.6", Fauske and Associates, Inc., Burr Ridge, IL, August 1988.

19E.2-4 "CORCON-MOD2 User's Manual", NUREG/CR-3920, SAND84-1246, Rev. 3, August 1984.

19E.2-5 R.E. Henry, "Key Phenomenological Models for Assessing Explosive Steam Generation Rates", IDCOR Technical Report 14.1A, 1983.

19E.2-6 R.E. Henry, "Key Phenomenological Models for Assessing Explosive Steam Generation Rates", IDCOR Technical Report 14.1B, 1983.

19E.2-7 "Reactor Safety Study: An Assessment of Accident Risks in U.S. Commercial Nuclear Power Plants", NUREG-75/014, WASH 1400, October 1975.

19E.2-8 T.G. Theofanous, "Scaling Considerations in Steam Explosions", Procedures 1987 National Heat Transfer Conference, Pittsburgh, August 9-12, 1987, pp. 58-67.

19E.2-9 Sir Horace Lamb, “Hydrodynamics”, Dover.

19E.2-10 F. Kreith, “Principles of Heat Transfer”, 3rd Edition, IEP - A Dun-Donnelley Publisher, N.Y., 1976.

19E.2-11 P.J. Berenson, “Film Boiling Heat Transfer from a Horizontal Surface”, Transactions of the ASME, Series C, Volume 83, 1961.

19E.2-12 G.A. Green, “Experiments on Melt Spreading and Bubbling Heat Transfer”, Severe Accident Research Partners Meeting, Bethesda, MD, October 17-21, 1981.

19E.2-13 F.J. Moody, “Pressure Suppression Containment Thermal-Hydraulics State of the Art”, NUREG/CP-0014, Volume 1, 1980.

19E.2-14 “GESSAR II, 238 Nuclear Island”, 22A7007 Revision 21, General Electric Company, March 1982.

19E.2-15 Crane, “Flow of Fluids Through Valves, Fitting, and Pipe”, Technical Paper 410, 1969.

19E.2-16 Not Used.

19E.2-17 A.M. Rozen, S.I. Golub and T. I. Vitintseva, “Calculating the Transported Entrainment During Sparging”, Translated by Polyglot Language Service.

19E.2-18 S. Kutateladze, “Elements of the Hydrodynamics of Gas-Liquid Systems”, Fluid Mechanics - Soviet Research, 1, 4, 1972.

19E.2-19 “Severe Accident Risks: An Assessment for Five U.S. Nuclear Power Plants”, NUREG-1150, Nuclear Regulatory Commission, June 1989.

19E.2-20 “Evaluation of Severe Accident Risks: Peach Bottom, Unit 2”, NUREG/CR-4551 Volume 4, Nuclear Regulatory Commission, December 1990.

19E.2-21 “Evaluation of Severe Accident Risks: Grand Gulf, Unit 1”, NUREG/CR-4551 Volume 6, Nuclear Regulatory Commission, December 1990.

19E.2-22 “Individual Plant Examination: Submittal Guidance”, NUREG-1335, Nuclear Regulatory Commission, August 1989.

19E.2-23 “Individual Plant Examination for Severe Accident Vulnerabilities”, Nuclear Regulatory Commission, Generic Letter No. 88-20, November 23, 1988.

19E.2-24 “Probabilistic Risk Assessment for Kuosheng Nuclear Power Station, Unit 1”, Republic of China Atomic Energy Council, July 1985.

19E.2-25 "Recommended Sensitivity Analyses for an Individual Plant Examination Using MAAP 3.0B", Draft 1992, Electric Power Research Institute.

19E.2-26 "MAAP 3.0B Code Evaluation - Final Report", Draft, Nuclear Regulatory Commission, December 1991.

19E.2-27 "Advanced Light Water Reactor Utility Requirements Document", Volume II, Chapter 1, Appendix A: PRA Key Assumptions and Guidelines, EPRI Report NP-6780-L.

19E.2-28 R. O. Gauntt, R. D. Gasser, L. J. Ott, "The DF-4 Fuel Damage Experiment in ACRR with a BWR Control Blade and Channel Box", NUREG/CR-4671, SAND 86-1443, November 1989.

19E.2-29 R. Tokraz and R. Libby, "Recriticality in a Boiling Water Reactor Following a Core Damage Accident", Proceedings of the 17th Water Reactor Safety Meeting, October 1989.

19E.2-30 K.C. Wagner, "Analysis of a High Pressure ATWS with Very Low Makeup Flow", DOE/ID 10211, October 1988.

19E.2-31 "Iodine Chemical Forms in LWR Severe Accidents, Final Report", NUREG/CR-5732, January 1992.

19E.2-32 D. B. Clauss, W. A. von Riesemann, and M. B. Parks, "Containment Penetrations", SAND88-0331C.

19E.2-33 E. C. Beahm, R. A. Lorenz, and C. F. Weber, "Iodine Evolution and pH Control", NUREG/CR-5950, November 1992.

19E.2-34 Theofanous, T.G., Additon, S., Liu, C., Kymäläinen, O., Angelini, S., and Salmassi, T. (1993), "The Probability of In-Vessel Coolability and Retention of a Core Melt in the AP600", DOE Draft, September 1993.

19E.2-35 J. L. Rempe, et. al., "BWR Lower Head Failure Head Failure Assessment for CSNI Comparison Exercise", EGG-EAST-9609, April 1991.

19E.2-36 Cheung et. al., "TRACB04 Study on Suppression Pool Swelling During Containment Venting", Transient Thermal-Hydraulics Safety ANS Transactions Vol. 53, Nov. 1986.

19E.2-37 A.H. Shapiro, "The Dynamics and Thermodynamics of Compressible Fluid Flow", The Ronald Press, 1953.

19E.2-38 R.H. Cole, “Underwater Explosions”, Princeton University Press, 1948; or F.J. Moody, “Introduction to Unsteady Thermofluid Mechanics”, Wiley Interscience, 1990; or other books on acoustic theory.

19E.2-39 Md. Alamgir, “BWR Refill-Reflood Program Task 4.8 - TRAC-BWR Model Qualification For BWR Safety Analysis Final Report”, NUREG/CR-2571, October 1983.

19E.2-40 “ABWR Severe Accident Evaluations”, UTLR-0014.

19E.2-41 “ABWR Severe Accident Analysis”, UTLR-0016.

19E.2-42 Joseph F. Quirk (GE) letter to R.W. Borchardt (NRC), December 21, 1994, “NEPA/SAMDA Submittal for the ABWR,” Attachment A. (This reference is not incorporated into Tier 2 of the DCD.)

Table 19E.2-1 Potential Suppression Pool Bypass Lines

Description	Number of Lines	Pathway From	Pathway To	Pathway Size (mm) (1 in. = 25.4 mm)	Isolation Valves	Basis For Exclusion (See Notes)
Main Steam	4	RPV	ST	700	(AO, AO)	-
Main Steam Line Drain	1	RPV	ST	80	MO, MO	3
Feedwater	2	RPV	ST	550	CK, CK	-
Reactor Inst. Lines	37	RPV	RB	6	CK	-
CRD Insert	205	RPV	RB	1	CK, MA	1
HPCF Discharge	2	RPV	RB	200	CK, MO	-
HPCF Equalizing	2	RPV	RB	20	MO, MO	-
HPCF Suction	2	SP	RB	400	MO	2
Supp Pool Instrumentation	6	SP	RB	6	CK	2
SLC Injection	1	RPV	RB	40	CK, CK	-
RCIC Steam Supply	1	RPV	RB	150	(MO, MO)	-
RCIC Discharge	1	RPV	RB	150	CK, MO	5
RCIC Min. Flow	1	SP	RB	150	MO	2
RCIC Suction	1	SP	RB	200	MO	2
RCIC Turbine Exhaust	1	SP	RB	350	MO, CK	2
RCIC Turb. Exh Vac Bkr	1	SP	RB	40	CK, CK	2
RCIC Vac Pump Discharge	1	SP	RB	50	MO, CK	2
RHR LPFL Discharge	2	RPV	RB	250	CK, MO	-
RHR Equalizing Lines	2	RPV	RB	20	MO, MO	-
RHR Wetwell Spray	2	WW	RB	100	MO	2,4
RHR Drywell Spray	2	DW	RB	200	MO, MO	4
RHR SDC Suction	3	RPV	RB	350	MO, MO	3
CUW Suction	1	RPV	RB	200	(MO, MO, MO)	-
CUW Return	1	RPV	RB	200	MO, MO	5
CUW Head Spray Line	1	RPV	RB	150	CK, MO, MO	3
CUW Instrument Lines	4	RPV	RB	6	CK	-
Post Accident Sampling	4	RPV	RB	25	(MO, MO)	-
RIP Motor Purge	10	RPV	RB	<1	CK, CK	1
RIP Cooling Water	4	RPV	RB	200	MO, MO	1

Table 19E.2-1 Potential Suppression Pool Bypass Lines (Continued)

Description	Number of Lines	Pathway From	Pathway To	Pathway Size (mm) (1 in. = 25.4 mm)	Isolation Valves	Basis For Exclusion (See Notes)
LDS Instruments	9	RPV	RB	6	CK	-
SPCU Suction	1	SP	RB	200	MO, MO	2
SPCU Return	1	SP	RB	250	MO, CK	2
Cont. Atmosphere Monitor	6	DW	RB	20	MO	-
LDS Samples	2	DW	RB	30	(SO, SO)	-
Drywell Sump Drains	2	DW	RB	100	MO, MO	-
HVCW/RBCW Supply	4	DW	RB	125	CK, MO	1
HVCW/DWCW Return	4	DW	RB	125	MO, MO	1
DW Exhaust/SGTS	1	DW	RB	550	AO, AO	7
Wetwell Vent to SGTS	1	WW	RB	550	AO, AO	2
DW Purge	1	DW	RB	350	AO	-
Inerting Makeup	1	DW	WW	50	AO, AO	-
WW Inerting/Purge	1	WW	RB	550	AO, AO	2
Instrument Air (and Service Air)	2	DW	RB	50	CK, MO	1
SRV Pneumatic Supply	3	DW	RB	50	CK, MO	1
ADS/SRV Discharge	8	RPV	WW	300	RV	-
ACS Supply	2	DW	WW	550	AO, AO	-
WW/DW Vacuum Breaker	8	DW	WW	500	CK	-
Miscellaneous Leakage	1	DW	RB	---	NONE	6
Access Tunnels	2	DW	RB	---	NONE	6

NOTES:

Legends and Acronyms

Pathway

Source (From)		Termination (To)	
RPV	Reactor Pressure Vessel	WW	Wetwell
DW	Drywell	RB	Reactor Building
SP	Suppression Pool	WW	Wetwell
		ST	Steam Tunnel

Isolation Valve Types

AO Air Operated

MO Motor Operated

RV Relief Valve

SP Suppression Pool

CK Check Valve

MA Manually Actuated

SO Solenoid Operated

( ) Common Mode Failure Potential [Subsection 19E.2.3.3.3(2)]

Bases for Exclusion

(1) Closed system such as closed cooling water systems which do not directly connect to the RPV or containment atmosphere require two failures to become a bypass pathway: a leak or break within the cooled component and a line break outside of containment. Very low flow is expected out of the break or leak at the cooled component is likely due to the high degree of restriction. These pathways are not considered further on the basis of this very low flow rate. Similarly, internal restrictions within the CRD and the ball check valve in the drive flange provides the basis for excluding these lines.

(2) Pathways which originate in the primary containment wetwell airspace or the suppression pool are excluded because fission product aerosols would first be trapped in the suppression pool and would thus not be available for release through the bypass path.

(3) Some lines are closed during normal plant operation and would not be expected to be opened in the short term following a plant accident. These lines are excluded on the basis of low frequency of use. Furthermore, should a bypass pathway develop later when the line is used, the fission product source term would be expected to have been already significantly reduced due to decay and other removal mechanisms.

(4) Some lines which originate in the primary containment are designed for operating pressures higher than would be expected in the containment during a severe accident. These lines [with design pressures greater than about 0.790 MPa] were excluded since the probability of a break under less than normal operating pressures and coincident with the severe accident is extremely small.

(5) Some lines return to the feedwater line. These pathways (such as LPFL loop A and CUW) are excluded since they are bounded by the evaluation of feedwater.

(6) Acceptable long term leakage from the containment to the reactor building following a design basis accident is specified at 0.5% of containment volume per 24 hours. During severe accident conditions this leakage could be somewhat greater due to

higher than design basis containment pressure. The contribution of this leakage to overall risk is considered in Subsection 19E.2.3.4. A discussion of the drywell access tunnels is included in Appendix 19F.

(7) Drywell purge lines are normally closed a fail closed. The potential for inadvertent opening is considered remote and is addressed by Emergency Procedure guidelines.

Table 19E.2-2 ABWR Plant Ability to Cope with Station Blackout for up to 8 Hours

Plant Parameter		Design Basis Value	Station Blackout Basis
a)	RPV Level	Core covered	Core covered
	RPV Pressure	0.446 MPa RCIC trip	>1.1356 MPa
		1.1356 MPa RCIC rated flow	
b)	D.C. Battery Capacity	11,400 amp-h	Sufficient with load shedding
		Div. 1, 2, 3 & 4	
c)	RCIC Water Source	1) CST - 566 m^3 (20 x 10^3 ft^3) 2) Suppression pool - 3566 m^3 (126 x 10^3 ft^3)	CST sufficient with RPV pressurized
d)	RCIC Room Temperature	339 K (66°C)	<339 K (66°C)
e)	Drywell Temperature	444 K (171°C)	<444 K (171°C)
f)	Drywell Pressure	0.41 MPa	<0.41 MPa
g)	Wetwell Temperature	377 K (104°C)	<377 K (104°C)
h)	Wetwell Pressure	0.41 MPa	<0.41 MPa
i)	Control Rooms		
	- Main	331 K (58°C)	331 K (58°C)
	- Lower	331 K (58°C)	331 K (58°C)
	- Computer	331 K (58°C)	331 K (58°C)

Table 19E.2-3 Definition of Accident Sequence Codes

Characters 1 to 4: General Condition Indicator	
LCLP	Loss of All Core Cooling with Vessel Failure occurring at Low Pressure
LCHP	Loss of All Core Cooling with Vessel Failure occurring at High Pressure
SBRC	Station Blackout with RCIC operating for 8 hours
LHRC	Loss of Heat Removal in the Containment
LBLC	Large Break LOCA with Loss of All Core Cooling
NSCL	Transient without Scram and with Failure of All Core Cooling, Vessel Failure occurs at Low Pressure
NSCH	Transient without Scram and with Failure of All Core Cooling, Vessel Failure occurs at High Pressure
NSRC	Station Blackout without Scram, RCIC operates
Characters 5 and 6: Mitigating Features	
00	No mitigating features operated
IV	In-Vessel Recovery
PF	Passive Flooder
FA	Firewater Addition System Injects into the Vessel
HR	Containment Heat Removal
PS	Passive Flooder and Drywell Spray
FS	Firewater Addition System switched to Drywell Spray Mode
PB	Passive Flooder with Suppression Pool Bypass
Character 7: Mode of Release	
N	Normal Containment Leakage
P	Leakage through Moveable Penetrations
R	Containment Overpressure Protection System Rupture Disk Opening
D	Drywell Head Failure
E	Early Containment Structural Failure
S	Suppression Pool Failure
Character 8: Magnitude of Release	
0	No core damage, no fission product release
N	Negligible: Less than 0.1% volatile fission products
L	Low: 0.1% to 1% volatile fission products
M	Medium: 1% to 10% volatile fission products
H	High: More than 10% volatile fission products

Table 19E.2-4 Grouping of Accident Classes into Base Sequences

Accident Class	Initiator Code	Base Sequence Subsection Number
IA	LCHP	19E.2.2.2
IB-1	LCLP	19E.2.2.1
	LCHP	19E.2.2.2
IB-2	SBRC	19E.2.2.3
IB-3	LCLP	19E.2.2.1
	LCHP	19E.2.2.2
IC	NSCL	19E.2.2.6
ID	LCLP	19E.2.2.1
IE	NSCH	19E.2.2.7
II	LHRC	19E.2.2.4
IIIA	LCHP	19E.2.2.2
IIID	LBLC	19E.2.2.5
IV-1	NSRC	19E.2.2.8

Table 19E.2-5 Sequence of Events for LCLP-PF-R-N

Loss of All Core Cooling with Vessel Failure at Low Pressure
Passive Flooder Operates and Drywell Head Fails

Time	Event
0.0	MSIV Closure
4.2 s	Reactor Scrammed
0.4 h	Indicated Water Level at 2/3 Core Height One SRV Opened by Operator
1.8 h	Vessel Failed
2.7 h	Water in Lower Drywell Boiled Off Corium Heatup Begins
5.4 h	Passive Flooder Opens
20.2 h	Rupture Disk Opens

Table 19E.2-6 Sequence of Events for LCLP-FS-R-N

Loss of All Core Cooling with Vessel Failure at Low Pressure
Firewater Addition System Injects and Rupture Disk Opens

Time	Event
0.0	MSIV Closure
4.2 s	Reactor Scrammed
0.4 h	Indicated Water Level at 2/3 Core Height One SRV Opened by Operator
1.8 h	Vessel Failed
2.7 h	Water in Lower Drywell Boiled Off Corium Heatup Begins
4.0 h	Firewater Spray Started
7.0 h	Suppression Pool Overflows to the Lower Drywell
23.6 h	Firewater Spray Stopped
31.1 h	Rupture Disk Opened
56.6 h	Water in Lower Drywell Boiled Off
61.1 h	Passive Flooder Opened

Table 19E.2-7 Sequence of Events for LCHP-PS-R-N

Loss of All Core Cooling with Vessel Failure at High Pressure
Passive Flooder and Drywell Spray Operates, Rupture Disk Opens

Time	Event
0.0	MSIV Closure
4.2 s	Reactor Scrammed
0.3 h	Core Uncovered
2.0 h	Vessel Fails Corium and Water Entrained into Upper Drywell
2.0 h	Passive Flooder Opens
4.0 h	Drywell Spray Initiated
25.0 h	Rupture Disk Opens

Table 19E.2-8 Sequence of Events for LCHP-PF-P-M

Loss of All Core Cooling with Vessel Failure at High Pressure
Passive Flooder Operates, Penetration Leakage Occurs

Time	Event
0.0	MSIV Closure
4.2 s	Reactor Scrammed
0.3 h	Core Uncovered
2.0 h	Vessel Fails Corium and Water Entrained into Upper Drywell
2.0 h	Passive Flooder Opens
2.1 h	Seal Degradation Temperature Reached
18.1 h	Leakage Begins through Moveable Penetrations Fission Product Release Begins

Table 19E.2-9 Sequence of Events for SBRC-FA-R-0

Station Blackout with RCIC Operational for 8 Hours
Firewater Addition to Vessel Used to Prevent Core Damage, Rupture Disk Opens

Time	Event
0.0	MSIV Closure
4.2 s	Reactor Scrammed
52.0 s	RCIC Injection, Suction from CST
1.3 h	RCIC Suction Switched to Suppression Pool
4.4 h	RCIC Suction Switched to CST
8.0 h	RCIC Failure
9.0 h	Suppression Pool began to overflow to Lower Drywell
9.8 h	Manual ADS
9.9 h	Collapsed Water Level Falls below Top of Active Fuel Firewater Addition System Injection Begins
32.3 h	Rupture Disk Opened

Table 19E.2-10 Sequence of Events for SBRC-PF-R-N

Station Blackout with RCIC Operational for 8 Hours
Passive Flooder Operates and Rupture Disk Opens

Time	Event
0.0	MSIV Closure
4.2 s	Reactor Scrammed
52.0 s	RCIC Injection, Suction from CSP
1.3 h	RCIC Suction Switched to Suppression Pool
4.4 h	RCIC Suction Switched to CSP
8.0 h	RCIC Failure
9.3 h	Core Uncovered
9.7 h	One SRV opened by operator
12.3 h	Vessel Fails
21.1 h	Lower Drywell Water Boils Away
23.5 h	Passive Flooder Opens Rupture Disk Opens

Table 19E.2-11 Sequence of Events for LHRC-00-R-0

Isolation with Loss of Containment Heat Removal
Rupture Disk Opens

Time	Event
0.0	MSIV Closure
4.2 s	Reactor Scrammed
1.1 min	RCIC Injection
2.9 h	Manual Open 1 SRV
3.0 h	HPCF Injection
3.1 h	RCIC Trip on Low Turbine Pressure
21.7 h	Rupture Disk Opens
>72 h	Potential Loss of Core Cooling

Table 19E.2-12 Sequence of Events for LBLC-PF-R-N

Large Break LOCA With Loss of Core Cooling
Passive Flooder Operates and Rupture Disk Opens

Time	Event
0.0	Main Steam Line Break
0.2 s	High Drywell Pressure Signal
4.4 s	Reactor Scrammed
14.9 s	MSIV Closed
2.8 min	Core Uncovered
1.4 h	Vessel Failed
5.7 h	Passive Flooder Opened
19.1 h	Rupture Disk Opens

Table 19E.2-13 Sequence of Events for NSCL-PF-R-N

Concurrent Loss of All Core Cooling and ATWS with Vessel Failure at Low Pressure
Passive Flooder Operates and Rupture Disk Opens

Time	Event
0.0	MSIV Closure
3.7 s	Core Uncovered
0.5 h	One SRV Opened by Operator
1.3 h	Vessel Failed
1.9 h	Water in Lower Drywell Boiled Off Corium Heatup Begins
4.4 h	Passive Flooder Opens
18.7 h	Rupture Disk Opens

Table 19E.2-14 Sequence of Events for NSCH-PF-P-M

Concurrent Loss of All Core Cooling and ATWS with Vessel Failure at High Pressure
Passive Flooder Operates, Penetration Leakage Occurs

Time	Event
0.0	MSIV Closure
3.6 min	Core Uncovered
1.3 h	Vessel Fails Corium and Water Entrained into Upper Drywell
1.4 h	Passive Flooder Opens
1.4 h	Seal Degradation Temperature Reached
17.8 h	Leakage Begins Through Moveable Penetrations Fission Product Release Begins

Table 19E.2-15 Sequence of Events for NSRC-PF-R-N

Concurrent Station Blackout and ATWS
Passive Flooder Operates, Rupture Disk Opens

Time	Event
0.0	MSIV Closure
4.1min	Core Uncovered
1.9 h	Suppression Pool Began to Overflow to Lower Drywell
3.6 h	RCIC Tripped
3.8 h	SRV Opened
5.6 h	Vessel Failed
8.6 h	Rupture Disk Opened Fission Product Release Begins

Table 19E.2-16 Summary of Critical Parameters for Severe Accident Sequences

Accident	Time of Vessel Failure	Fission Product Release Time	Time of Rupture Disk Failure	End of CsI Release	Release Fraction of CsI @ 72 hours
LCLP-PF-R-N	1.8 h	20.2 h	20.2 h	100 h	<1E–7
LCLP-FS-R-N	1.8 h	31.1 h	31.1 h	76 h	1E–7
LCHP-PS-R-N	2.0 h	25.0 h	25.0 h	50 h	<1E–7
LCHP-FS-R-N	2.0 h	50 h*	50 h*	125 h*	<1E–7*
LCHP-PF-P-M	2.0 h	18.1 h	N/A	70 h	8.8E–2
SBRC-PF-R-N	12.3 h	23.5 h	23.5 h	100 h	<1E–7
LBLC-PF-R-N	1.4 h	19.1 h	19.1 h	125 h	<1E–7
LBLC-FS-R-N	1.4 h	29.5 h	29.5 h	67 h	<1E–7
NSCL-PF-R-N	1.3 h	18.7 h	18.7 h	105 h	<1E–7
NSCL-FS-R-N	1.3 h	30.7 h	30.7 h	69 h	<1E–7
NSCH-PF-P-M	1.3 h	17.8 h	N/A	65 h	7E–2
NSCH-FS-R-N	1.3 h	50 h*	50 h*	125 h*	<1E–7*
NSRC-PF-R-N	5.6 h	8.6 h	8.6 h	110 h	<1E–7
NSRC-FS-R-N	5.6 h	26.4 h	26.4 h	120 h	<1E–7

* Release parameters are approximate. See sequence discussion for more detail.

Table 19E.2-17 Important Parameters for Steam Explosion Analysis

Symbol	Value	Description
m'	500 kg/s	Mass Flow Rate of Corium from Vessel
Q	0.056 m^3/s	Volumetric Flow of Corium from Vessel
α	7.E-6 m^2/s	Thermal Diffusivity of Corium
c_v	480 J/kg-K	Specific Heat of Corium
ρ	9000 kg/m^3	Density of Corium
σ	1.0 N/m	Surface Tension of Molten Corium
h	390 W/m^2-K	Heat Transfer Coefficient for Corium Droplet
T_i	2600 K	Initial Temperature of Corium Droplet
ρ_a	1.1 kg/m^3	Density of Air
ρ_L	1000 kg/m^3	Density of Water
$v_{fg}(P_\infty)$	1.7 m^3/kg	Specific Volume of Evaporation for Water
$h_{fg}(P_\infty)$	2257 kJ/kg	Specific Enthalpy of Evaporation for Water
L	5.5 m	Height of Water in Lower Drywell
A_L	88.2 m^2	Area of Lower Drywell
H	6 m	Distance from Bottom of Vessel to Surface of Water in Lower Drywell

Table 19E.2-18 Potential Bypass Pathway Matrix*

	From			
To	RPV	Drywell	Wetwell Airspace	Suppression Pool
Drywell	No	NA	NA	NA
Wetwell Airspace	Yes†	Yes†	NA	NA
Reactor Building	Yes	Yes	Yes	Yes
Turbine Building	Yes	Yes	Yes	Yes

* This matrix shows the paths that potentially bypass the suppression pool.

† Pathways which originate in the drywell and potentially release into the wetwell are potential bypass paths if the containment is vented or the wetwell fails during the severe accident.

Table 19E.2-19 Flow Split Fractions

Line Size		Flow Split Fraction	
mm	in	RPV Source	Drywell Source
6	0.25	1.5E–05	5.4E–05
12	0.5	9.4E–05	3.4E–04
25	1	5.7E–04	2.0E–03
50	2	3.3E–03	1.2E–02
100	4	1.8E–02	6.2E–02
150	6	4.8E–02	1.5E–01
200	8	8.9E–02	2.5E–01
250	10	1.4E–01	3.6E–01
300	12	2.0E–01	4.6E–01
350	14	2.6E–01	5.4E–01
400	16	3.2E–01	6.2E–01
450	18	3.8E–01	6.7E–01
500	20	4.3E–01	7.2E–01
700	28	6.1E–01	8.4E–01
1000	40	7.7E–01	9.2E–01

Table 19E.2-20 Failure Probabilities

Symbol	Description	Prob/Event*	Basis
P1	Main Steam Isolation Valve Common Mode Failure		a
P2	MSIV leakage probability		b
P3	Turbine Bypass Isolation		c
P4	Main condenser failure		c
P5	MSL break outside containment		d
P6	Air operated valve (NO)		e
P7	Motor -operated valve (NO)		e
P8	Motor-operated valve (NO)		f
P9	Check Valve		g
P10	Motor-operated valves (NC)		h
P11	Motor-operated valves (NC)		i
P12	Inadvertent opening		j
P13	Small line break		k
P14	Medium line break		k
P15	Large line break		k
P16	CUW line break		k

* Probabilites not part of DCD (Refer to Reference 19E.2-40)

Table 19E.2-21 Summary of Bypass Probabilities

Pathway	Flow Split Fraction	Bypass Probability Equation	Bypass Probability*	Bypass Fraction*	Figures 19E.2-19a to 19E.2-19k
Lines from the RPV					
Main Steam	6.7E–1	4*P1*(P3*P4+P5)			a
Main Steam Leakage	2.2E–5	4*P2*(P3*P4+P5)			a
Feedwater	5.2E–1	2*P9*P9*P15			b
Reactor Inst. Lines	3.1E–5	30*P13*P9			d
HPCF Discharge†	1.1E–1	2*P9*P10*P14			c
HPCF Equalizing Line†	1.0E–3	2*P10*P11*P13			c
SLC Injection	3.0E–3	1*P9*P13			b
RCIC Steam Supply	6.9E–2	1*P8*P14			e
LPFL Discharge†	1.7E–1	2*P9*P10*P15			c
LPFL Equalizing Line†	1.0E–3	2*P10*P11*P13			c
CUW Suction	1.2E–1	1*P8*P14			e
CUW Inst Lines	3.1E–5	4*P13*P9			d
Post Acc Sampling	1.0E–3	4*P8*P11			j
LDS Instruments	3.1E–5	9*P13*P9			d
SRV Discharge	6.9E–2	8*P14			k
Lines from the Drywell					
Cont Atmos Monitor	8.9E-4	6*P8*P13			j
LDS Samples	1.7E-3	2*P8*P11			j
Drywell Sump Drain	3.0E-2	2*P8*P13			j
DW Purge	5.4E-1	1*P6*P11			i
Inerting Makeup	1.2E-2	1*P6			i
ACS Supply	7.5E-1	2*P12*P6			h
WW-DW Vac Bkr‡	2.6E-1	8*P9			g
		Grand Total excluding vacuum breaker			
		Goal			

* Probabilites not part of DCD (refer to Reference 19E.2-40).
† These lines may be excluded for station blackout events.
‡ Addressed on Containment Event Trees.

Table 19E.2-22 NUREG/CR-4551 Grand Gulf APET Events by Category

Event Number	Description
Plant Damage State Grouping Events	
1	Initiating Event Type
2	Station Blackout
3	DC Power Availability
4	S/RV Fails to Reclose
5	HPCI Failure
6	RCIC Failure Initially
7	CRD Injection Failure
8	Condensate System Failure
9	LPCS/LPCI Systems Failure
10	RHR Failure
11	Service Water/LPCI Crosstie Failure
12	Fire Protection Crosstie Failure
13	Containment Spray Failure
14	Vessel Depressurization
15	Time Core Damage
20	Plant Damage State Summary
Structural Capacity/Initial Containment Status	
16	Containment Isolation (Pre-existing Leakage)
17	Extent of Pool Bypass Initially
18	Containment Capacity (Quasi-static/Dynamic Loading)
19	Drywell Capacity (Quasi-static/Dynamic Loading)
Systems Behavior/Operator Actions	
21	Ignitors Turned On Before Core Damage
22	Containment Vented Before Core Damage
23	SRV Vacuum Breakers Stick Open
26	RV Pressure During Core Damage
27	Status of Hydrogen Ignitors Before Vessel Breach
28	RV Injection Restored During Core Damage
30	Containment Spray Status
53	Upper Pool Dump

Table 19E.2-22 NUREG/CR-4551 Grand Gulf APET Events by Category

Event Number	Description
81	Containment Spray Status Following Vessel Breach
103	Containment Vented Following Vessel Breach
106	Containment Spray Status Late
119	Containment Vented Late
AC/DC Power Availability	
24	AC Power Recovered During Core Damage
25	DC Power Available During Core Damage
79	AC Power Recovered Following Vessel Breach
80	DC Power Available Following Vessel Breach
104	AC Power Recovered Late
105	DC Power Available Late
Criticality	
29	Core in Critical Configuration Following Injection Recovery
Hydrogen Related Phenomena/Issues	
31	Amount Oxygen in Wetwell During Core Damage
32	Amount Oxygen in Drywell During Core Damage
33	Amount Steam in Containment During Core Damage
34	Amount Steam in Drywell During Core Damage
35	Amount Hydrogen Released In-vessel During Core Damage
36	Level In-vessel Zirconium Oxidation
39	Max. Hydrogen Concentration in Wetwell Before Vessel Failure
40	Extent Wetwell Inert During Core Damage
41	Diffusion Flames Consume Hydrogen Before Vessel Breach
42	Max. Hydrogen Concentration in Drywell Before Vessel Failure
43	Deflagrations in Wetwell Before Vessel Breach
44	Detonation in Wetwell Before Vessel Breach
45	Containment Impulse Load Before Vessel Breach
46	Hydrogen Burn Efficiency Before Vessel Breach
47	Peak Hydrogen Burn Containment Pressure
48	Extent of Drywell Leakage Due to Early Detonation in Containment
49	Extent of Containment Leakage Due to Early Detonation in Containment

Table 19E.2-22 NUREG/CR-4551 Grand Gulf APET Events by Category

Event Number	Description
56	Extent Drywell Inert at Vessel Breach
57	Sufficient Hydrogen in Drywell for Combustion/Detonation Before Vessel Breach
65	Detonation in Drywell at Vessel Breach
66	Deflagration in Drywell at Vessel Breach
68	Amount Hydrogen Released at Vessel Breach
69	How Much Hydrogen Released at Vessel Breach
78	Hydrogen Concentration in Containment Immediately After Vessel Breach
82	Extent Wetwell Inert After Vessel Breach
83	Sufficient Oxygen in Containment for Combustion
84	Hydrogen Ignition in Containment at Vessel Breach
85	Hydrogen Ignition in Containment Following Vessel Breach
86	Hydrogen Detonation in Wetwell Following Vessel Breach
87	Impulse Loading to Containment Following Vessel Breach
88	Hydrogen Burn Efficiency Following Vessel Breach
89	Peak Containment Pressure From Hydrogen Burn at Vessel Breach
91	Extent of Drywell Leakage Due to Detonation in Containment at Vessel Breach
92	Extent of Containment Leakage Due to Detonation at Vessel Breach
101	Hydrogen (and CO) Produced During CCI
102	Level Zirconium Oxidation in Pedestal Before CCI
107	Late Concentration Combustible Gases in Containment
108	Level Wetwell Inert After Vessel Breach
109	Sufficient Oxygen in Containment for Late Combustion
110	Hydrogen Ignition in Containment Late
111	Detonation in Wetwell Following Vessel Breach
112	Containment Impulse Load Late
113	Hydrogen Burn Efficiency Late
114	Peak Containment Pressure From Late Hydrogen Burn
115	Extent of Drywell Leakage Due to Detonation in Containment Late
116	Extent of Containment Leakage Due to Late Detonation
117	Level of Containment Leakage Due to Late Combustion
118	Level of Drywell Leakage Due to Late Combustion

Table 19E.2-22 NUREG/CR-4551 Grand Gulf APET Events by Category

Event Number	Description
Containment/Drywell Pressurization/Failure	
37	Containment Pressure During Core Damage
38	Extent of Containment Leakage Due to Slow Pressurization Before Vessel Breach
50	Level Containment Leakage Before Vessel Breach
51	Level of Drywell Leakage Due to Containment Pressurization
52	Level Pool Bypass Following Early Combustion Events
55	Containment Pressure Before Vessel Breach
70	Drywell/Wetwell Pressure Differential Resulting from Vessel Breach
71	Peak Pedestal Pressure at Vessel Breach
72	Drywell Impulse Load at Vessel Breach Sufficient to Cause Failure
73	Drywell Pressurization at Vessel Breach Sufficient to Cause Failure
74	Pedestal Failure Due to Pressurization at Vessel Breach
76	Pedestal Failure Causes Drywell Failure
77	Containment Pressure at Vessel Breach Prior to Hydrogen Burn
90	Level Containment Pressurization At Vessel Breach
93	Level Containment Leakage Following Vessel Breach
94	Level of Drywell Leakage Due to Containment Pressurization
95	Level Pool Bypass Following Vessel Breach
96	Containment Pressure After Vessel Breach
122	Level Late Pool Bypass
123	Late Containment Pressure Due to Non-condensables or Steam
124	Late Containment Failure Due to Non-condensables or Steam
125	Long Term Level Containment Leakage
Core Concrete Interactions/Pedestal Failure	
54	Water in Reactor Cavity
97	Water Supplied to Debris Late
98	Water in Cavity After Vessel Breach
99	Nature of Core Concrete Interactions (CCI)
100	Fraction of Core Not Participating in HPME Participates in CCI
120	Amount Concrete Erosion to Fail Pedestal
121	Time of Pedestal Failure

Table 19E.2-22 NUREG/CR-4551 Grand Gulf APET Events by Category

Event Number	Description
Steam Explosion Related	
58	Alpha Mode Event Fails Vessel and Containment
60	Large In-vessel Steam Explosion
62	In-vessel Steam Explosion Fails Vessel
67	Large Ex-vessel Steam Explosion
75	Pedestal Failure From Ex-vessel Steam Explosion
Core Damage Progression and Vessel Breach	
59	Fraction of Core Participating in Core Slump
61	Fraction Core Debris Mobile at Vessel Breach
63	Mode of Vessel Breach
64	High Pressure Melt Ejection

Table 19E.2-23 NRC Identified Parameters for Sensitivity Study from NUREG-1335

- Performance of containment heat removal systems during core meltdown accidents
  - In-vessel phenomena (primary system at high pressure)
  - H_2 production and combustion in containment
  - Induced failure of the reactor coolant system pressure boundary
  - Core relocation characteristics
  - Mode of reactor vessel melt-through
- In-vessel phenomena (primary system at low pressure)
  - H_2 production and combustion in containment
  - Core relocation characteristics
  - Fuel/coolant interactions
  - Mode of reactor vessel melt-through
- Ex-vessel phenomena (primary system at high pressure)
  - Direct containment heating concerns
  - Potential for early containment failure due to pressure load
  - Long-term disposition of core debris (coolable or not coolable)
- Ex-vessel phenomena (primary system at low pressure)
  - Potential for early containment failure due to direct contact by core debris
  - Water availability in cases with long-term core-concrete interactions
  - Long-term disposition of core debris (Coolable or not coolable)

Table 19E.2-24 Issues to be investigated in ABWR Sensitivity Analysis

In-vessel
Hydrogen generation
Core Blockage and Melt Progression
Fission Product release from core
CsI revaporization
Time of vessel failure
Recriticality following in-vessel recovery
Ex-vessel
Debris entrainment and direct containment heating
Mass of molten material at time of vessel failure
Mode of vessel breach
Potential for pedestal failure
Steam explosions
Mass of molten material at time of vessel failure
Presence of water in lower drywell at vessel failure
Potential for pedestal failure
Core concrete interaction and debris coolability
Debris-to-water heat transfer
Debris-to-crust heat transfer
Mass of molten material at time of vessel failure
Presence of water in lower drywell at vessel failure
Potential for pedestal failure
Non-condensable gas generation
Containment failure location and pressure
Containment failure area
Pool bypass
High temperature failure of drywell
Suppression Pool decontamination factor

Table 19E.2-25 Not Used

Table 19E.2-26 Not Used

Table 19E.2-27 Not Used

Table 19E.2-28 Not Used

Table 19E.2-29 Equipment and Instrumentation Required to Survive Severe Accident Scenarios

Equipment and Instrumentation	10CFR50.34(f)	In-Vessel Severe Accident	Ex-Vessel Severe Accident
Equipment			
RHR	+	+	+
ADS	+	+	-
ACIWA	+	+	+
Containment Structure	+	+	+
Pedestal	+	+	+
CIVs - Inboard	+	+	+
CIVs - Outboard	+	+	+
Electrical Penetrations	+	+	+
Mechanical Penetrations	+	+	+
Hatches	+	+	+
Passive Flooder	-	-	+
COPS	-	+	+
Vacuum Breakers	+	+	+
RIP Vertical Restraints	+	+	+
Instrumentation			
RPV Water Level	+	+	-
RPV Pressure	+	+	-
Suppression Pool Water Temperature	+	+	+
DW/WW Radiation Monitor	+	+	+
DW/WW H_2 Concentration	+	+	+
DW/WW O_2 Concentration	+	+	+
DW Temperature	+	+	+
DW Pressure	+	+	+
WW Pressure	+	+	+
DW Water Level	+	+	+
WW Water Level	+	+	+

+ Indicates that the equipment/instrumentation is required for the event,

- Indicates that the equipment/instrumentation is not required for the event.

Table 19E.2-30 Material Properties Used in Tunnel Integrity Analysis

Steel	
K_{St}	30 W/mK
ρ_{St}	8000 kg/m^3
Cp_{St}	550 J/kgK
α_{St}	6.8 x 10^{-6} m^2/s
Debris	
k_C	8 W/mK
ρ_C	8000 kg/m^3
Cp_c	500 J/kgK
α_C	1.9 x 10^{-6} m^2/s

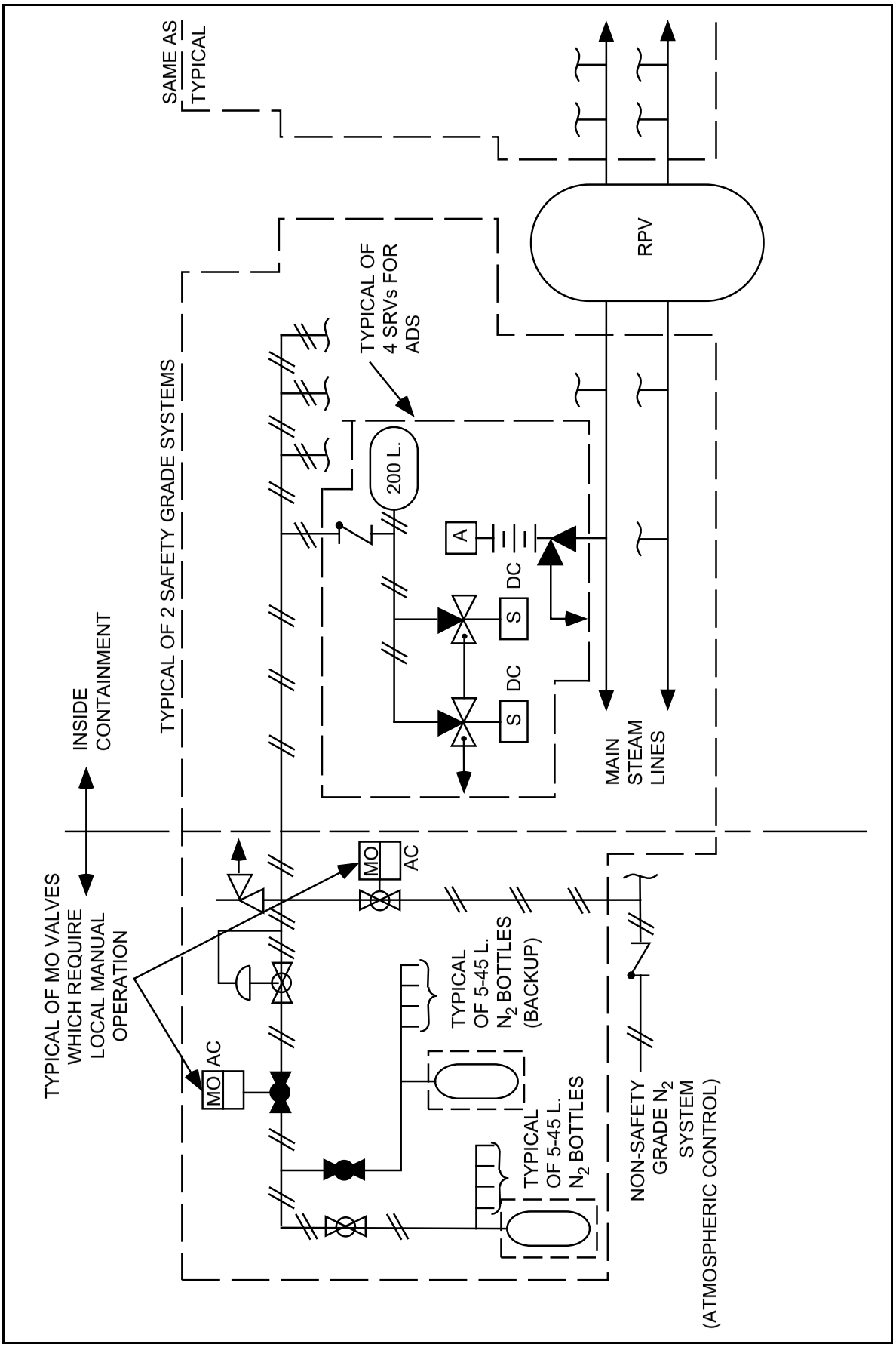

Figure 19E.2-1 Simplified Sketch of N_2 Supplies to Safety Grade ADS Valves

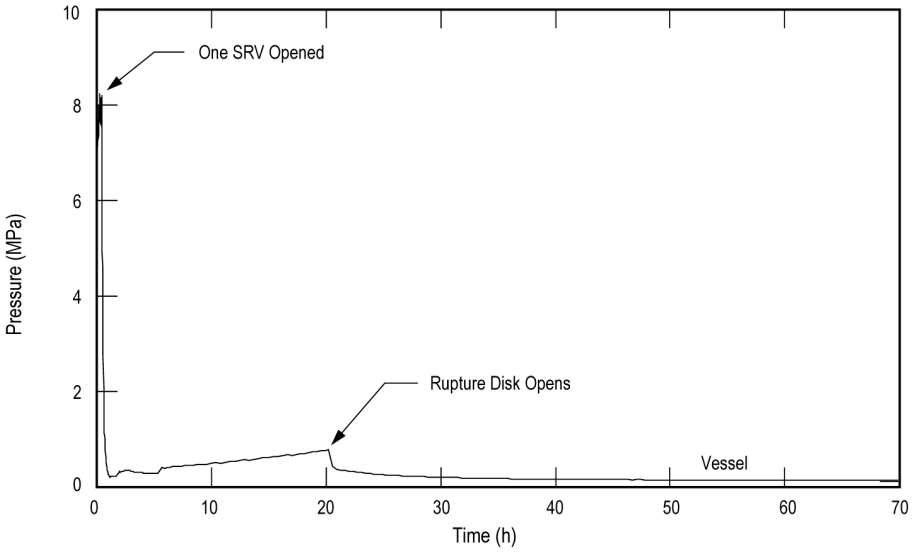

Figure 19E.2-2a LCLP-PF-R-N: Loss of all Core Cooling with Vessel Failure at Low Pressure, Passive Flooder Operates and Rupture Disk Opens: Vessel Pressure

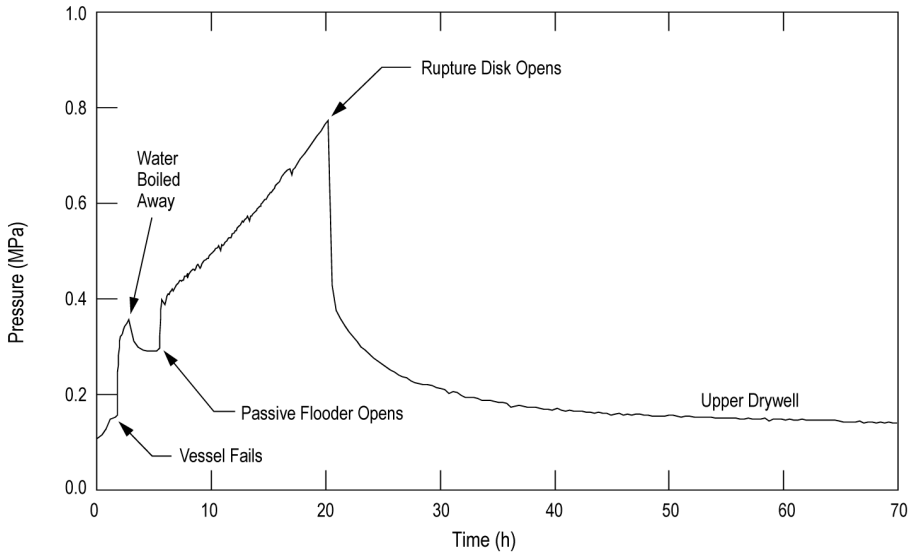

Figure 19E.2-2b LCLP-PF-R-N: Loss of all core Cooling with Vessel Failure at Low Pressure, Passive Flooder Operates and Rupture Disk Opens: Drywell Pressure

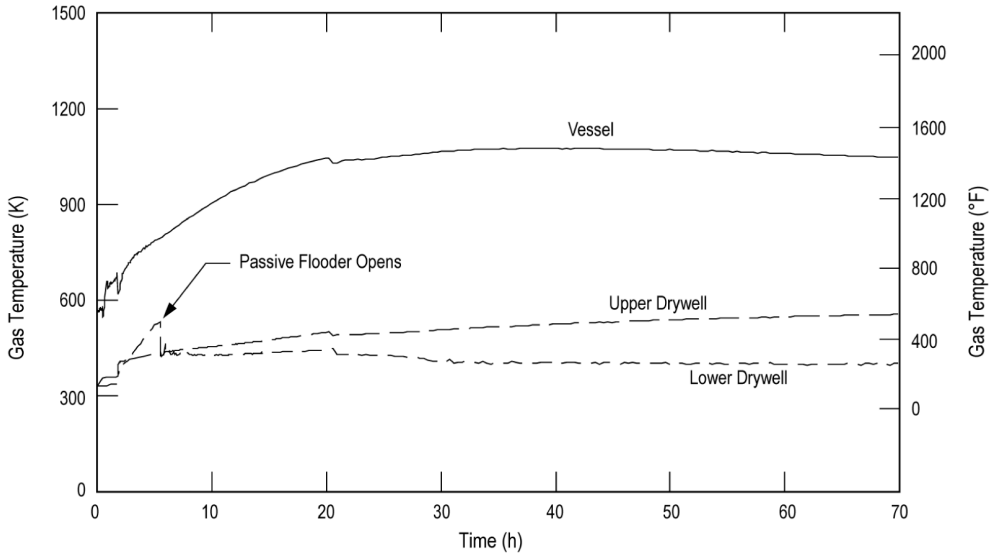

Figure 19E.2-2c LCLP-PF-R-N: Loss of all Core Cooling with Vessel Failure at Low Pressure, Passive Flooder Operates and Rupture Disk Opens: Gas Temperature

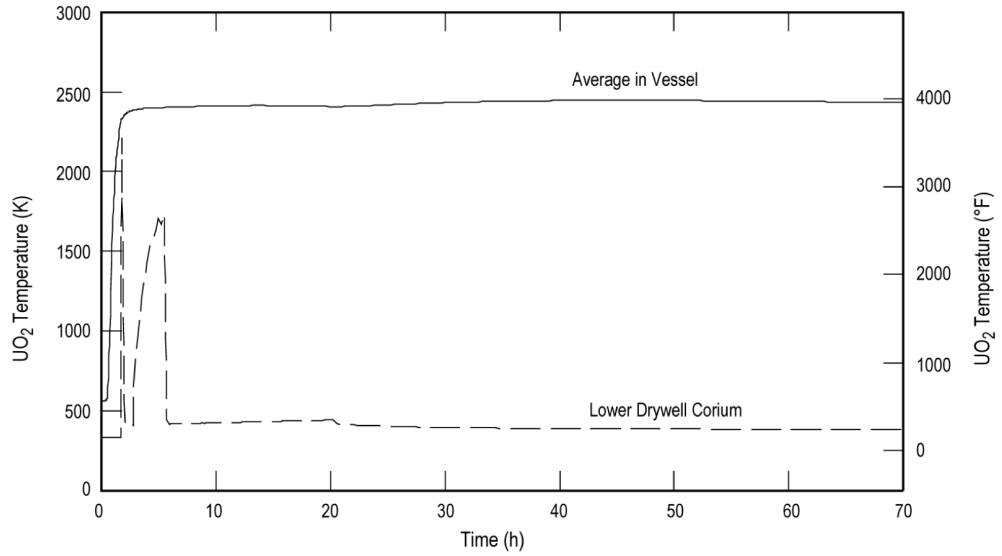

Figure 19E.2-2d LCLP-PF-R-N: Loss of all Core Cooling with Vessel Failure at Low Pressure, Passive Flooder Operates and Rupture Disk Opens: UO_2 Temperature

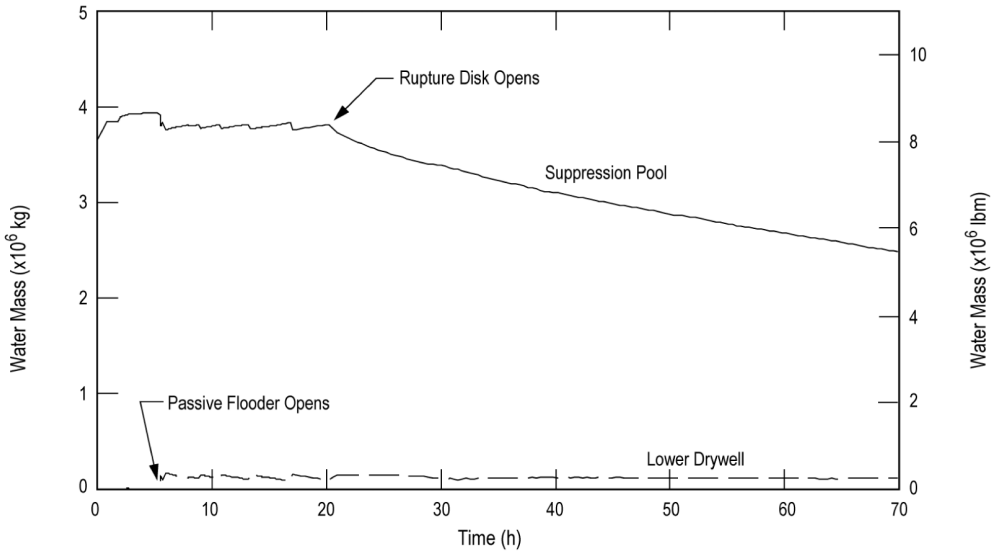

Figure 19E.2-2e LCLP-PF-R-N: Loss of all Core Cooling with Vessel Failure at Low Pressure, Passive Flooder Operates and Rupture Disk Opens: Water Mass

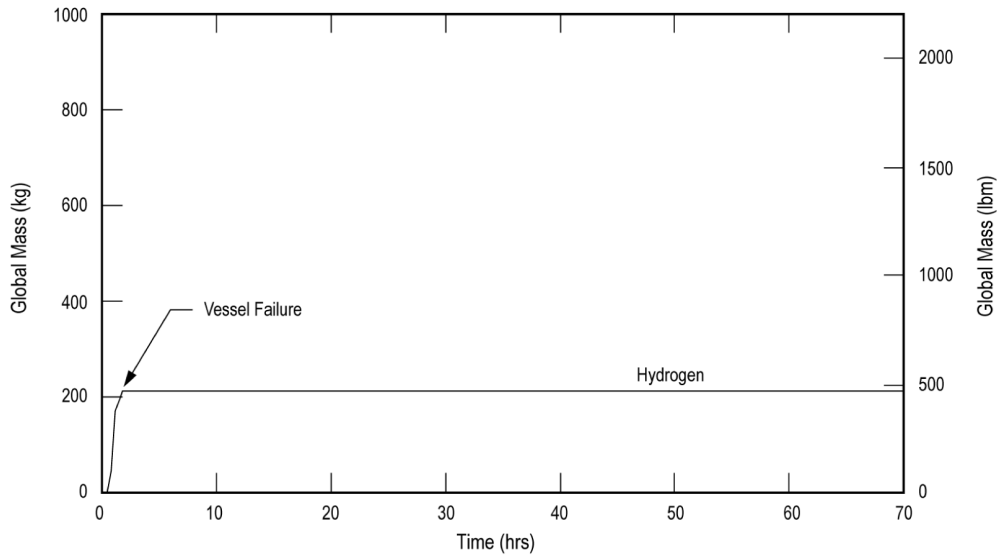

Figure 19E.2-2f LCLP-PF-R-N: Loss of all Core Cooling with Vessel Failure at Low Pressure, Passive Flooder Operates and Rupture Disk Opens: Mass of Non-Condensables

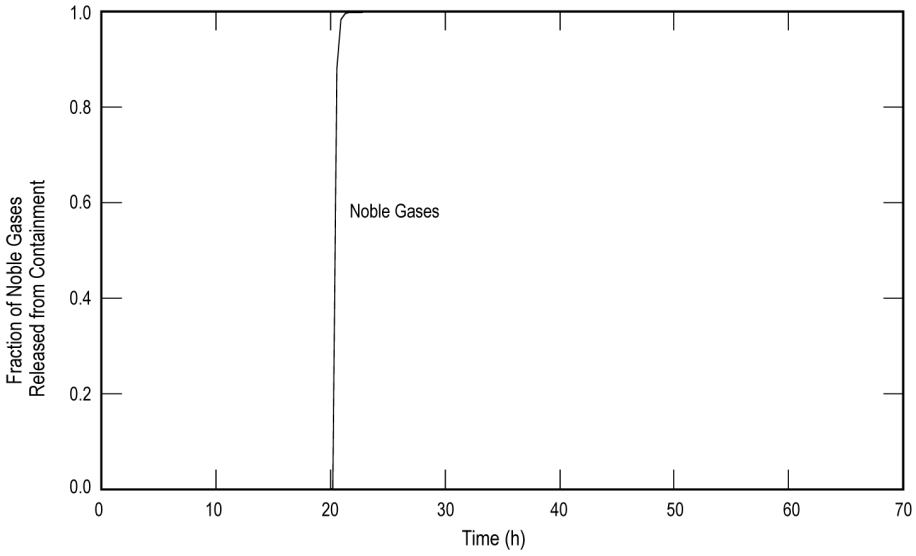

Figure 19E.2-2g LCLP-PF-R-N: Loss of all Core Cooling with Vessel Failure at Low Pressure, Passive Flooder Operates and Rupture Disk Opens: Noble Gases

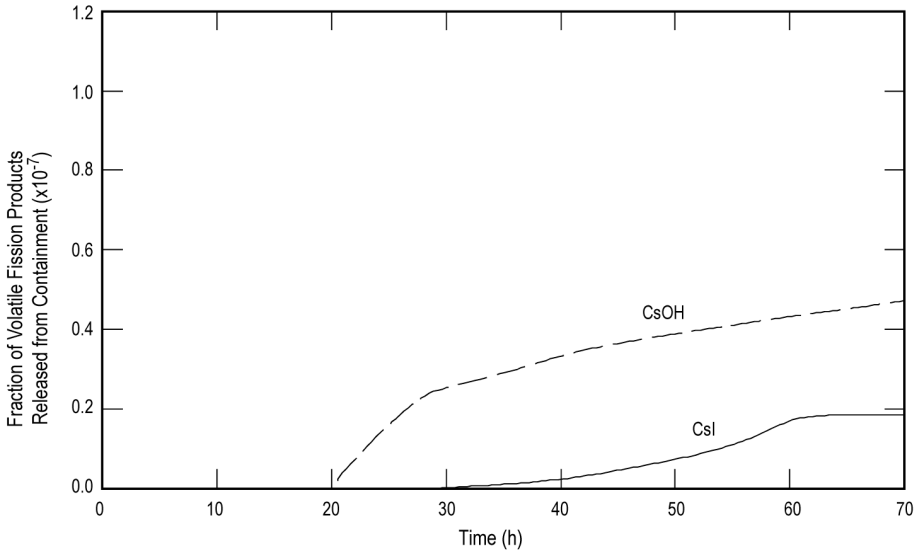

Figure 19E.2-2h LCLP-PF-R-N: Loss of all Core Cooling with Vessel Failure at Low Pressure, Passive Flooder Operates and Rupture Disk Opens: Volatile Fission Products

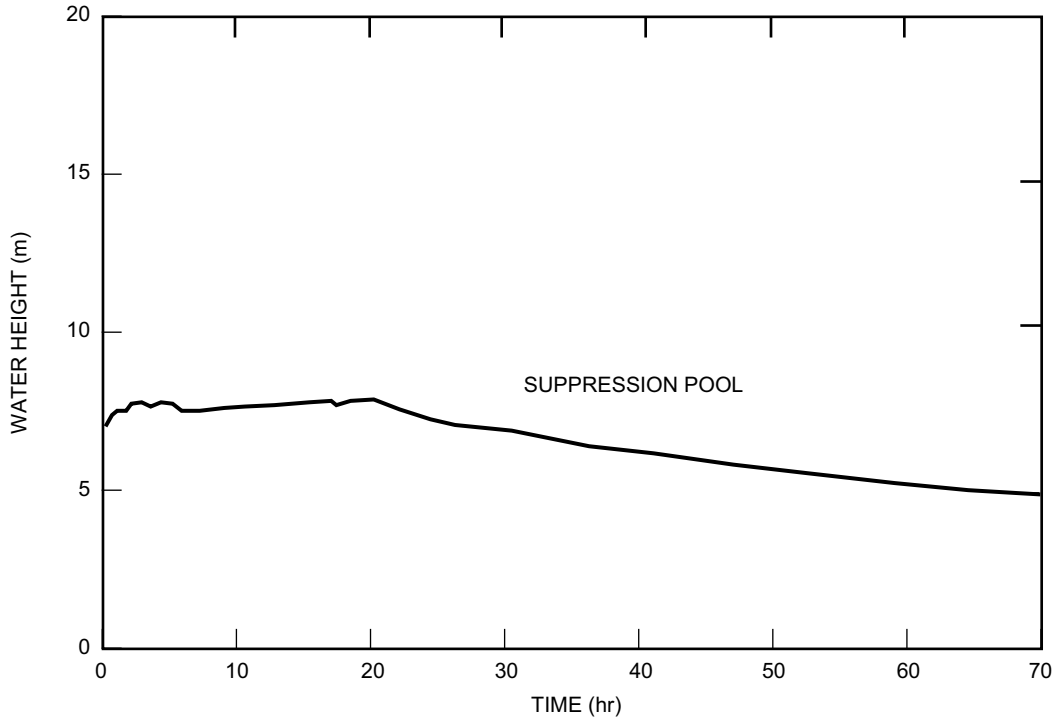

Figure 19E.2-2i LCLP-PF-R-N: Loss of All Core Cooling with Vessel Failure at Low Pressure, Passive Flooder Operates and Rupture Disk Opens: Water Height

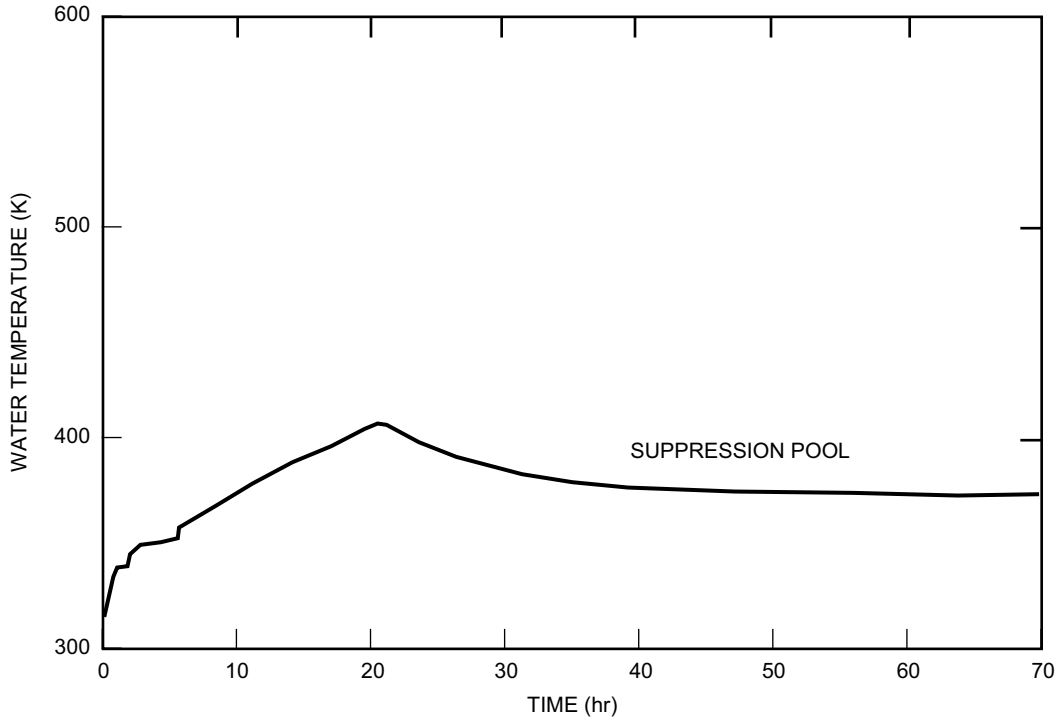

Figure 19E.2-2j LCLP-PF-R-N: Loss of All Core Cooling with Vessel Failure at Low Pressure, Passive Flooder Operates and Rupture Disk Opens: Water Temperature

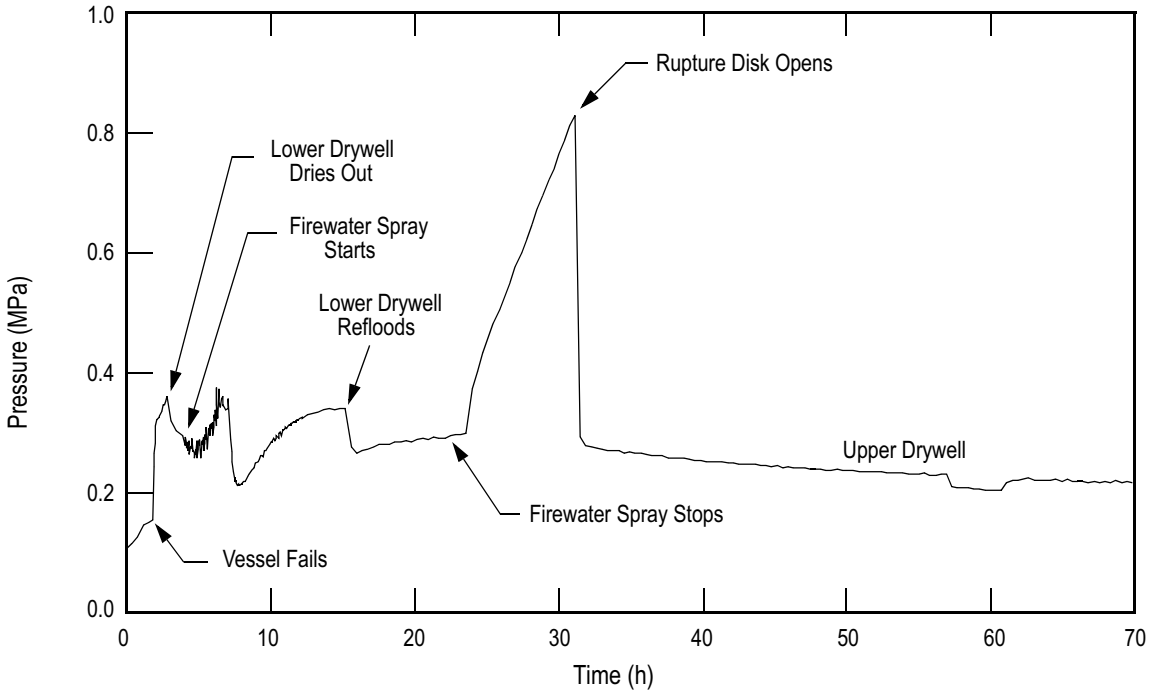

Figure 19E.2-3a LCLP-FS-R-N: Loss of all Core Cooling with Vessel Failure at Low Pressure, Firewater Spray Operates and Rupture Disk Opens: Drywell Pressure

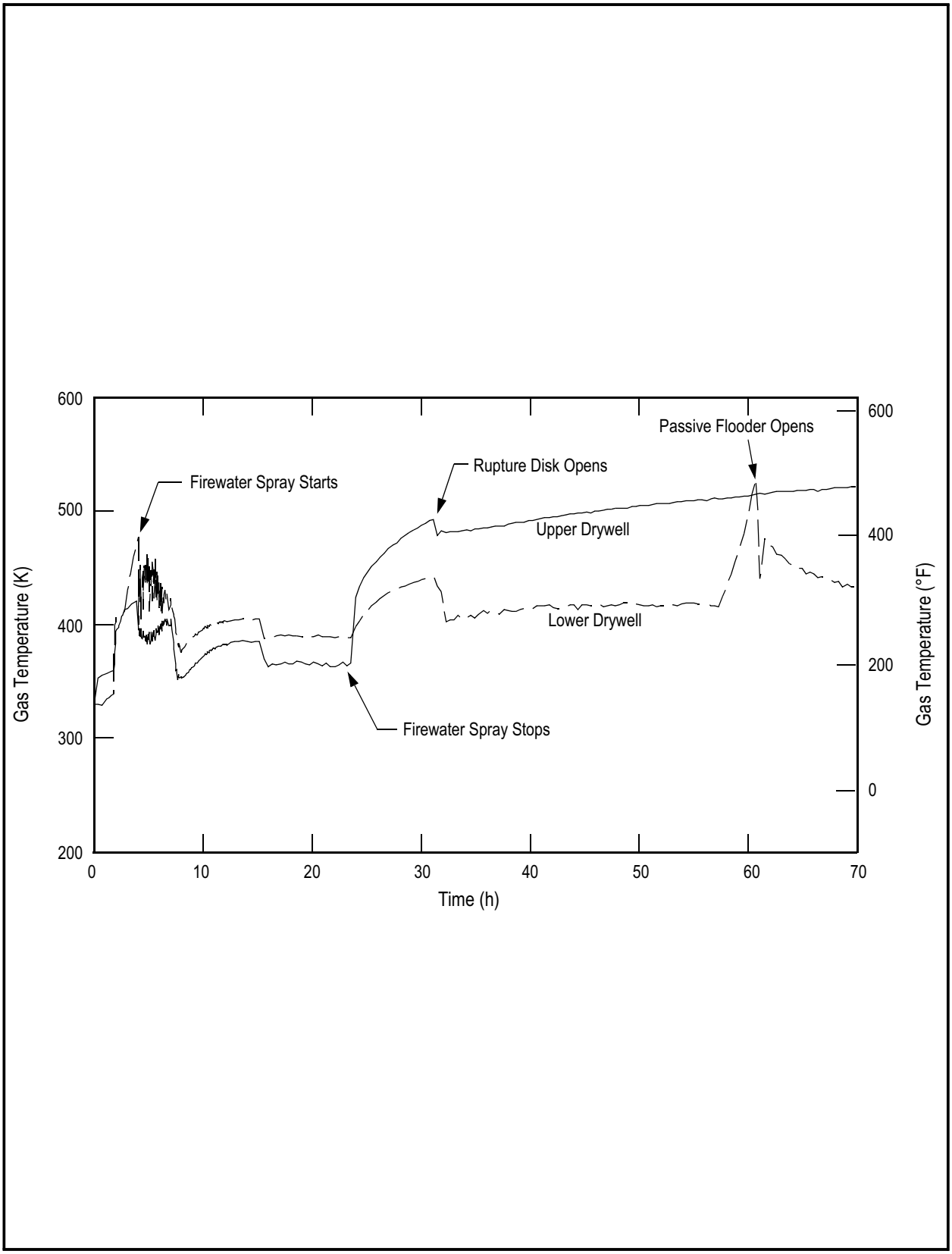

Figure 19E.2-3b LCLP-FS-R-N: Loss of all Core Cooling with Vessel Failure at Low Pressure, Firewater Spray Operates and Rupture Disk Opens: Gas Temperature

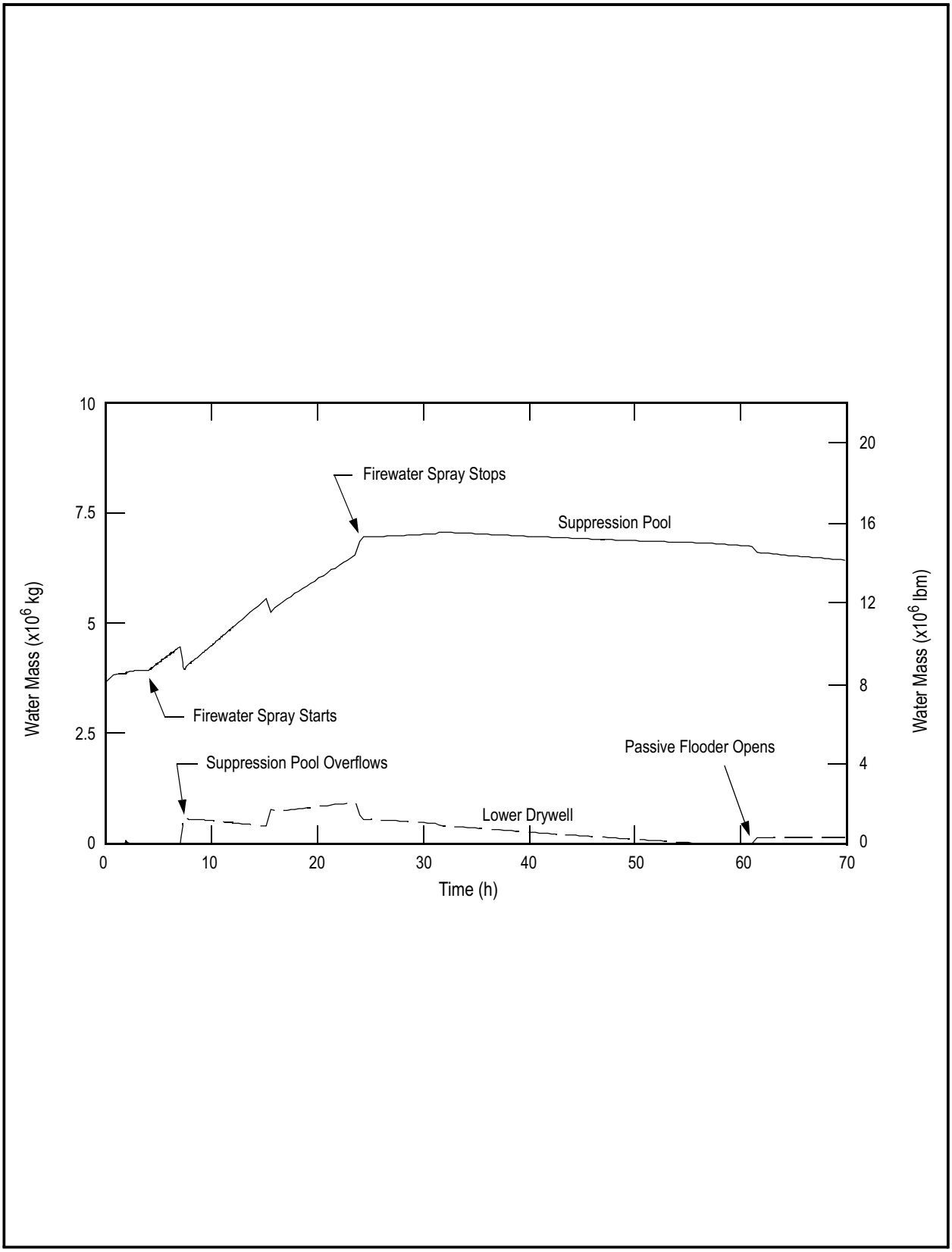

Figure 19E.2-3c LCLP-FS-R-N: Loss of all Core Cooling with Vessel Failure at Low Pressure, Firewater Spray Operates and Rupture Disk Opens: Water Mass

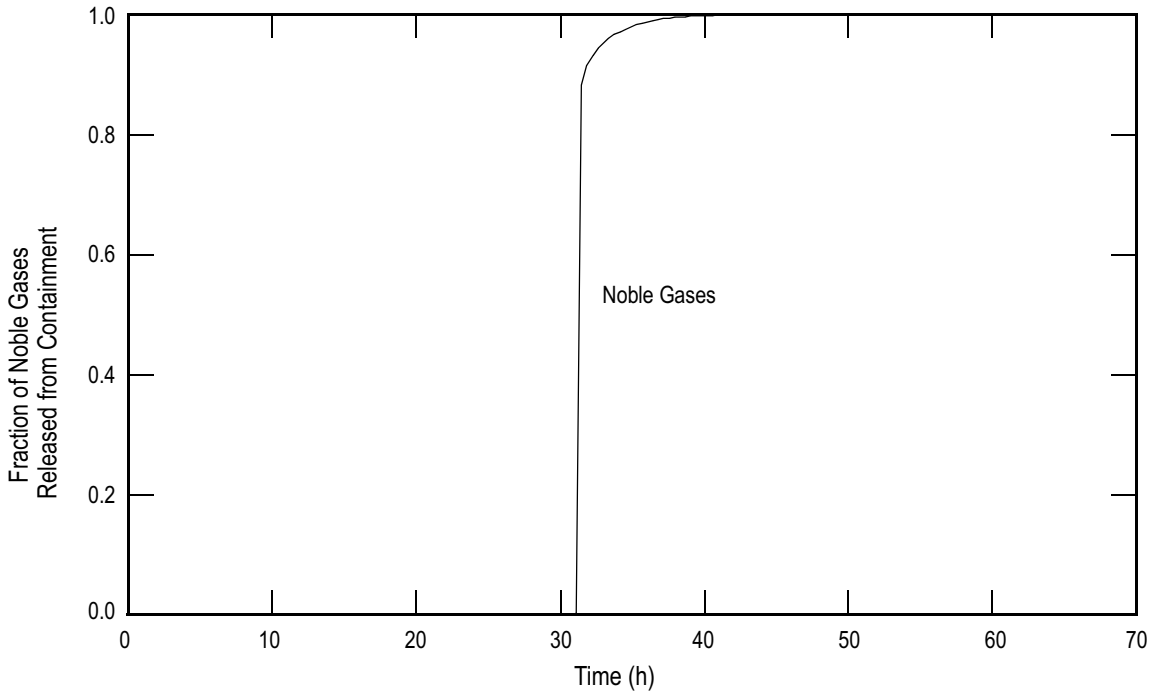

Figure 19E.2-3d LCLP-FS-R-N: Loss of all Core Cooling with Vessel Failure at Low Pressure, Firewater Spray Operates and Rupture Disk Opens: Noble Gas

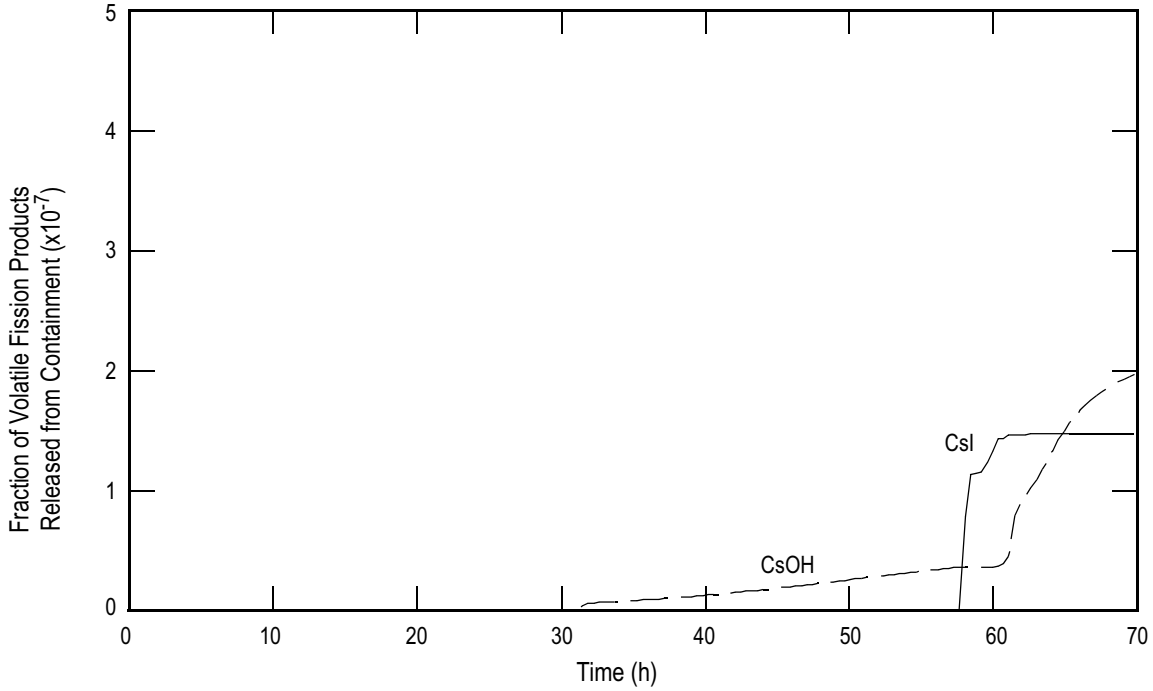

Figure 19E.2-3e LCLP-FS-R-N: Loss of all Core Cooling with Vessel Failure at Low Pressure, Firewater Spray Operates and Rupture Disk Opens: Volatile Fission Products

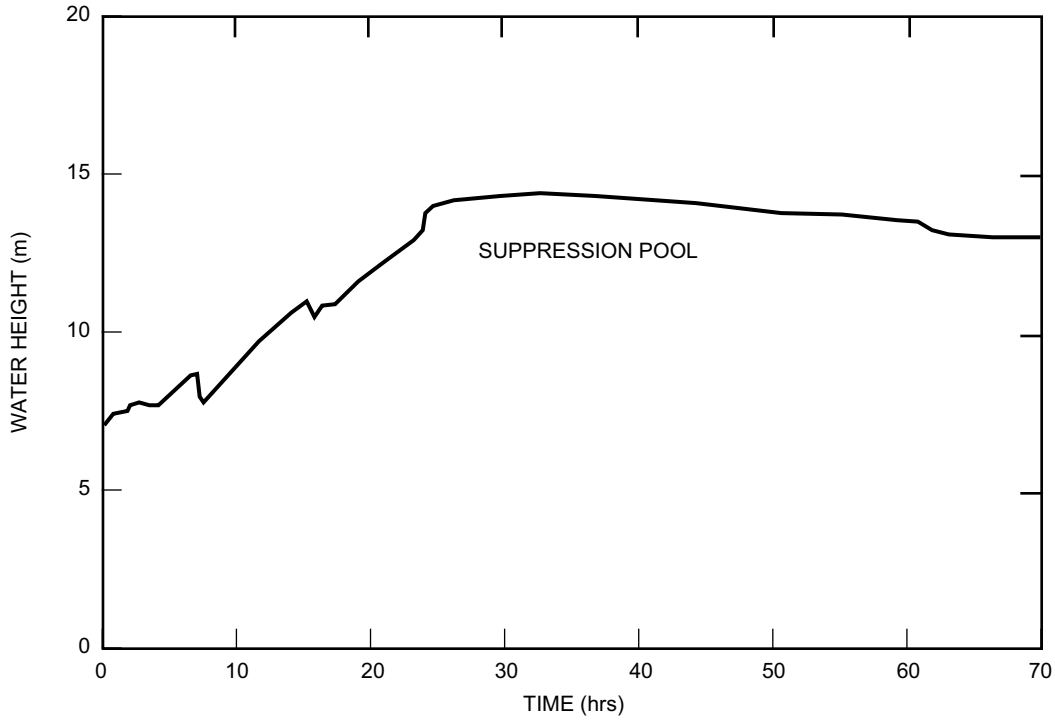

Figure 19E.2-3f LCLP-FS-R-N: Loss of All Core Cooling with Vessel Failure at Low Pressure, Firewater Spray Operates and Rupture Disk Opens: Water Height

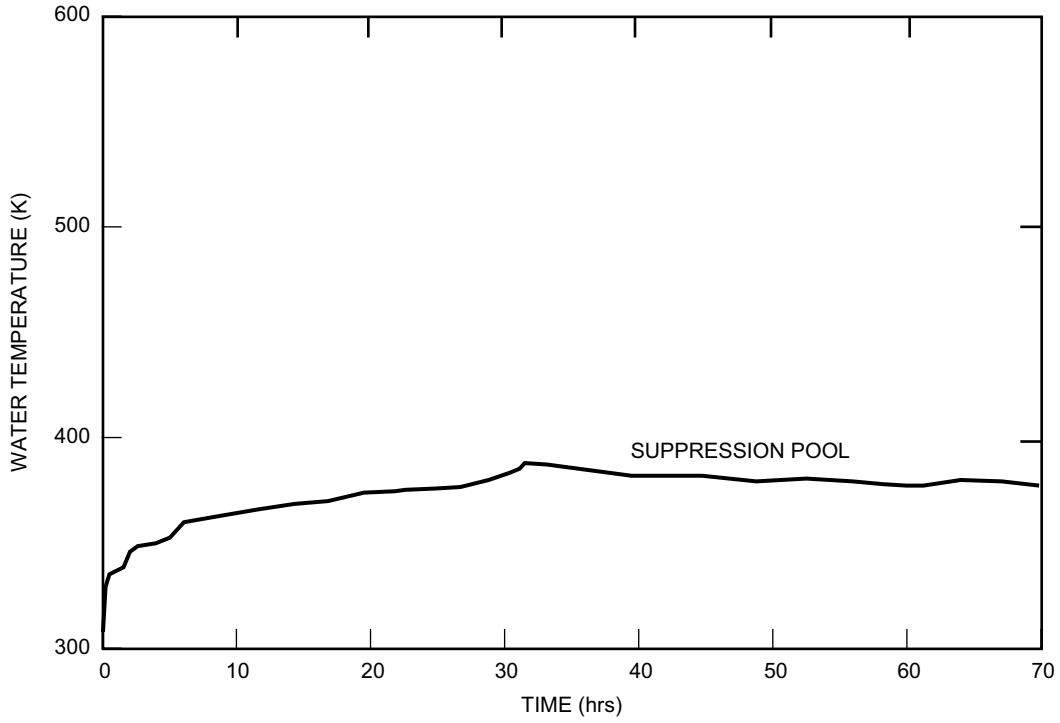

Figure 19E.2-3g LCLP-FS-R-N: Loss of All Core Cooling with Vessel Failure at Low Pressure, Firewater Spray Operates and Rupture Disk Opens: Water Temperature

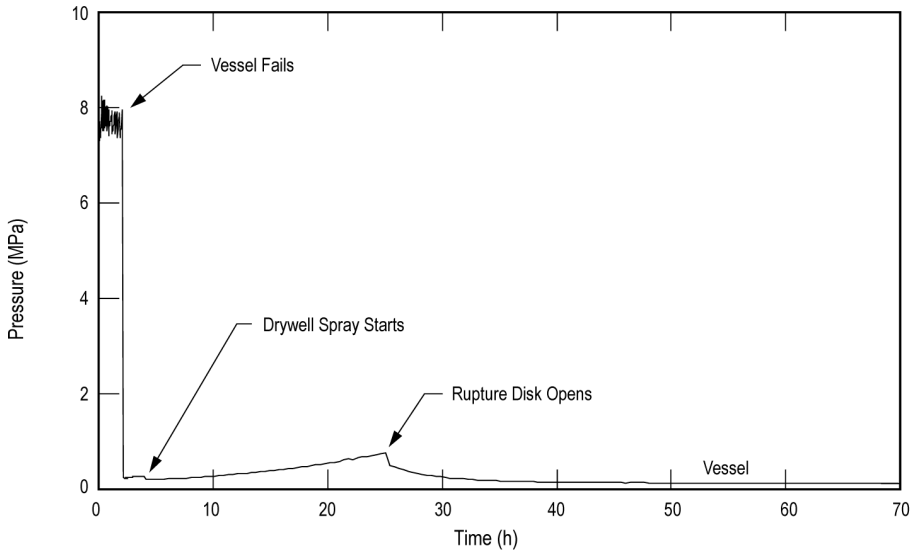

Figure 19E.2-4a LCHP-PS-R-N: Loss of all Core Cooling with Vessel Failure at High Pressure, Passive Flooder and Drywell Sprays Operate, Rupture Disk Opens: Vessel Pressure

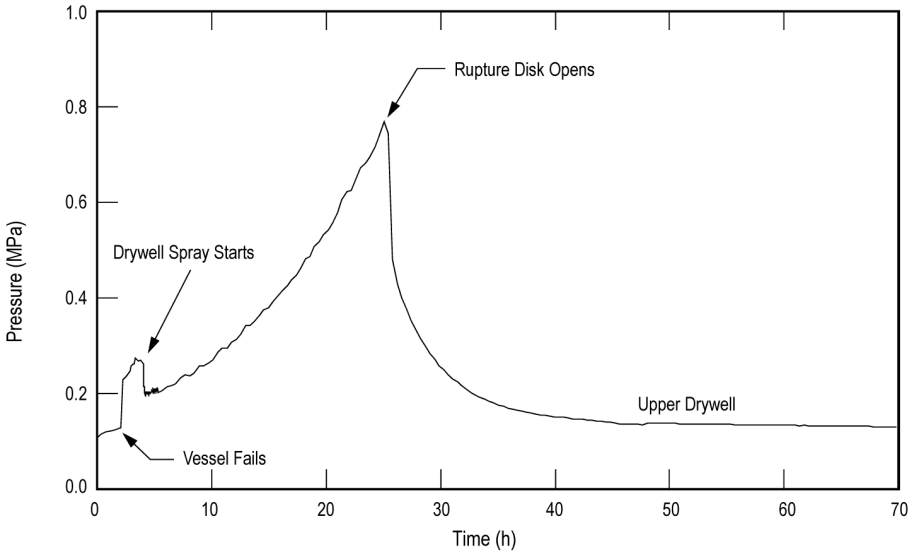

Figure 19E.2-4b LCHP-PS-R-N: Loss of all Core Cooling with Vessel Failure at High Pressure, Passive Flooder and Drywell Sprays Operate, Rupture Disk Opens: Drywell Pressure

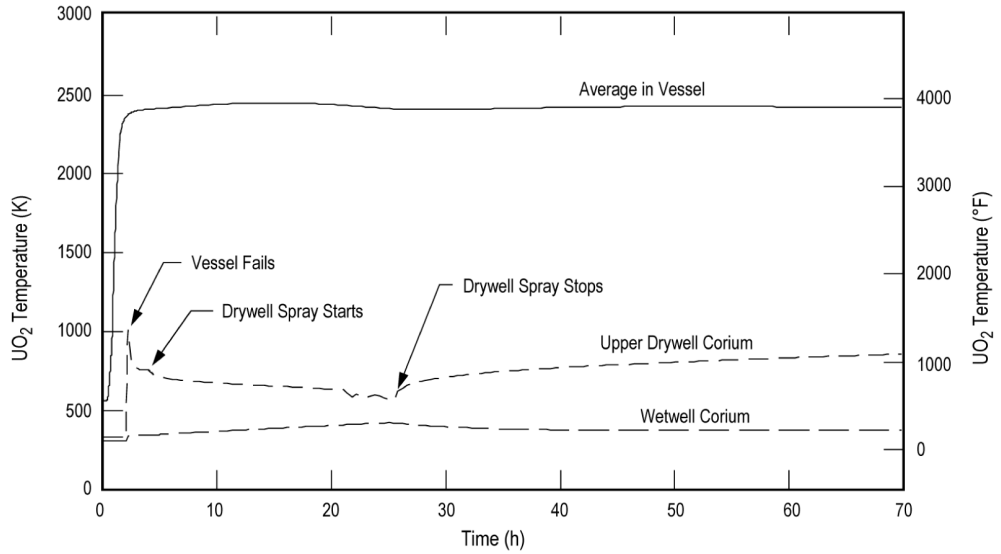

Figure 19E.2-4c LCHP-PS-R-N: Loss of all Core Cooling with Vessel Failure at High Pressure, Passive Flooder and Drywell Sprays Operate, Rupture Disk Opens: UO_2 Temperature

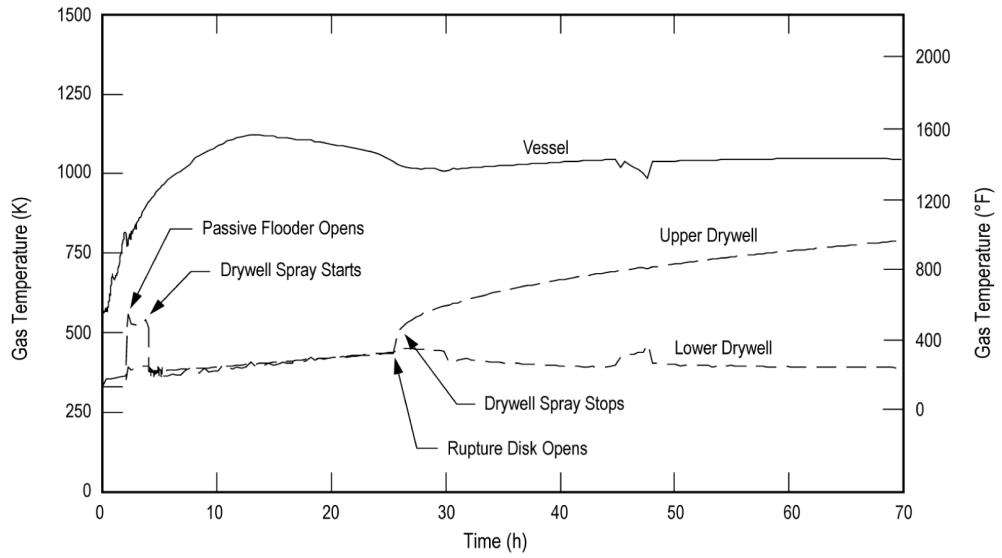

Figure 19E.2-4d LCHP-PS-R-N: Loss of all Core Cooling with Vessel Failure at High Pressure, Passive Flooder and Drywell Sprays Operate, Rupture Disk Opens: Gas Temperature

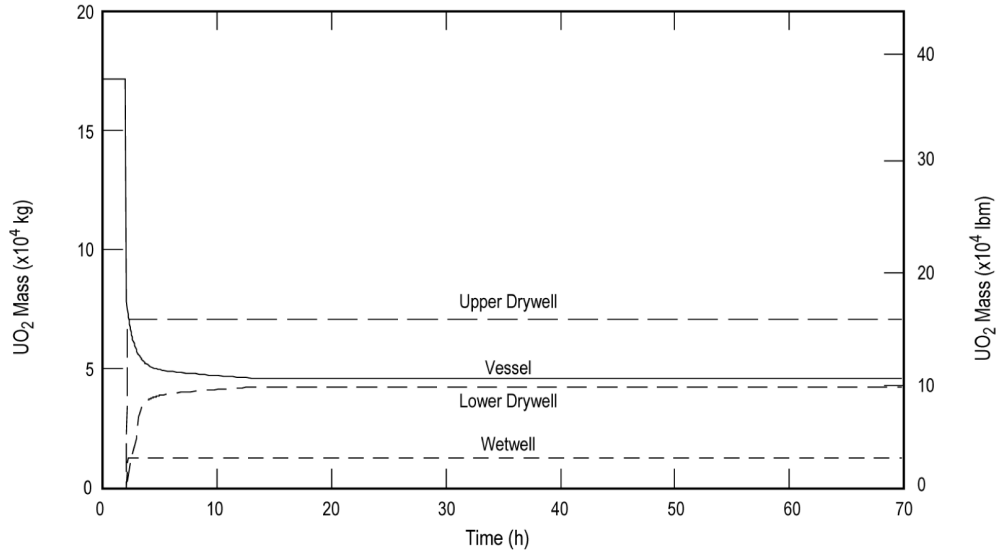

Figure 19E.2-4e LCHP-PS-R-N: Loss of all Core Cooling with Vessel Failure at High Pressure, Passive Flooder and Drywell Sprays Operate, Rupture Disk Opens: UO_2 Mass

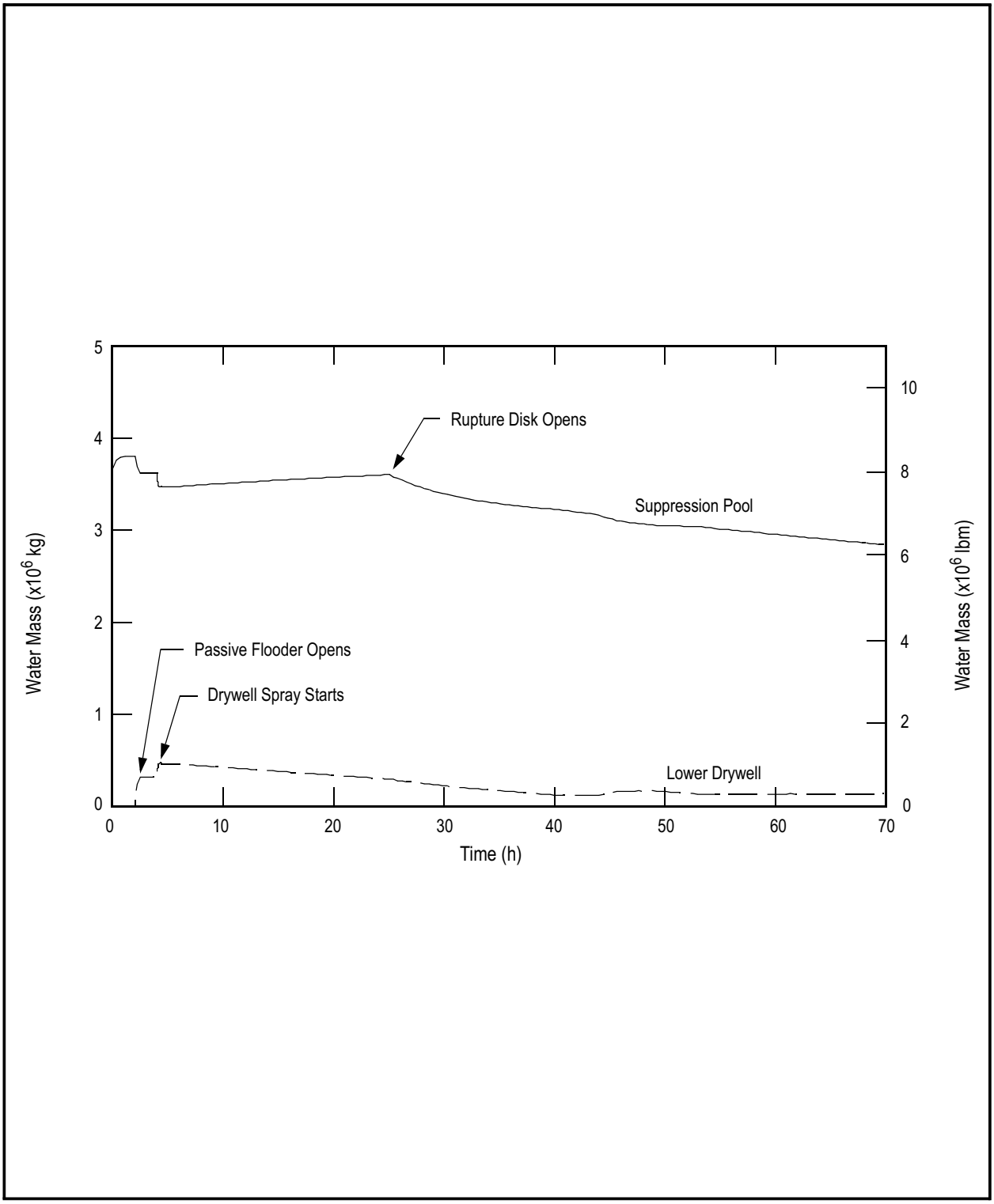

Figure 19E.2-4f LCHP-PS-R-N: Loss of all Core Cooling with Vessel Failure at High Pressure, Passive Flooder and Drywell Sprays Operate, Rupture Disk Opens: Water Mass

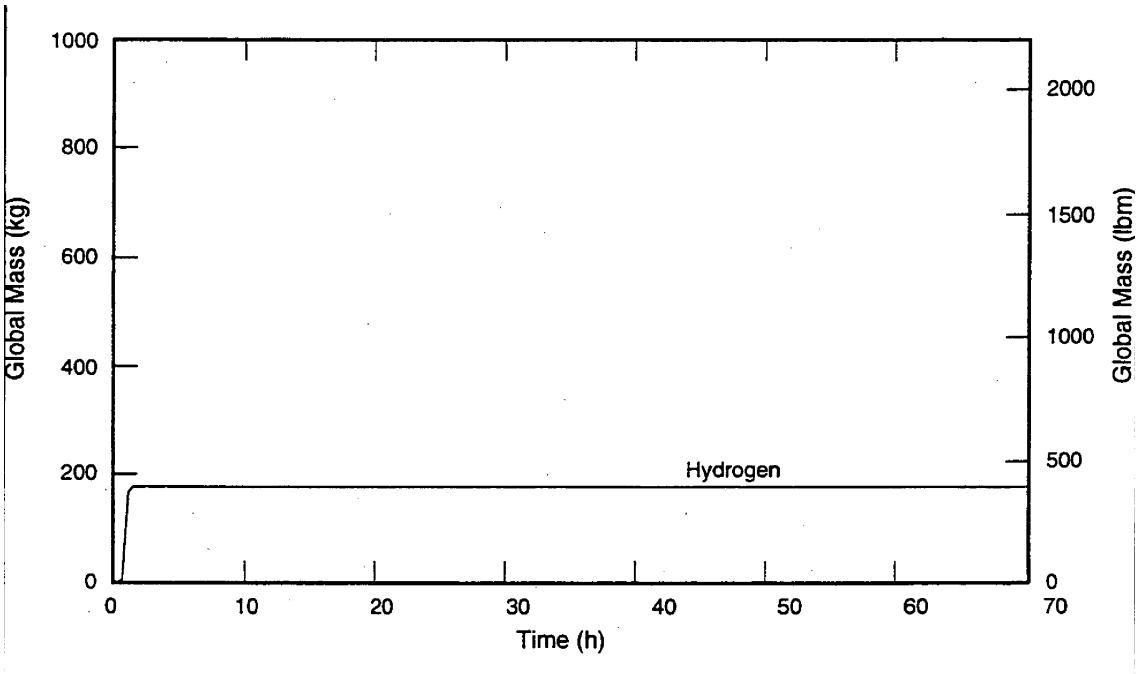

Figure 19E.2-4g LCHP-PS-R-N: Loss of all Core Cooling with Vessel Failure at High Pressure, Passive Flooder and Drywell Sprays Operate, Rupture Disk Opens: Global Mass

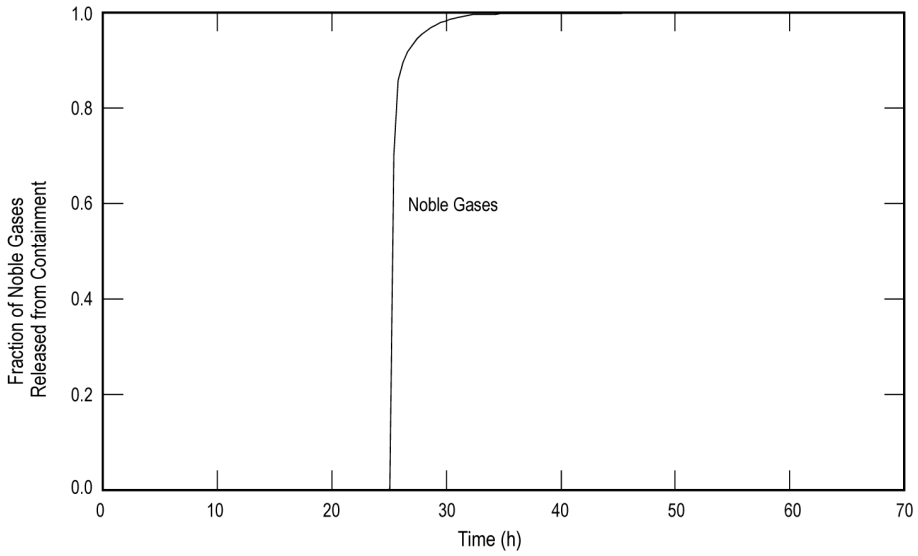

Figure 19E.2-4h LCHP-PS-R-N: Loss of all Core Cooling with Vessel Failure at High Pressure, Passive Flooder and Drywell Sprays Operate, Rupture Disk Opens: Noble Gases

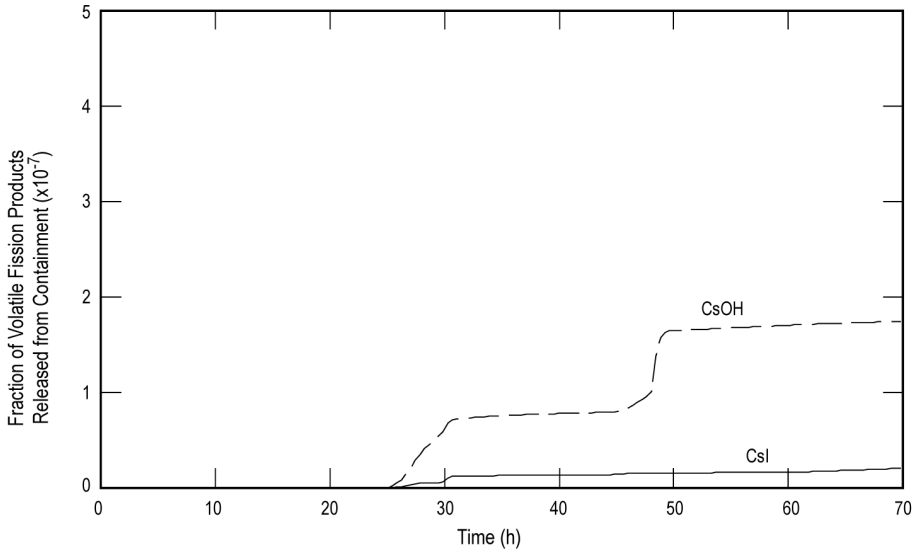

Figure 19E.2-4i LCHP-PS-R-N: Loss of all Core Cooling with Vessel Failure at High Pressure, Passive Flooder and Drywell Sprays Operate, Rupture Disk Opens: Volatiles

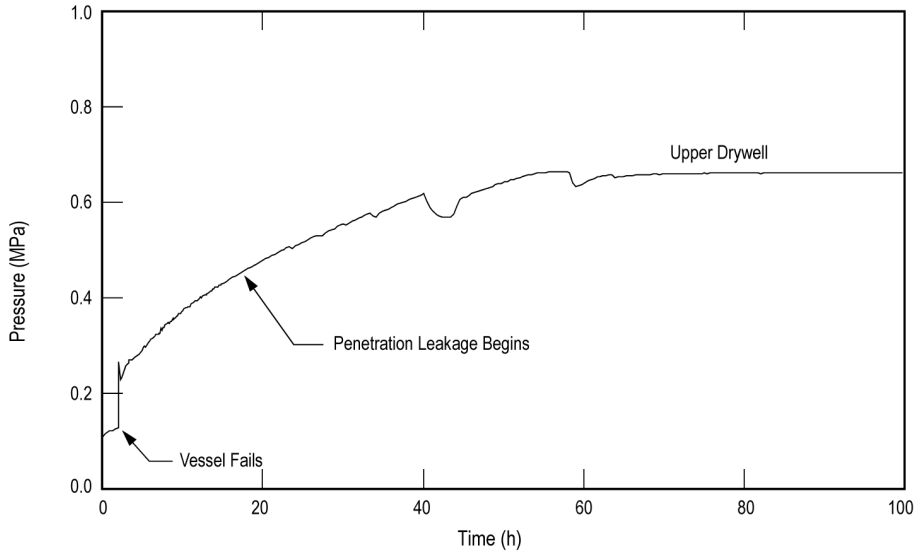

Figure 19E.2-5a LCHP-PF-P-M: Loss of all Core Cooling with Vessel Failure at High Pressure, Passive Flooder Operates, Penetration Leakage: Drywell Pressure

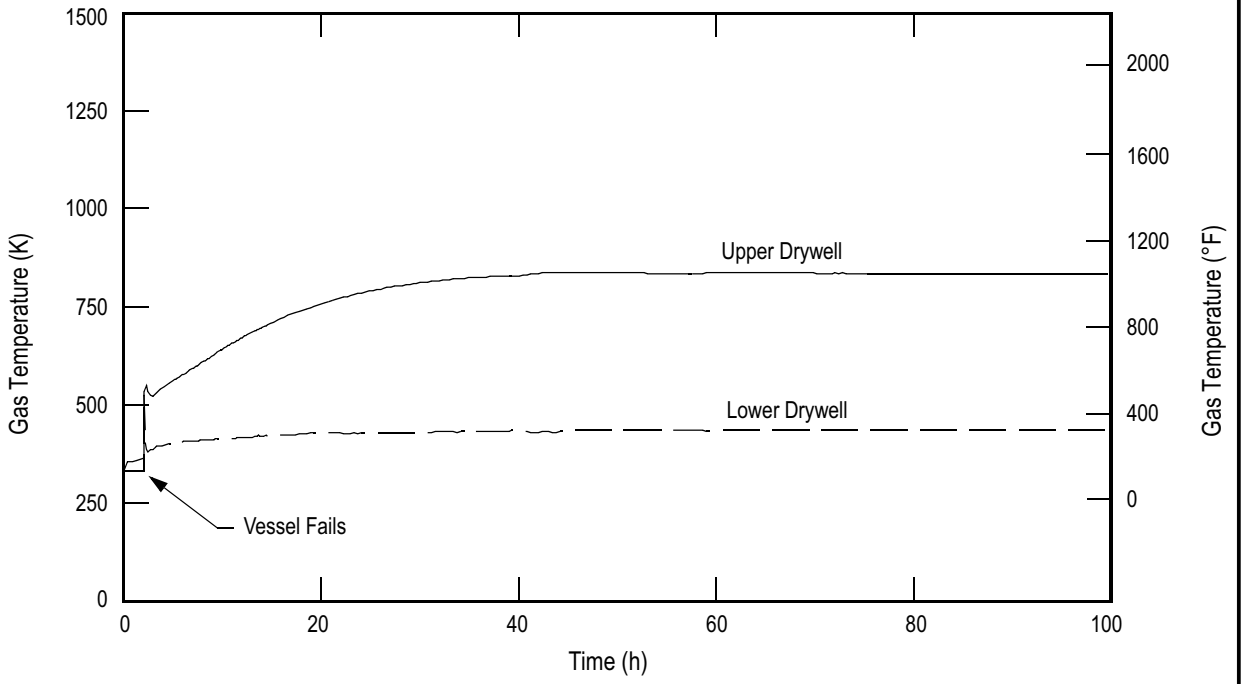

Figure 19E.2-5b LCHP-PF-P-M: Loss of all Core Cooling with Vessel Failure at High Pressure, Passive Flooder Operates, Penetration Leakage: Gas Temperature

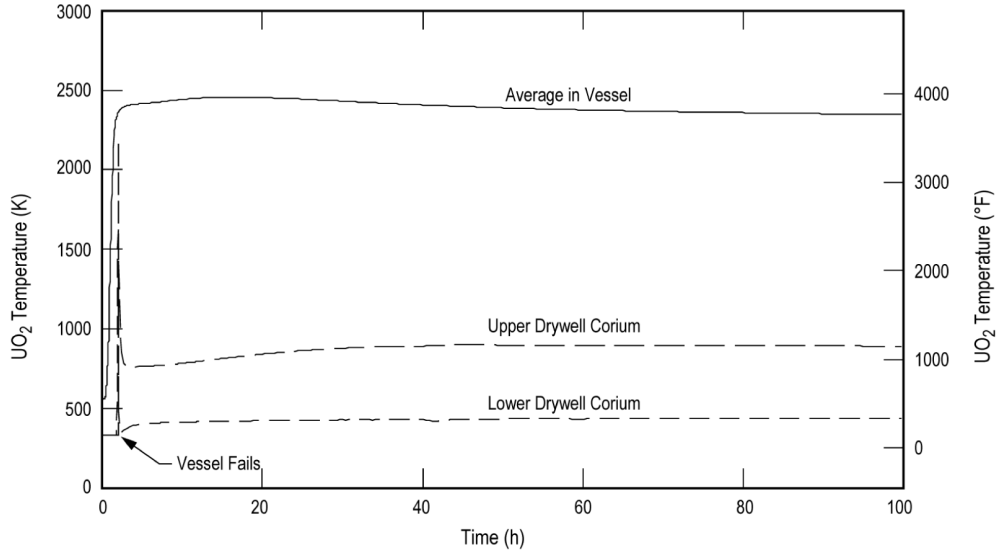

Figure 19E.2-5c LCHP-PF-P-M: Loss of all Core Cooling with Vessel Failure at High Pressure, Passive Flooder Operates, Penetration Leakage: UO_2 Temperature

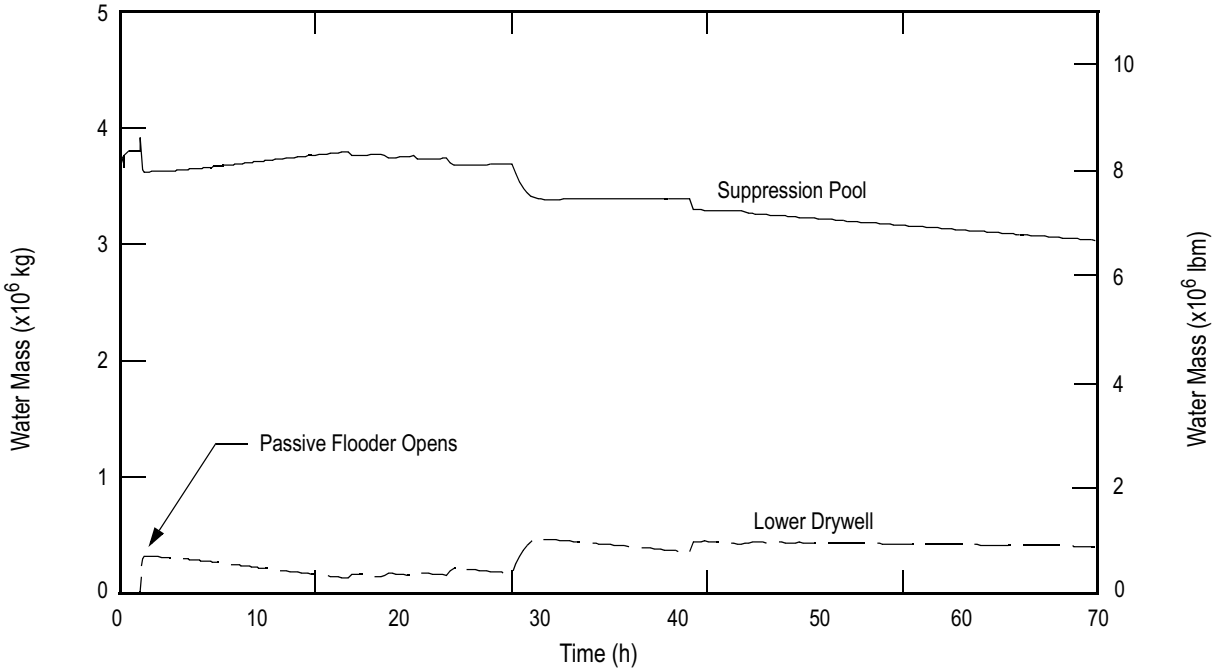

Figure 19E.2-5d LCHP-PF-P-M: Loss of all Core Cooling with Vessel Failure at High Pressure, Passive Flooder Operates, Penetration Leakage: Water Mass

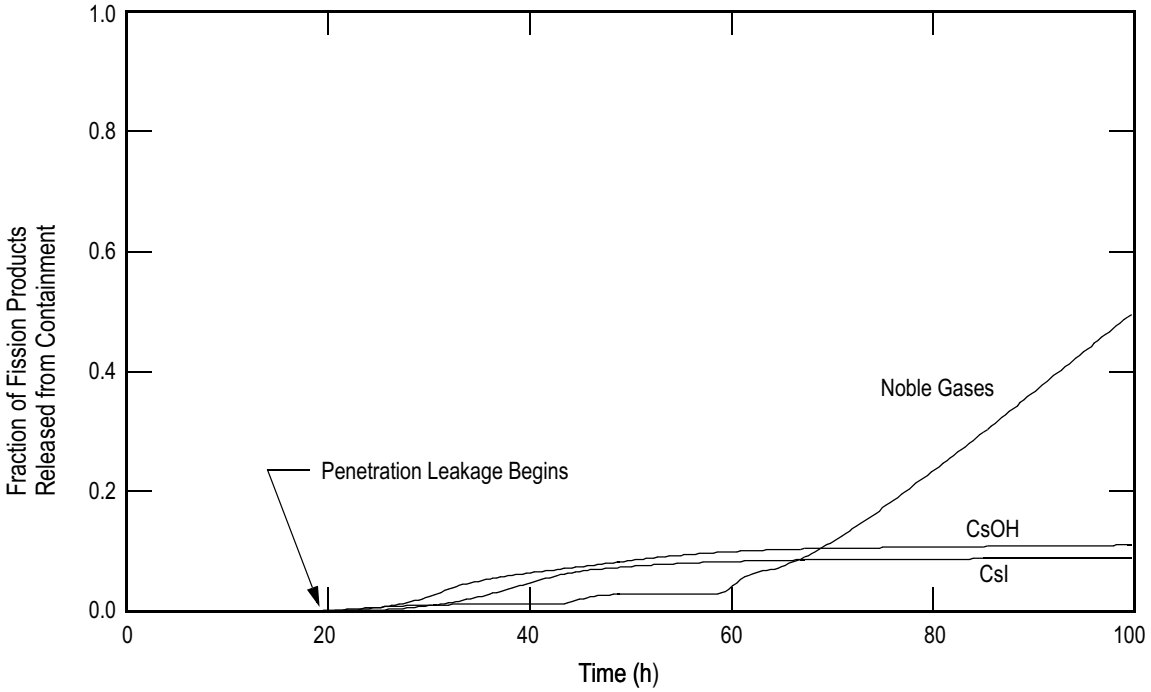

Figure 19E.2-5e LCHP-PF-P-M: Loss of all Core Cooling with Vessel Failure at High Pressure, Passive Flooder Operates, Penetration Leakage: Fission Product Release

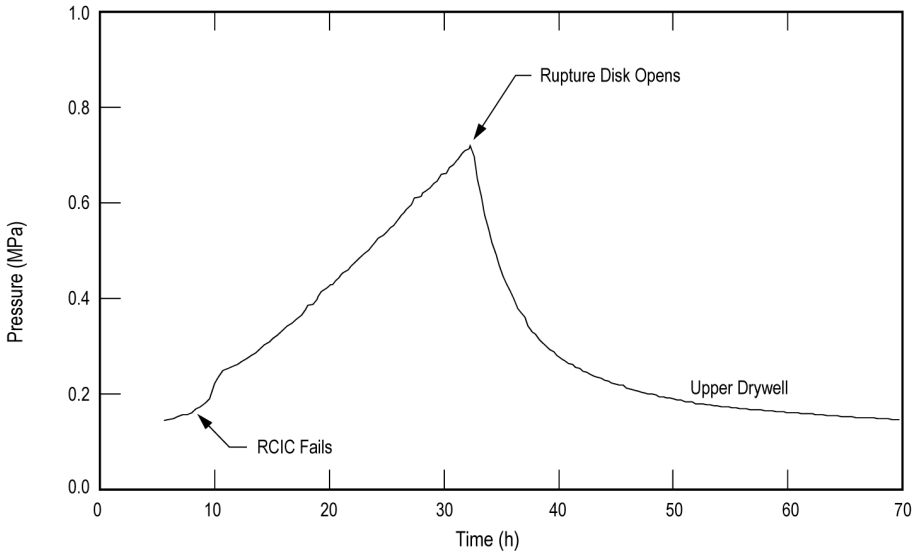

Figure 19E.2-6a SBRC-FA-R-0: Station Blackout, RCIC Runs Eight Hours, Firewater Addition Prevents Core Damage, Rupture Disk Opens: Drywell Pressure

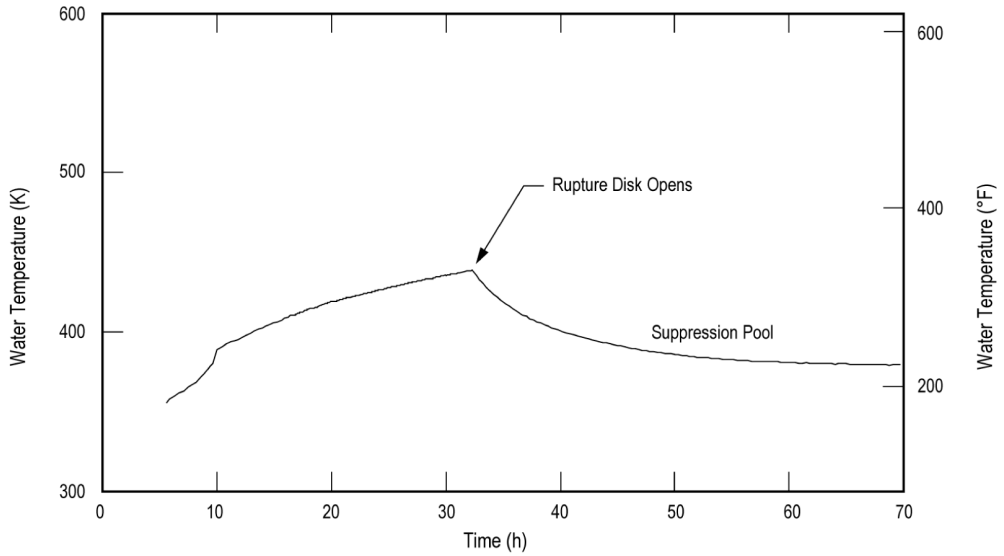

Figure 19E.2-6b SBRC-FA-R-0: Station Blackout, RCIC Runs Eight Hours, Firewater Addition Prevents Core Damage, Rupture Disk Opens: Water Temperature

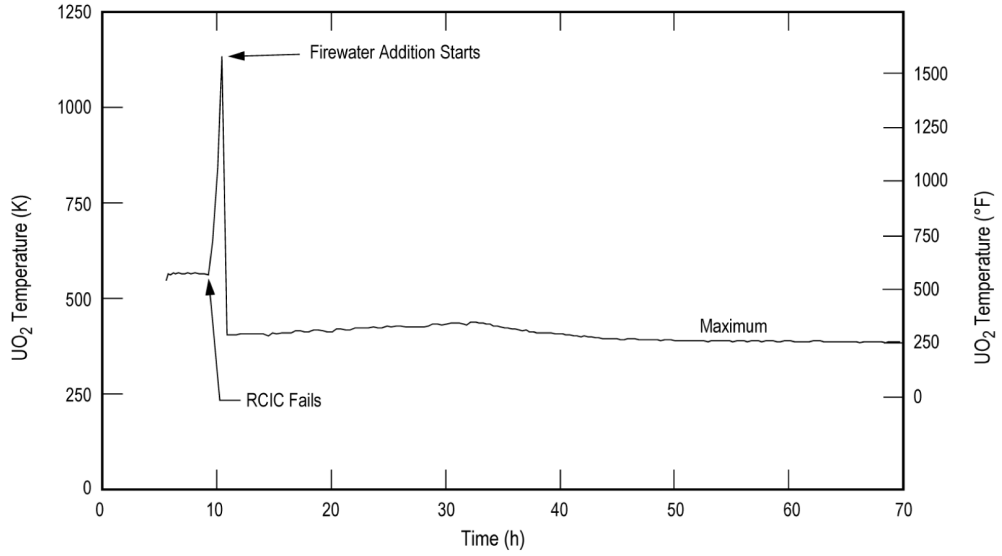

Figure 19E.2-6c SBRC-FA-R-0: Station Blackout, RCIC Runs Eight Hours, Firewater Addition Prevents Core Damage, Rupture Disk Opens: UO_2 Temperature

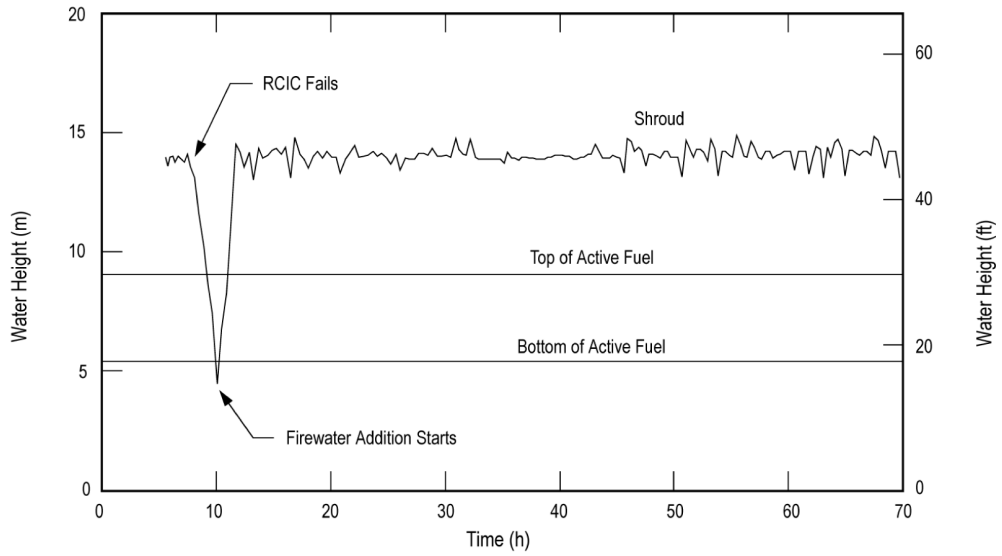

Figure 19E.2-6d SBRC-FA-R-0: Station Blackout, RCIC Runs Eight Hours, Firewater Addition Prevents Core Damage, Rupture Disk Opens: Vessel Water Height

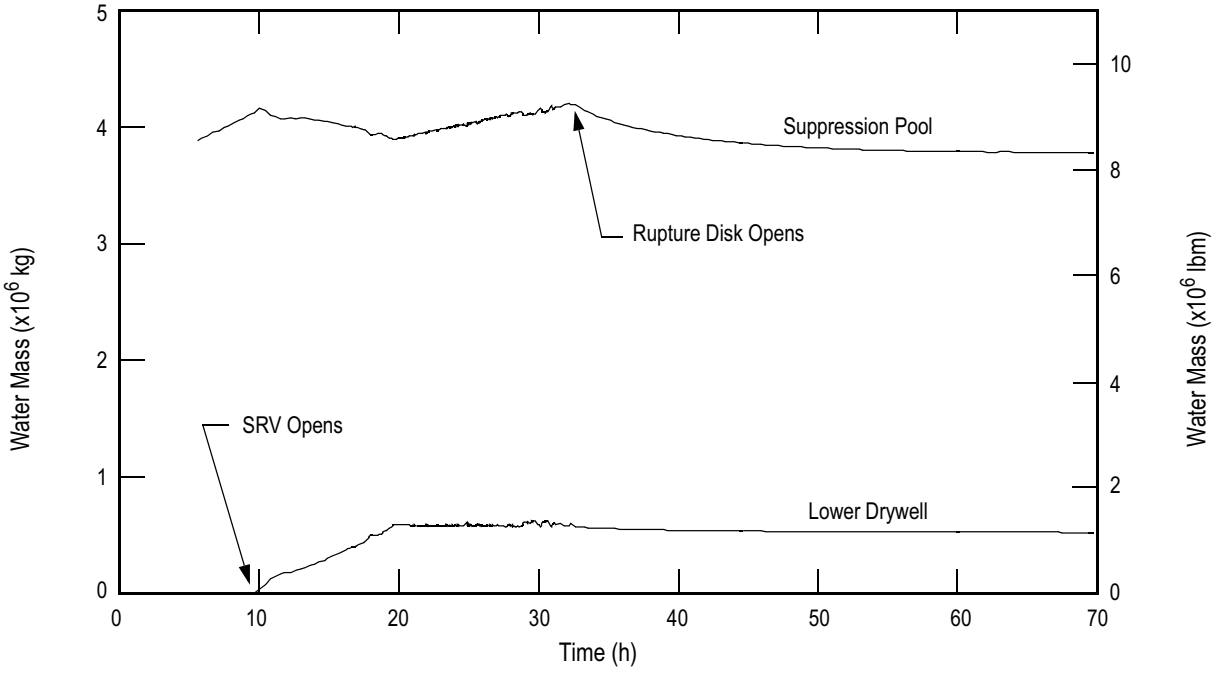

Figure 19E.2-6e SBRC-FA-R-0: Station Blackout, RCIC Runs Eight Hours, Firewater Addition Prevents Core Damage, Rupture Disk Opens: Water Mass

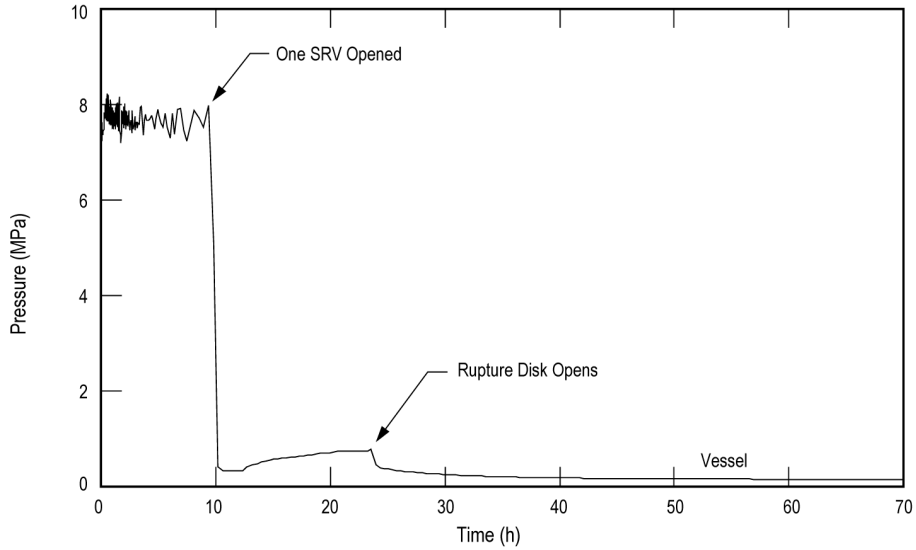

Figure 19E.2-7a SBRC-PF-R-N: Station Blackout with RCIC Operating, Passive Flooder Operates and Rupture Disk Opens: Vessel Pressure

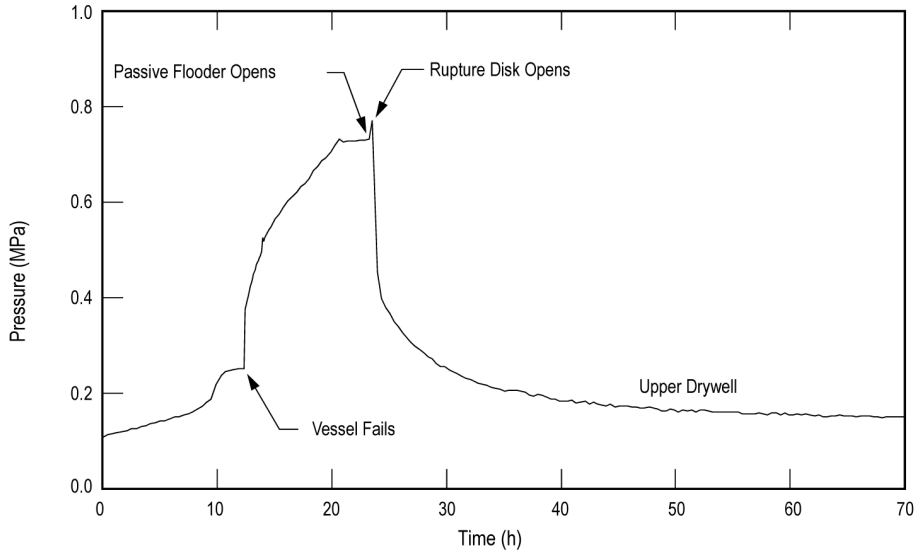

Figure 19E.2-7b SBRC-PF-R-N: Station Blackout with RCIC Operating, Passive Flooder Operates and Rupture Disk Opens: Drywell Pressure

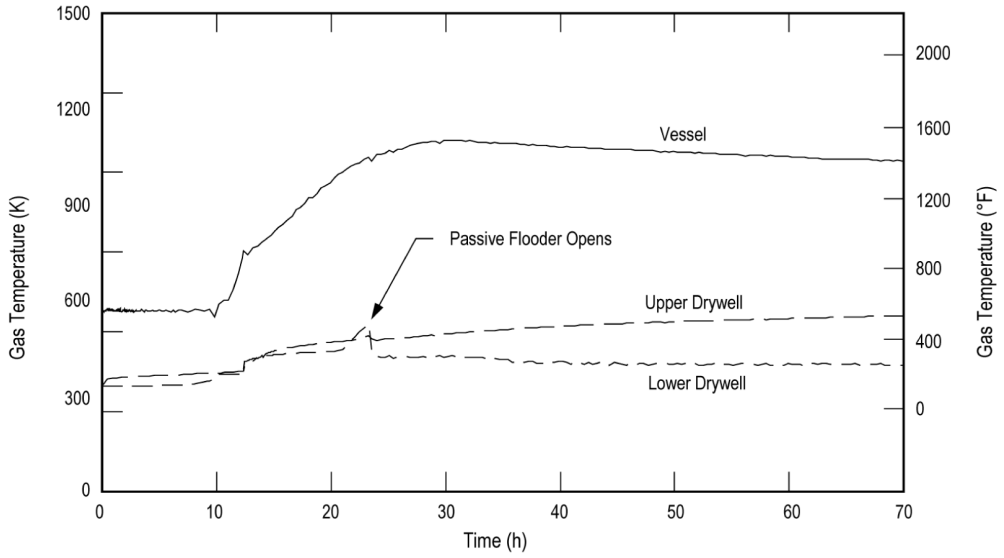

Figure 19E.2-7c SBRC-PF-R-N: Station Blackout with RCIC Operating, Passive Flooder Operates and Rupture Disk Opens: Gas Temperature

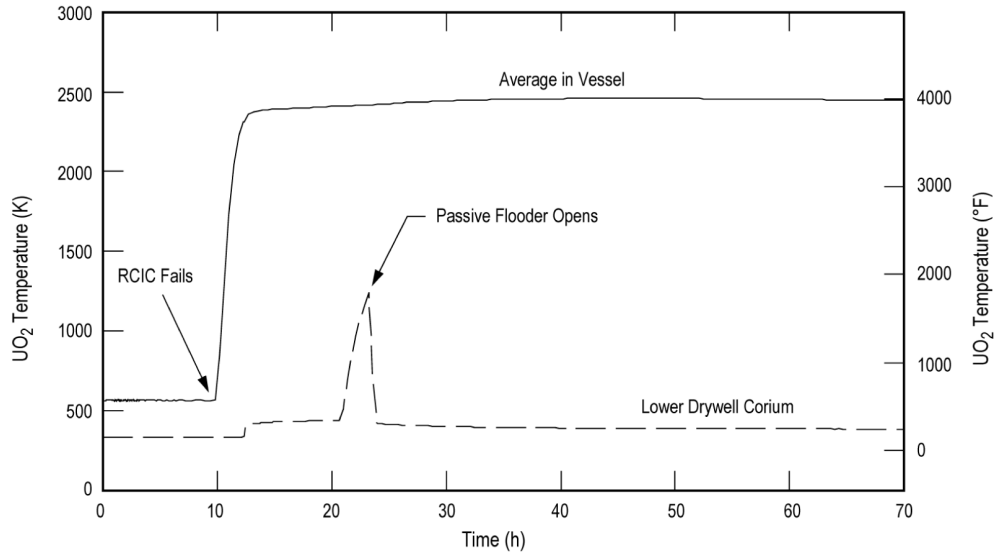

Figure 19E.2-7d SBRC-PF-R-N: Station Blackout with RCIC Operating, Passive Flooder Operates and Rupture Disk Opens: UO_2 Temperature

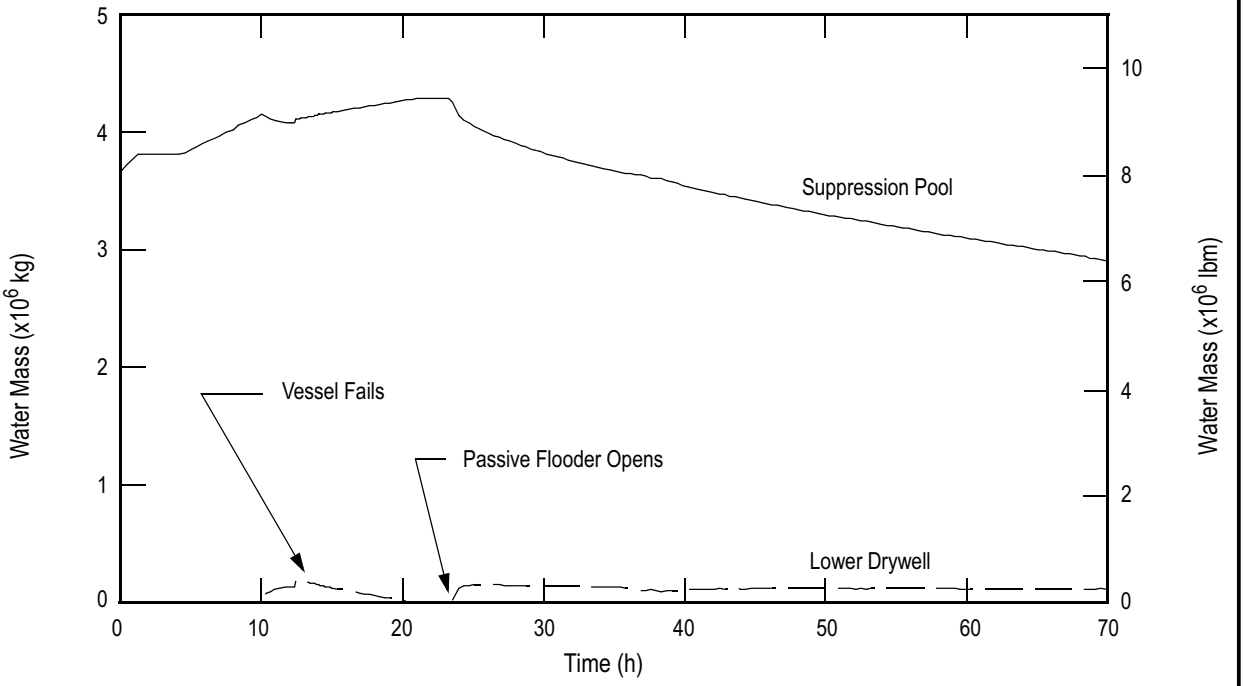

Figure 19E.2-7e SBRC-PF-R-N: Station Blackout with RCIC Operating, Passive Flooder Operates and Rupture Disk Opens: Water Mass

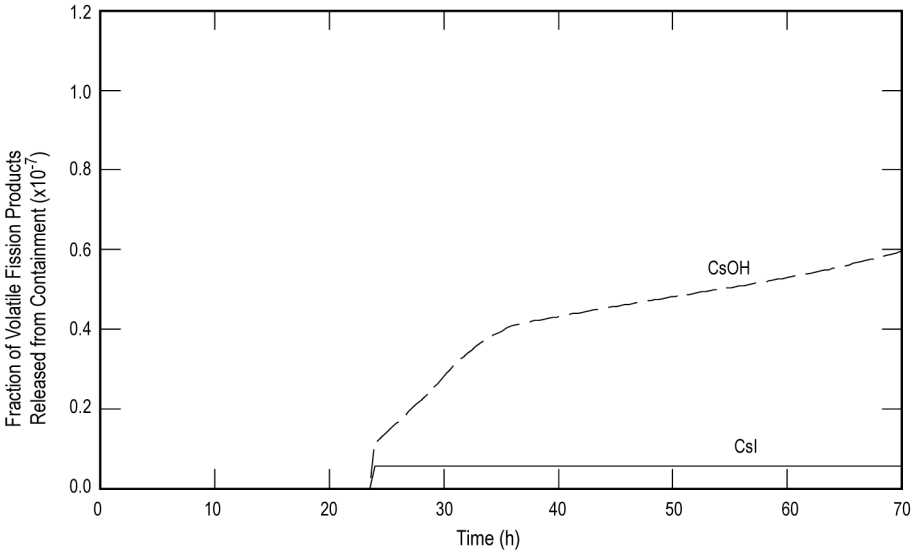

Figure 19E.2-7f SBRC-PF-R-N: Station Blackout with RCIC Operating, Passive Flooder Operates and Rupture Disk Opens: Volatile Fission Product Release

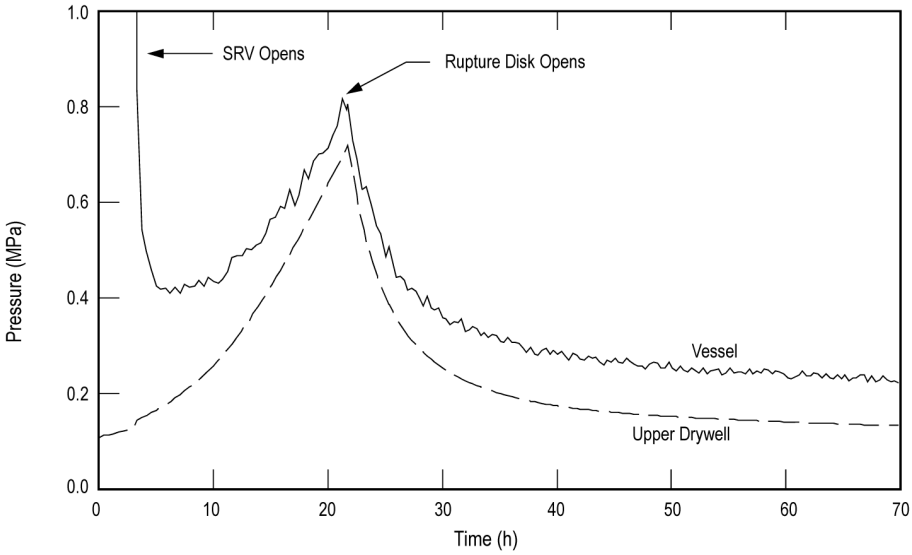

Figure 19E.2-8a LHRC-00-R-0: Isolation with Loss of Containment Heat Removal and Rupture Disk Opens: Pressure

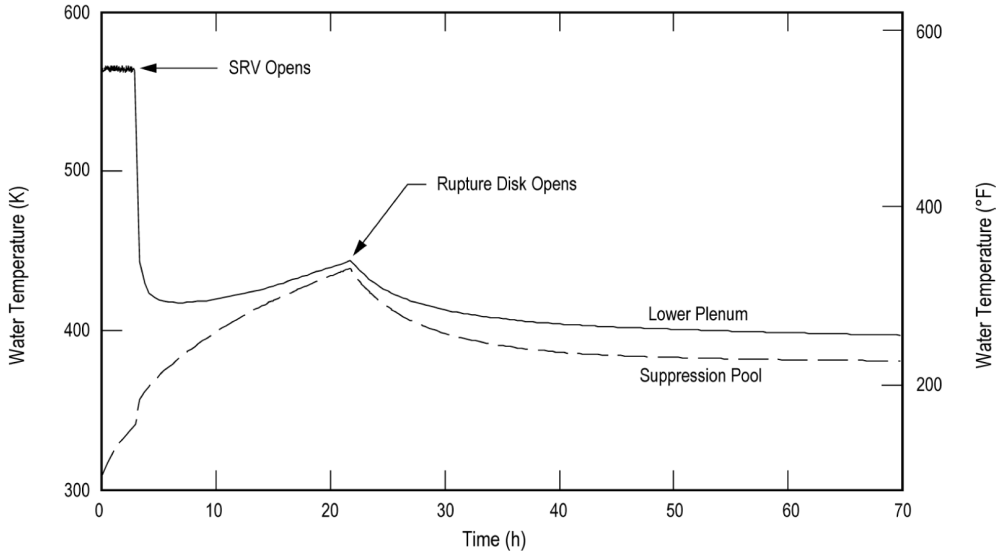

Figure 19E.2-8b LHRC-00-R-0: Isolation with Loss of Containment Heat Removal and Rupture Disk Opens: Water Temperature

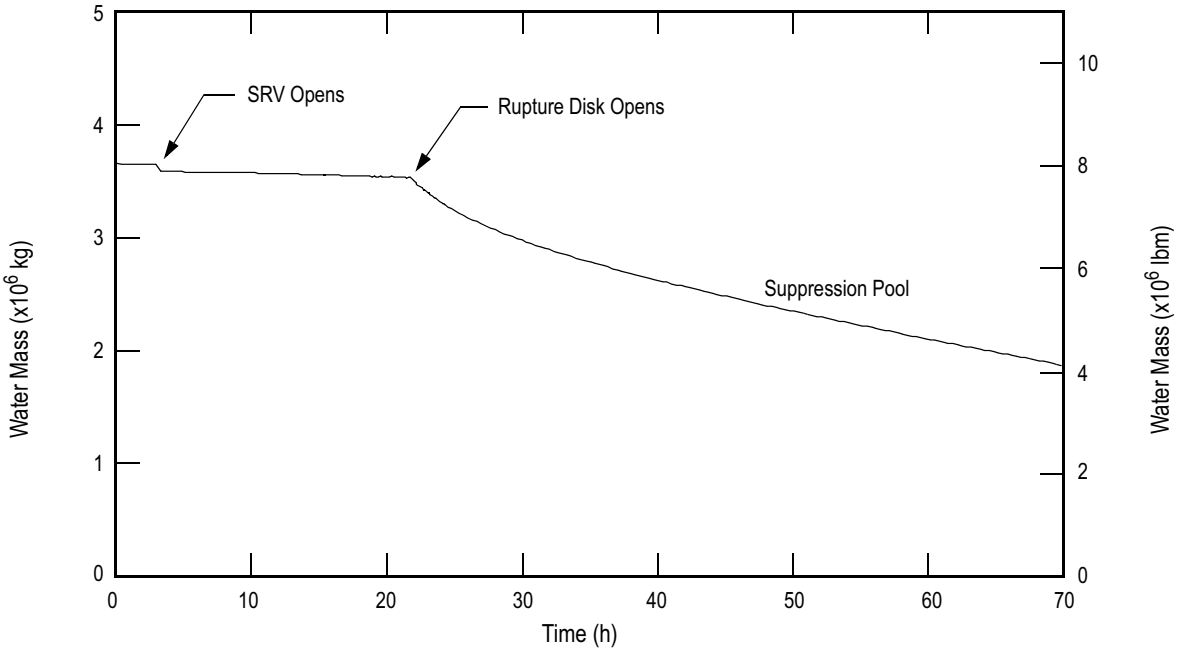

Figure 19E.2-8c LHRC-00-R-0: Isolation with Loss of Containment Heat Removal and Rupture Disk Opens: Water Mass

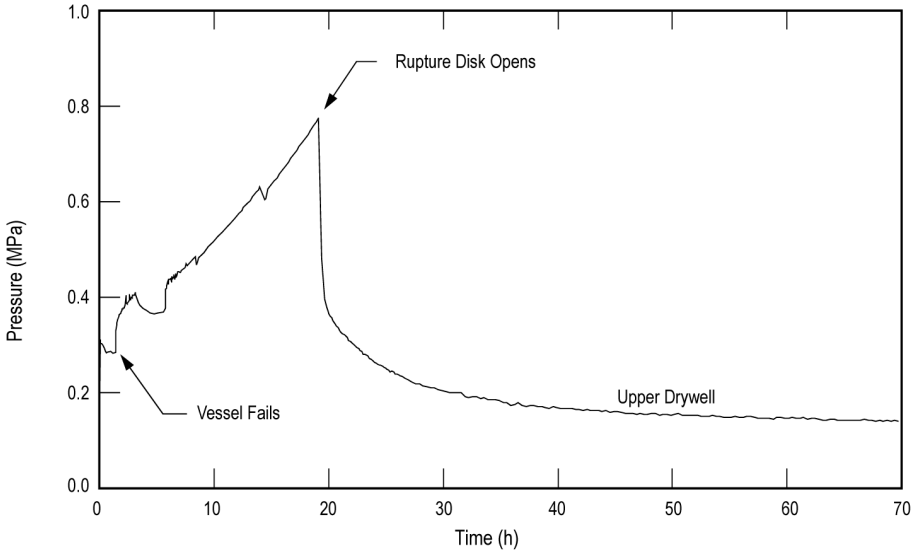

Figure 19E.2-9a LBLC-PF-R-N: Large Break LOCA with Loss of all Core Cooling, Passive Flooder Operates and Rupture Disk Opens: Drywell Pressure

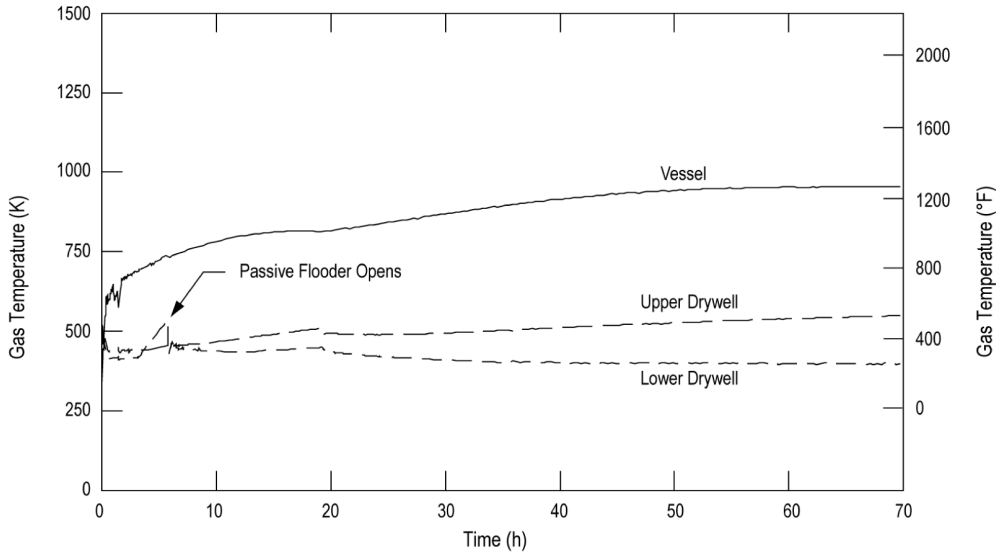

Figure 19E.2-9b LBLC-PF-R-N: Large Break LOCA with Loss of all Core Cooling, Passive Flooder Operates and Rupture Disk Opens: Gas Temperature

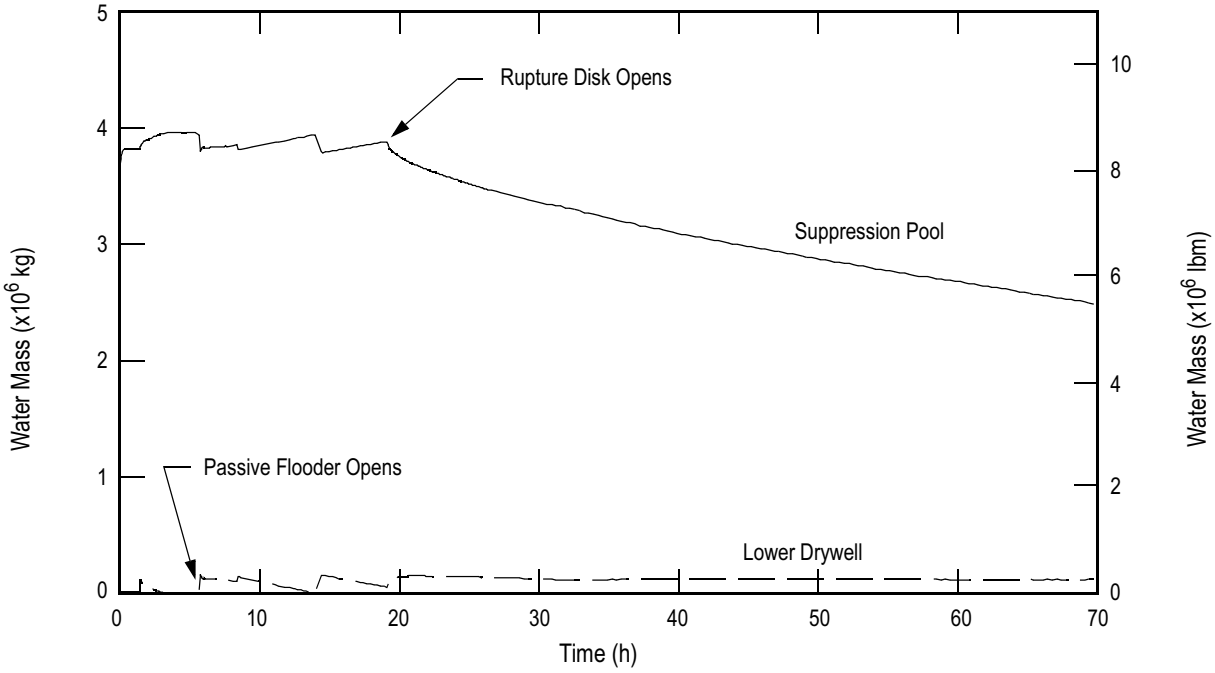

Figure 19E.2-9c LBLC-PF-R-N: Large Break LOCA with Loss of all Core Cooling, Passive Flooder Operates and Rupture Disk Opens: Water Mass

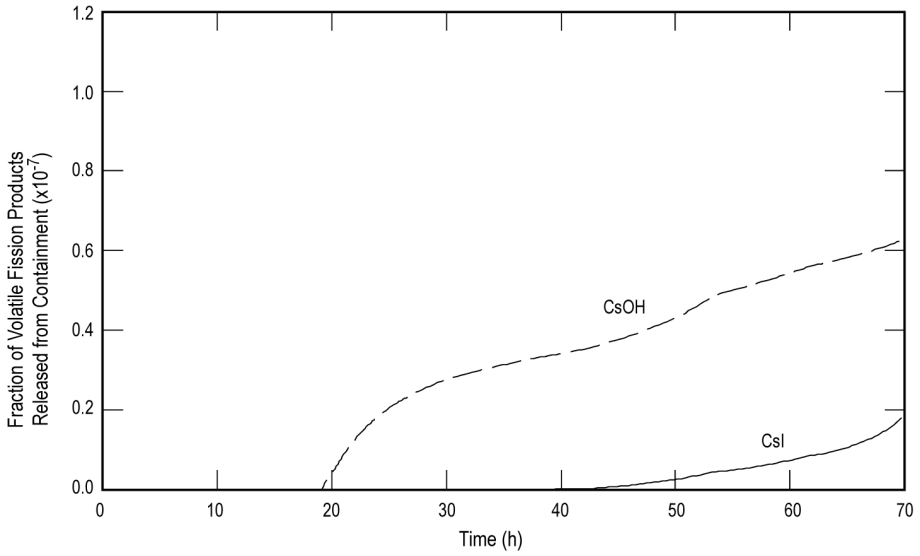

Figure 19E.2-9d LBLC-PF-R-N: Large Break LOCA with Loss of all Core Cooling, Passive Flooder Operates and Rupture Disk Opens: Volatile Fission Product Release

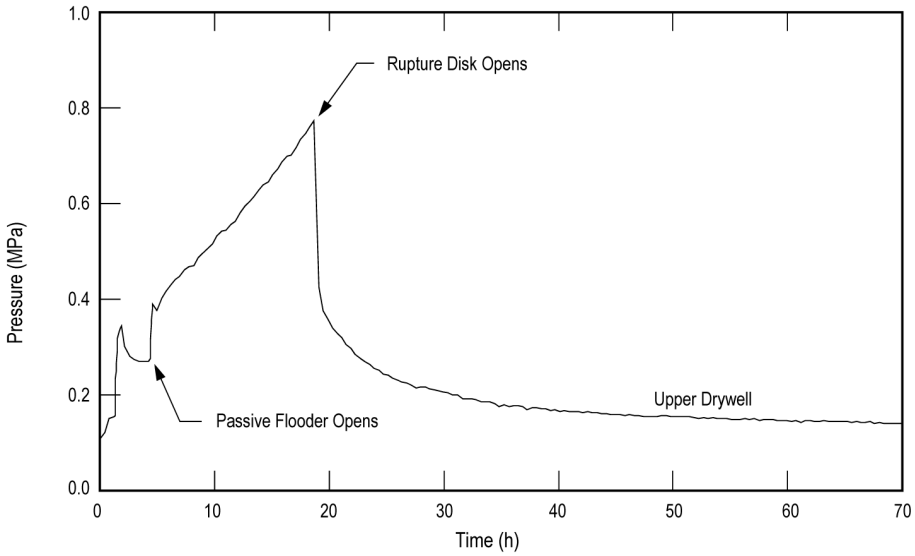

Figure 19E.2-10a NSCL-PF-R-N: Concurrent Loss of all Core Cooling and ATWS with Vessel Failure at Low Pressure, Passive Flooder and Rupture Disk: Drywell Pressure

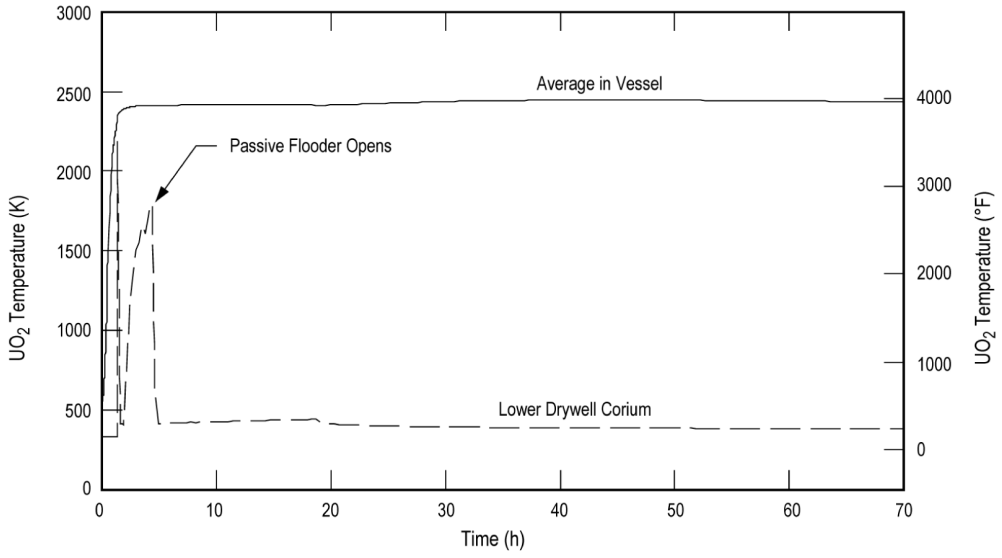

Figure 19E.2-10b NSCL-PF-R-N: Concurrent Loss of all Core Cooling and ATWS with Vessel Failure at Low Pressure, Passive Flooder and Rupture Disk: UO_2 Temperature

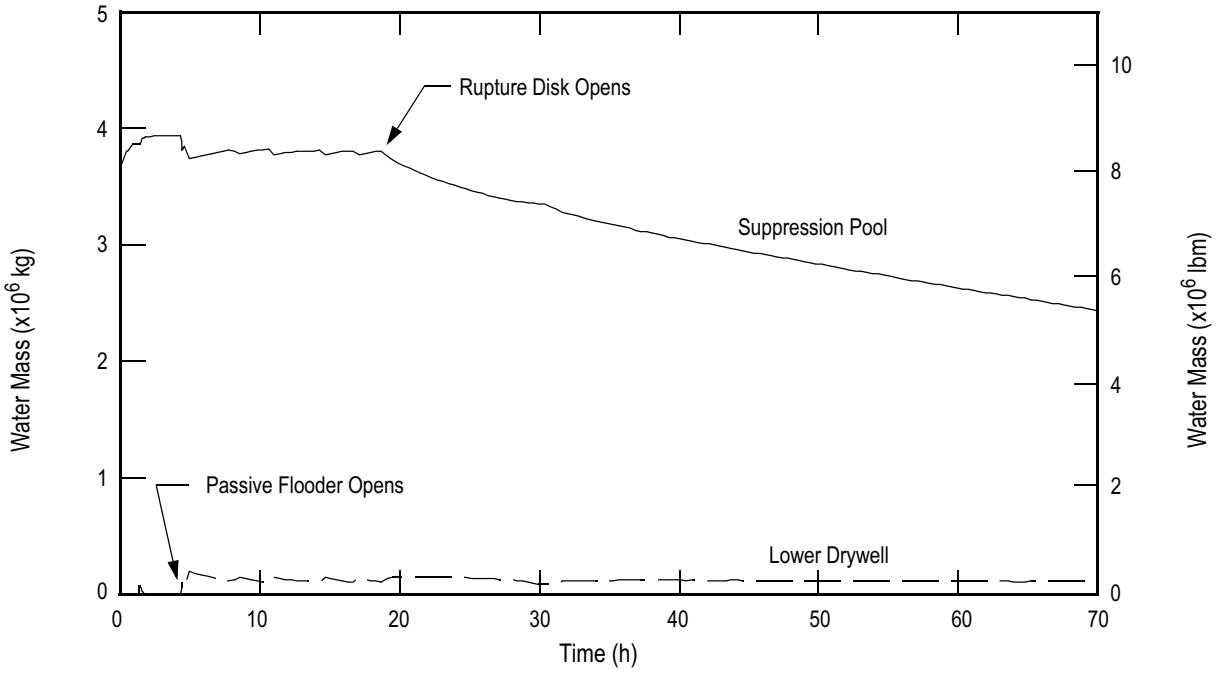

Figure 19E.2-10c NSCL-PF-R-N: Concurrent Loss of all Core Cooling and ATWS with Vessel Failure at Low Pressure, Passive Flooder and Rupture Disk: Water Mass

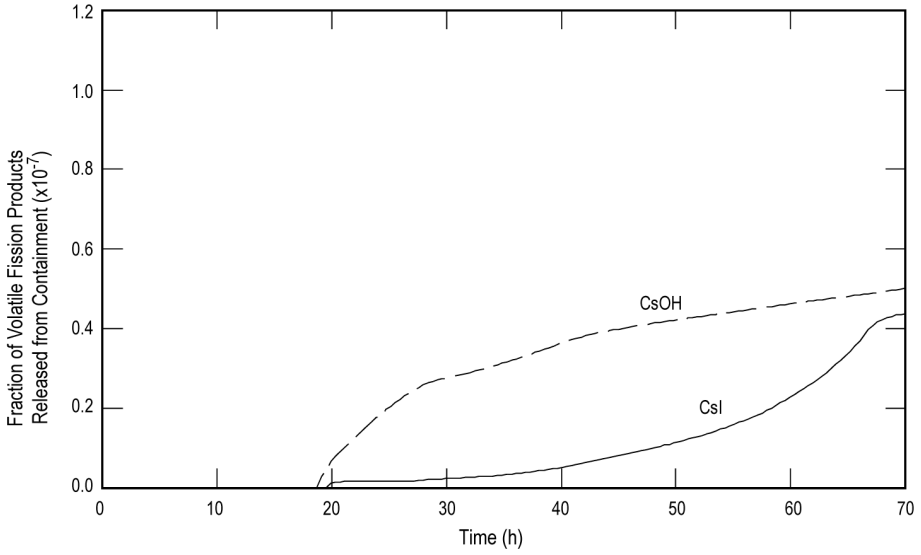

Figure 19E.2-10d NSCL-PF-R-N: Concurrent Loss of all Core Cooling and ATWS with Vessel Failure at Low Pressure, Passive Flooder and Rupture Disk: Volatile Fission Products

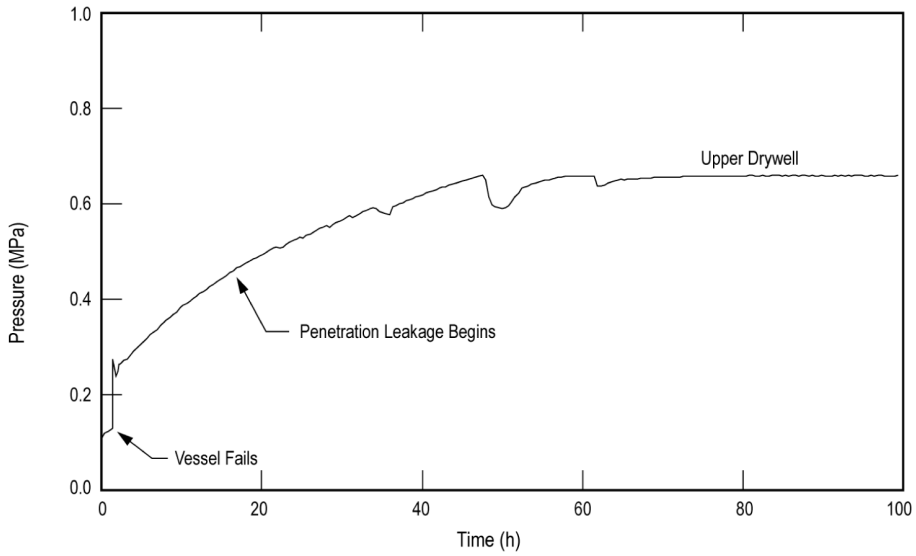

Figure 19E.2-11a NSCH-PF-P-M: Concurrent Loss of all Core Cooling and ATWS with Vessel Failure at High Pressure, Passive Flooder, Penetration Leakage: Drywell Pressure

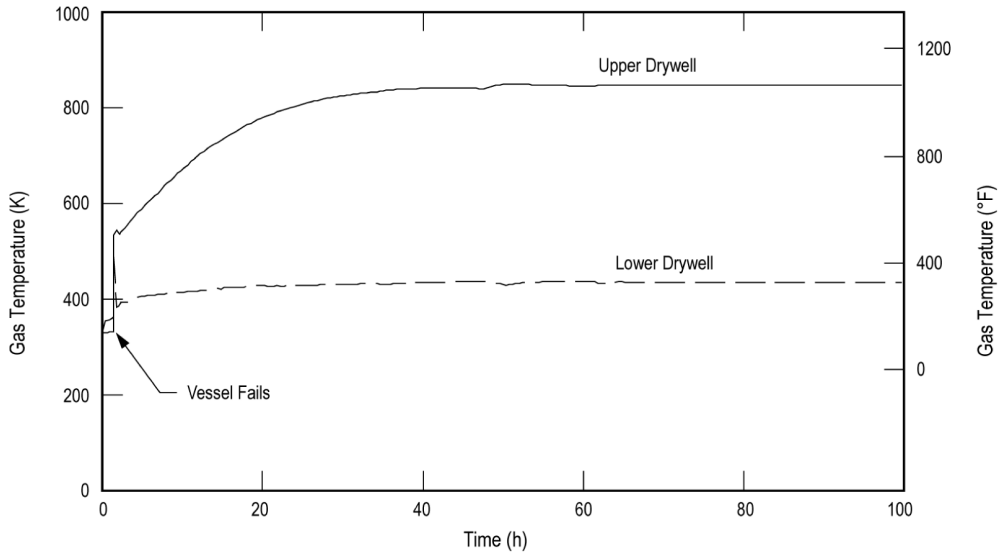

Figure 19E.2-11b NSCH-PF-M: Concurrent Loss of all Core Cooling and ATWS with Vessel Failure at High Pressure, Passive Flooder, Penetration Leakage Rupture Disk Opens: Gas Temperature

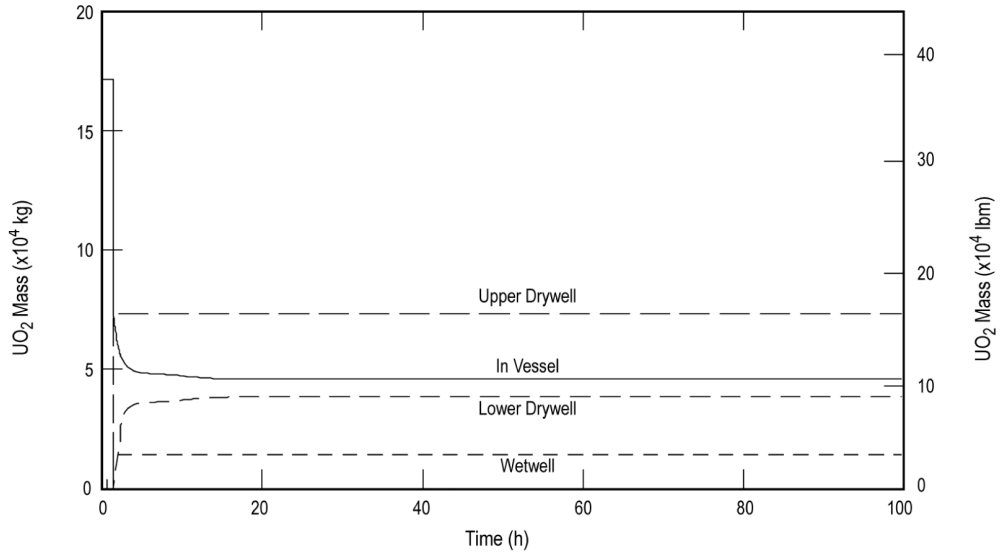

Figure 19E.2-11c NSCH-PF-P-M: Concurrent Loss of all Core Cooling and ATWS with Vessel Failure at High Pressure, Passive Flooder, Penetration Leakage: UO_2 Mass

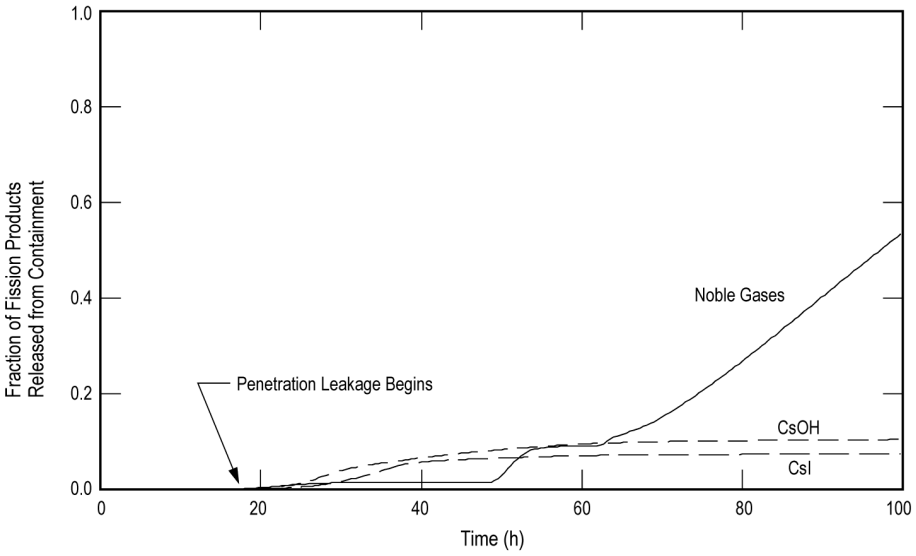

Figure 19E.2-11d NSCH-PF-P-M: Concurrent Loss of all Core Cooling and ATWS with Vessel Failure at High Pressure, Passive Flooder, Penetration Leakage: Fission Products

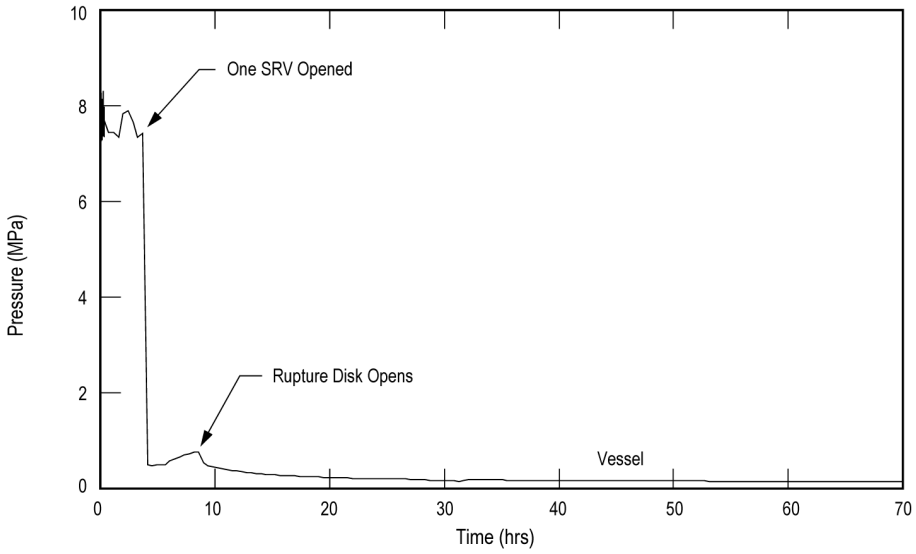

Figure 19E.2-12a NSRC-PF-R-N: Concurrent Station Blackout with ATWS, Passive Flooder Operates and Rupture Disk Opens: Vessel Pressure

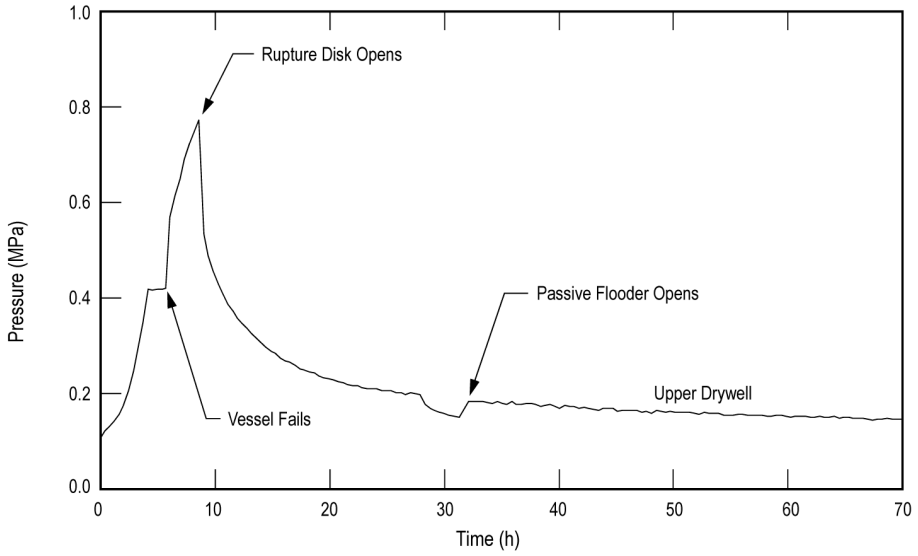

Figure 19E.2-12b NSRC-PF-R-N: Concurrent Station Blackout with ATWS, Passive Flooder Operates and Rupture Disk Opens: Drywell Pressure

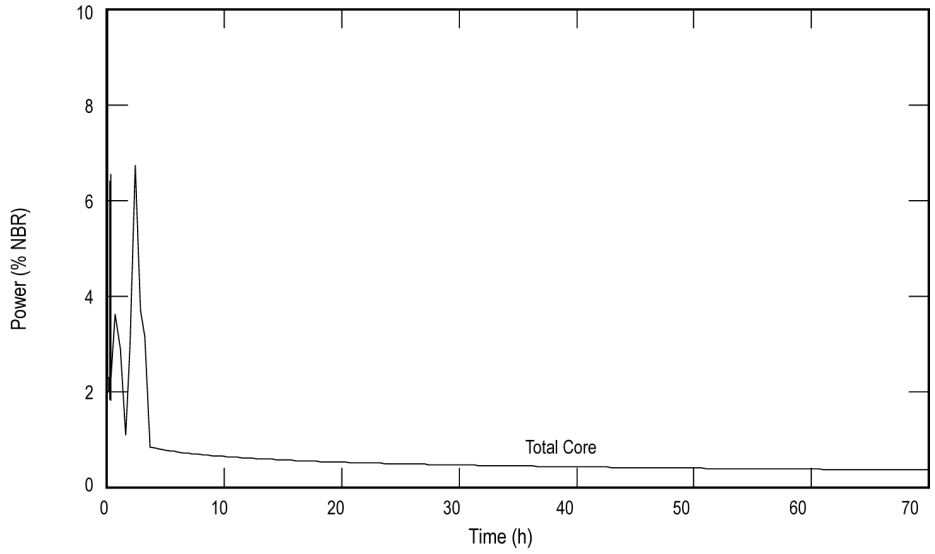

Figure 19E.2-12c NSRC-PF-R-N: Concurrent Station Blackout with ATWS, Passive Flooder Operates and Rupture Disk Opens: Power

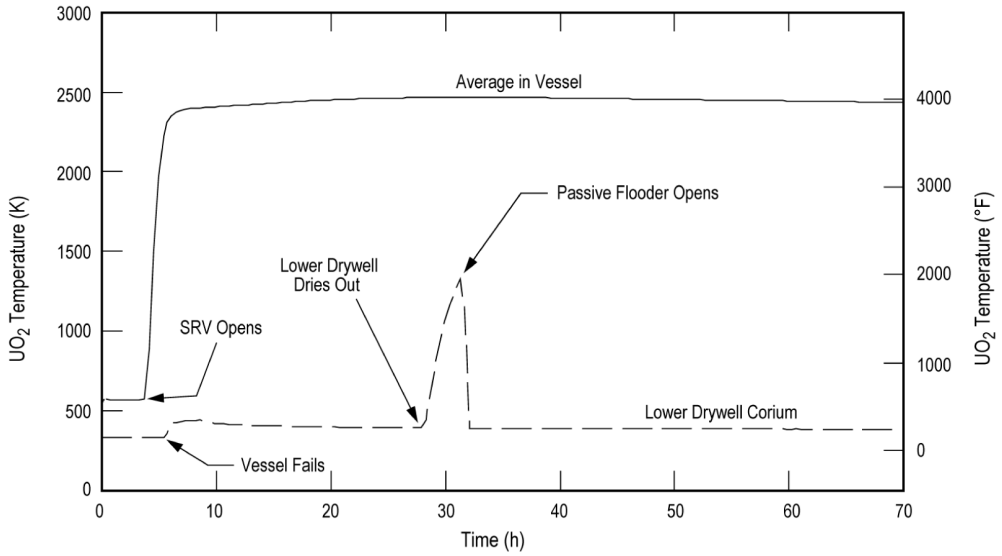

Figure 19E.2-12d NSRC-PF-R-N: Concurrent Station Blackout with ATWS, Passive Flooder Operates and Rupture Disk Opens: UO_2 Temperature

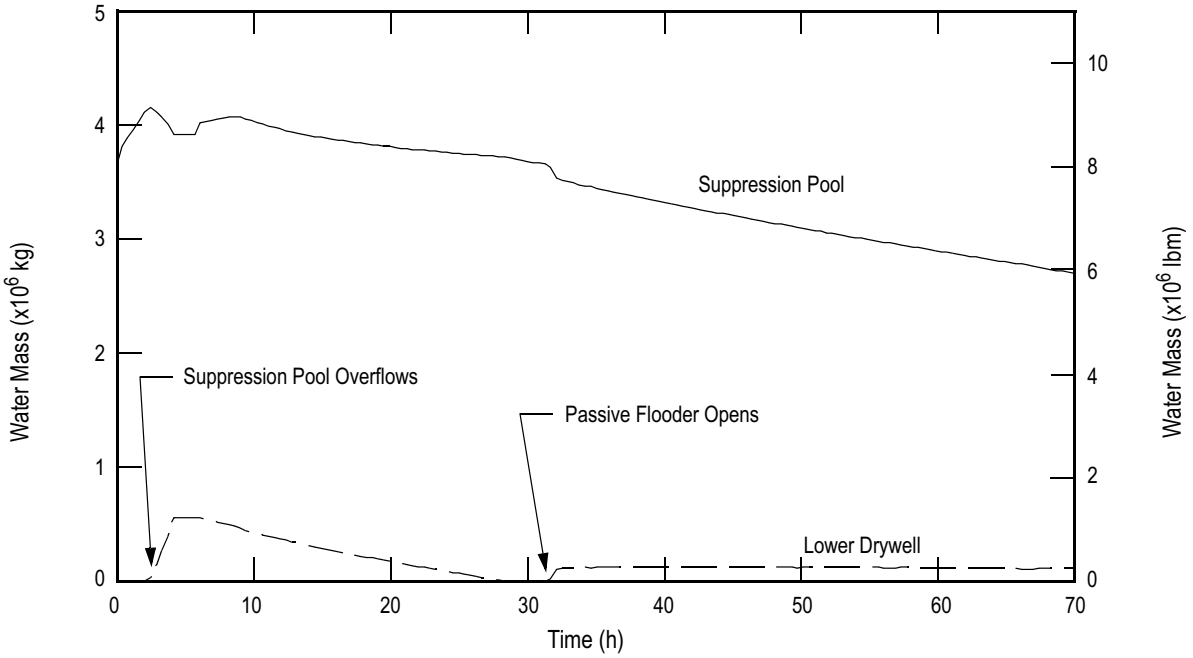

Figure 19E.2-12e NSRC-PF-R-N: Concurrent Station Blackout with ATWS, Passive Flooder Operates and Rupture Disk Opens: Water Mass

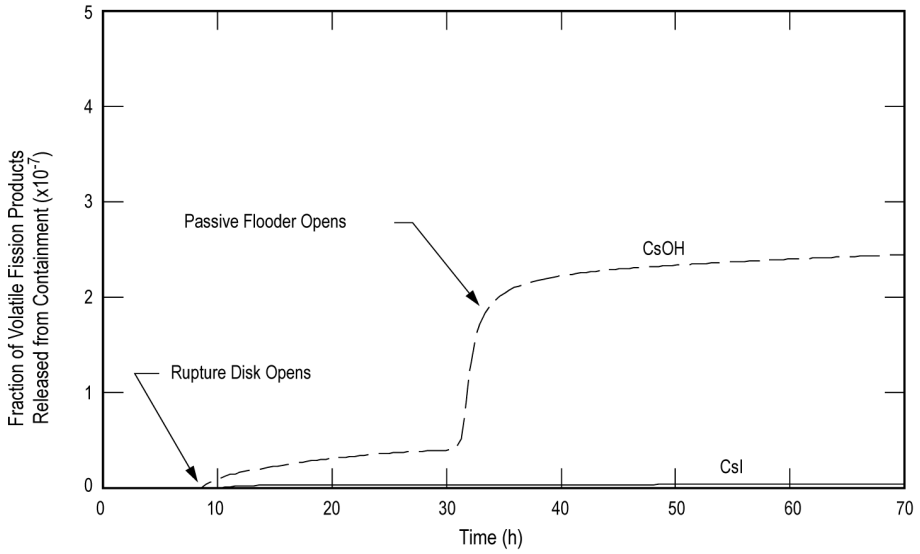

Figure 19E.2-12f NSRC-PF-R-N: Concurrent Station Blackout with ATWS, Passive Flooder Operates and Rupture Disk Opens: Volatile Fission Product Release

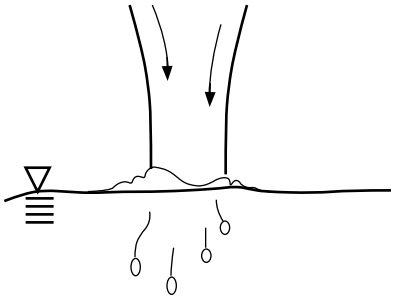

• MOLTEN DEBRIS WITH HIGH THERMAL ENERGY ENTERS WATER

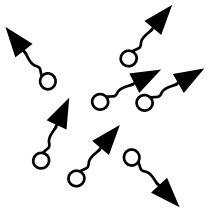

• RAPID FORMATION OF SMALL PARTICLES (FRACTURING, TRIGGERING)

• RAPID FORMATION OF A SUBMERGED HIGH PRESSURE STEAM REGION AND EXPANSION

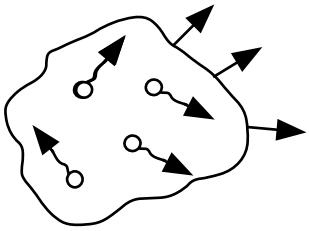

• RAPID HEAT TRANSFER FROM DEBRIS TO WATER

• WATER ACCELERATION

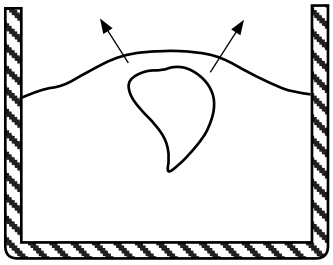

• SUBSTANTIAL PRESSURE AND IMPACT FORCES

Figure 19E.2-13 Steam Explosion Process

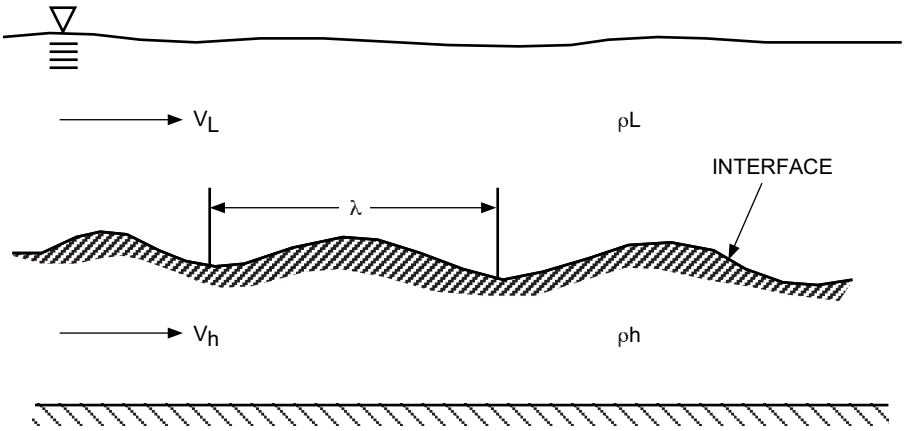

Figure 19E.2-14a Interfacial Instability

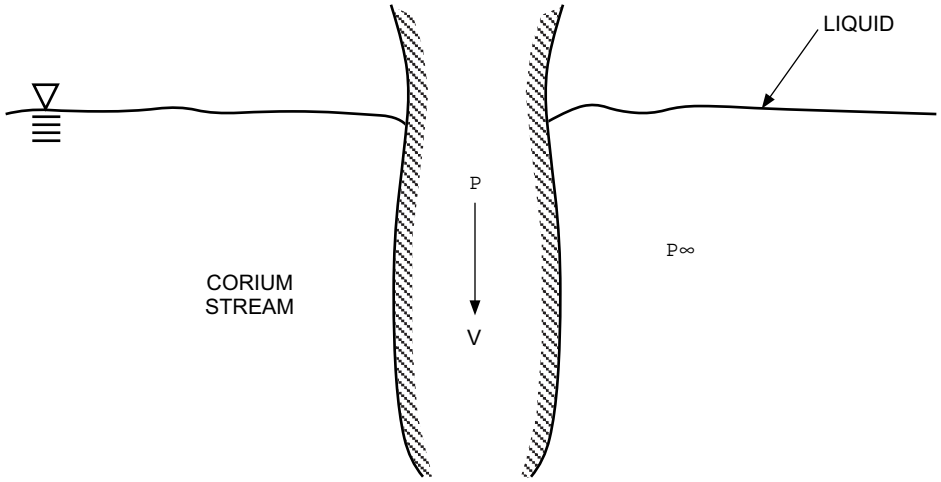

Figure 19E.2-14b Corium Stream in Liquid

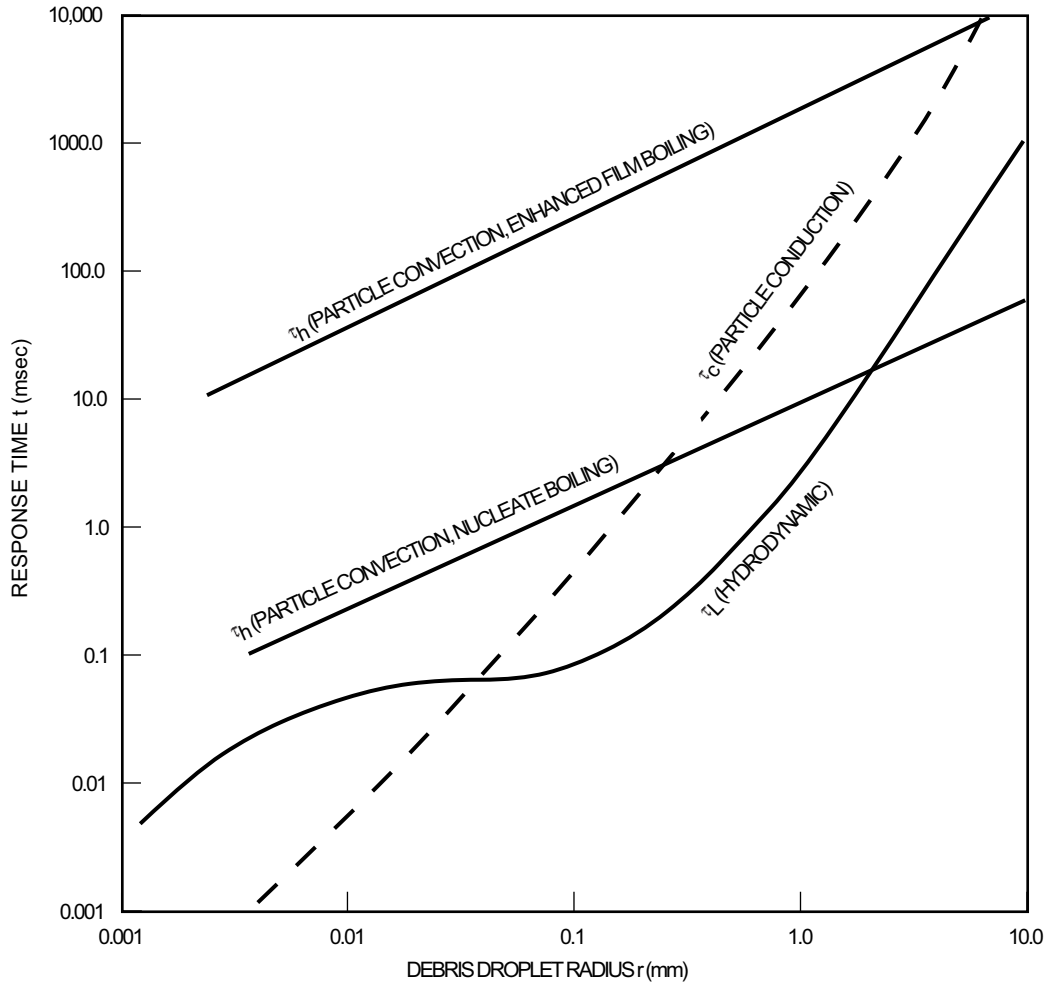

Figure 19E.2-15 Important Response Times

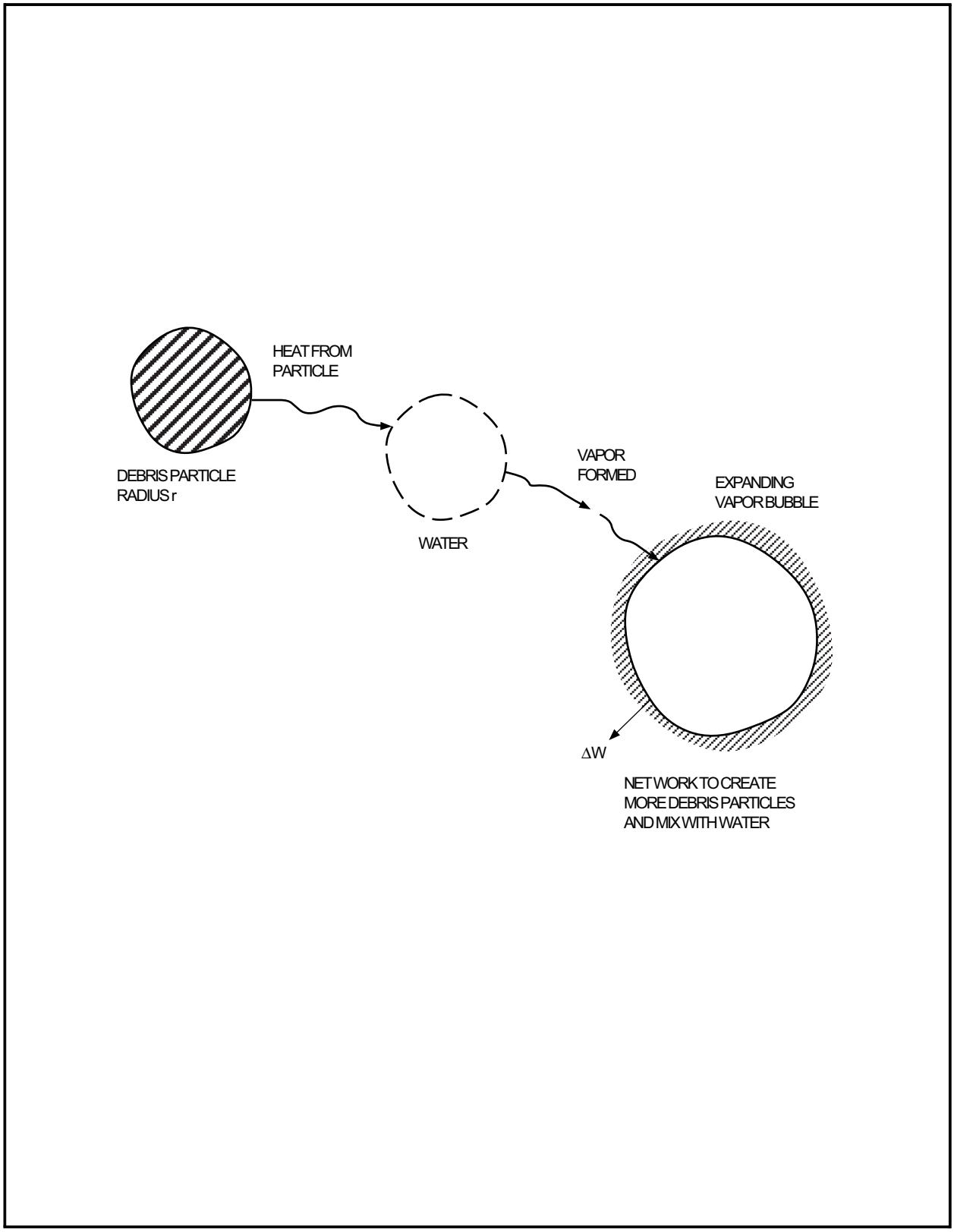

Figure 19E.2-16 Self-Triggering Process

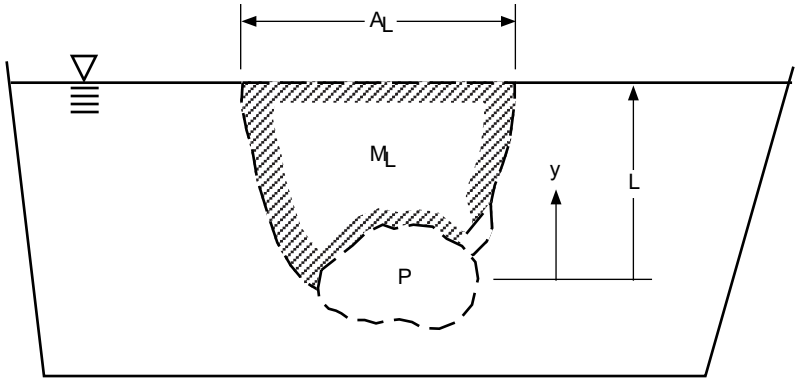

Figure 19E.2-17 Conditions for Steam Explosion

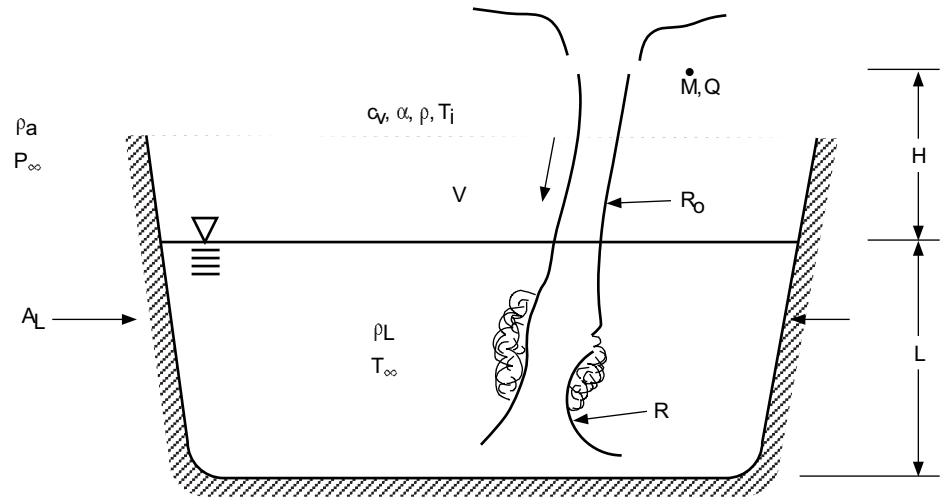

Figure 19E.2-18 Application to ABWR

Figure 19E.2-19a Suppression Pool Bypass Paths and Configurations

Not Part of DCD (Refer to Reference 19E.2-40)

Figure 19E.2-19b Suppression Pool Bypass Paths and Configurations

Not Part of DCD (Refer to Reference 19E.2-40)

Figure 19E.2-19c Suppression Pool Bypass Paths and Configurations

Not Part of DCD (Refer to Reference 19E.2-40)

Figure 19E.2-19d Suppression Pool Bypass Paths and Configurations

Not Part of DCD (Refer to Reference 19E.2-40)

Figure 19E.2-19e Suppression Pool Bypass Paths and Configurations

Not Part of DCD (Refer to Reference 19E.2-40)

Figure 19E.2-19f Suppression Pool Bypass Paths and Configurations

Not Part of DCD (Refer to Reference 19E.2-40)

Figure 19E.2-19g Suppression Pool Bypass Paths and Configurations

Not Part of DCD (Refer to Reference 19E.2-40)

Figure 19E.2-19h Suppression Pool Bypass Paths and Configurations

Not Part of DCD (Refer to Reference 19E.2-40)

Figure 19E.2-19i Suppression Pool Bypass Paths and Configurations

Not Part of DCD (Refer to Reference 19E.2-40)

Figure 19E.2-19j Suppression Pool Bypass Paths and Configurations

Not Part of DCD (Refer to Reference 19E.2-40)

Figure 19E.2-19k Suppression Pool Bypass Paths and Configurations

Not Part of DCD (Refer to Reference 19E.2-40)

Figure 19E.2-20a Small LOCAs Outside Containment

Not Part of DCD (Refer to Reference 19E.2-40)

Figure 19E.2-20b Intermediate LOCAs Outside Containment

Not Part of DCD (Refer to Reference 19E.2-40)

Figure 19E.2-20c Large LOCAs Outside Containment

Not Part of DCD (Refer to Reference 19E.2-40)

Figure 19E.2-21 Not Used

Figure 19E.2-22 Not Used

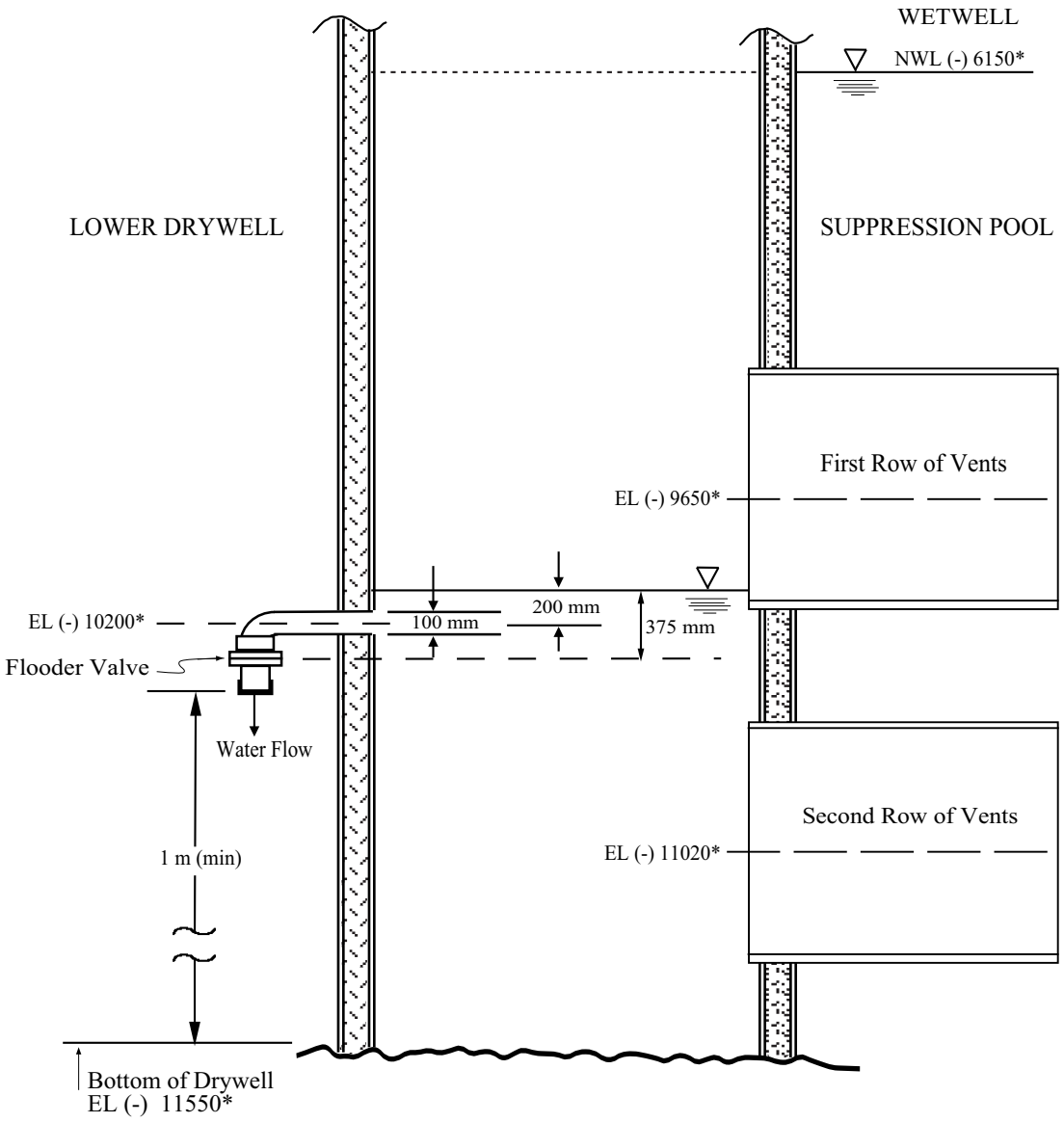

* Elevations based on RPV bottom at EL 0. All dimensions in millimeters.

Figure 19E.2-23 Lower Drywell Flooder System

Figure 19E.2-24 Not Used

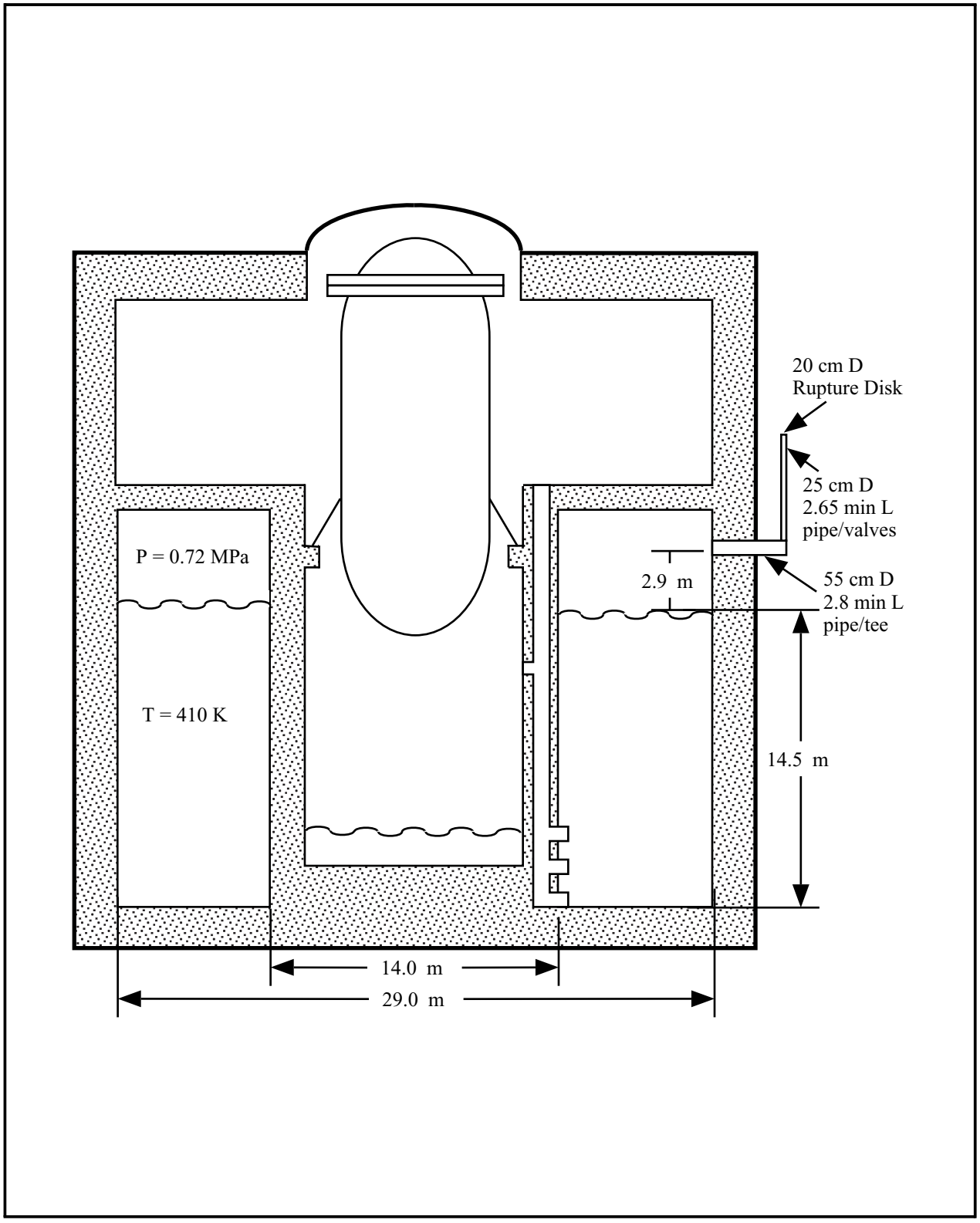

Figure 19E.2-25 Limiting Configuration for COPS Blowdown Study

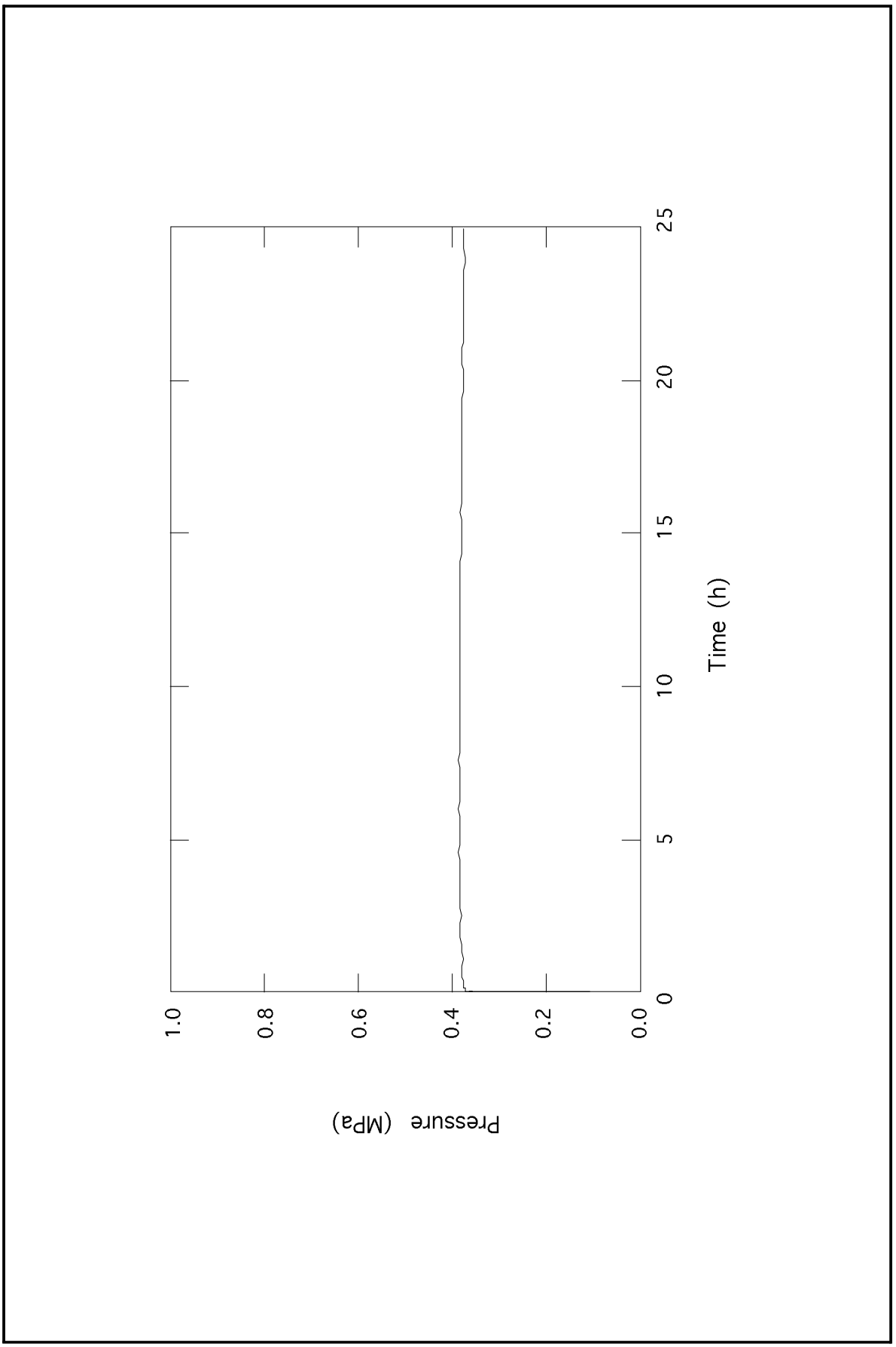

Figure 19E.2-26a Drywell Pressure for 100% Metal-Water Reaction Scenario

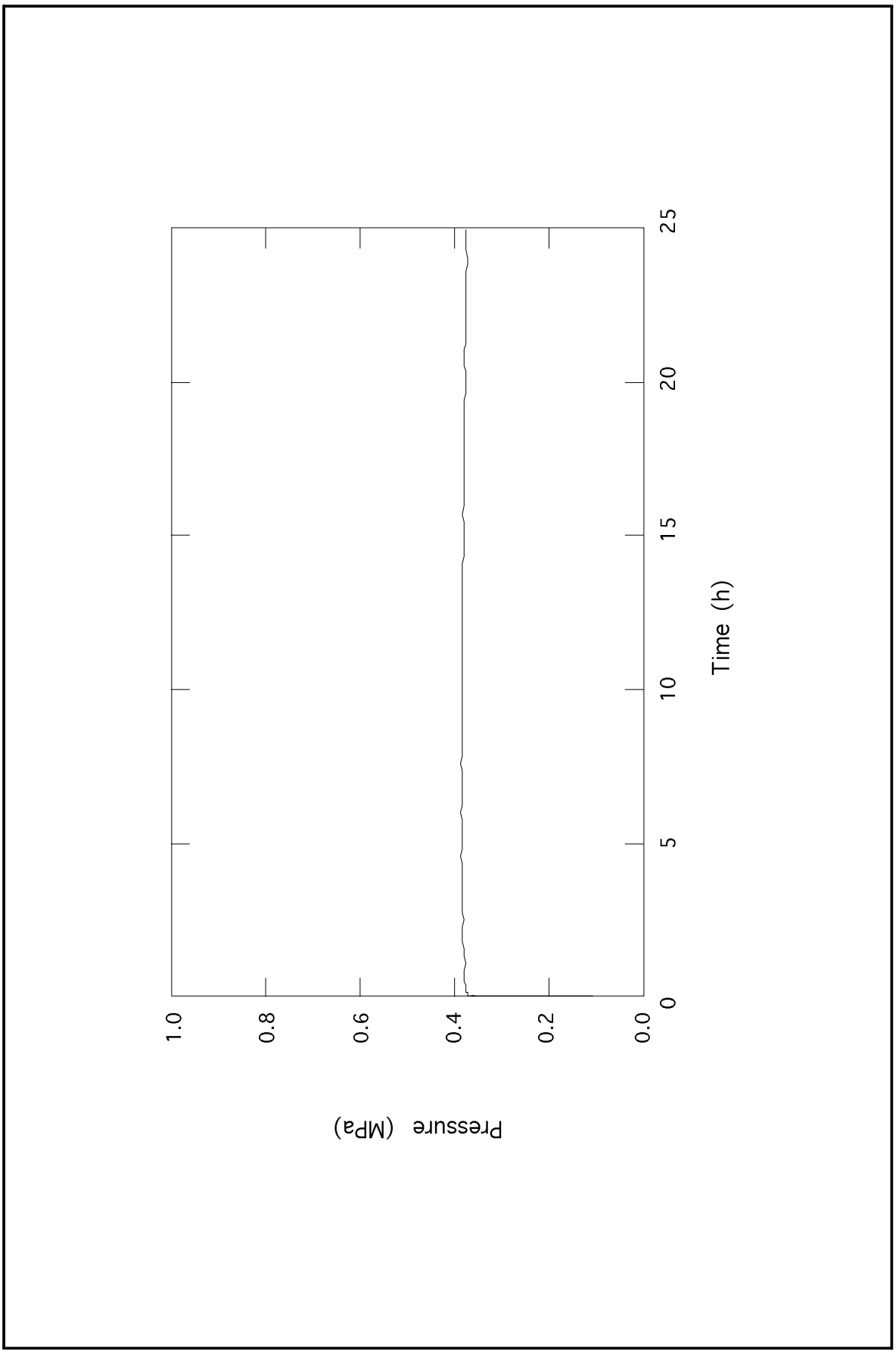

Figure 19E.2-26b Wetwell Pressure for 100% Metal-Water Reaction Scenario

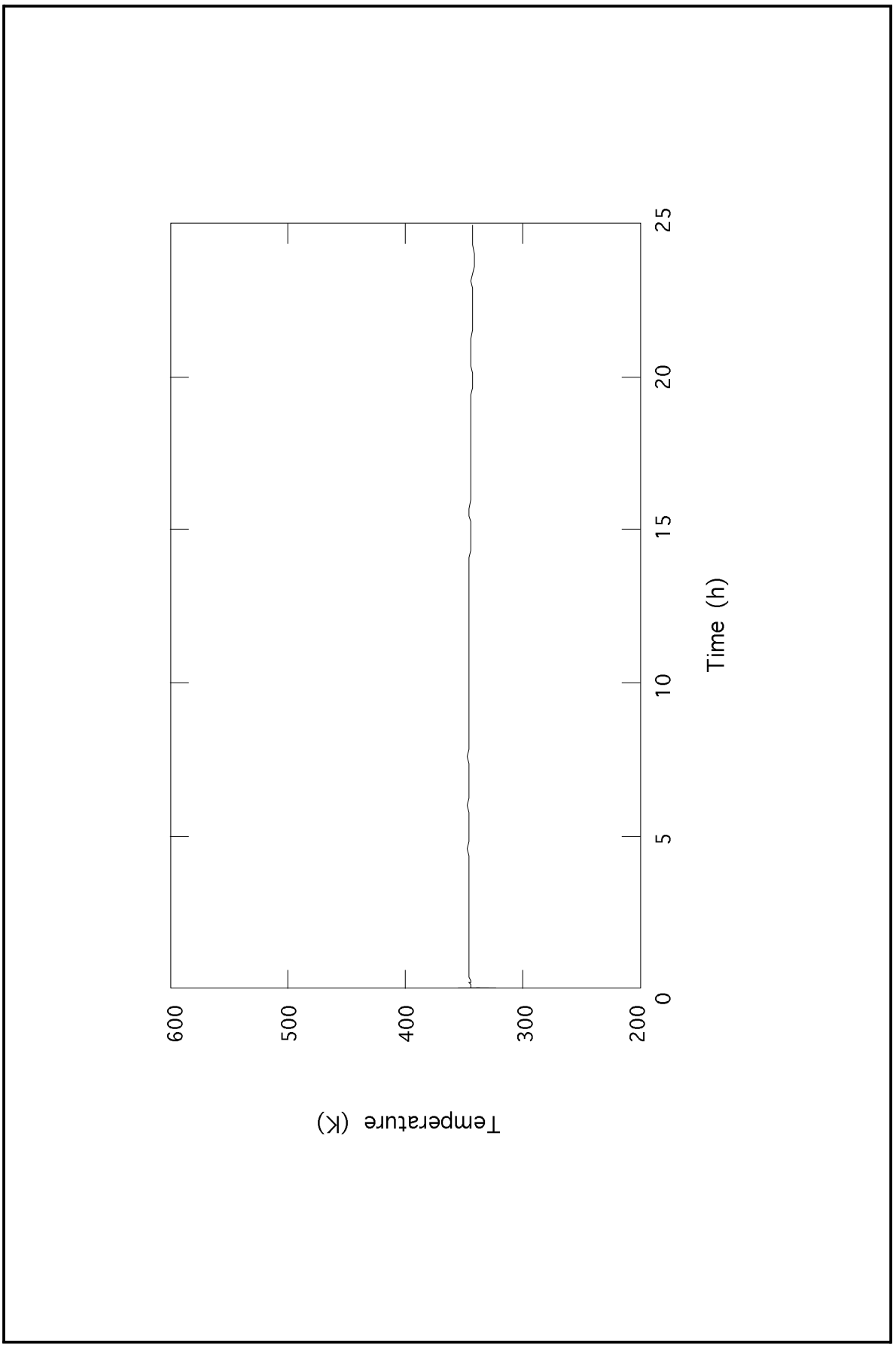

Figure 19E.2-26c Drywell Temperature for 100% Metal-Water Reaction Scenario

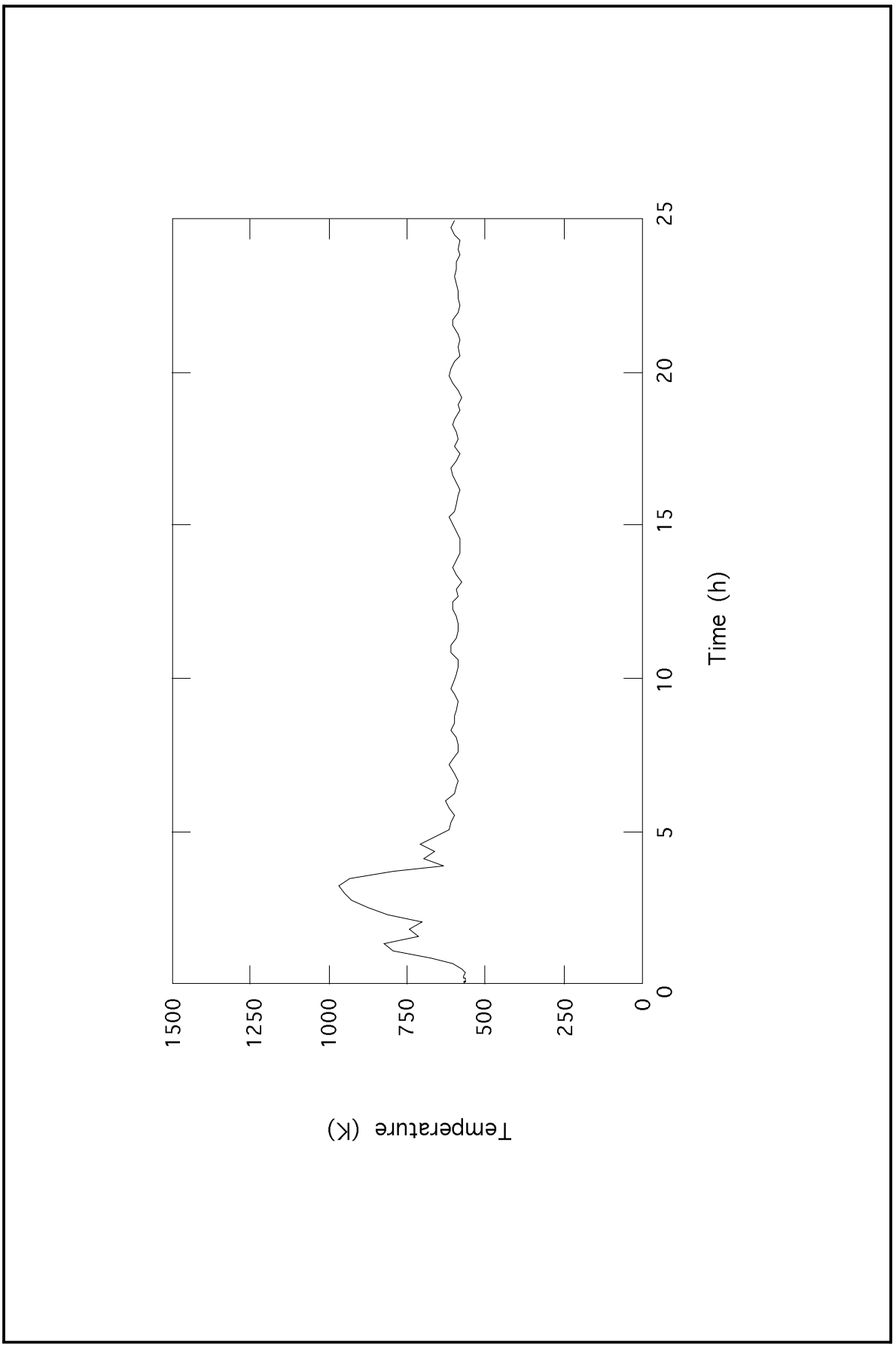

Figure 19E.2-26d Vessel Temperature for 100% Metal-Water Reaction Scenario

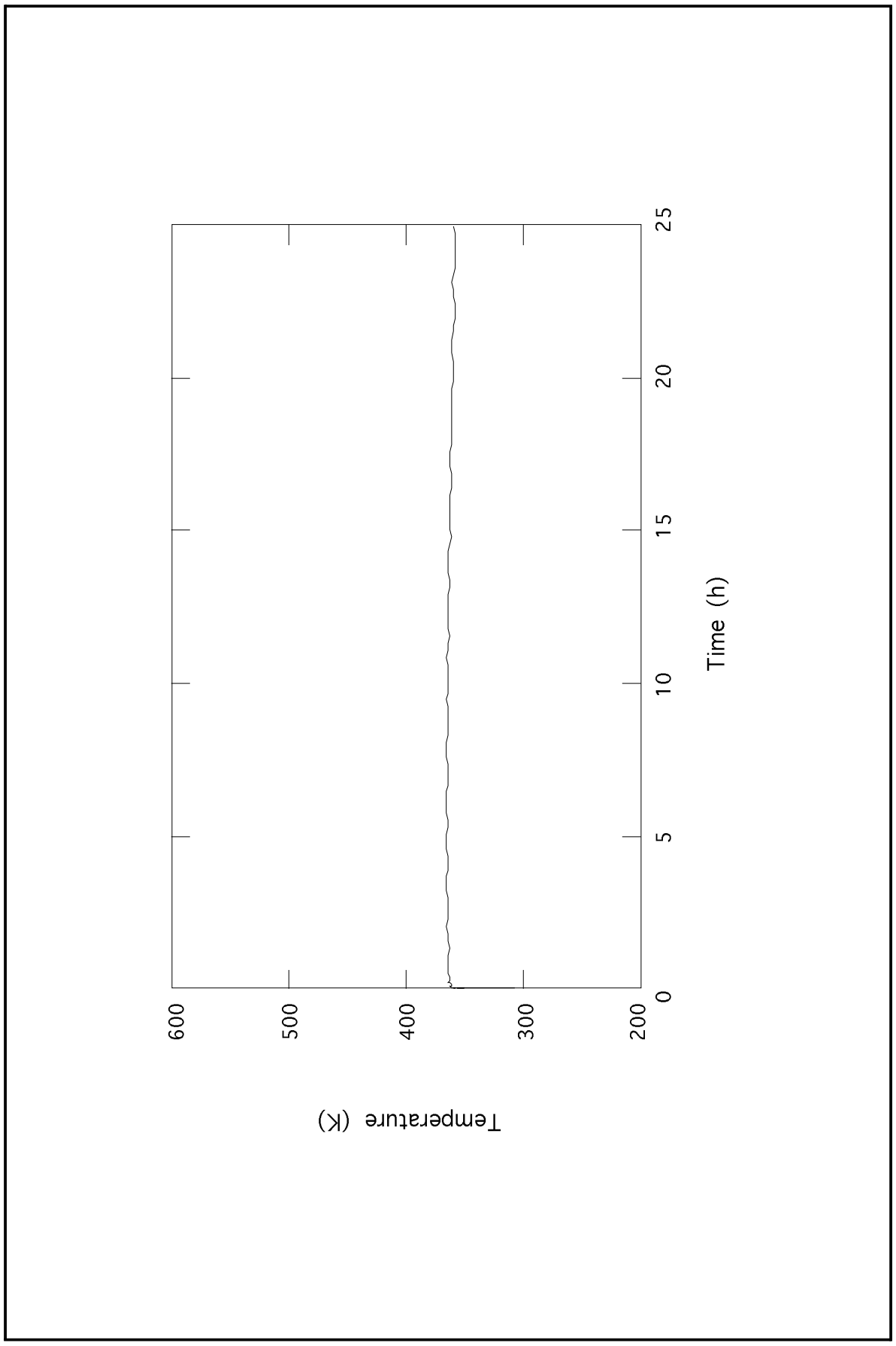

Figure 19E.2-26e Suppression Pool Water Temperature for 100% Metal-Water Scenario

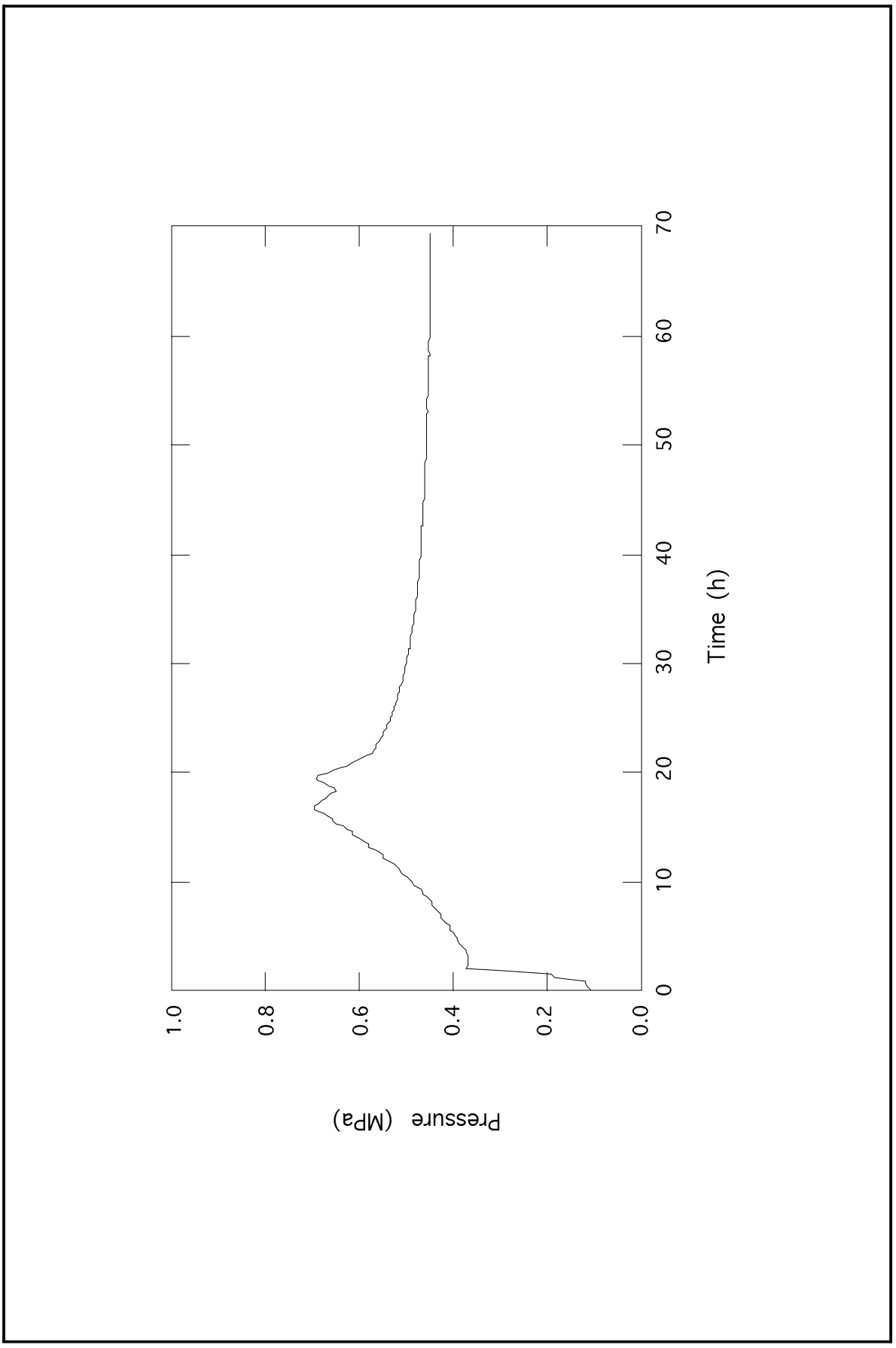

Figure 19E.2-27a Drywell Pressure for In-Vessel Core Melt Scenario

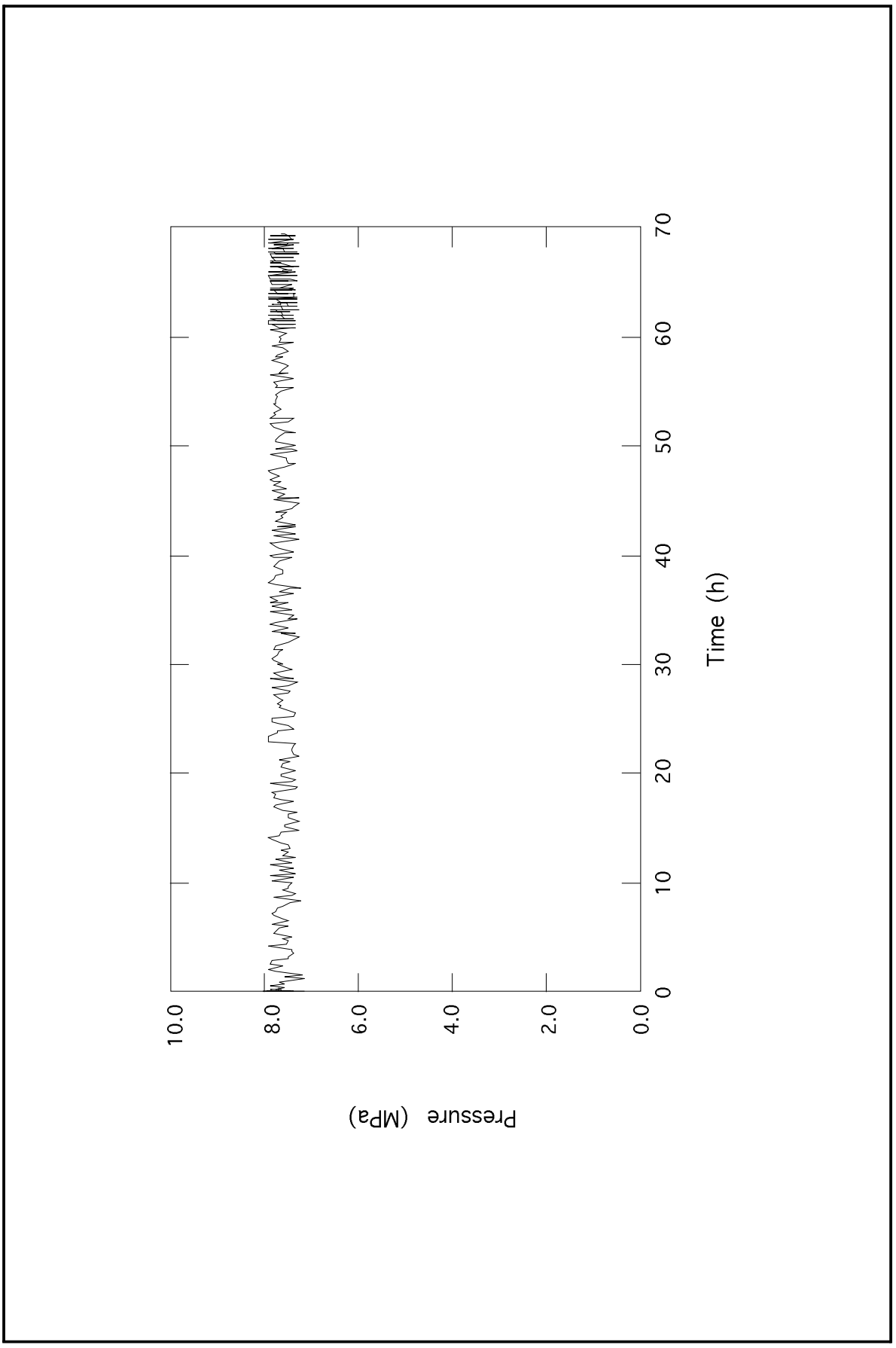

Figure 19E.2-27b Vessel Pressure for In-Vessel Core Melt Scenario

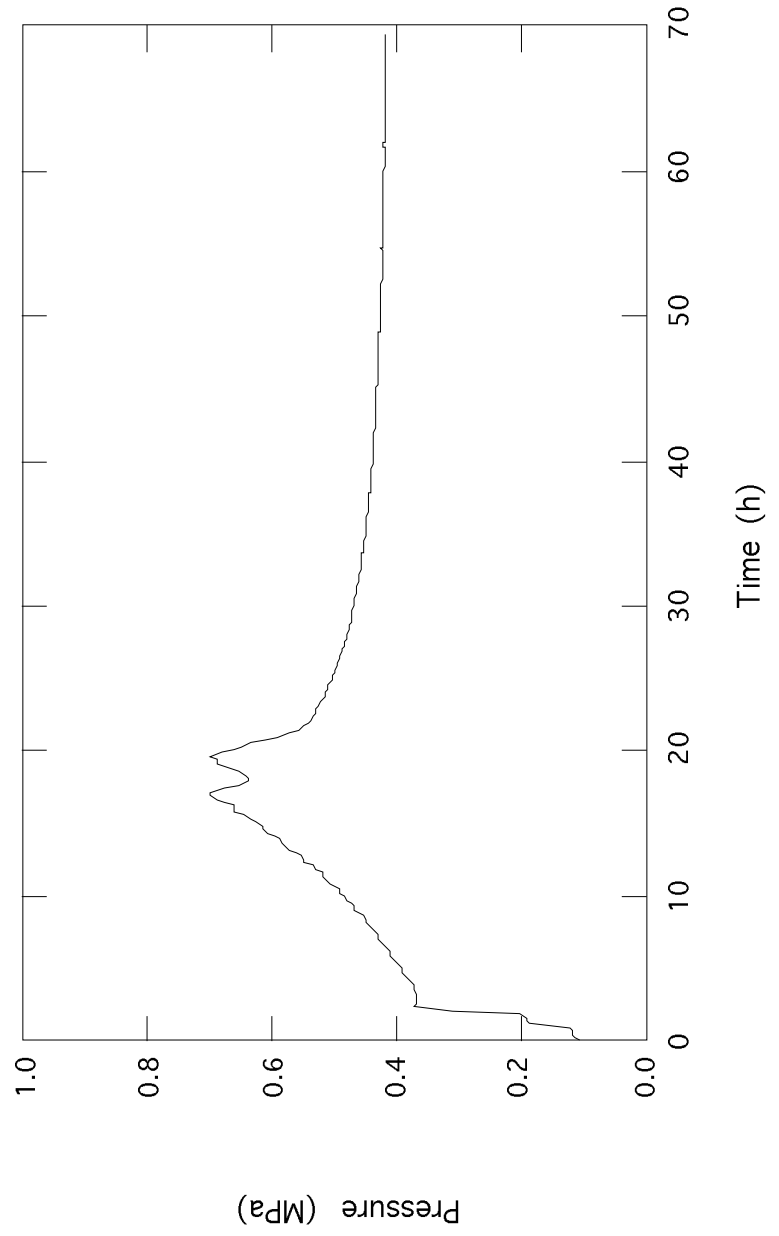

Figure 19E.2-27c Wetwell Pressure for In-Vessel Core Melt Scenario

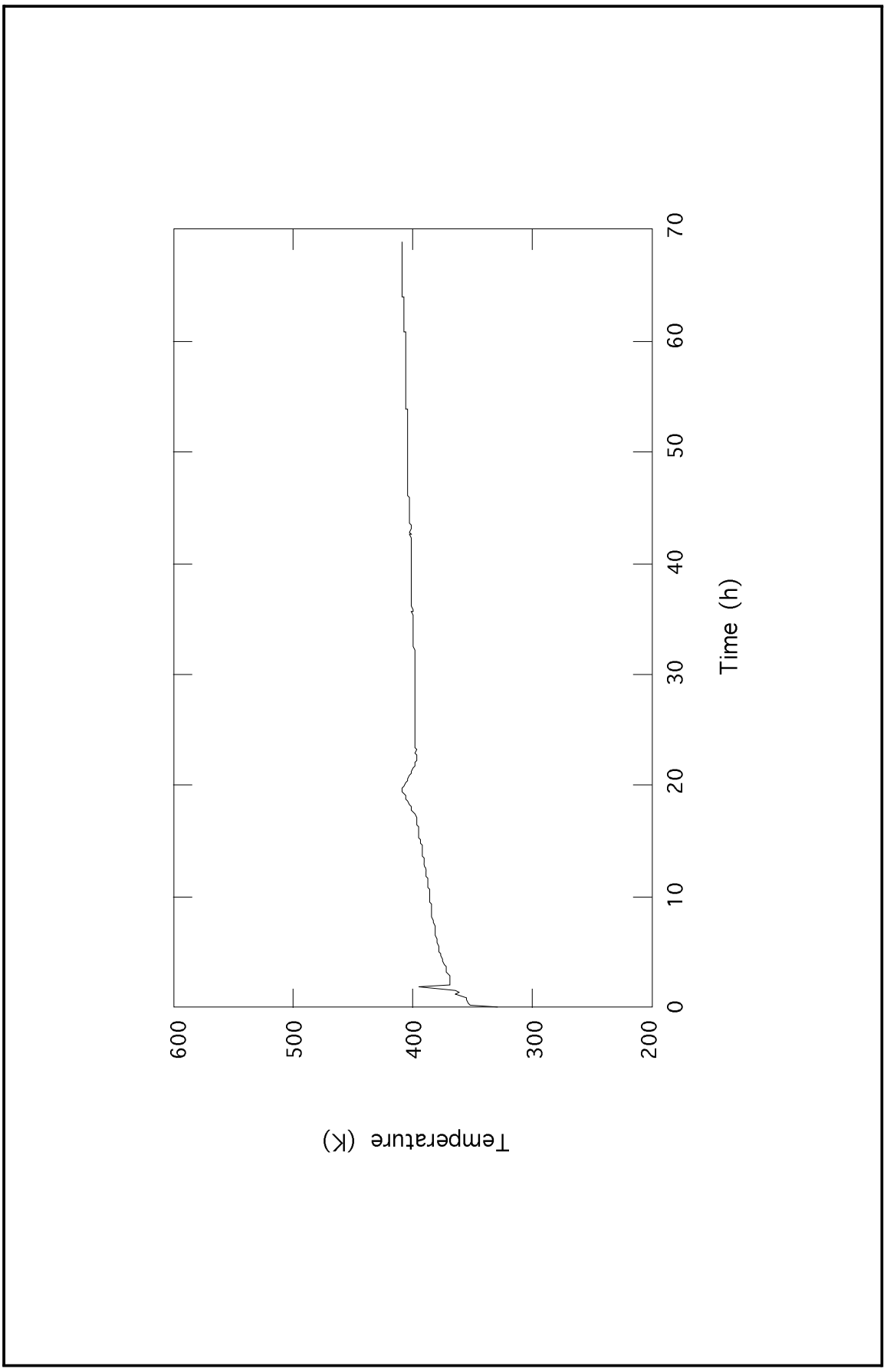

Figure 19E.2-27d Drywell Temperature for In-Vessel Core Melt Scenario

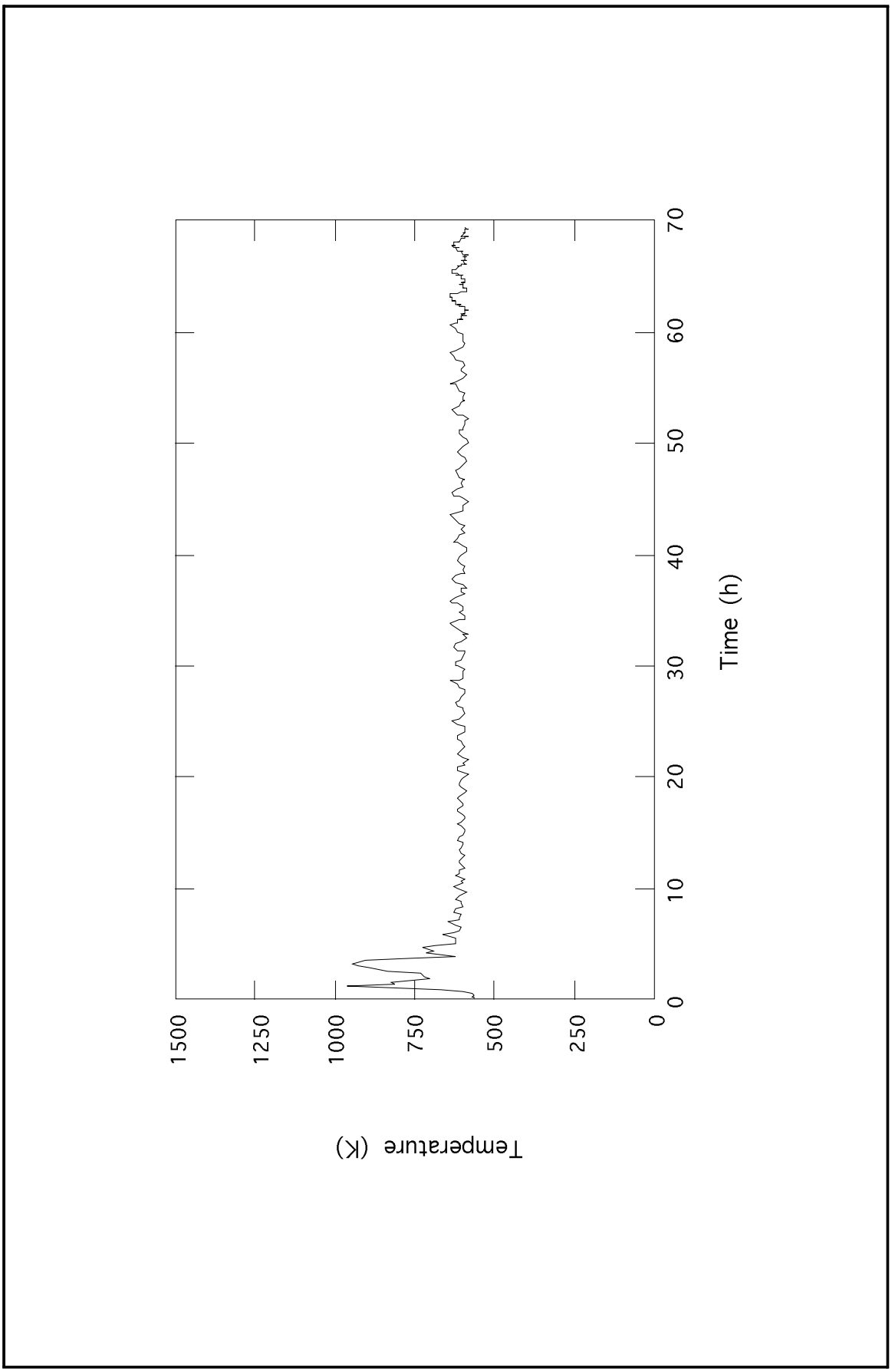

Figure 19E.2-27e Vessel Temperature for In-Vessel Core Melt Scenario

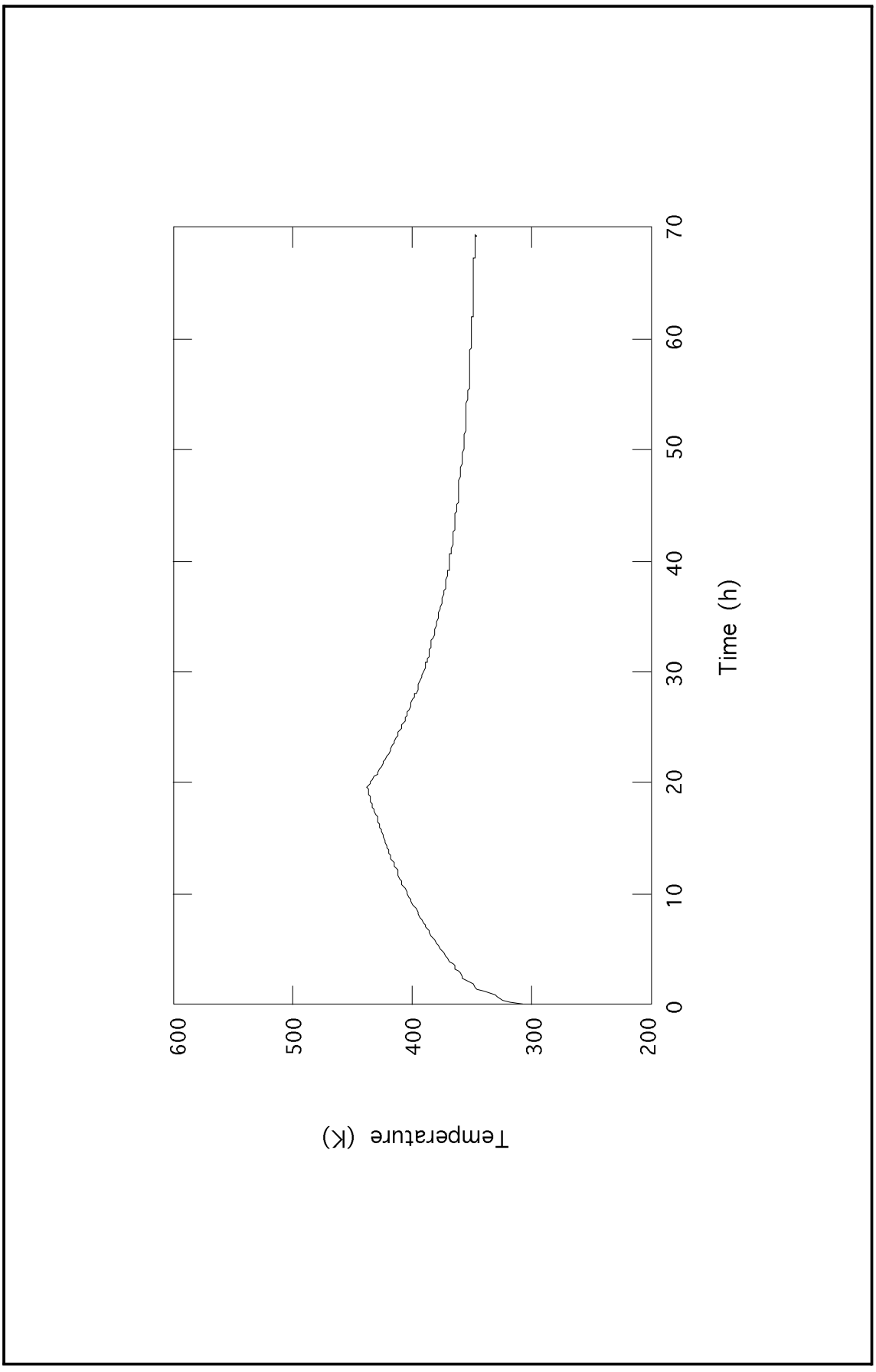

Figure 19E.2-27f Suppression Pool Water Temperature for In-Vessel Core Melt

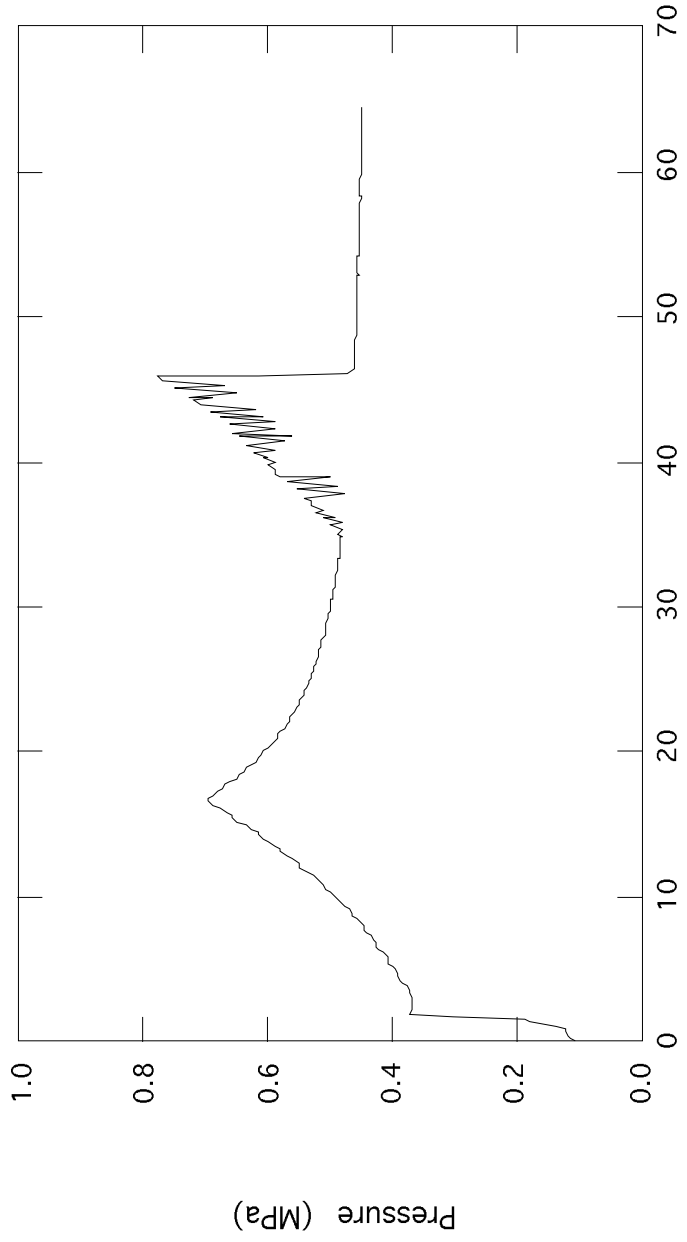

Figure 19E.2-28a Drywell Pressure for High Pressure Ex-Vessel Core Melt Scenario

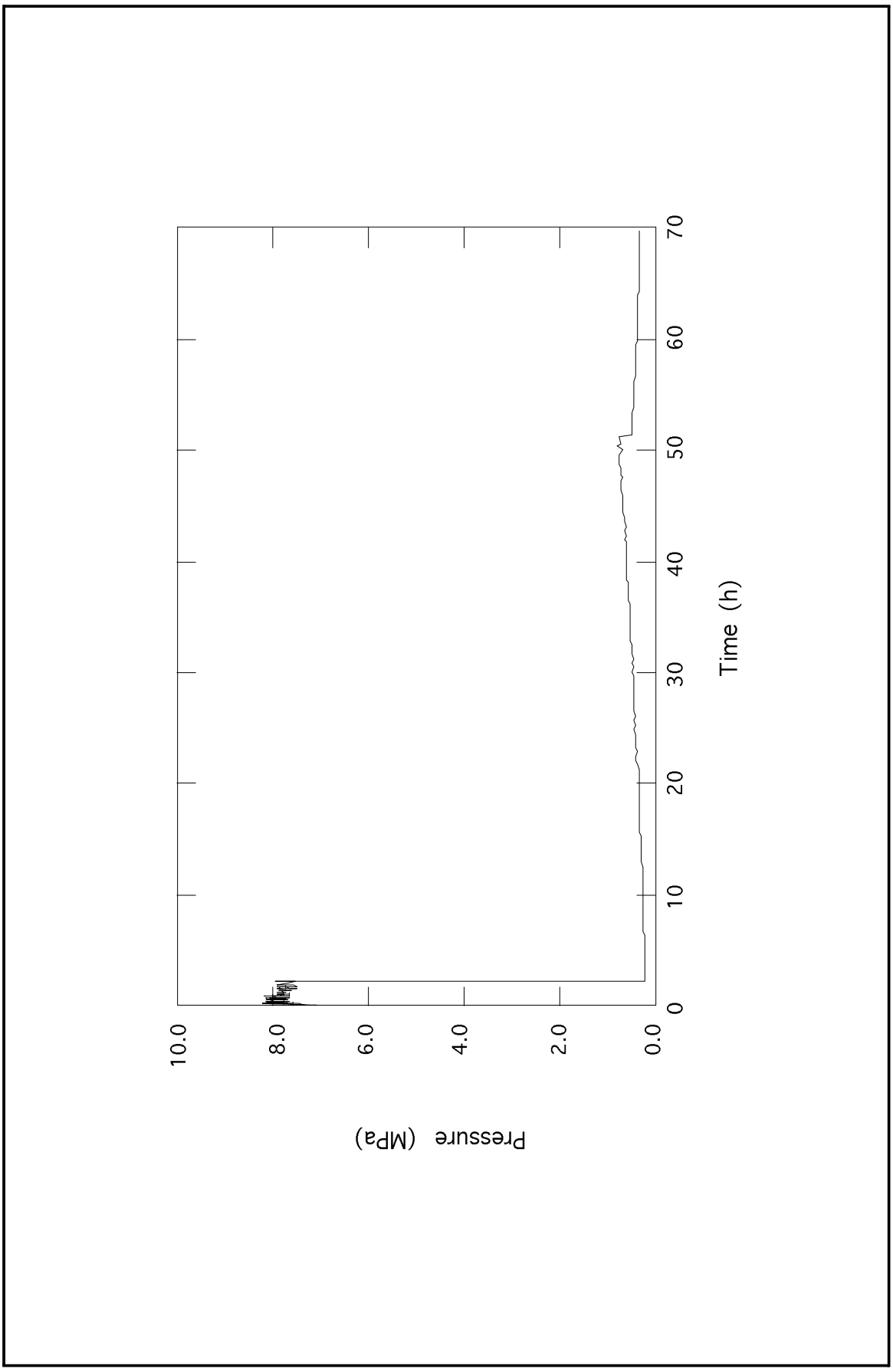

Figure 19E.2-28b Vessel Pressure for Ex-Vessel High Pressure Core Melt Scenario

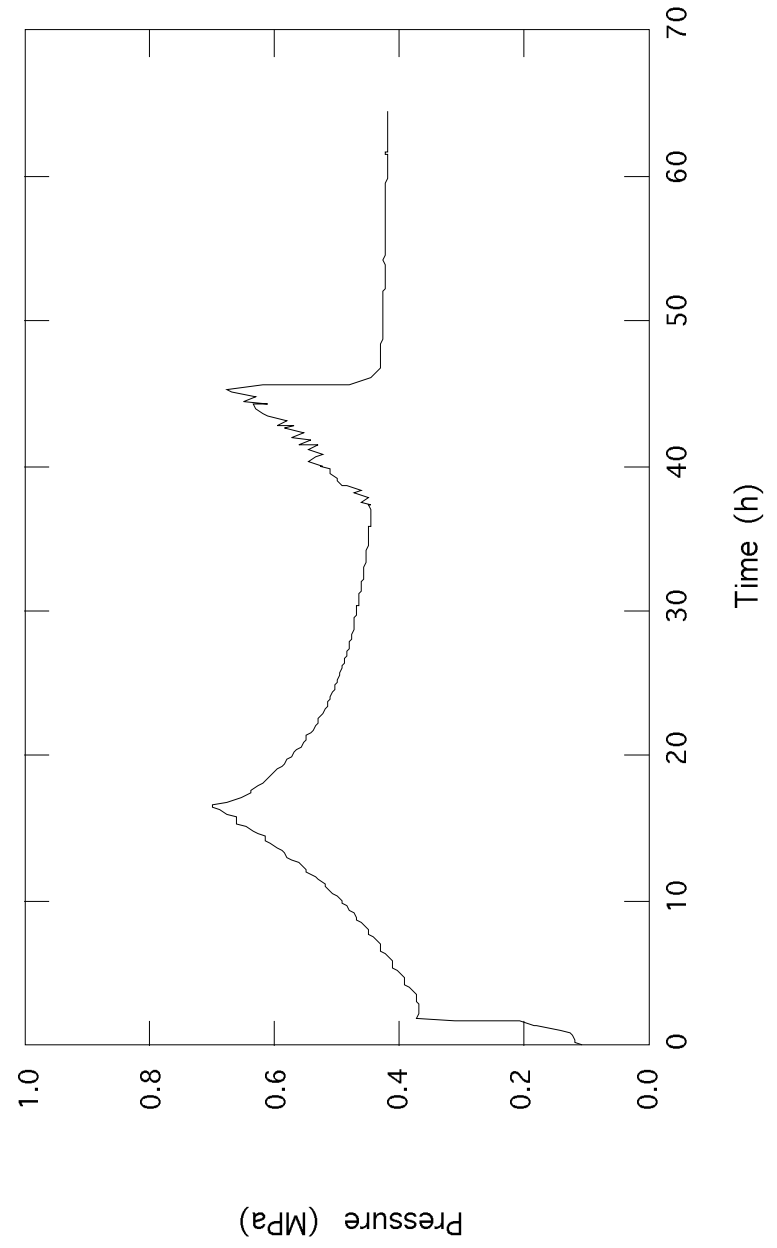

Figure 19E.2-28c Wetwell Pressure for Ex-Vessel High Pressure Core Melt Scenario

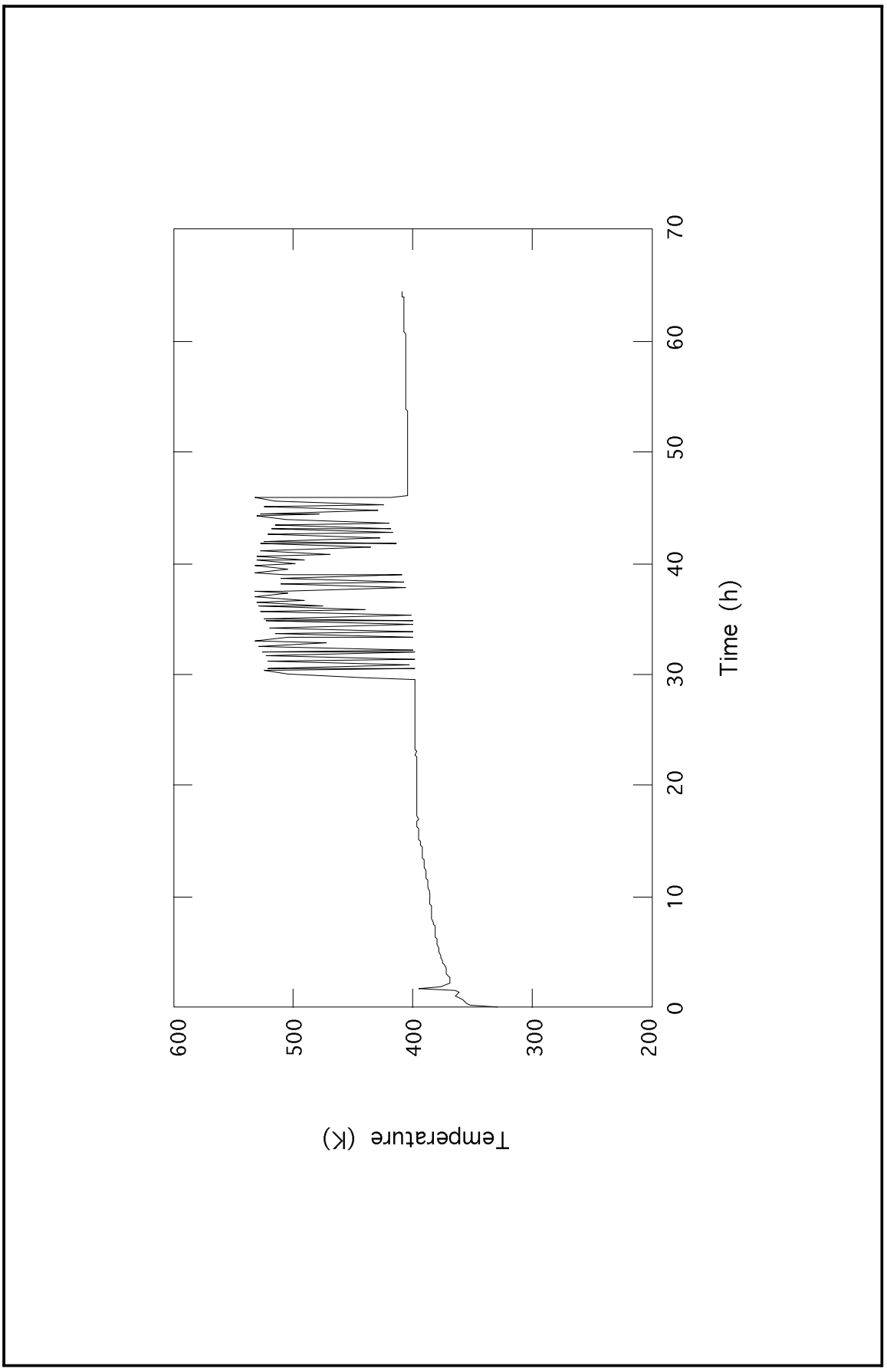

Figure 19E.2-28d Drywell Temperature for Ex-Vessel High Pressure Core Melt Scenario

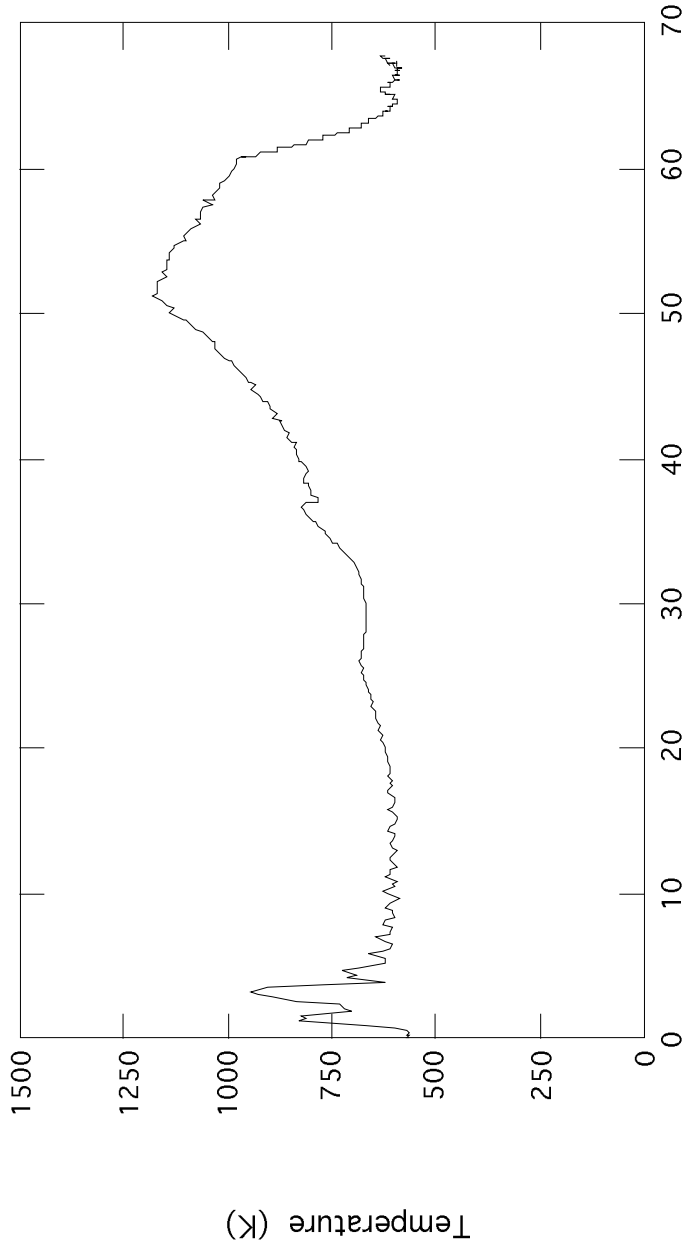

Figure 19E.2-28e Vessel Temperature for Ex-Vessel High Pressure Core Melt

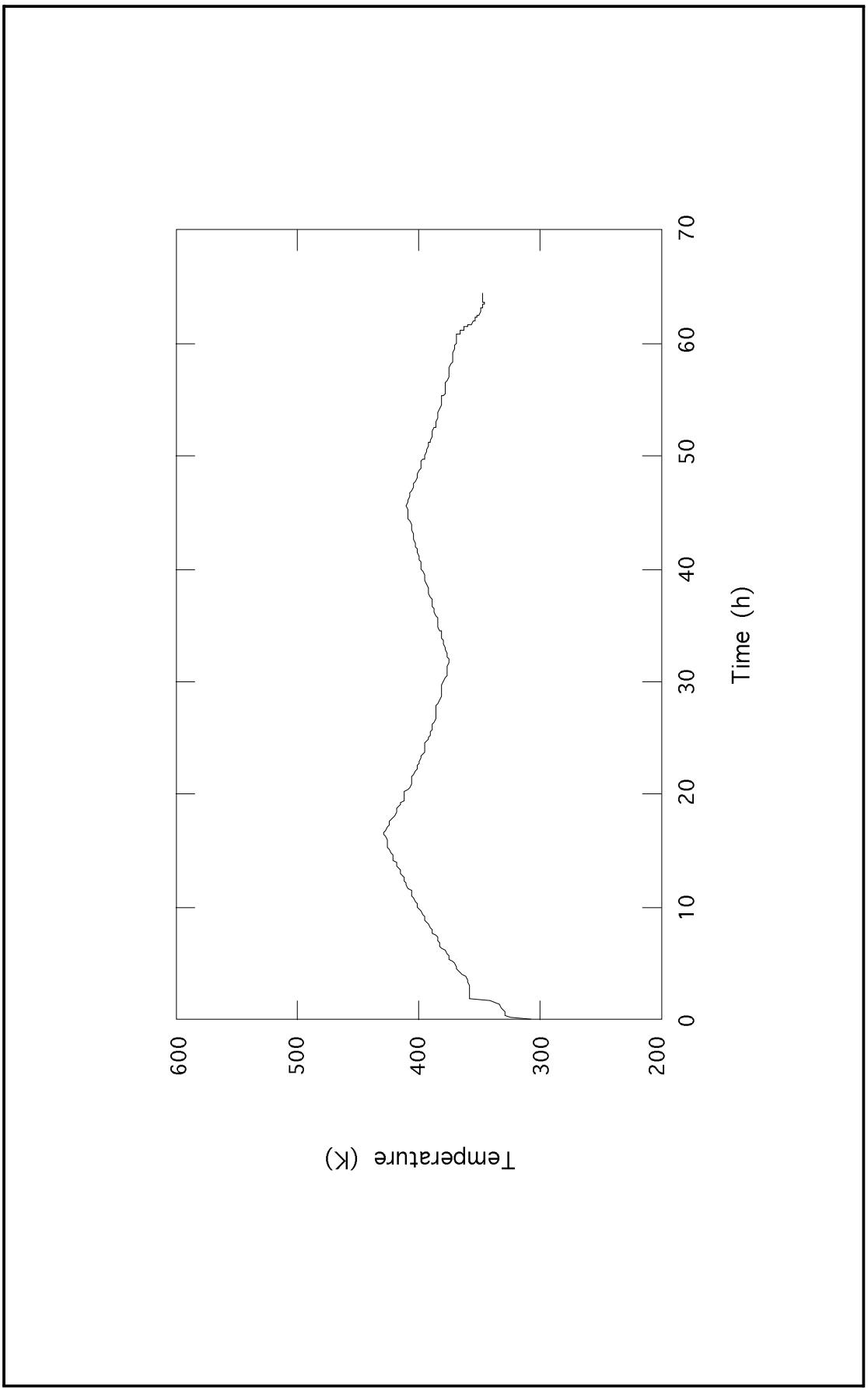

Figure 19E.2-28f Suppression Pool Water Temperature for High Pressure Ex-Vessel Core Melt Scenario

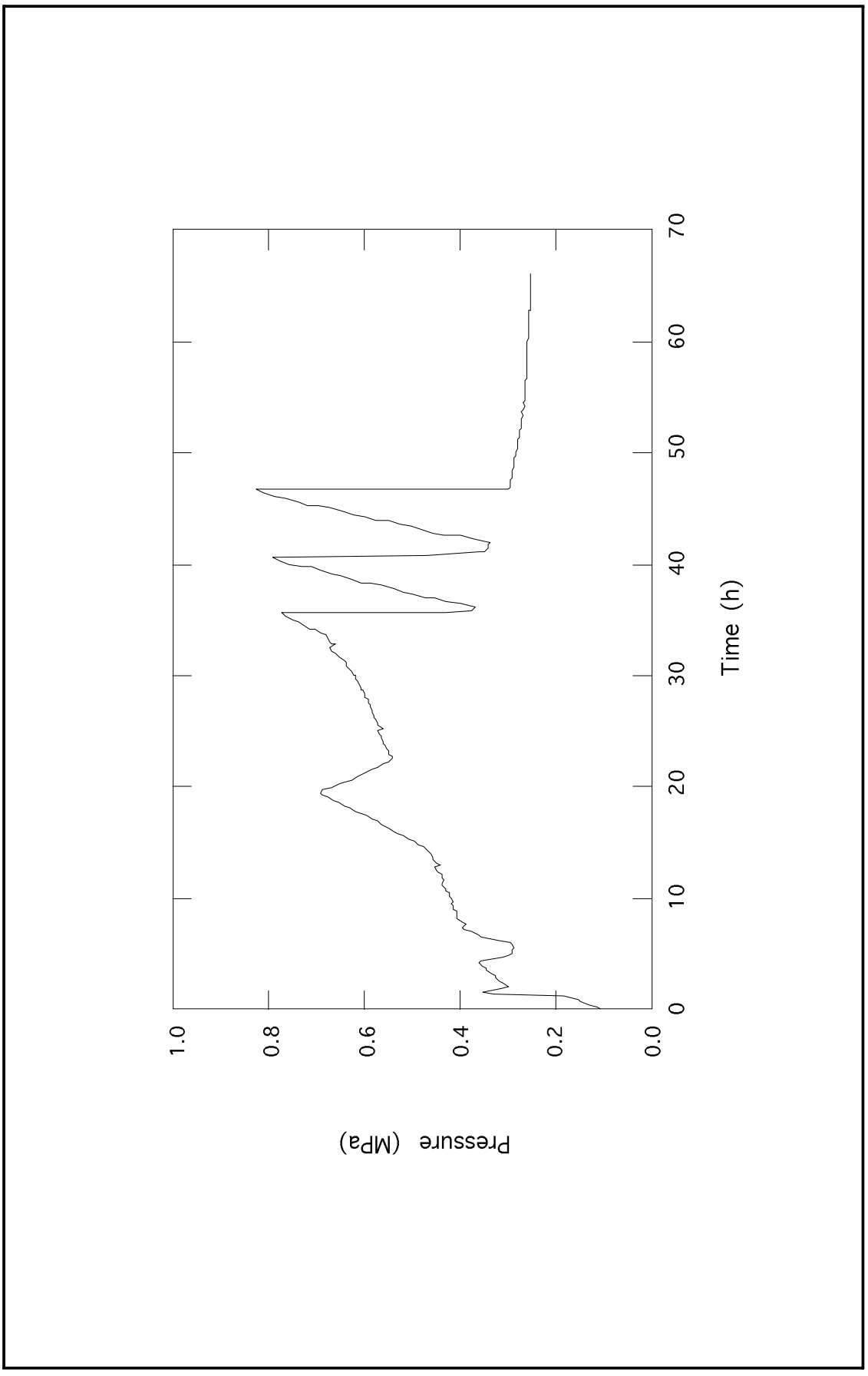

Figure 19E.2-29a Drywell Pressure for Low Pressure Ex-Vessel Core Melt Scenario

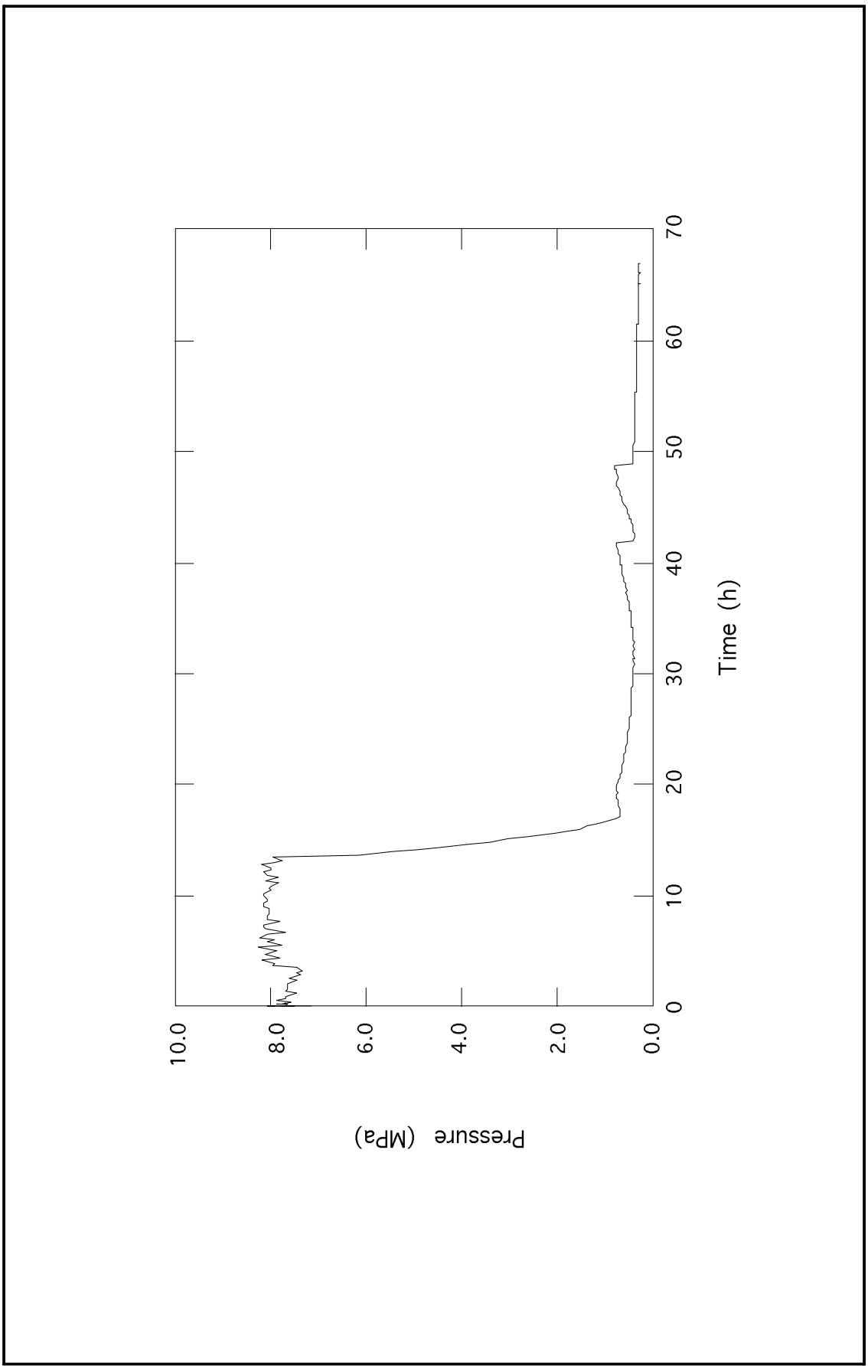

Figure 19E.2-29b Vessel Pressure for Ex-Vessel Low Pressure Core Melt Scenario

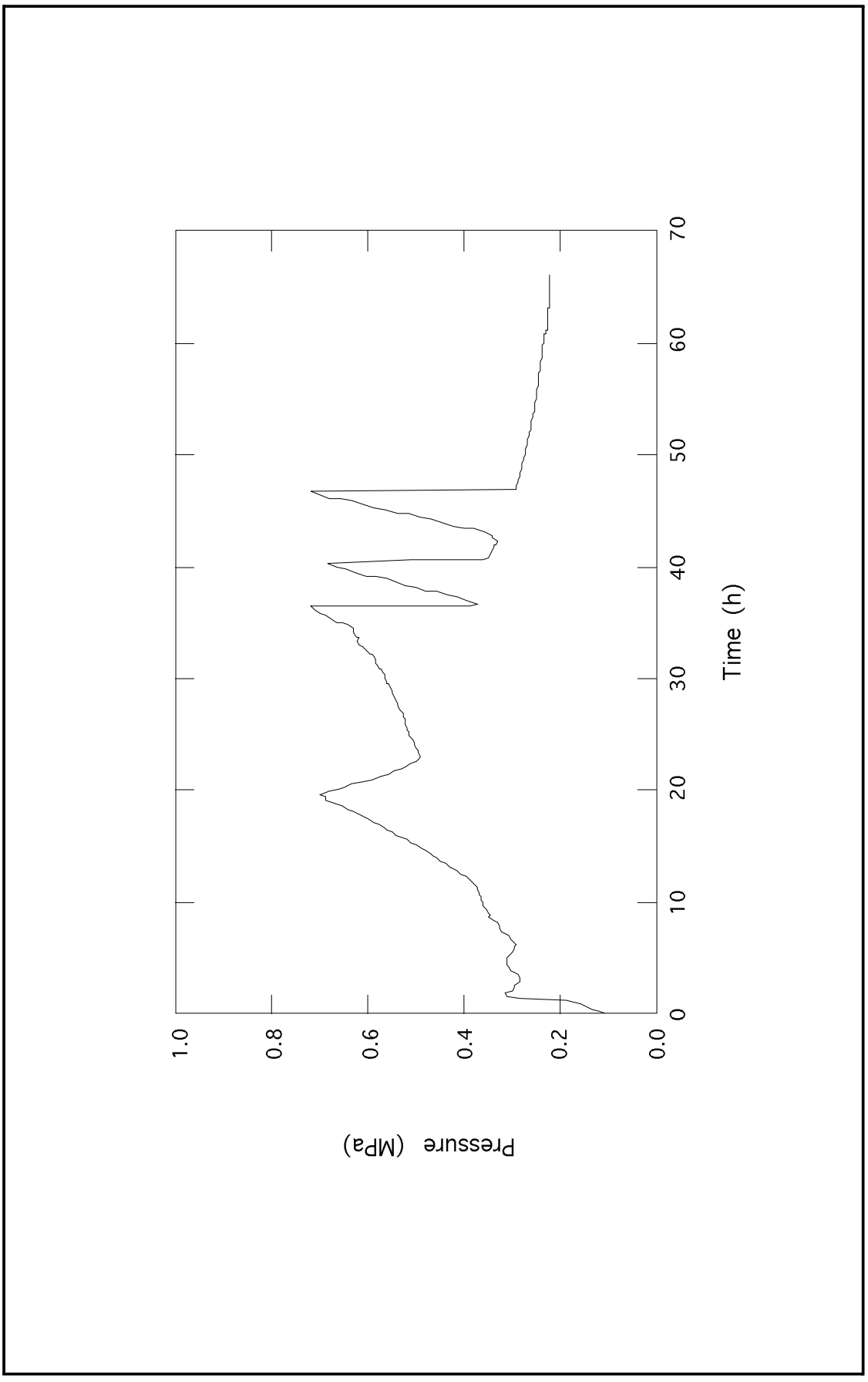

Figure 19E.2-29c Wetwell Pressure for Ex-Vessel Low Pressure Core Melt Scenario

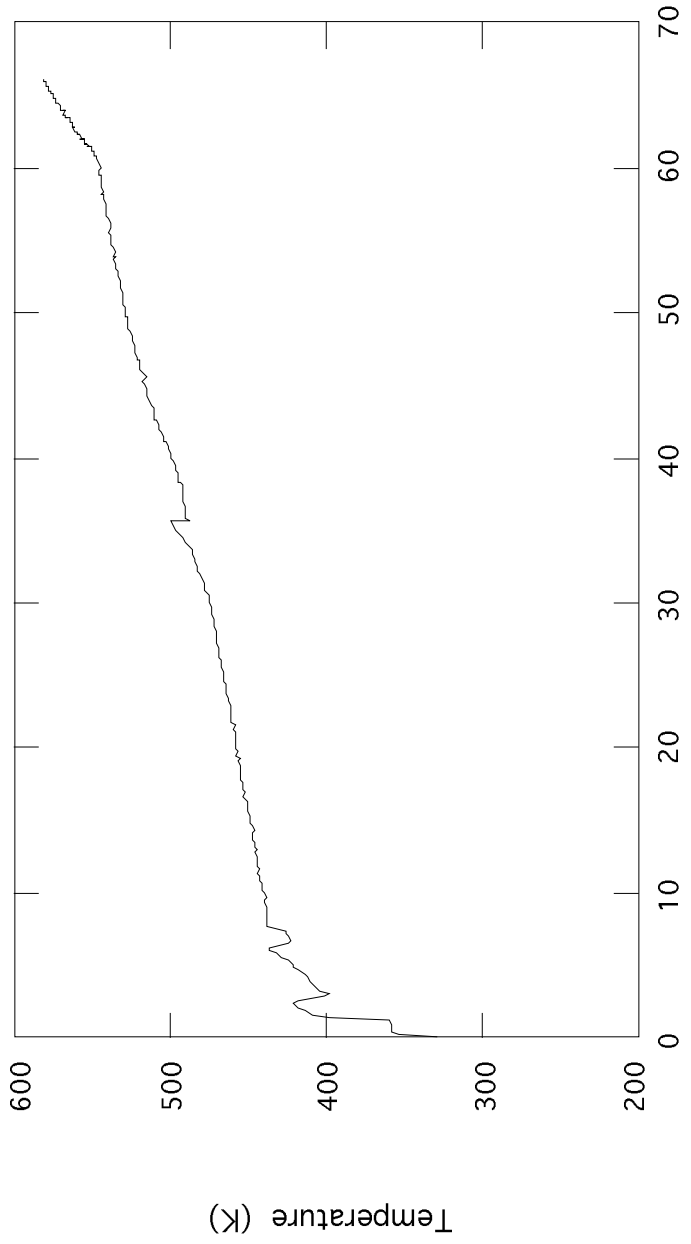

Figure 19E.2-29d Drywell Temperature for Ex-Vessel Low Pressure Core Melt

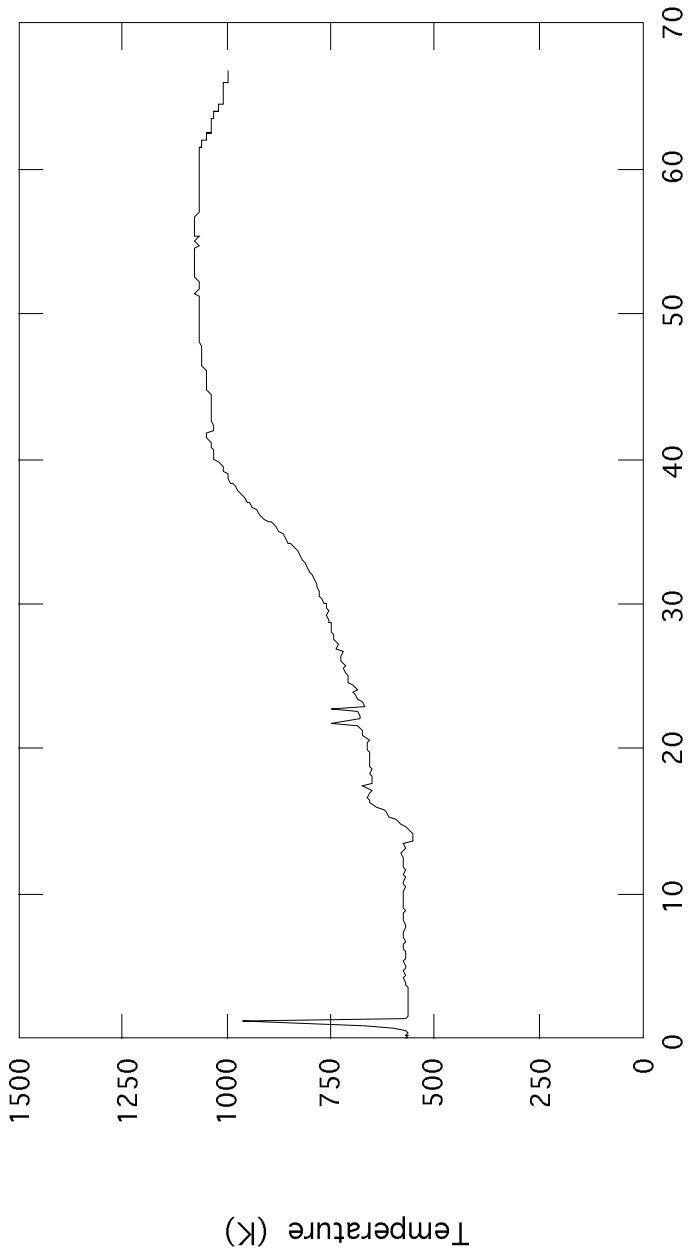

Figure 19E.2-29e Vessel Temperature for Ex-Vessel Low Pressure Core Melt Scenario

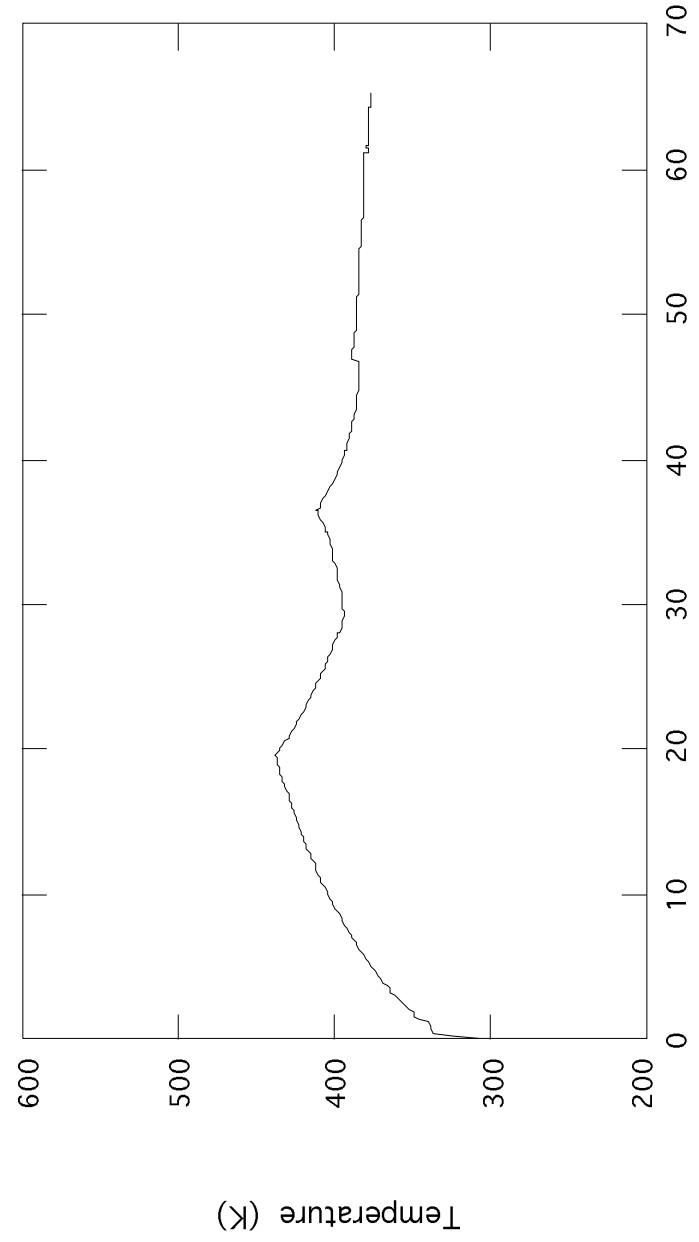

Figure 19E.2-29f Suppression Pool Water Temperature for Low Pressure Ex-Vessel Core Melt Scenario

19E.3 Consequence Analysis

This subsection describes the consequence evaluation. Key inputs and assumptions are described. The calculated results are compared to consequence-related goals to show that the goals are satisfied.

The CRAC-2 computer code (Reference 19E.3-1) was used to determine the consequences of potential reactor accidents. The CRAC code evaluates offsite dose and consequences for each accident category over a range of possible weather conditions and evacuation assumptions. The CRAC code models are described in Reference 19E.3-2. The rationale for site related input selection is presented in Subsection 19E.3.1. This data and data from the plant performance analysis is presented in Subsection 19E.3.2. The calculated results are compared to the goals in Subsection 19E.3.3.

19E.3.1 Site Assumptions

The evaluation of the consequences of a reactor accident are closely tied to the site parameters (e.g., weather, population, and land use). Envelope site parameters for deterministic evaluations are provided in Chapter 2. For probabilistic consequence evaluations, additional site related assumptions were required. They are described below.

19E.3.1.1 Meteorology

In the original WASH-1400 analysis (Reference 19E.3-3), a number of actual site meteorologies were used. However, the original WASH-1400 meteorology data files are not compatible with the CRAC-2 code. A set of meteorological data files suitable for use with the CRAC-2 code was obtained from Sandia National Laboratory. This data was used in the study given in Reference 19E.3-4. These files define hourly weather data for a one year period for twenty-six U.S. Sites. Five sites representing five geographical regions throughout the U.S. were chosen for this ABWR study. These regions were termed NE(northeast), NW (northwest), S (south), W (west), and SW (southwest) as is shown in Figure 3-1 of Reference 19E.3-4.

For each of these geographical regions, one meteorological data file was chosen. The basis for this choice was an evaluation for each meteorology using reactor release parameters for five accidents representing a very large percentage of the risk calculated in the GESSAR II PRA (Reference 19E.3-5). This accident data set is given in Table 19E.3-1. It was chosen since the GESSAR II design is closer to the ABWR design in terms of offsite releases than other designs for which PRA's were available. In determining the variations in consequence due to different meteorological data sets, each data file was input to the CRAC-2 code with all other information being identical. From these results, the site in each geographical region most closely approximating the mean total latent fatality result for that region was chosen to represent the region. The consequence results reported here (Subsection 19E.3.3) represent the average of five runs, one for each meteorological region.

19E.3.1.2 Population

For the ABWR consequence evaluation, the population density tables from Reference 19E.3-4, Tables 3-2 and 3-3, were used to develop regional populations corresponding to each regional meteorology. The mean values used are given in Table 19E.3-2.

19E.3.1.3 Evacuation

Many evacuation related characteristics (local roads, population demographics, emergency services) are quite site specific. No general guidance has been given for generic evacuation evaluations by the NRC. The evacuation parameters used in this study are given in Table 19E.3-3. Five percent of the people are assumed not to evacuate. Ninety-five percent are assumed to wait 1.5 hours after notification and then move radially outward at 4.47 meters per second (10 mph). Values used for shielding were the standard CRAC assumptions. Definitions for the parameters given in Table 19E.3-3 are provided in Table 19E.3-4.

These evacuation assumptions were used for individual and societal risk calculations. For the purposes of evaluating dose levels for comparison to the dose goal (Subsection 19E.3.3.1 item 3), no evacuation or shielding was assumed.

19E.3.2 CRAC Input Data

19E.3.2.1 Input Which Differs From Standard CRAC Assumptions

The following table describes these inputs.

Table	Inputs
19E.3-2	Population Density
19E.3-3	Evacuation Parameters
19E.3-5	Site and Reactor Data for Meteorological Modeling
19E.3-6	Event Release Parameters

19E.3.2.2 Input to CRAC from Performance Analysis

The plant performance analysis results which are input parameters to the CRAC-2 code are described here and are shown in Table 19E.3-6. These inputs describe the data used which are plant specific and are not related to radiological modeling which is discussed in Subsection 19E.3.1. The plant input parameters are described below with the subsection of Tier 2 in which the parameters are developed indicated at the end of each section in parenthesis.

In addition to the accident case probability, for each accident case, which represents the accident sequence listed below it, the following data are used (Table 19E.3-6):

Release Category Name, LNAME(j) - Abbreviated name given to release which results from the event. (Subsection 19E.2)

TL(j) - time(hr) from reactor shutdown (defined as the end of neutron generation) to release to the atmosphere. The value is used to determine isotopic decay prior to release from the plant. For an ATWS event, containment failure is postulated to occur before core damage. Since neutron production may continue up to the time of core melt, TL may be zero for an ATWS event. (Subsection 19E.2)

DR(j) - duration of initial release (h) of radionuclides from the plant. This value is used to determine the expansion of the cloud. The maximum value of this parameter is 10 hours (CRAC limitation for plume modeling). (Subsection 19E.2)

TLL(j) - warning time (h) between official notification of public and release of radioactivity from the plant. The basis for the warning time is the onset of severe core damage. The emergency action levels specified in Reference 19E.3-6, Appendix I require that a site area emergency be delayed when “delayed core with possible loss of coolable geometry” occurs.

FPR(j) - Sensible heat release rate in calories/s in the release cloud. This value is used to determine the initial buoyancy of the released cloud plume.

RH(j) - Plume release height in meters from the ground. If this value is less than the building height, a ground release with building wake effect is assumed. Otherwise, the plume will be buoyed to a height equal to the release height plus a buoyancy height.

FLEAK(j,k) - fraction of core inventory at the beginning of the accident for each isotope group which is eventually released into the atmosphere. The standard isotopes groups are:

(1) Noble gases (Kr, Xe)

(2) Not used, originally used for organic iodide

(3) Iodine, including organic iodide

(4) Cesium, including Rb

(5) Tellurium, including Sb

(6) Barium, including Sr

(7) Cobalt, including Mo, Tc, Ru, Rh

(8) Lanthanum, including Y, Zr, Nb, Ce, Pr, Nd, Np, Pu, Am, Cm

19E.3.3 Comparison of Results to Goals

19E.3.3.1 Goals

Three major consequence-related goals were established in the ABWR Licensing Review Bases (Reference 19E.3-7) which referenced the Safety Goal Policy Statement. These goals are:

(1) Individual Risk Goal

The risk to an average individual in the "vicinity" of a nuclear power plant of prompt fatalities that might result from reactor accidents should not exceed one-tenth of one percent (0.1%) of the sum of "prompt fatality risks" resulting from other accidents to which members of the U.S. Population are generally exposed. As noted in the Safety Goals Policy statement, "vicinity" is defined as the area within 1.61 km (1 mile) of the plant site boundary. "Prompt Fatality Risks" are defined as those risks to which the average individual residing in the vicinity of the plant is exposed to as a result of normal daily activities. Such risks are the sum of risks which result in fatalities from such activities as driving, household chores, occupational activities, etc. For this evaluation, the sum of prompt fatality risks was taken as the U.S. accidental death risk value of 39.1 deaths per 100,000 people per year based upon Reference 19E.3-8 (i.e., $<3.9 \times 10^{-7}$ per year).

(2) Societal Risk Goal

The risk to the population in the area "near" a nuclear power plant of cancer fatalities that might result from nuclear power plant operation should not exceed one-tenth of one percent (0.1%) of the sum of the "cancer fatality risks" resulting from all other causes. As noted in the Safety Goal Policy Statement, "near" is defined as within 16.1 km (10 miles) of the plant. The "cancer fatality risk" was taken as 169 deaths per 100,000 people per year based upon 1983 statistics in Reference 19E.3-9 (i.e., $<1.7 \times 10^{-6}$ per year).

(3) Radiation Dose Goal

The probability of exceeding a whole body dose of 0.25 Sv at a distance of 805 m (one-half mile) from the reactor shall be less than one in a million per reactor year.

19E.3.3.2 Results

The results from the PRA demonstrate that the Core Damage Frequency alone is below the Individual Risk Goal probability. When considering the additional protection provided by containment to prevent release of large amounts of radioactivity, the ABWR probability is far below the goals for societal risk and radiation dose. Based upon the results of the analysis, the ABWR meets the established consequence related goals.

19E.3.4 References

19E.3-1 Ritchie, L.T., et al, "Calculation of Reactor Accident Consequences Version 2 CRAC2: Computer Code", NUREG/CR-2326, February 1983.

19E.3-2 Ritchie, L.T., et al, "CRAC2 Model Description", NUREG/CR-2552, March 1984.

19E.3-3 "Reactor Safety Study, Appendix 6: Calculation of Reactor Accident Consequences", WASH-1400 (NUREG 75/014), October 1975.

19E.3-4 Aldrich, D.C., et al, "Technical Guidance for Siting Criteria Development", NUREG/CR-2239, December 1982.

19E.3-5 "General Electric Company GESSAR II BWR/6 Nuclear Island Design (22A7007)", March 1982.

19E.3-6 "Criteria for preparation and Evaluation of Radiological Emergency Response Plans and Preparedness in Support of Nuclear Power Plants", NUREG-0654.

19E.3-7 Murley, T.E., "Advanced Boiling Water Reactor Licensing Review Bases", Project No. 671, August 7, 1987.

19E.3-8 "Accident Facts", 1988, National Safety Council.

19E.3-9 "1986 Cancer Facts & Figures", American Cancer Society, 90 Park Ave, New York, NY 10016.

19E.3-10 "ABWR Severe Accident Evaluations," Toshiba UTLR-0014.

Table 19E.3-1 GESSAR Reactor Release Parameters

Category	$P_{(j)}$*	$TL_{(j)}$	$DR_{(j)}$	$TLL_{(j)}$	$FPR_{(j)}$	$RH_{(j)}$	Isotopic Release Fractions by Group						
Group =							1	3	4	5	6	7	8
C1-TR-E2		1.66	0.1	0.7	4.0E+07	10.0	1.0E+0	1.3E-03	1.0E-03	1.0E-03	1.1E-03	2.6E-04	1.5E-07
C1-TR-E3		1.7	4.3	0.7	1.5E+06	10.0	1.0E+0	1.3E-03	1.0E-03	1.0E-03	2.2E-04	3.1E-04	4.9E-05
C1-TR-L3		11.9	10.0	10.9	5.0E+05	49.0	1.0E+0	4.8E-04	1.8E-04	1.8E-04	3.9E-05	5.7E-05	9.0E-06
C1-TR-12		3.0	0.1	2.0	4.4E+07	10.0	1.0E+0	1.3E-03	9.9E-04	9.9E-04	1.0E-03	2.5E-04	1.5E-07
C1-TR-13		3.0	3.6	2.0	2.1E+06	10.0	1.0E+0	1.3E-03	1.0E-03	1.0E-03	2.2E-04	3.1E-04	4.8E-05

* Probabilites not part of DCD (Refer to Reference 19E.3-10).

Note:

See Subsection 19E.3.2.2 for definition of parameters in this table.

Table 19E.3-2 Population Density for Each Geographical Region

Radial Interval (mi)	Mean Population by Geographic Sector (people per sq. mi.)				
	NE	MW	S	W	SW
0-5	100	60	30	20	10
5-10	130	60	80	30	20
10-20	170	90	70	60	30
20-30	180	120	100	50	40
30-50	400	100	80	40	130

Note:
Data taken from Reference 19E.3-4, Table 3-2.

Table 19E.3-3 Evacuation Parameters

Parameter	Strategy	
	1	2
Fraction of Population Evacuating	0.95	0.05
Time Delay Before Evacuation — h	1.5	0
Evacuation Speed — m/s (mph)	4.47 (10)	0
Maximum Distance of Evacuation — m (mi)	4827 (3)	0
Distance Moved by Evacuees — m (mi)	1260 (7)	0
Sheltering Radius — m (mi)	24140 (15)	0

Note:
See Subsection 19E.3.1.3 for additional description of parameters in this table.

Table 19E.3-4 Evacuation Parameter Definition

Parameter	Definition
Fraction of Population Evacuating	Fraction of population following the evacuation strategy.
Time Delay Before Evacuating	Time between notice to evacuate and start of evacuation.
Evacuation Speed	Once evacuation begins, it is assumed that the public moves directly outward and away from the plant site at this speed.
Maximum Distance of Evacuation	Once evacuation begins, individuals within this distance are assumed to evacuate as above with their exposure determined by detailed tracking of their position relative to the radioactive cloud plume. People living beyond this distance are assumed to not be evacuated initially. They are assumed to be exposed to ground contamination for 24 hours and then evacuated.
Distance moved by Evacuees before Sheltering	Distance at which evacuees are assumed to take shelter. This parameter is nominally designed to represent the use of prearranged evacuation shelters.
Sheltering Radius	People living within this distance are assumed to take shelter if they do not evacuate. Sheltering is assumed for 24 hours at which time these people are assumed to be relocated out of the contaminated area, without further exposure.

Table 19E.3-5 Site and Reactor Data for Meteorological Modeling

Reactor Building Length	54.0 m	177 ft.
Reactor Building Height	37.7 m	124 ft.
Interval for Special Wake Effects	2.41 km	1.5 mi.

Table 19E.3-6 Event Release Parameters

Accident	P(i)*	TL	DR	TLL	FPR	RH	Release Fractions†		
							NG	Iodine	Cesium
NCL		2.7	10	1.7	3.3E+5	37	0.044	2.3E-05	2.3E-05
CASE 1		20	1	19.2	3.3E+5	37	1	1.5E-07	1.3E-05
LCHPFSRN									
LCHPPSRN									
LBLCFSRN									
SBRCPFRN									
LCLPPFRN									
LCPFSRN									
CASE 2		19	1	18.2	3.3E+5	37	1	5.0E-06	5.0E-06
LCLPPFCR									
LCLPFSCR									
CASE 3		50	10	49.2	3.3E+5	37	1	2.8E-04	2.2E-03
LCHPFSD90									
CASE 4		20	1	19.2	3.3E+5	37	1	1.6E-03	1.6E-03
DF100FSR									
DF100PFR									
CASE 5		19	1	19.2	3.3E+5	37	1	6.0E-03	5.3E-04
LBLCPFRN									
CASE 6		19	10	18.2	3.3E+5	37	1	3.1E-02	7.7E-02
LCHPPSD90									
LBLCPFD90									
LBLCFSD90									
CASE 7		20	10	19.2	3.3E+5	37	1	8.9E-02	9.9E-02
LCLPFSD90									
LCHPPFPM									
LCLPPFD90									
CASE 8		2	10	1.2	1.0E+6	37	1	1.9E-01	2.5E-01
LCHPPFEH									
LCHPPFBR									
LCHPPFBD									
CASE 9		23.6	10	12.2	3.3E+5	37	1	3.7E-01	3.6E-01
SBRCPFD90									

* Probabilites not part of DCD (Refer to Reference 19E.3-10).

† Group 5-8 negligible release

Note:

See Subsection 19E.3.2.2 for definition of parameters in this table.

Table 19E.3-7 Not Used

Figure 19E.3-1 Not Used